UNIVERSITÉ DE MONTRÉAL

MODÉLISATION DES SYSTÈMES DE PLAQUES EN INTERACTION AVEC UN FLUIDE AU REPOS OU EN ÉCOULEMENT

KERBOUA YOUCEF
DÉPARTEMENT DE GÉNIE MÉCANIQUE
ÉCOLE POLYTECHNIQUE DE MONTRÉAL

THÈSE PRÉSENTÉE EN VUE DE L'OBTENTION
DU DIPLÔME DE PHILOSOPHIAE DOCTOR (Ph.D.)
(GÉNIE MÉCANIQUE)
JANVIER 2007

Your file Votre référence
ISBN: 978-0-494-24555-2
Our file Notre référence
ISBN: 978-0-494-24555-2

UNIVERSITÉ DE MONTRÉAL

ÉCOLE POLYTECHNIQUE DE MONTRÉAL

Cette thèse intitulée:

MODÉLISATION DES SYSTÈMES DE PLAQUES EN INTERACTION AVEC UN FLUIDE AU REPOS OU EN ÉCOULEMENT

Présentée par: KERBOUA YOUCEF

en vue de l'obtention du diplôme de: Philosophiae Doctor

a été dûment acceptée par le jury d'examen constitué de:

M. SHIRAZI-ADL Aboulfazl, Ph.D., président

M. LAKIS Aouni A., Ph.D., membre et directeur de recherche

M. MUREITHI Njuki W., Ph.D., membre

M. HOJJATI Mehdi, Ph.D., membre

DÉDICACE

À l'âme de ma mère et à mon père

À ma femme et mon fils Louaï

À mes frères et mes sœurs

REMERCIEMENTS

Je tiens à exprimer mes remerciements les plus profonds à mon directeur de recherche, le Prof. Aouni. A. Lakis, qui m'a offert la possibilité de réaliser cette thèse et de découvrir un domaine de recherche très intéressant. Je le remercie également pour son suivi et ses conseils judicieux tout au long de mon doctorat.

Ce travail est supporté financièrement grâce à une subvention de recherche et développement coopérative pour le projet (RDC, N CRDPJ-311188-04) intitulé « Analyse dynamique des turbines hydrauliques » (CRSNG – Hydro Québec). Ce support est grandement apprécié.

Je tiens aussi à remercier tous les membres du jury, présidé par le professeur A.Shirazi-Adl de l'École Polytechnique de Montréal et composé des professeurs N.W. Mureithi de l'École Polytechnique de Montréal et du docteur M. Hojjati, chercheur au Conseil national de recherches Canada section Aérospatiale Montréal, qui ont consacré une partie de leur temps à la lecture de cette thèse.

RÉSUMÉ

Lorsqu'une structure est en contact avec un fluide au repos ou en écoulement, son comportement dynamique subit des changements considérables. La chute importante des fréquences constatée lors de l'interaction du fluide avec la structure peut même affecter la stabilité dynamique du système.

Très peu de travail a été fait sur les plaques et les réservoirs rectangulaires par rapport aux structures ayant une symétrie géométrique axiale telles que les coques cylindriques et les plaques circulaires.

Nous développons dans ce travail un élément fini de plaque qui sera capable de prédire le comportement dynamique des plaques et des coques en interaction avec un fluide incompressible, non visqueux et irrotationnel.

L'idée de notre travail provient de l'approche hybride utilisée lors du développement des deux éléments finis solide-fluide au sein de notre équipe de recherche. Le premier élément est une portion circonférentielle de la coque cylindrique fermée ayant deux nœuds selon la direction axiale et le second est une portion longitudinale d'une coque cylindrique ouverte ayant deux nœuds dans la direction circonférentielle. Les deux éléments ont été utilisés pour l'analyse des coques cylindriques ouvertes et fermées en interaction avec un fluide au repos ou en écoulement. Les fonctions de déplacement ont été dérivées de la solution exacte des équations d'équilibre des coques. Cette caractéristique a permis d'avoir des éléments finis hybrides très précis et qui convergent rapidement.

L'élément fini développé dans ce travail est en quelque sorte une combinaison entre les deux éléments de coques déjà développés par Lakis et al. et qui ne sera pas limité

à une géométrie spécifique. Il sera capable de calculer les hautes et les basses fréquences avec précision et il pourra tenir compte de n'importe quelle condition aux limites au milieu ou aux bords de la structure.

L'élément fini que nous développons ici est une portion de plaque rectangulaire ayant quatre nœuds, deux selon l'axe des X et deux selon l'axe des Y. Chacun des nœuds possède des degrés de liberté décrivant les mouvements membranaires et flexionnels.

Les équations d'équilibre et de mouvement d'une portion de plaque sont obtenues à partir de la théorie de Sanders. Les équations d'équilibre tiennent compte de l'effet de membrane et de l'effet de flexion. Les équations de Sanders sont basées sur la première approximation de Love pour les coques minces.

Nous approchons les déplacements de membrane par des polynômes bilinéaires et la déflexion de la plaque par une fonction exponentielle ayant la forme générale de la solution des équations d'équilibre. Comme le couplage solide-fluide s'impose avec le déplacement transversal, le choix de la fonction exponentielle convient à la solution des équations de fluide et au calcul de la pression.

En se basant sur le champ de déplacement mentionné précédemment, la méthode des éléments finis est utilisée pour calculer les matrices élémentaires de masse et de rigidité par intégration exacte pour une plaque rectangulaire. Les modes et les fréquences sans fluide calculés éprouvent une très bonne précision lorsqu'on les compare avec les résultats obtenus par d'autres logiciels ou avec le recueil de solutions analytiques de Leissa.

Lorsque la plaque est en interaction avec un fluide au repos ou en écoulement potentiel, la pression hydrodynamique est exprimée en fonction de la masse volumique du fluide, des conditions aux limites du fluide (mur rigide, surface libre, ...), de la vitesse moyenne d'écoulement et du champ de déplacement de la paroi solide et ses dérivées par rapport au temps.

L'élément fini solide-fluide de plaque tient compte de la pression de fluide appliquée sur la plaque en utilisant l'équation de Bernoulli à l'interface fluide-solide et l'équation différentielle gouvernant le potentiel de vitesse. La condition d'imperméabilité assure le couplage entre le fluide et la structure. La limite du fluide peut être une surface libre a potentiel nul, une surface libre avec effet de surface ou un mur rigide. La pression de fluide s'introduit dans le système comme une masse ajoutée fictive de fluide.

Les systèmes de plaques parallèles et radiales ainsi que les réservoirs cylindriques et rectangulaires ont été analysés dans ce travail en utilisant un élément fini de plaque. L'utilisation d'une matrice de transformation géométrique s'impose afin de pouvoir écrire les matrices élémentaires calculées au niveau local dans un repère global et commun pour toutes les parties de la structure et par la suite les équations globales d'équilibre dynamique. Le problème de singularité numérique causé par l'apparition d'un nouveau degré de liberté lorsque nous passons du repère local au repère global est résolu en introduisant des raideurs et des masses fictives aux termes diagonaux correspondant à ce degré de liberté dans chaque nœud de l'élément. La pression hydrodynamique est calculée en fonction des conditions aux limites du fluide. Les

modes en phase et en antiphase des différentes parois de réservoirs ou de systèmes de plaques sont considérés.

Dans la dernière partie de cette thèse, nous développons un modèle d'éléments finis fluide-solide qui nous permettra d'étudier les plaques rectangulaires ayant des conditions aux limites quelconques soumises aux efforts induits par le passage d'un écoulement potentiel.

Le potentiel de vitesse, l'équation de Bernoulli et l'imperméabilité linéaire appliquée à l'interface sont utilisés pour écrire une expression explicite de la pression. Cette dernière est exprimée en fonction de l'inertie du fluide, de la force de Coriolis et de la force centrifuge, écrites respectivement en terme d'accélération, de vitesse et de déplacement transversaux.

Un code de calcul en langage Fortran a été conçu pour calculer et assembler les matrices élémentaires et puis par la suite introduire les conditions aux limites spécifiques à chaque structure et calculer les fréquences et les modes de vibration.

Chaque structure étudiée en utilisant les modèles d'éléments finis solide-fluide développés dans ce travail est validée d'abord lorsque la structure vibre à vide puis lorsqu'elle est en interaction avec un fluide. En comparant les résultats obtenus en utilisant nos modèles avec ceux d'autres travaux analytiques, numériques ou expérimentaux, nous pouvons conclure que notre formulation éprouve une bonne précision.

Les avantages de cet élément résident dans le fait qu'il n'est pas limité par des conditions aux limites imposées par des fonctions de déplacement assumées. Aussi, ces éléments peuvent être utilisés pour l'étude de structure ayant des discontinuités

ou des épaisseurs variables. Le fait que la pression se calcule indépendamment pour chaque élément nous permet d'étudier des structures en contact partiel avec le fluide ou une structure en contact avec un fluide ayant une hauteur variable d'un point à l'autre.

ABSTRACT

When in contact with fluid at rest or in flow, structures undergo considerable changes in their dynamic behaviour. The significant decrease in the frequencies observed during the fluid-structure interaction can also affect the dynamic stability of the system. While many works have been carried out to study the axisymetric structures, such as cylindrical shells and circular plates, only few have addressed the rectangular plates and tanks.

The current study aims to develop a finite element model of a plate in order to predict the dynamic behaviour of plates and shells subjected to an incompressible, inviscid, irrotationnal fluid. The basic idea of the work comes from the hybrid approach used previously by our group in which two solid-fluid finite elements were developed. The first element was a circumferential portion of a cylindrical shell with two nodes in the axial direction while the second one was a longitudinal portion of the open cylindrical shells with two nodes in the circumferential direction. These two elements were used to investigate open and closed cylindrical shells subjected to a flowing fluid. Displacement functions were derived from exact solution of the equilibrium equations of shells; a characteristic that provides a very accurate and rapidly converging hybrid finite element.

The finite element developed in the present work can be considered as a combination of the two above-mentioned finite elements, but its applications are not limited to a specific geometry. Such an element is able to accurately compute both high and low frequencies while taking into account any type of boundary condition. This element

is a rectangular portion of a plate with four nodes. The effects of membrane (in-plane) and flexural (out-of-plane) motions are taken into account.

The equilibrium equations of the plate are derived using Sanders' theory in which both membrane and bending effects are incorporated. Sanders' equations are established based on Love's first approximation for thin shells. The membrane and transversal displacement fields are approximated by bilinear polynomial and exponential functions, respectively. The latter one is general form of solution of the equilibrium equations. Since the solid-fluid coupling is mainly introduced by transverse displacement, the exponential form of this displacement will be appropriate for solving the fluid equations as well as calculating the pressure.

Mass and stiffness matrices are calculated using the exact integration approach, the foregoing displacement fields, and the finite element method. The calculated mode shapes and frequencies in vacuum show good agreement when compared to those obtained by other software and analytical results summarized by Leissa in an extensive study.

When the plate is in interaction with fluid at rest or in potential flow, the hydrodynamic pressure will be a function of fluid density, boundary conditions of the fluid (rigid wall, free surface.... etc.), mean velocity of the flow, and finally displacement of the elastic wall and its temporal derivatives. Using the equation of Bernoulli at the fluid-solid interface and the differential equation which governs the potential velocity, the solid-fluid finite element is able to take into account the fluid pressure applied to the plate. The impermeability condition ensures the existence coupling between the fluid and structure. The fluid boundary can be a rigid wall or a

free surface with either zero velocity potential or surface effect. The fluid pressure is introduced into the system as an added mass.

In the present study, parallel/radial-plates as well as the cylindrical and rectangular tanks were analyzed by using the plate finite element. However, it is necessary to use a geometrical matrix to transfer the local elementary matrices into a global one in which dynamic equations are subsequently written. New degree-of-freedom at the global system generated after geometrical transformation causes a numerical singularity problem. Such problem is tackled by adding virtual stiffness and masses to diagonal terms for this new degree of freedom at each node of the element. It is also known that the hydrodynamic pressure varies with boundary conditions of the fluid. The in-phase and out-of-phase modes of the tank walls and the parallel-plate assemblies are also considered.

In the final phase of the thesis, we describe the development of a fluid-solid finite element to model plates subjected to flowing fluid under various boundary conditions. The velocity potential, Bernoulli's equation as well as linear impermeability applied at the solid-fluid interface are employed to yield an explicit expression for fluid pressure which, in turn, is a function of the fluid inertia, Coriolis, and centrifugal forces. These forces are written in terms of acceleration, velocity, and transverse displacement, respectively.

An in-house FORTRAN code has been developed to calculate and assemble the elementary matrices, to introduce the boundary conditions for each structure as well as to calculate frequencies/mode shapes of vibration. Each considered structure is first validated for the case of in vacuum vibrations and then in interaction with a

fluid. Comparison of our results with those of other analytical, numerical and experimental works shows good agreement.

One of the most important advantages, among others, of this element lies in not being limited by specific boundary conditions imposed by the assumed displacement functions. Furthermore, these elements can be used to study structures with discontinuities or variable thicknesses. The fact that the pressure is independently calculated for each element allows for the investigation of partially submerged structures and those in contact to a fluid with a variable height from one point to another.

TABLE DES MATIÈRES

CHAPITRE II. HYBRID METHOD FOR VIBRATION ANALYSIS OF RECTANGULAR PLATES

CHAPITRE III : VIBRATION ANALYSIS OF RECTANGULAR PLATES COUPLED WITH FLUID

LISTE DES TABLEAUX

LISTE DES FIGURES

CHAPITRE I – INTRODUCTION

1.1 GÉNÉRALITÉS

L'interaction fluide-structure est un phénomène qui traduit les effets réciproques de deux milieux continus, fluide et solide. Le couplage des deux milieux est imposé par un ensemble de conditions qui contraignent leurs mouvements relatifs de telle sorte que l'évolution de chaque milieu dépend de celle de l'autre.

Nous rencontrons dans la pratique un grand nombre de problèmes d'interaction fluide-structure dans des domaines différents. Nous citons à titre d'exemple des réservoirs remplis de liquide dans le domaine du transport, les piles et les tabliers de ponts dans le génie civil, les écoulements bi-phasiques dans les échangeurs thermiques des centrales nucléaires, les ailes d'avions et les fusées en aéroélasticité, les aubes de turbines dans le domaine de l'énergie et l'écoulement sanguin dans les artères en hémodynamique.

Les efforts fournis à l'étude des problèmes d'interaction fluide-structure se sont multipliés au cours des dernières années. L'essor constant connu par la simulation numérique des phénomènes couplés est dû au développement des performances des calculateurs. Les modèles numériques développés ont permis de mieux comprendre et d'améliorer le comportement de certains systèmes en interaction avec le fluide lorsque le coût des essais expérimentaux en grandeur réelle n'est plus raisonnable.

Si nous examinons de près les cas pratiques mentionnés ci-haut, nous trouvons que les fuselages d'avion, les turboréacteurs, les réservoirs de tout genre, les pipelines, les aubes de turbines, les échangeurs sont tous des structures de type coque ou

plaque. La présence large de ces structures dans des industries stratégiques et économiquement très importantes a favorisé le développement de ce domaine de recherche. Au début, tous les travaux visaient la compréhension des caractéristiques statiques et dynamiques de ces structures afin d'éviter tous les effets destructifs lors de leur utilisation industrielle.

La première tentative de formulation des coques en flexion a été faite par Aron en 1874 en utilisant les équations générales de l'élasticité. Il a été suivi par Love en 1888 qui a développé une série d'équations fondamentales décrivant le comportement des coques minces élastiques [1]. Ces équations et les hypothèses sur lesquelles elles sont basées sont souvent identifiées comme la première approximation de Love. Reissner [2] et puis Knowles et Reissner [3] ont fait une nouvelle dérivation pour les coordonnées orthogonales. Une autre théorie a été développée par Sanders [4] tout en conservant les hypothèses originales de Love. Il a redéfini les forces et les moments de telle façon que les déformations de mouvement rigides disparaissent. Plusieurs autres travaux ont été faits pour résoudre des problèmes spécifiques de coques tels que les grands déplacements, la non-uniformité de la structure, l'inertie de rotation, l'anisotropie, la courbure initiale, la non-linéarité des propriétés mécaniques, etc. Les travaux continuent jusqu'à nos jours afin d'améliorer et corriger les formulations déjà existantes.

Les plaques sont des structures de la même famille des coques, les équations gouvernant le comportement des plaques peuvent être déduites des équations des coques. Elles ont été étudiées depuis plus de cent ans. Au 18^{e} siècle, Euler a formulé le premier modèle mathématique de comportement en membrane. Plus tard, Lagrange a développé la première équation exacte pour modéliser les vibrations

d'une plaque libre. Navier a introduit une méthode pour calculer les modes et les fréquences propres d'une plaque pour certaines conditions aux limites. Il a utilisé les séries de Fourrier pour représenter la déflexion de la plaque. Kirchhoff [5] est considéré le fondateur de la théorie moderne des plaques, il a tenu compte simultanément de l'effet membrane et de la flexion. Il a calculé les modes et les fréquences en se basant sur le travail virtuel. Love [1] a appliqué le travail de Kirchhoff aux plaques épaisses. Les bases d'une théorie prenant en compte les déformations au cisaillement ont été posées par Reissner [6]. Puis la théorie complète a été publiée par Mindlin [7].

Les travaux cités ci-haut font la plateforme du calcul des structures de type plaque et coque. Ces théories ont endossé la plupart des modèles analytiques ou numériques développés pour étudier le comportement de ces structures lorsqu'elles sont soumises à des charges ou à des excitations déterminées. En revanche, lorsque le milieu entourant la structure est un fluide, un couplage des modèles mathématiques gouvernant les deux milieux continus s'impose. Jusqu'à nos jours, la modélisation du couplage fluide-structure se heurte à des difficultés dont un bon nombre n'est pas encore résolu.

1.2 ORGANISATION DE LA THÉSE

Cette thèse a été élaborée sous forme d'articles intégrés dans le corps du travail. Chaque article constitue un chapitre dans la thèse. Le travail est réparti en sept chapitres de la manière suivante :

Le premier chapitre donne un bref aperçu de la nature du sujet et des disciplines liées au domaine de l'interaction fluide-structure ainsi qu'une recherche bibliographique

mentionnant selon un ordre chronologique par classe de structure les travaux réalisés dans ce domaine, que ce soit analytiques, numériques ou expérimentaux. À l'image des éléments développés dans ce travail, la revue bibliographique est divisée en trois parties comme suit :

a) plaques en interaction avec un fluide au repos ;

b) réservoirs en interaction avec un fluide au repos ;

c) plaques et systèmes de plaques soumis aux efforts induits par un écoulement potentiel.

À la suite de cette introduction, le deuxième chapitre présente le modèle d'éléments finis solide de plaque utilisé. Cette étude est présentée sous forme d'un article intitulé: **Hybrid Method for Vibration Analysis of Rectangular Plates**. Cet article développe un nouvel élément fini pour la détermination des fréquences et modes de vibrations des plaques rectangulaires. Cet article a été accepté comme publication dans Nuclear Engineering and Design.

Dans le troisième chapitre, nous présentons le développement d'un élément fini solide-fluide qui nous permet d'étudier le comportement des plaques rectangulaires en interaction avec un fluide. Des conditions aux limites variées de la plaque ou de fluide ont été considérées. Cette étude est présentée sous forme d'un article intitulé : **Vibration Analysis of Rectangular Plates Coupled with Fluid.** Cet article a été soumis à International Journal for Numerical Methods in Fluids.

Au quatrième chapitre, nous développons un élément fini solide-fluide de la même nature que celui du chapitre précédent destiné pour étudier le comportement dynamique des systèmes de plaques parallèles ou radiales submergées dans le fluide. Nous utilisons dans ce travail un élément fini solide-fluide de plaque qui tient compte

simultanément des effets de membrane et de flexion. Les matrices élémentaires calculées au niveau local sont transformées à un repère global de la structure. Des applications de ce modèle ont été élaborées pour des réservoirs cylindriques ou parallélépipédiques remplis de liquide. Cette étude est présentée sous forme d'un article intitulé : **Computational Modeling of Coupled Fluid-Structure Systems with Applications.** Cet article a été soumis au journal Computers and Structures.

Dans le cinquième chapitre, nous étudions le comportement des plaques et des systèmes de plaques ayant des conditions aux limites quelconques soumis aux efforts induits par le passage d'un écoulement potentiel de fluide. La pression du fluide sur la structure est exprimée en fonction de l'inertie du fluide, de la force de Coriolis et de la force centrifuge, écrites respectivement en terme d'accélération, de vitesse et de déplacement transversal. Les résultats obtenus sont validés par des modèles analytiques disponibles dans la littérature. Nous avons présenté ce modèle sous forme d'un article intitulé : **Modeling of Plates Subjected to Flowing Fluid under Various Boundary Conditions.** Cet article a été soumis à International Journal for Numerical Methods in Fluids.

Nous recueillons dans le sixième chapitre les principales remarques soulignées dans les quatre articles. Et finalement, nous présentons au dernier chapitre les principales conclusions tirées de cette thèse et nous énumérerons les perspectives des travaux futurs à la suite de cette recherche.

1.3. REVUE BIBLIOGRAPHIQUE

Lorsqu'on fait vibrer un système solide élastique en contact avec un fluide, le mouvement des parois entraîne une certaine masse du fluide, ce qui augmente l'énergie cinétique du système couplé.

Comme nous l'avons déjà mentionné, l'interaction fluide-structure consiste à étudier le comportement d'une structure en contact ou submergée dans un fluide en repos ou en écoulement. Un très grand nombre de travaux de recherche de toutes natures (expérimentaux, analytiques et numériques) ont été réalisés dans ce domaine. Nous divisons ces travaux en trois catégories :

a) plaques en interaction avec un fluide au repos ;

b) réservoirs en interaction avec un fluide au repos ;

c) plaques et systèmes de plaques soumis aux efforts induits par un écoulement potentiel.

1.3.1. Plaques en interaction avec un fluide au repos

Au 18^{e} siècle, Lord Rayleigh [8] a initié le travail sur les structures en contact avec le fluide. Il a développé une approche analytique pour calculer l'augmentation de l'inertie d'un disque rigide placé dans l'ouverture d'un mur rigide de dimensions infinies.

Lamb [9] a étudié le changement de la fréquence de résonance d'une plaque circulaire mince encastrée sur toute la circonférence lorsqu'elle est en contact avec un fluide. La plaque étudiée est placée dans l'ouverture d'un mur rigide plat de dimensions infinies. La méthode développée est basée sur le calcul de l'énergie cinétique du fluide. Le premier mode axisymétrique en flexion a été calculé en

utilisant la méthode de Rayleigh et en assumant une déflexion de la plaque polynomiale de quatrième ordre. Lamb est considéré un des pionniers dans ce domaine.

Powell et Roberts [10] ont fait un travail expérimental pour vérifier les résultats de Lamb. Ils ont étudié des plaques de différentes tailles en contact avec le fluide. Les résultats obtenus s'accordent bien avec ceux de Lamb.

MacLachlan [11] a calculé analytiquement l'inertie additionnelle lorsqu'un disque circulaire libre sur toute la circonférence vibre en contact avec un fluide. Le disque est placé dans l'ouverture d'un mur rigide infini.

Peake et Thurston [12] ont utilisé le modèle analytique de Lamb pour calculer les fréquences de résonance d'une plaque circulaire simplement supportée ou encastrée en contact avec un fluide agissant sur une de ses surfaces.

Les travaux théoriques mentionnés précédemment fournissent seulement les modes de résonance en assumant que les rayons des plaques sont très faibles par rapport à la longueur d'onde des radiations acoustiques dans le fluide.

Montero et al. [13] ont développé une méthode analytique permettant de calculer les fréquences de tous les modes axisymétriques dont la forme est connue à vide. La plaque circulaire étudiée est libre et est totalement submergée dans un réservoir de fluide. Des tests expérimentaux ont été élaborés pour vérifier le modèle analytique. Ils ont calculé aussi les fréquences de vibration d'une plaque en contact avec le fluide d'un seul côté. Une comparaison a été faite avec le modèle de MacLachlan, l'écart entre les résultats ne dépassait pas 5% malgré que la plaque de MacLachlan ait été placée dans l'ouverture d'un mur rigide.

Lindholm et al. [14] ont étudié théoriquement et expérimentalement le comportement dynamique d'une série de quinze plaques rectangulaires toutes encastrées sur un seul côté lorsqu'elles vibrent dans l'air et dans l'eau. Les plaques étudiées ont des épaisseurs et des rapports de dimensions (largeur/longueur) variées. Le système conçu permet d'étudier des plaques horizontales, verticales ou inclinées à 45 degrés lorsqu'elles sont totalement ou partiellement submergées dans l'eau. Une méthode analytique basée sur les théories des poutres et des plaques minces avec l'introduction des facteurs de correction hydrodynamiques a été développée. Une bonne corrélation entre les fréquences théoriques et expérimentales a été obtenue. Ce travail a dévoilé plusieurs informations sur le comportement des structures submergées dans un fluide. Les résultats obtenus montrent que : a) la hauteur de fluide au-delà de laquelle les fréquences cessent de changer est égale à la moitié de la longueur de la plaque et à cette hauteur l'effet de la surface libre du fluide devient négligeable, b) pour une plaque verticale totalement submergée dans l'eau, nous avons le même comportement que celui de la plaque horizontale totalement submergée au fond du réservoir, c) si la plaque verticale est partiellement submergée, la chute majeure des fréquences d'une plaque verticale a lieu lorsque la partie submergée est moins que la moitié de la longueur.

Un modèle d'éléments finis a été développé par Muthuveerappan et al. [15] pour calculer les fréquences d'une plaque encastrée-libre submergée dans l'eau en utilisant des éléments finis ordinaires [16] pour la plaque et des éléments finis cubiques à huit ou à treize nœuds pour le fluide. La fréquence fondamentale obtenue en utilisant ce modèle d'interaction continue à changer même pour des hauteurs de fluide qui dépassent deux fois la longueur de la plaque, ce qui contredit la majorité

des travaux consultés. Le même modèle a été utilisé par la suite pour étudier des plaques ayant des conditions aux limites et des rapports de formes variées [17] ainsi que des plaques carrées faites en matériaux composites [18].

Un autre modèle d'éléments finis a été développé par Aggarwal et al. [19] pour calculer les modes de vibrations d'une plaque mince simplement supportée submergée dans l'eau. Le fluide a été modélisé par un super élément fini à treize nœuds composé de huit éléments prismatiques auxquels on enlève un certain nombre de degrés de liberté. Les fréquences obtenues en utilisant ce super élément s'accordent bien avec les fréquences mesurées lors des tests expérimentaux.

Fu et Price [20] ont étudié la réponse d'une plaque encastrée-libre partiellement ou totalement submergée dans le fluide. Une méthode combinant les éléments finis et les fonctions de singularités a été utilisée. Les modes de la plaque en interaction avec le fluide sont assumés identiques à ceux des vibrations dans l'air. Plusieurs paramètres ont été étudiés dans ce travail tels que l'effet de surface libre, le niveau de fluide pour les plaques horizontales et la longueur immergée des plaques verticales. Les résultats obtenus s'accordent bien avec ceux obtenus par le modèle numérique de Lindholm [14].

La réponse dynamique d'une plaque rectangulaire en vibration dans l'air et dans le liquide a été étudiée analytiquement et expérimentalement par Haddara et Cao [21]. Ils ont discuté l'effet des conditions aux limites, de l'amortissement et de niveau de liquide en contact avec la plaque. Le facteur de masse ajoutée (FMA) a été calculé pour différents cas. Ce dernier représente le rapport entre l'énergie cinétique de la structure et celle du fluide. Ils ont conclu que l'amortissement mesuré augmente

lorsque la plaque est submergée et qu'il n'est pas très sensible au changement de niveau de fluide.

Kwak [22] a développé un modèle analytique pour étudier la réponse dynamique d'une plaque circulaire en contact avec la surface libre du fluide. La méthode de Rayleigh a été utilisée pour calculer les facteurs incrémentaux adimensionnels de la masse virtuelle ajoutée NAVMI (non-dimensionalized added virtual mass incremental) correspondant aux modes axisymétriques pour des plaques circulaires simplement supportées, encastrées et libres. Ces facteurs reflètent l'augmentation de l'énergie cinétique du système causée par la présence du fluide et ils varient en fonction de la géométrie, des propriétés du matériau et du fluide et des conditions aux limites. Les équations couplées du potentiel du fluide et de la déflexion de la plaque ont été résolues en employant les transformées de Hankel afin de tenir compte des conditions aux limites mixtes. Dans ce travail, Kwak [22] a essayé d'expliquer pourquoi il y a un écart entre les résultats expérimentaux et analytiques dans les travaux précédents [9-12]. L'effet de surface libre du fluide a été négligé dans ce travail. Kwak [23] a généralisé son premier travail [22] pour l'analyse des vibrations asymétriques des plaques circulaires. Il a calculé une nouvelle expression des facteurs NAVMI. Ces facteurs calculés dans [22, 23] peuvent être utilisés pour l'étude du comportement d'une plaque totalement submergée, en prenant le double de la valeur calculée lorsqu'un seul côté de la plaque est en contact avec le fluide.

De plus, Kwak [24] a étudié une membrane circulaire placée dans l'ouverture d'un mur rigide infini ou en contact avec la surface libre (sans mur rigide). Il a conclu que la membrane circulaire encastrée et la plaque circulaire simplement supportée ont les

mêmes facteurs NAVMI et la membrane libre et la plaque libre ont les mêmes facteurs NAVMI.

Amabili et Kwak [25] ont reproduit les mêmes conditions aux limites adoptées par Lamb et MacLachlan [9, 11] lors du développement de leurs premiers modèles analytiques. Ils ont placé la plaque circulaire en contact avec le fluide d'un seul côté dans l'ouverture d'un mur rigide plat de dimensions infinies. Les expressions analytiques des facteurs NAVMI ont été calculées pour une plaque ayant des conditions aux limites axisymétriques. Initialement, ils ont supposé que les modes à vide et en contact avec fluide restent invariables. Mais contrairement aux autres travaux, les modes de la plaque en contact avec le fluide sont recalculés par la suite en utilisant la méthode de Rayleigh-Ritz. Les résultats obtenus s'accordent bien avec ceux de Lamb et MacLachlan [9, 11] et ils ont été calculés pour des plaques simplement supportées, encastrées et libres sur toute la circonférence.

Amabili et al. [26] ont utilisé le modèle développé dans [25] pour étudier la plaque annulaire en contact avec le fluide d'un seul côté. La plaque est placée dans l'ouverture d'un mur rigide infinie. Différentes conditions aux limites à la circonférence interne ou externe de la plaque ont été étudiées. La différence entre les modes avec et sans fluide n'était pas considérable, presque dans tous les cas calculés.

La hauteur du fluide est un paramètre significatif dans le calcul des fréquences de vibration. Amabili [27] a étudié analytiquement l'effet du niveau de fluide sur le comportement des plaques circulaires et annulaires placées dans l'ouverture d'un mur rigide de dimensions infinies. Les plaques sont en contact avec un fluide incompressible d'un seul côté. Les facteurs de masse ajoutée sont calculés lorsque la limite du fluide est une surface libre ainsi que lorsqu'elle est un mur rigide. Les

modes de vibration dans le fluide sont recalculés en utilisant les fonctions de déflexion assumées et la méthode de Rayleigh-Ritz. Les résultats obtenus montrent que si la limite du fluide est une surface libre, les fréquences diminuent lorsque le niveau de fluide augmente. Le contraire est observé lorsque la surface du fluide est limitée par un mur rigide. Les facteurs NAVMI sont calculés pour des plaques annulaires encastrées sur les circonférences internes et externes et des plaques circulaires simplement supportées sur toute la circonférence.

Plus tard, Kwak et Han [28] ont fait une étude théorique afin de déterminer l'effet de la hauteur de fluide sur une plaque circulaire libre se reposant sur la surface libre d'un fluide incompressible. La limite inférieure du fluide est assumée comme un mur rigide. La théorie de Kirchhoff a été utilisée pour modéliser la plaque circulaire mince. Les résultats théoriques et expérimentaux montrent que les fréquences chutent rapidement lorsque le niveau de fluide est faible.

Kwak [29] a étudié les vibrations libres d'une plaque rectangulaire uniforme en contact avec un fluide d'un seul côté. Il a calculé la matrice de masse ajoutée pour le cas où la plaque se repose sur la surface libre du fluide sans mur rigide et pour le cas où la plaque est placée dans l'ouverture d'un mur rigide en contact avec la surface libre du fluide. Les plaques analysées sont simplement supportées ou encastrées sur les quatre côtés. La méthode des éléments aux frontières (BEM) combinée avec la méthode de Rayleigh Ritz a été utilisée afin de surmonter certaines difficultés de conditions aux limites. Une autre fois, les facteurs NAVMI calculés sont plus importants lorsque la plaque est placée dans l'ouverture d'un mur rigide que ceux du cas de la plaque se reposant sur la surface libre. Cela est dû au fait que le mur augmente l'énergie cinétique du fluide. Il a été prouvé que les modes de vibrations de

la structure en contact avec le fluide changent légèrement pour les plus basses fréquences alors que le changement est considérable pour les fréquences élevées.

Amabili et Kwak [30] ont étudié l'effet de la surface libre du fluide sur le comportement dynamique d'une plaque circulaire. Avec la présence du champ de gravité, il existe deux types d'effet de surface libre, l'effet " Sloshing" dû aux oscillations de fluide (les fréquences de ces modes de vibration sont généralement faibles) et l'effet "Bulging" dû aux vibrations de la structure. Les résultats obtenus pour des plaques circulaires simplement supportées, encastrées et libre montrent que l'effet de la surface libre est important lorsque les plaques sont très flexibles, c'est-à-dire lorsque les fréquences naturelles des plaques circulaires sont proches de celles des modes de "Sloshing" ou de "Bulging".

Cheung et Zhou [31] ont calculé les fréquences naturelles d'une plaque élastique formant la base d'un réservoir rectangulaire remplie de fluide. La limite supérieure du fluide est une surface libre. Les parois verticales du réservoir sont supposées rigides. La base du réservoir peut être une plaque élastique ou un mur rigide ayant une ouverture au milieu dans laquelle se situe la plaque rectangulaire élastique. Cela nous permet d'étudier l'effet diffusif du mouvement dans le domaine du fluide de dimensions infinies. L'effet de la surface libre de fluide n'a pas été considéré. La solution analytique a été basée sur la méthode de Ritz pour l'analyse du système fluide-structure. Le cas où la plaque est une partie intégrante du fond rigide de réservoir a été considéré, cela permet d'étudier le cas des plaques en contact avec un domaine de fluide infini. Les plaques étudiées sont simplement supportées et encastrées sur les quatre côtés.

Le cas de la plaque circulaire composant la base d'un réservoir cylindrique rigide rempli de fluide a été étudié par Cheung et Zhou [32]. L'effet de la surface libre a été considéré. Après avoir calculé la solution exacte de potentiel de vitesse, la méthode de Galerkin a été utilisée pour calculer les fréquences d'interaction fluide-structure.

Un volume de travail très important a été consacré pour mieux comprendre l'interaction des plaques avec le fluide, d'autres aspects de comportement dynamique ont été étudiés dans [33-38]. Mais malgré ça, nous constatons que la majorité des travaux concerne des plaques circulaires ayant des conditions aux limites uniformes sur toute la circonférence. Cela est lié à la facilité des solutions analytiques vu la symétrie axiale de ces structures. Peu d'efforts ont été consacrés à l'analyse des plaques rectangulaires. En plus, les modèles existants sont développés pour des conditions aux limites bien définies.

1.3.2 Réservoirs en interaction avec un fluide au repos

On rencontre dans différents domaines de l'industrie des réservoirs et des conduites qui sont utilisés en contact avec un fluide. L'importance de cette classe de structures a incité les chercheurs à fournir des efforts énormes afin de maîtriser leur comportement dynamique.

Les coques cylindriques continuent de faire l'objet de beaucoup de sujets de recherche dès les premiers travaux de Rayleigh [8] et Lamb [39] qui constituent la théorie de base du comportement d'un fluide à l'intérieur d'une coque axisymétrique, jusqu'à nos jours. Ceci revient à leur champ d'application large dans différents domaines de l'industrie.

Dans les années soixante, Berry et Reissner [40] ont étudié théoriquement le comportement d'une coque cylindrique remplie de fluide lourd sous pression en utilisant la théorie des coques peu profondes "shallow shells".

Lindholm et al. [41] ont étudié les vibrations d'une coque cylindrique totalement remplie de liquide et ils ont calculé expérimentalement les fréquences de vibration d'une coque cylindrique partiellement remplie.

Coale et Nagano [42] ont calculé les modes axisymétriques d'une coque cylindrique jointe à une coque hémisphérique, les deux remplies de liquide.

Un élément fini hybride circonférentiel a été développé par Lakis et Paidoussis [43] en se basant sur la théorie classique des coques et la méthode des éléments finis. Cet élément a été utilisé pour l'analyse du comportement dynamique d'un réservoir cylindrique vertical totalement ou partiellement rempli de liquide. L'effet de la surface libre du fluide lorsque le réservoir vertical est partiellement rempli a été étudié par Neagu et Lakis [44] en utilisant le même élément fini hybride [43].

Jain [45] a étudié les vibrations d'une coque cylindrique orthotrope partiellement remplie de liquide incompressible en tenant compte du cisaillement transversal et de l'inertie de rotation.

Une étude théorique a été faite par Amabili et Dalpiaz [46] sur le comportement dynamique d'une coque cylindrique horizontale partiellement remplie de liquide. Des mesures expérimentales ont été prises sur des réservoirs industriels pour valider le modèle théorique. La variation des fréquences en fonction du niveau de fluide a été étudiée.

Selmane et Lakis [47] ont développé un autre élément fini hybride longitudinal pour l'analyse des coques cylindriques horizontales fermées ou ouvertes totalement ou

partiellement remplies de liquide. Le même élément [47] a été utilisé par Lakis et Bursuc [48] pour étudier l'effet de la surface libre lorsque le réservoir cylindrique, horizontal, est partiellement rempli de liquide.

Pour modéliser une coque cylindrique totalement ou partiellement remplie de liquide, Mistry et Menezes [49] ont utilisé des éléments finis axisymétriques à deux nœuds pour les parois solides et des éléments finis axisymétriques à huit nœuds pour le fluide. Les équations de Navier-stockes sont utilisées pour décrire le comportement du fluide supposé visqueux et incompressible. Les résultats obtenus sont validés par des tests expérimentaux effectués dans le même travail.

L'interaction entre le fluide et la structure ne se réduit pas à un échange de l'énergie cinétique à l'interface solide-fluide, mais le fluide peut transporter cette énergie d'une paroi élastique à l'autre dans le même système. Dans ce contexte, Jeong et al. [50] ont développé un modèle analytique en utilisant la méthode de Rayleigh pour étudier les vibrations libres de deux plaques élastiques circulaires formant la base et le haut d'un réservoir cylindrique fermé ayant les parois latérales rigides. Le mouvement des deux plaques circulaires encastrées aux murs latéraux est couplé en vibration avec le fluide contenu dans le réservoir. Une analyse en éléments finis a été faite afin de valider les résultats du modèle théorique. Les modes de vibration en phase et en antiphase ont été considérés. Les résultats obtenus montrent que le modèle développé peut prédire correctement les fréquences naturelles du système couplé pour tous les modes en phase. Cependant, le modèle ne se prête pas bien pour le calcul des modes de vibration en antiphase à l'exception du premier mode (m=0).

Afin d'améliorer les fréquences des modes de vibrations latérales antiphase calculées dans [50], Jeong [51] a développé un autre modèle analytique basé sur l'expansion

des séries de Fourrier-Bessel et la méthode de Rayleigh Ritz. Les modes en phase et en antiphase sont calculés et comparés avec les résultats obtenus par éléments finis. Une bonne concordance des résultats a été éprouvée. L'influence de la hauteur de fluide entre les deux plaques sur le comportement dynamique a été étudiée. Il a été conclu que lorsque la hauteur de fluide entre les deux plaques augmente, les fréquences en phase diminuent et les fréquences en antiphase augmentent.

Le cas de deux plaques élastiques rectangulaires formant la base et le haut d'un réservoir rectangulaire rempli d'eau a été étudié analytiquement par Jeong et al. [52]. Les parois latérales du réservoir sont supposées rigides. Chaque mode de vibration en phase est une combinaison de modes de poutre et chaque mode de vibration en antiphase est approché par des polynômes satisfaisant les conditions aux limites de la plaque et de la conservation de masse de fluide. Les fréquences naturelles de couplage ont été obtenues en utilisant la méthode de Rayleigh.

Kim et Lee [53] ont analysé le comportement hydroélastique d'un réservoir rectangulaire découvert (topless) totalement rempli d'eau en se basant sur la formulation de MSC/NASTRAN DMAP. Les fréquences de ballottement de fluide ont été calculées en supposant que le réservoir est totalement rigide. En ce qui concerne les vibrations des parois, seulement la fréquence fondamentale correspondant au mode en phase et celle du mode en antiphase ont été calculées. Les fréquences de ballottement et de vibrations hydroélastiques ont été validées en les comparant à des résultats analytiques.

Bauer [54] a étudié le comportement hydroélastique d'un réservoir rectangulaire totalement ou partiellement rempli de fluide incompressible en tenant compte de l'effet de la surface libre. Le réservoir a des parois latérales rigides et une base

définie comme une plaque élastique ou une membrane flexible. Il a étudié aussi le cas où la base du réservoir est rigide et la surface libre de fluide est couverte par une plaque élastique ou par une membrane flexible. Ce travail ne concerne pas seulement le design de véhicules aérospatiaux ou aéronautiques, mais il est aussi utile pour la construction de bateaux spécialement les larges "tankers".

La réponse dynamique des réservoirs aux excitations provenant des tremblements de terre est un problème de grande importance dans le domaine du calcul des structures. Kim et Lee [53] ont développé un modèle analytique pour évaluer la réponse d'un conteneur rectangulaire flexible à des excitations séismiques horizontales et verticales. Le réservoir rectangulaire considéré est une structure symétrique ayant quatre côtés et une base fixée au sol. Les quatre parois sont modélisées comme étant des plaques à épaisseur uniforme. Le mouvement de la structure est exprimé par des modes de plaques compatibles avec les conditions aux limites du réservoir. Les équations de mouvement du système couplé sont obtenues en utilisant la méthode de Rayleigh-Ritz et les modes à vide comme fonctions assumées. L'effet de la flexibilité des murs sur le ballottement de fluide a été étudié. La pression dynamique appliquée sur les parois, les déplacements et les accélérations des parois ont été calculés.

Dans le même contexte, Koh et al. [55] ont étudié le comportement dynamique d'un réservoir rectangulaire tridimensionnel à une excitation sismique horizontale en utilisant une méthode variationnelle couplée entre la méthode des éléments finis et la méthode des éléments frontières. Le ballottement de la surface libre a été considéré comme une condition aux limites dans le modèle développé. Le mouvement de réservoir a été modélisé par la méthode des éléments finis. Le fluide contenu dans le réservoir supposé inviscide incompressible a été modélisé en utilisant la méthode des

éléments frontières. La validation du modèle a été faite en comparant les résultats obtenus avec les données expérimentales obtenues par les tests effectués sur un petit réservoir en acrylique sur une table excitatrice (Shaking-table). Ils ont conclu que le ballottement en lui-même n'est pas un paramètre significatif, mais il peut être amplifié à cause de la flexibilité des parois du réservoir.

1.3.3 Plaques et systèmes de plaques soumis aux efforts induits par un écoulement potentiel.

Les systèmes de plaques soumis aux efforts induits par le passage d'un écoulement de fluide sont utilisés dans les échangeurs de chaleur nucléaires, dans l'industrie navale ou dans le domaine de l'aérospatiale. Lorsque le fluide en contact avec la structure s'écoule à grande vitesse, le système solide risque de perdre sa stabilité de fonctionnement ou de subir la ruine totale.

Plusieurs travaux ont été faits dans ce domaine spécialement sur les systèmes ETR (engineering test reactor) dont ils se composent d'un empilement de plaques identiques parallèles. Une formulation théorique a été présentée par Miller [56] pour prédire la vitesse de fluide à laquelle un système ETR s'écroule. Il s'est basé sur l'équilibre neutre entre la pression de fluide et les forces de rappel dans le système élastique. Des formules analytiques exprimant la vitesse critique pour des systèmes de plaques parallèles courbes et plates avec différentes conditions aux limites ont été calculées. Les formules de Miller ont été validées par un travail expérimental fait par Rosenberg et Youngdahl [57].

Une étude expérimentale a été faite par Groninger et Kane [58] sur trois systèmes de plaques parallèles soumis aux efforts d'un écoulement de fluide. La vitesse critique a

été observée à un régime d'écoulement presque égal au double de la vitesse théorique de Miller. Ils ont trouvé que les plaques adjacentes vibrent selon un mode antiphase en ouvrant et en fermant alternativement les canaux d'écoulement de fluide.

Dowell [59] a examiné la stabilité d'une plaque rectangulaire soumise à un écoulement de fluide. Il a considéré un comportement non linéaire pour la plaque et il a gardé le potentiel de fluide linéaire. Il a mentionné que l'utilisation de la théorie linéaire des plaques ne peut pas être utilisée pour la modélisation de l'instabilité dynamique "flutter" puisque durant ce phénomène l'hypothèse des faibles déplacements n'est pas conservée et en plus ces déplacements peuvent causer la fatigue. Il a montré qu'il y a une divergence à une certaine vitesse, mais pas d'instabilité dynamique après la divergence.

Une étude composée d'une partie expérimentale et d'une partie théorique portant sur les différents types d'instabilité qu'une plaque faisant partie d'un système MTR a été faite par Smissaert [60, 61]. Le système est sous forme d'un empilement de plaques ayant les côtés latéraux encastrés à des murs rigides. La disposition des plaques forme des canaux dans lesquels le fluide de refroidissement s'écoule souvent à grande vitesse. Les tests expérimentaux [60] montrent que pour des vitesses de fluide faibles, la plaque se déforme comme si elle était soumise à une pression statique; cette déformation change le long de la plaque vu la redistribution de la vitesse causée par la déformation. Pour des vitesses trop élevées, des vibrations à grande amplitude ont été observées, ces amplitudes n'apparaissent pas à des vitesses inférieures à celles de Miller, cette instabilité dynamique commence en amont puis voyage le long de la plaque dans la direction de l'écoulement. Dans la partie théorique, Smissaert [61] a développé un modèle analytique d'interaction pour un système de plaques

parallèles ayant des dimensions infinies, cela permet de faire une étude bidimensionnelle du problème de fluide et de la plaque. Leur travail a montré que le système d'assemblage de plaque est caractérisé par deux vitesses, la vitesse de Miller et celle d'instabilité dynamique "Flutter". Ils ont conclu que le système peut subir plusieurs types d'instabilité. L'instabilité de classe "A" survenant à la vitesse de Miller cause une déflexion de la plaque sous forme d'onde de longueur infinie. L'instabilité de type "B" génère des ondes à faibles amplitudes traversant la plaque dans le sens de l'écoulement, le seuil de vitesse de cette instabilité est faible, cette instabilité n'est pas très dangereuse. Lorsqu'on atteint la vitesse d'instabilité dynamique "Flutter", un couplage d'instabilité de type "B" et de "Flutter" naît en amont, ce couplage génère une onde à grande amplitude se déplaçant dans le sens de l'écoulement. La vitesse de "flutter" est presque le double de la vitesse de Miller. Dans ce cas, la plaque vibre avec une onde ayant une longueur égale à trois et demie à cinq fois la largeur de la plaque. Selon les expériences, il a été constaté que le "flutter" n'est pas forcément destructif s'il est de courte durée. Par contre, s'il persiste, il devient un problème de fatigue.

Weaver et Unny [62] ont étudié la stabilité hydroélastique d'une plaque soumise aux efforts induits par le passage d'un écoulement de fluide sur la plaque. La plaque est simplement supportée en amont et en aval et sa largeur est supposée être infinie. En examinant la variation des fréquences naturelles de vibration en fonction de la vitesse d'écoulement du fluide, ils ont mentionné que pour un rapport de masse donné, la zone de stabilité neutre est suivie par une zone d'instabilité statique. Après cette étape, la plaque revient dans un petit intervalle à la stabilité neutre suivi par l'instabilité dynamique.

Une étude expérimentale sur la divergence et la post-divergence d'une plaque rectangulaire soumise à un écoulement de fluide a été faite par Gislason [63]. Il a trouvé qu'il n'y a pas d'instabilité dynamique (flutter) pour une plaque ayant le rapport de dimensions "chord-to-span" égal à deux, même si la vitesse d'écoulement dépasse deux fois la vitesse de Miller. Cette conclusion est en bon accord qualitatif avec le modèle non-linéaire de Dowell.

Afin de prévoir la nature de l'instabilité des plaques soumises à un écoulement potentiel de fluide incompressible, Kornecki et al. 1976 [64] ont développé un modèle analytique, unidimensionnel pour la plaque élastique et bidimensionnel pour l'écoulement. Les plaques étudiées sont simplement supportées et encastrées en amont et en aval. Le cas de la plaque encastrée libre a été étudié théoriquement et expérimentalement. D'après ce modèle, les conditions aux limites de la plaque déterminent la nature de l'instabilité qui pourra survenir dans la plaque. Ils ont conclu que la plaque perd sa stabilité par divergence (instabilité statique) si elle est simplement supportée ou encastrée en amont et en aval. Par contre, si elle est encastrée-libre, elle perd sa stabilité par "flutter". Ceci a été confirmé par les tests expérimentaux.

La stabilité d'une plaque et d'une coque cylindrique exposées à un écoulement de fluide a été examinée par Holmes 1977 [65] en tenant compte de la non-linéarité de la plaque et de l'amortissement. Il a reconstruit les équations différentielles de mouvement en se basant sur la théorie de Galerkin et la troncature modale. L'approche générale est illustrée en analysant un système de tube ou de plaque de deux degrés de liberté. Il a discuté certaines omissions commises par les modèles

d'interaction fluide-solide linéaires. Les résultats obtenus s'accordent bien avec ceux de Dowell [59] .

Un système de plaques parallèles et identiques (ETR) a été étudié par Davis et Kim [66]. Ils ont développé un modèle analytique pour calculer les vitesses de fluide provoquant l'instabilité du système. Les plaques ont les deux côtés parallèles au sens de l'écoulement bloqués élastiquement aux murs latéraux. Ceci permet d'étudier en même temps le cas des plaques simplement supportées et le cas des plaques encastrées en changeant un paramètre adimensionnel de la rigidité de rotation. Ils ont calculé les vitesses de divergence et d'instabilité dynamique en tenant compte de plusieurs paramètres tels que l'effet de la hauteur de fluide entre les plaques, le rapport d'aspect des plaques et les modes en phase et en antiphase. Ils ont conclu que la divergence survient à une vitesse égale à 1.2 fois la vitesse de Miller, alors que l'instabilité dynamique a lieu à une vitesse presque égale au double de la vitesse de Miller.

L'instabilité d'une plaque soumise à un écoulement potentiel de fluide dans un canal a été examinée analytiquement par Guo et Paidoussis 2000 [67]. La plaque est modélisée par des équations unidimensionnelles et le fluide par des équations bidimensionnelles. La méthode de Galerkin a été utilisée pour résoudre les équations de la plaque. La pression induite par l'écoulement potentiel est calculée en utilisant la technique des transformées de Fourrier. Des plaques ayant des conditions aux limites variées ont été étudiées. Ils ont conclu que la divergence et l'instabilité dynamique des modes couplés (coupled mode flutter) peut arriver à des plaques ayant n'importe quelle condition aux limites, alors que l'instabilité dynamique d'un

seul mode (single mode flutter) peut avoir lieu seulement si la plaque a des conditions aux limites non symétriques en amont et en aval.

Guo et Paidoussis [68] ont aussi étudié la stabilité d'un système composé d'un assemblage de plaques parallèles, en considérant la plaque une structure bidimensionnelle et le potentiel de fluide une fonction tridimensionnelle. Ils ont mentionné deux types d'instabilité, le "single mode divergence" qui survient généralement au premier mode et les modes d'instabilité dynamique couplés "coupled mode flutter". Ce type d'instabilité concerne généralement les modes adjacents. Ils ont conclu aussi que les fréquences à une vitesse donnée diminuent lorsque : a) le rapport (longueur/largeur) de la plaque augmente, b) le rapport (hauteur du canal/largeur de la plaque) diminue et c) lorsque le rapport de masse diminue. Ils ont conclu que l'amortissement a un effet faible sur les fréquences et la vitesse critique, mais il change le comportement de post-divergence et des modes couplés dynamiquement instables "coupled modes flutter".

1.4 BUT DU TRAVAIL

En examinant l'étude bibliographique, nous pouvons dire que des efforts énormes ont été fournis pour maîtriser le comportement des plaques et coques en interaction avec le fluide. Mais malgré ça, la majorité des travaux reste limitée à l'analyse des structures ayant une symétrie axiale (coques cylindriques et plaques circulaires) ou une direction privilégiée selon laquelle les caractéristiques géométriques et les conditions aux limites sont uniformes.

Nous proposons dans cette thèse le développement d'un élément fini solide-fluide capable de prédire le comportement dynamique des plaques et coques à vide et en

interaction avec un fluide se trouvant autour et/ou dans la structure. Le but ultime de ce travail est de pouvoir modéliser les aubes d'une turbine hydraulique.

Les principales étapes de ce travail sont :

I) Le calcul des matrices élémentaires de masse et de rigidité ainsi que la pression hydrodynamique correspondant à chaque élément fini solide-fluide de plaque. Ces matrices seront utilisées pour calculer les modes et les fréquences de vibrations lorsque la plaque rectangulaire est : a) en vibration dans l'air, b) en contact avec la surface libre d'un fluide d'un seul côté, c) totalement submergée et d) verticalement immergée partiellement dans le fluide. Le modèle d'éléments finis développé couvre toutes les conditions aux limites de la plaque rectangulaire et du fluide.

II) Transformation des matrices élémentaires de masse, de rigidité et de masse ajoutée à un repère global défini pour toute la structure afin de pouvoir modéliser les coques cylindriques, les réservoirs rectangulaires et les systèmes de plaques radiales et parallèles.

III) le développement d'un élément fini solide-fluide pour modéliser une plaque rectangulaire soumise aux efforts induits par le passage d'un écoulement potentiel de fluide. En plus des matrices de masse et de rigidité solide, il est nécessaire de calculer des matrices supplémentaires qui représentent les forces d'inertie, de Coriolis et centrifuge exprimées respectivement en fonction de l'accélération, de la vitesse et du déplacement transversal de la plaque.

IV) L'écriture d'un code de calcul en langage FORTRAN pour calculer et assembler les matrices élémentaires correspondant aux milieux solide et fluide, introduire les conditions aux limites et calculer les modes et les fréquences de vibration, en se basant sur les modèles analytiquement développés en utilisant le logiciel Maple.

V) La validation des modèles développés en comparant les résultats obtenus avec ceux calculés par d'autres modèles déjà existants, que ce soit analytiques, numériques ou expérimentaux.

Cette étude fait partie d'un projet de recherche dont le but ultime est de modéliser une aube de turbines d'Hydro-Québec soumise à un effort induit par un écoulement de fluide turbulent. Certaines applications sont faites dans ce travail pour bien comprendre et pour prévoir l'influence de tous les paramètres qui peuvent altérer le comportement dynamique de structures plus complexes.

CHAPITRE II

HYBRID METHOD FOR VIBRATION ANALYSIS OF RECTANGULAR PLATES

Y. Kerboua [a], A.A. Lakis [a], M. Thomas [b], L. Marcouiller [c]

[a] *Mechanical Engineering Dept., École Polytechnique of Montréal, Canada*

[b] *Mechanical Engineering Dept., École de Technologie Supérieure, Canada*

[c] *Institut de Recherche d'Hydro Québec, Montréal (Québec) Canada*

Received 12 June; received in revised form 17 September2006; accepted 17 September2006

2.1 Abstract

This paper presents a semi-analytical approach for the dynamic analysis of rectangular plates. The mathematical model is developed using a combination of the finite element method and Sanders' shell theory. The in-plane, membrane displacement components are modelled by bilinear polynomials and the out-of-plane, normal to mid-surface displacement component is modelled by an exponential function that represents a general form of the exact solution of the equations of motion. The mass and stiffness matrices are then determined by exact analytical integration to establish the plate's dynamic equations. The effect of various geometrical parameters and boundary conditions on the dynamic responses of the rectangular plates has been explored in this

work. The results are in satisfactory agreement with those of experiments and other theories.

2.2 INTRODUCTION

Plates and shells constitute important components of complex structures and are of great significance to modern construction engineering, aerospace and aircraft structures, nuclear power plant components and naval structures to name a few. Knowledge of dynamic characteristics, i.e. natural frequencies and mode shapes, of structural components is therefore of great interest in the study of structural responses to various excitations.

Plates have been the subject of a great many research studies over the past century. The dynamic study of the plates backs to the eighteenth century when Euler presented the first mathematical model of plate membrane theory. One half century later, Lagrange developed differential equations describing free vibrations of plates. Navier presented an exact method to calculate the frequency and vibrational mode shapes of rectangular plates for certain boundary conditions. Kirchhoff [1] is considered the founder of the modern theory for plates in which the both membrane and bending effects are taken into consideration. Love applied Kirchhoff's theory to thick plates. Evolution in design of modern aircraft and space vehicles encouraged researchers to take further steps. Numerous computational approaches have been implemented for dynamic analysis of complex structures following the introduction of the finite element method and fast growth of high-speed computing capability.

Vibration analysis of rectangular plates has received considerable attention and has been the subject of numerous studies, many of which are well documented by Leissa [2]. A variety of computational methods have been employed successfully for such analysis. These include the Rayleigh method, Ritz variational methods, methods of finite strips and spline strip, the series expansion and methods of differential quadrature. However, alternative approaches might provide more accurate results for plate analysis. The dynamic behaviour of thin rectangular plates with partial intermediate supports, which are used in many engineering structures such as solar panels supported at a few points, is studied by Escalante et al. [3]. Free vibration of isotropic and orthotropic rectangular plates with mixed boundary conditions is investigated by Hsu [4].

Composite plates are increasingly used in a variety of modern engineering fields. They offer a unique advantage compared to isotropic materials because of their high strength- and stiffness-to-weight ratios. Recent developments of intelligent systems incorporating piezoelectric and piezomagnetic materials have also stimulated considerable studies on the dynamic behaviour of rectangular plates made of non-isotropic materials. Piezoelectric materials have the ability to convert energy from one form to another (magnetic to electric, electric to mechanical etc.).

Improving performance, reducing operation costs, lowering noise and other undesirable phenomenon and enhancing the structural reliability of complex and advanced structures are necessary to meet the challenges of the new century. A representative mathematical model is the prime factor in obtaining satisfactory modal definition for a structure. If the model is of poor quality, mathematical rigor in solving the equations of motion will not

improve results. The stiffness and mass distribution as well as the boundary conditions are basic factors that should be given careful consideration in the synthesis of the mathematical model for structural dynamic analysis. Neglecting any of these parameters may result in a model that is not dynamically similar to the actual structure. It can be concluded that the accuracy of solutions reached by the finite element displacement formulation depends on the functions developed to accurately model the deformation modes of the structure.

Based on the aforementioned discussions, the need for accurate and efficient methods for static/and dynamic analysis of rectangular plates is apparent. To achieve the desired solution accuracy a new model is developed here, which is a combination of classical finite element method and Sanders' shell theory [5]. The displacement functions of plate are derived using the equations of motion. Then, mass and stiffness matrices required by the finite element method are determined by precise analytical integration to form the dynamic equations. These are applied to the dynamic analysis of rectangular plates and generate satisfactory results when compared to experimental data and results from other theoretical approaches.

2.3 METHOD OF ANALYSIS

The geometry of the mean surface of the rectangular plate and the co-ordinate systems used for this analysis are shown in Figure 2.1.B. A typical four-node element and nodal degrees of freedom are shown in Figure 2.1.A. Each node has six degrees of freedom consisting of in-plane and out-of-plane displacement components and their spatial

derivatives (see Figure 2.1.A). To develop the equilibrium equations for rectangular plates, the Sanders' equations for cylindrical shells are used assuming the radius to be infinite, $\theta = y$ and $rd\theta = dy$. Both membrane and bending effects are taken into account in this theory. It is worthy to note that Sanders' shell theory is based on Love's first approximation theory but leads to zero strains for the case of rigid body motion. The developed displacement functions therefore satisfy the convergence criteria for the proposed finite element.

2.3.1 Equilibrium Equations and Displacement Functions

The equilibrium equations of a rectangular plate according to Sanders' theory can be written as a function of displacement components with respect to the reference surface:

$$P_{22}\frac{\partial^2 V}{\partial y^2} + P_{21}\frac{\partial^2 U}{\partial x \partial y} + P_{33}\left(\frac{\partial^2 U}{\partial x \partial y} + \frac{\partial^2 V}{\partial x^2}\right) = 0 \tag{2.1}$$

$$P_{11}\frac{\partial^2 U}{\partial x^2} + P_{12}\frac{\partial^2 V}{\partial x \partial y} + P_{33}\left(\frac{\partial^2 V}{\partial x \partial y} + \frac{\partial^2 U}{\partial y^2}\right) = 0 \tag{2.2}$$

$$P_{44}\frac{\partial^4 W}{\partial x^4} + \frac{\partial^4 W}{\partial x^2 \partial y^2}(P_{45} + P_{54} + 2P_{66}) + P_{55}\frac{\partial^4 W}{\partial y^4} = 0 \tag{2.3}$$

where U and V represent the in-plane displacement components of the middle surface in X and Y directions, respectively. W is the transversal displacement of the middle surface. P_{ij} (i=1,6 j=1,6) are the coefficients of elasticity matrix.

Note that both circumferential and longitudinal hybrid elements used in dynamic analysis of vertical [6] and horizontal [7] open cylindrical shells were developed based on exact solution of the equilibrium equations. This approach resulted in a very precise element which leads to fast convergence and less numerical difficulties from the computational point of view. This encouraged us to develop a new element using the same approach for dynamic analysis of rectangular plates. Generally, exact solution of the equilibrium equations for the case of rectangular plates is difficult. To overcome this we present the in-plane membrane displacement components in terms of bilinear polynomials and the out-of-plane bending displacement component by an exponential function. Hence, the displacement field may be defined as follows:

$$U(x,y,t) = C_1 + C_2\frac{x}{A} + C_3\frac{y}{B} + C_4\frac{xy}{AB} \tag{2.4}$$

$$V(x,y,t) = C_5 + C_6\frac{x}{A} + C_7\frac{y}{B} + C_8\frac{xy}{AB} \tag{2.5}$$

$$W(x,y,t) = \sum_{i=9}^{24} C_j e^{i\pi\left(\frac{x}{A}+\frac{y}{B}\right)} e^{i\omega t} \tag{2.6}$$

where A and B are the plate dimensions in X and Y directions. "ω" is the natural frequency of the plate (rad/sec) and "*i*" is a complex number. Finally, C_j are unknown constants.

Solution of bending equation (2.3) is presented as follows:

$$W(x,y,t)=\sum_{q=0}^{3}\frac{A_q}{q!}\left(\frac{x}{A}\right)^q\sum_{p=0}^{3}\frac{B_p}{p!}\left(\frac{y}{B}\right)^p \tag{2.7}$$

Equation (2.7) can be developed in Taylor's series as [8]:

$$\begin{aligned}W(x,y,t)=C_9+C_{10}\frac{x}{A}+C_{11}\frac{y}{B}+C_{12}\frac{x^2}{2A^2}+C_{13}\frac{xy}{AB}+C_{14}\frac{y^2}{2B^2}+C_{15}\frac{x^3}{6A^3}+C_{16}\frac{x^2y}{2A^2B}+C_{17}\frac{xy^2}{2AB^2}+\\ C_{18}\frac{y^3}{6B^3}+C_{19}\frac{x^3y}{6A^3B}+C_{20}\frac{x^2y^2}{4A^2B^2}+C_{21}\frac{xy^3}{6AB^3}+C_{22}\frac{x^3y^2}{12A^3B^2}+C_{23}\frac{x^2y^3}{12A^2B^3}+C_{24}\frac{x^3y^3}{36A^3B^3}\end{aligned} \tag{2.8}$$

The displacement field may be rewritten in the form of matrix relations as follows:

$$\begin{Bmatrix}U\\V\\W\end{Bmatrix}=[R]\{C\} \tag{2.9}$$

with:

$$\{C\}=\{C_1,C_2,\ldots,C_{24}\}^T \tag{2.10}$$

where [R] is a matrix of order (3× 24) given in the Appendix and {C} is the unknown constants' vector. The components of this last vector can be determined using twenty-four degrees of freedom and are presented for a plate element in Figure 1A. The nodal displacement vector is given as:

$$\{\delta\}=\left\{\{\delta_i\}^T,\{\delta_j\}^T,\{\delta_k\}^T,\{\delta_l\}^T\right\}^T \tag{2.11}$$

Each node, i.e. "node i", possesses a nodal displacement vector composed of the following terms:

$$\{\delta_i\} = \{U_i, V_i, W_i, \partial W_i/\partial x, \partial W_i/\partial y, \partial^2 W_i/\partial x \partial y\}^T \tag{2.12}$$

where U_i and V_i are in-plane displacement components and W_i represent the displacement component normal to the middle surface. By introducing equations (2.4) to (2.6) into relation (2.12), the nodal displacement vector can be defined as:

$$\{\delta\} = [A]\{C\} \tag{2.13}$$

The unknown constants will then be replaced by the generalized displacement vector of a quadrilateral finite element. Multiplying equation (2.13) by $[A]^{-1}$ results in the following expression:

$$\{C\} = [A]^{-1}\{\delta\} \tag{2.14}$$

The terms of matrix $[A]^{-1}$ are given in Appendix A. Substituting equation (2.14) into equation (2.9), the displacement field may be expressed using the following relation:

$$\begin{Bmatrix} U \\ V \\ W \end{Bmatrix} = [R][A]^{-1}\{\delta\} = [N]\{\delta\} \tag{2.15}$$

where matrix [N] of order (3 ×24) is the displacement shape function of the finite element.

2.3.2 Kinematic relations

The strain-displacement relations for rectangular plates are given as [5]:

$$\begin{Bmatrix} \varepsilon_x \\ \varepsilon_y \\ 2\varepsilon_{xy} \\ \kappa_x \\ \kappa_x \\ \kappa_{xy} \end{Bmatrix} = \begin{Bmatrix} \partial U/\partial x \\ \partial V/\partial y \\ \partial V/\partial x + \partial U/\partial y \\ -\partial^2 W/\partial x^2 \\ -\partial^2 W/\partial y^2 \\ -2\partial^2 W/\partial x \partial y \end{Bmatrix} \tag{2.16}$$

Substituting the displacement components defined in equation (2.15) into the strain-displacement relationship (2.16), one obtains an expression for the strain vector as a function of nodal displacements.

$$\{\varepsilon\} = [Q][A]^{-1}\{\delta\} = [B]\{\delta\} \tag{2.17}$$

where matrix [Q], of order (6 ×24), is given in the Appendix.

2.3.3 Constitutive Equations

The stress-strain relationships for an anisotropic rectangular plate are defined as follows:

$$\{\sigma\} = [P]\{\varepsilon\} \tag{2.18}$$

where [P] is the elasticity matrix. The elements of the elasticity matrix for an isotropic plate where no bending-membrane coupling is present are defined as:

$$\begin{gathered} P_{11} = P_{22} = D \quad P_{44} = P_{55} = K \quad P_{12} = P_{21} = \nu D \quad P_{45} = P_{54} = \nu K \\ P_{33} = (1-\nu)D/2 \quad P_{66} = (1-\nu)K/2 \end{gathered} \tag{2.19}$$

where

$$K = \frac{Eh^3}{12(1-\nu^2)} \tag{2.20}$$

$$D = \frac{Eh}{1-\nu^2}$$

E is the modulus of elasticity, ν is Poisson's coefficient and h is the plate thickness. Substituting equation (2.17) into (2.18) results in the following expression for the stress vector as a function of nodal displacements.

$$\{\sigma\} = [P][B]\{\delta\} \tag{2.21}$$

The mass and stiffness matrices for one finite element can be expressed as:

$$[k]^e = \iint_A [B]^T [P][B] dA \tag{2.22.a}$$

$$[m]^e = \rho_s h \iint_A [N]^T [N] dA \tag{2.22.b}$$

where dA is the element surface area, ρ is the material density and [P], [N] and [B] are defined in equations (2.15, 2.17 and 2.19). Substituting these into equation (2.22) and carrying out analytical integration with respect to x and y, we obtain:

$$[k]^e = \left[[A]^{-1}\right]^T \left(\int_0^{y_e} \int_0^{x_e} [Q]^T [P][Q] dx dy \right) [A]^{-1} \tag{2.23.a}$$

$$[m]^e = \rho h \left[[A]^{-1}\right]^T \left(\int_0^{y_e} \int_0^{x_e} [R]^T [R] dx dy \right) [A]^{-1} \tag{2.23.b}$$

where x_e and y_e are dimensions of an element according to X and Y coordinates. These integrals are calculated using Maple mathematical software.

2.4 ANALYSIS OF FREE VIBRATIONS

The rectangular plate is subdivided into finite elements, each of which is a smaller rectangular plate (see Figure 2.1.A). The positions of the nodal points of these elements are chosen in such a way that the local and global coordinates are parallel. The global matrices are obtained by superimposing the mass and stiffness matrices for each individual element. After applying the boundary conditions, these matrices are reduced

to square matrices of order NDF*N-NC where NDF, N and NC are, respectively; the number of degrees of freedom at each node, the number of node and the imposed constraint. The equations of motion will be:

$$[M]\{\ddot{\Delta}\}+[K]\{\Delta\}=0 \tag{2.24}$$

where;

$$\{\Delta\}=\{\delta_1 \quad \delta_2 \quad \cdots \quad \delta_N\} \tag{2.25}$$

[M] and [K] are the global mass and stiffness matrices. An in-house computer code has been developed to calculate the structural matrices of each element on the basis of these theoretical equations. The global matrices are obtained by superimposing the mass and stiffness matrices for each element. Once the global mass and stiffness matrices are constructed, equation (2.24) can be solved to obtain 6*(N)-NC eigenvalues and eigenvectors. Using equation (2.24) and definition (2.25), one may obtain a typical eigenvalues problem, written as:

$$\det[[K]-\omega^2[M]]=0 \tag{2.26}$$

2.5 RESULTS AND DISCUSSIONS

2.5.a Convergence Test

The precision of the finite element method depends on the number of elements used to discretize the physical problem. The first set of calculations is therefore to determine the

requisite number of elements for a precise determination of the natural frequencies. The variation of the first five frequencies versus the number of finite elements is plotted in Figure 2.2, and shows the minimum required number of elements to assure fast convergence in determining both low and high frequencies. Eight elements are sufficient to calculate the two first modes, whereas for other modes convergence requires at least twenty-five elements. This number of elements required by the proposed method is much lower than that of other existing approaches. In all of the following examples sixty-four elements are used, which assures that the results will be independent of mesh size.

2.5.b Numerical examples

The next example involves the determination of natural frequencies of a steel rectangular plate which is simply supported on its four sides (Figure 2.3-A). The mechanical and geometrical parameters used are given as:

$E = 196$ GPa, $\rho = 7860$ kg/m^3, $h = 2.54$ mm, $\nu = 0.3$, $A = 609.6$ mm and $B = 304.8$ mm

The first six natural frequencies are listed in Table 2.1 along with analytical results and ANSYS output data. It can be seen that the present method gives fairly good results compared to the exact solution and the commercial finite element code ANSYS.

The method is then applied to calculate the dynamic responses of a steel cantilever plate fixed at one short side (see Figure 2.3-D). The following dimensions are used for this plate:

$A = 70.1$ mm, $B = 130$ mm and $h = 1.35$ mm

The results are listed in Table 2.2 and compared with Martin's theory (2.10), Grinsted's experiment (2.11) as well as ANSYS and NASTRAN eigenvalues. As may be seen, results obtained are in good agreement with other theories and experiments. The first four mode shapes of this plate are presented in Figure (2.4).

The next example presents modal analysis of a steel plate simply supported at its two short sides. The same material and geometrical parameters as the second example are used in this case, and the results are presented in Table 2.3.

The natural frequencies of a cantilever square plate are calculated for this example and compared with those of other theories in Table 2.4. The plate dimensions are:

$$A = B = 10\text{m and } h = 0.238\text{m}$$

According to the listed results in Table 2.4, we can conclude that the dynamic responses of rectangular and square plates are computed with a relatively good precision. As the last example demonstrates, the non-dimensional natural frequency parameter λ can be obtained using this theory for various boundary conditions and plate dimension ratios (A/B) and compared with corresponding results presented by Leissa [9].

$$\lambda = \omega * A^2 / \sqrt{\rho h / K}$$

where:

$$K = Eh^3 / 12(1 - \nu^2)$$

The results are presented in Tables 2.5 through 2.12.

2.6 CONCLUSIONS

The objective of this paper is to develop a new finite element approach to predict the dynamic behaviour of thin rectangular plates for later use in dynamic analysis of these structures in contact with fluid. A structural finite element is developed using a bilinear polynomial for displacement in the in-plane directions and an exponential function for transversal displacement. This method combines the advantage of finite element analysis and the precision of an exact formulation for displacement functions derived from thin plate theory. The natural frequencies obtained by this method are in good agreement with those of other theories and experiments. An advantage of this method is its applicability to both uniform and non-uniform isotropic and anisotropic plates with any combination of boundary conditions. Convergence of the method was established and the natural frequencies were obtained for various boundary conditions and different modes. These results were compared with those of other selected theories and were found to be in satisfactory agreement.

The present approach supports future research for dynamic analysis of plates which are in contact with a stationary fluid or subjected to a flowing fluid (laminar or turbulent). Examples of industrial applications include; dynamic analysis of steam generator components, a set of parallel plates, or turbine blades that may be subjected to sinusoidal /or random excitations due to fluid forces. Further work is now under way to apply this theory to dynamic analysis of rectangular plates submerged in fluid.

2.7 REFERENCES

1. Kirchhoff, G., "UG berdas Gleichgewicht und die Bewegung einer elastischen Scheibe", Mathematical Journal (Crelle1s Journal) 40, pp. 51-58, 1850.
2. Leisaa, A.W., "Vibration of plates", NASA, SP-160, 1969.
3. Escalante, M. R., Rosales, M. B. and Filipich, C. P., "Natural frequencies of thin rectangular plates with partial intermediate supports", Latin American Applied Research, 34, pp. 217-224, 2004.
4. Hsu. M. H., "Vibration analysis of isotropic and orthotropic plates with mixed boundary conditions", Tamkang Journal of Science and Engineering, 6 (4), 217-226, 2003.
5. Sanders, J. L., "An improved first approximation theory for thin shell", NASA TR-24, 1959.
6 Lakis, A. A. and Paidoussis, M. P., "Free vibration of cylindrical shells partially filled with liquid", Journal of Sound and Vibration, 19 (1), pp1-15, 1971.
7 Lakis, A. A. and Selmane, A. "Vibration analysis of anisotropic open cylindrical shells subjected to a flowing fluid", Journal of Fluids and Structures, 11, pp111–134, 1997.
8 Charbonneau, E. and Lakis, A. A., "Semi-analytical shape functions in the finite element analysis of rectangular plates", Journal of Sound and vibration, 242 (3), 3, pp427-443, 2001.
9. Leissa, A. W., "The free vibration of rectangular plates", Journal of Sound and Vibration, 13 (3), pp. 257-293, 1973.

10. Martin, A. I., "On the vibration of Cantilever Plate", Quarterly Journal of Mechanics and Applied Mathematics, 9, pp94-102, 1956.

11. Grinsted, B., "Nodal pattern analysis", Proceedings of Institution of Mechanical Engineers, 166, pp309-326, 1952.

12. Gorman, D. J., "Free vibration analysis of rectangular plates", Amsterdam, Elsevier, 1982.

13. Lindholm, U.S., Kana, D. D., Chu, W. H. and Abramson, H.N., "Elastic vibration characteristics of cantilever plates in water", Journal of Ship Research, pp11-22, 1965.

14. Fu, Y., and PRICE, W. G., "Interactions between a partially or totally immersed vibrating cantilever plate and the surrounding fluid", Journal of Sound and Vibration, 118 (3), pp495-513, 1987.

2.8 APPENDIX

This appendix contains some equations, which are referred to in this work.

$$[R]=\begin{bmatrix}
1 & \frac{x}{A} & \frac{y}{B} & \frac{xy}{AB} & 0 & 0 & 0 & 0 & 0 & 0 & 0 & 0 & 0 & 0 & 0 & 0 & 0 & 0 & 0 & 0 & 0 & 0 & 0 & 0 & 0 \\
0 & 0 & 0 & 0 & 1 & \frac{x}{A} & \frac{y}{B} & \frac{xy}{AB} & 0 & 0 & 0 & 0 & 0 & 0 & 0 & 0 & 0 & 0 & 0 & 0 & 0 & 0 & 0 & 0 & 0 \\
0 & 0 & 0 & 0 & 0 & 0 & 0 & 0 & 1 & \frac{x}{A} & \frac{y}{B} & \frac{x^2}{2A^2} & \frac{xy}{AB} & \frac{y^2}{2B^2} & \frac{x^3}{6A^3} & \frac{x^2y}{2AB} & \frac{xy^2}{2AB^2} & \frac{y^3}{6B^3} & \frac{x^3y}{6A^3B} & \frac{x^2y^2}{4A^2B^2} & \frac{xy^3}{6AB^3} & \frac{x^3y^2}{12A^3B^2} & \frac{x^2y^3}{12A^2B^3} & \frac{x^3y^3}{36A^3B^3}
\end{bmatrix}$$

$$[Q]=\begin{bmatrix}
0 & \frac{1}{A} & 0 & \frac{y}{AB} & 0 & 0 & 0 & 0 & 0 & 0 & 0 & 0 & 0 & 0 & 0 & 0 & 0 & 0 & 0 & 0 & 0 & 0 & 0 & 0 & 0 \\
0 & 0 & 0 & 0 & 0 & 0 & \frac{1}{B} & \frac{x}{AB} & 0 & 0 & 0 & 0 & 0 & 0 & 0 & 0 & 0 & 0 & 0 & 0 & 0 & 0 & 0 & 0 & 0 \\
0 & 0 & \frac{1}{B} & \frac{x}{AB} & 0 & \frac{1}{A} & 0 & \frac{y}{AB} & 0 & 0 & 0 & 0 & 0 & 0 & 0 & 0 & 0 & 0 & 0 & 0 & 0 & 0 & 0 & 0 & 0 \\
0 & 0 & 0 & 0 & 0 & 0 & 0 & 0 & 0 & 0 & 0 & \frac{1}{A^2} & 0 & 0 & \frac{x}{A^3} & \frac{y}{A^2B} & 0 & 0 & \frac{xy}{A^3B} & \frac{y^2}{2A^2B^2} & 0 & \frac{xy^2}{2A^3B^2} & \frac{y^3}{6A^2B^3} & \frac{xy^3}{6A^3B^3} \\
0 & 0 & 0 & 0 & 0 & 0 & 0 & 0 & 0 & 0 & 0 & 0 & \frac{1}{B^2} & 0 & 0 & \frac{x}{AB^2} & \frac{y}{B^3} & 0 & \frac{x^2}{2A^2B^2} & \frac{xy}{AB^3} & \frac{x^3}{2A^3B^2} & \frac{x^2y}{6A^2B^3} & \frac{x^3y}{6A^2B^3B^2} \\
0 & 0 & 0 & 0 & 0 & 0 & 0 & 0 & 0 & 0 & 0 & 0 & \frac{2}{AB} & 0 & 0 & \frac{2x}{A^2B} & \frac{2y}{A^2B} & 0 & \frac{x^2}{A^3B} & \frac{2xy}{A^2B^2} & \frac{y^2}{AB^3} & \frac{x^2y}{A^3B^2} & \frac{xy^2}{A^2B^3} & \frac{x^2y^2}{2A^3B^3}
\end{bmatrix}$$

Non-zero elements of matrix $[A]^{-1}$

$A^{-1}(1,1) = 1, A^{-1}(2,1) = A^{-1}(2,7) = -\frac{A}{x_c}$, $A(3,1) = -A(3,19) = -\frac{B}{y_c}$, $A^{-1}(4,1) = -A^{-1}(4,7)) = A^{-1}(4,13) = -A^{-1}(4,19) = -\frac{AB}{x_c y_c}$

$A^{-1}(5,2) = 1$, $A^{-1}(6,2) = -A^{-1}(6,8) = -\frac{A}{x_c}$, $A^{-1}(7,2) = -\frac{B}{y_c}$, $A^{-1}(7,20) = -\frac{AB}{x_c y_c}$,

$A^{-1}(8,2) = -A^{-1}(8,8) = A^{-1}(8,14) = A^{-1}(8,14) = -A^{-1}(8,20) = \frac{AB}{x_c}$, $A^{-1}(9,3) = 1$, $A^{-1}(10,4) = A$, $A^{-1}(11,5) = B$,

$A^{-1}(12,3) = -A^{-1}(12,9) = -\frac{6A^2}{x_c^2}$, $A^{-1}(12,4) = 2A^{-1}(12,10) = -4\frac{A^2}{x_c}$, $A^{-1}(13,6) = A.B$, $A^{-1}(14,3) = -A^{-1}(14,21) = -12\frac{A^3}{x_c^2}$,

$A^{-1}(14,5) = A^{-1}(14,3) = 2A^{-1}(14,23) = 2\frac{B^2}{y_c}$, $A^{-1}(15,3) = -A^{-1}(15,9) = 12\frac{A^3}{x_c^3}$, $A^{-1}(15,4) = A^{-1}(15,10) = \frac{6A^3}{x_c^2}$,

$A^{-1}(16,5) = -A^{-1}(16,11) = -6\frac{A^2B}{x_c^2}$, $A^{-1}(16,6) = A^{-1}(16,12) = -2\frac{A^2B}{x_c}$, $A^{-1}(17,4) = -A^{-1}(17,22) = -6\frac{AB^2}{y_c^2}$,

$$A^{-1}(17,6) = A^{-1}(17,24) = -\frac{4AB^2}{y_e},\ A^{-1}(18,3) = -A^{-1}(18,21) = 12\frac{B^3}{y_e^3},\ A^{-1}(18,5) = A^{-1}(18,23) = 6\frac{B^3}{y_e^2},$$

$$A^{-1}(19,5) = A^{-1}(19,11) = 12\frac{A^3B}{x_e^3},\ A^{-1}(19,6) = A^{-1}(19,12) = 6\frac{BA^3}{x_e^2},$$

$$A^{-1}(20,4) = 2A^{-1}(20,10) = -A^{-1}(20,16) = -A^{-1}(20,22) = 24\frac{B^2A^2}{xy_e^2},$$

$$A^{-1}(20,5) = -\frac{2A^{-1}(20,9)}{3} = -A^{-1}(20,11) = -2A^{-1}(20,17) = 2A^{-1}(20,23) = 24\frac{A^2B^2}{x_e^2y_e},$$

$$A^{-1}(20,6) = 2A^{-1}(20,12) = 4A^{-1}(20,18) = \frac{2}{3}A(20,24) = 16\frac{A^2B^2}{x_ey_e},\ A^{-1}(21,4) = -A^{-1}(21,22) = 12\frac{AB^3}{y_e^3},$$

$$A^{-1}(21,6) = A^{-1}(21,24) = 6\frac{AB^3}{y_e^2},$$

$$A^{-1}(22,3) = -A^{-1}(22,9) = A^{-1}(22,15) = -A^{-1}(22,21) = 72\frac{AB^2}{x_e^3y_e^2},\ A^{-1}(22,4) = A^{-1}(22,10) = -A^{-1}(22,16) = -A^{-1}(22,22) = -36\frac{A^3B^3}{x_e^2y_e^2},$$

$$A^{-1}(22,5) = -A^{-1}(22,11) = -2A^{-1}(22,17) = 2A^{-1}(22,23) = -48\frac{A^3B^2}{x_e^3y_e},$$

$$A^{-1}(22,6) = A^{-1}(22,12) = 2A^{-1}(22,18) = 2A^{-1}(22,24) = -24\frac{A^3B^2}{x_e^2y_e}$$

$$A^{-1}(23,3) = -A^{-1}(23,9) = A^{-1}(23,15) = A^{-1}(23,21) = 72\frac{A^2B^3}{x_e^2y_e^2},$$

$$A^{-1}(23,4) = 2A^{-1}(23,10) = -2A^{-1}(23,16) = -A^{-1}(23,22) = -48\frac{A^2B^3}{x_ey_e^3},$$

$$A^{-1}(23,5) = -A^{-1}(23,11) = -A^{-1}(23,17) = A^{-1}(23,23) = -36\frac{A^2B^3}{x_e^2y_e^2},$$

$$A^{-1}(23,6) = 2A^{-1}(23,12) = 2A^{-1}(23,18) = A^{-1}(23,24) = -24\frac{A^2B^3}{x_ey_e^2}$$

$$A^{-1}(24,3) = -A^{-1}(24,9) = A^{-1}(24,15) = -A^{-1}(24,21) = 144\frac{A^3B^3}{x_e^3y_e^3},$$

$$A^{-1}(24,4) = A^{-1}(24,10) = -A^{-1}(24,16) = -A^{-1}(24,22) = 72\frac{A^3B^3}{x_e^2y_e^3}$$

$$A^{-1}(24,5) = -A^{-1}(24,11) = -A^{-1}(24,17) = A^{-1}(24,23) = -72\frac{A^3B^3}{x_e^2y_e^2},\quad A^{-1}(24,6) = A^{-1}(24,12) = A^{-1}(24,18) = A^{-1}(24,24) = 36\frac{A^3B^3}{x_e^2y_e^2}$$

2.9 NOMENCLATURE

U, V	Displacement components of the plate reference surface in the X and Y directions, respectively
W	Normal displacement of the plate middle surface
A, B	Plate side lengths along the X and Y directions, respectively
h	Plate thickness
U_i, V_i	Nodal displacement components at node *i* in X and Y directions, respectively
W_i	Normal displacement of the plate at node *i*
$W_{i,x}$; $iW_{i,y}$	The first derivative of the plate's normal displacement with respect to X and Y, respectively, at node *i*
$W_{i,xy}$	Crossed derivative of the plate's normal displacement with respect to X and Y
ω	Natural frequency of the plate in rad/sec
X, Y, Z	Orthogonal coordinate system
ρ	Material density
D	Membrane rigidity $Eh/(1-\nu^2)$
K	Bending rigidity $Eh^3/12(1-\nu^2)$
i	Complex number i^2=-1
C_i	Constants defined by equation (2.10)
ν	Poisson's coefficient
E	Modulus of elasticity
P_{ij}	Material elasticity matrix's components defined by equation (2.19)
x_e, y_e	Length of the element along the X and Y axes, respectively
n, m	Mode shape number in X and Y directions, respectively
λ	Nondimensional frequency parameter of the plate
[R]	Matrix (3 × 24), defined by equation (2.9)
$\{C\}$	Vector of unknown constants defined by equation (2.10)

$\{\delta\}$	Nodal displacement vector defined by equation (2.11)
[A]	Matrix (24 × 24) defined by equation (2.13)
$[N]$	Shape function matrix (3 × 24) defined by equation (2.15)
$\{\varepsilon\}$	Deformation vector
$[Q]$	Matrix (6 × 24) defined by equation (2.17)
[B]	Shape function derivative defined by equation (2.17)
$\{\sigma\}$	Stress vector
$[P]$	Elasticity matrix (6 × 6)
$[k]^e$	Stiffness matrix of an element (24 × 24)
$[m]^e$	Mass matrix of an element (24 × 24)
$\{F\}^e$	Nodal force vector
$[M]$	Global mass matrix
$[K]$	Global stiffness matrix
$\{\delta_T\}$	Global displacement vector
$\{\delta_{0T}\}$	Vector of mode shape amplitudes

Table 2.1: Natural frequency (Hz) of a plate, simply supported at its four sides (Figure 2.3.A)

Mode	Present element	ANSYS (Shell63)	Analytical Solution [9]	Error % Present element & ANSYS	Error % Present element & Ref. [9]
1	82.93	80.99	83.5	2.39	.68
2	133.44	129.33	133.61	3.17	.127
3	213.72	209.86	217.12	1.83	1.56
4	275.27	275.02	283.9	0.09	3.03
5	315.52	322.51	334	2.16	5.53
6	331.41	322.51	334	2.75	0.77

Table 2.2: Natural frequency (Hz) of a cantilever rectangular plate fixed at one short side (Figure 2.3-D), *m* and *n* are the modes number in the X and Y direction, respectively, see Figure (2.4)

(n, m)	Martin [10]	Experiment Grinsted [11]	NASTRAN (QUAD4)	ANSYS (Shell 63)	Present Theory
(1,1)	69.5	64	67.6	66.17	66.16
(1,2)	436	405	416.4	412.35	413.05
(1,3)	1220	1120	1151	1155.6	1159.04
(3,1)	1610	1606	1474	1558.2	1557.62
(3,2)	2260	N.A. (1)	1996	2155.5	2132.17

(1) Not available

Table 2.3: Natural frequency (Hz) of a plate simply supported at two-opposite-short sides (Figure 2.3.B), *m* and *n* are the mode numbers in X and Y direction, respectively

(n, m)	Analytical Solution [9]	ANSYS (Shell63)	Present Theory
(1,1)	16.70	15.65	15.67
(2,1)	66.80	63.47	63.61
(3,1)	150.3	143.94	144.34
(1,3)	178.5	173.18	181.54

Table 2.4: Natural frequency (Hz) of a cantilever square plate (Figure 2.3.D)

Mode	1	2	3	4	5
Mode Shape	Bending	Torsion	Bending	Bending	Torsion
Present Theory	12.929	31.7	79.55	101.121	115.34
Gorman [12]	12.92	31.21	78.77	101.407	114.10
Lindholm [13]	12.30	30.78	75.46	99.84	110.57
Fu et Price [14]	12.94	31.73	79.80	101.16	115.61

Table 2.5: Dimensionless frequencies variation of clamped rectangular plate (CCCC, See Figure 2.3.E) as a function of side-length ratio

CCCC	λ							
	A/B=0.4		A/B=1			A/B=2.5		
n-m	Present Theory	Leissa [9]	n-m	Present Theory	Leissa [9]	n-m	Present Theory	Leissa [9]
1-1	23.31	23.64	1-1	35.45	35.99	1-1	145.72	147.8
1-2	26.69	27.81	2-1	72.03	73.41	2-1	166.84	173.85
1-3	33.48	35.44	1-2	72.03	73.41	3-1	209.31	221.54
1-4	44.21	46.70	2-2	103.70	108.27	4-1	276.35	291.89
1-5	59.01	61.55	3-1	129.41	131.64	5-1	368.83	384.71
2-1	62.24	63.1	1-3	130.28	132.24	1-2	389.04	394.37

Table 2.6: Dimensionless frequencies variation of clamped-free rectangular plate (CCFF, See Figure 2.3-F) as a function of side-length ratio

CCFF	λ							
	A/B=0.4		A/B=1			A/B=2.5		
n-m	Present Theory	Leissa [9]	n-m	Present Theory	Leissa [9]	n-m	Present Theory	Leissa [9]
1-1	3.96	3.98	1-1	6.92	6.94	1-1	24.77	24.91
1-2	7.10	7.15	2-1	23.96	24.03	2-1	44.38	44.719
1-3	12.99	13.10	1-2	26.50	26.68	3-1	81.22	81.879
1-4	21.81	21.84	2-2	47.23	47.78	4-1	136.31	136.52
2-1	22.70	22.89	1-3	62.77	63.03	1-2	141.89	143.1
2-2	25.96	26.50	3-1	65.65	65.83	2-2	162.30	165.63

Table 2.7: Dimensionless frequencies variation of a free rectangular plate (FFFF, See Figure 2.3.G) as a function of side-length ratio

FFFF	λ							
	A/B=0.4		A/B=1			A/B=2.5		
n-m	Present Theory	Leissa [9]	n-m	Present Theory	Leissa [9]	n-m	Present Theory	Leissa [9]
1-3	3.431	3.46	2-2	13.48	13.48	3-1	21.47	21.64
2-2	5.28	5.28	1-3	19.61	19.78	2-2	33.01	33.05
1-4	9.56	9.62	3-1	24.31	24.43	4-1	59.78	60.13
2-3	11.34	11.43	3-2	34.79	35.02	3-2	70.90	71.48
1-5	18.72	18.79	2-3	34.79	35.02	5-1	117.04	117.45
2-4	18.94	19.1	4-1	61.32	61.52	4-2	118.42	119.38

Table 2.8: Dimensionless frequencies variation of a simply supported-free rectangular plate (SFFF, See Figure 2.3.H) as a function of side-length ratio

SFFF	λ							
	A/B=0.4		A/B=1			A/B=2.5		
n-m	Present Theory	Leissa [9]	n-m	Present Theory	Leissa [9]	n-m	Present Theory	Leissa [9]
1-2	2.69	2.69	1-2	6.64	6.64	2-1	14.82	14.93
1-3	6.47	6.50	2-1	14.93	15.02	1-2	16.23	16.24
1-4	12.58	12.63	2-2	25.38	25.49	3-1	48.57	48.84
2-1	15.29	15.33	1-3	25.98	26.12	2-2	51.97	52.08
2-2	17.33	17.51	3-1	48.49	48.71	3-2	77.52	97.22
1-5	21.57	21.69	2-3	50.43	50.84	4-1	96.73	102.34

Table 2.9: Dimensionless frequencies variation of a clamped-free rectangular plate (CCCF, See Figure 2.3.I) as a function of side-length ratio

CCCF	λ							
	A/B=0.4		A/B=1			A/B=2.5		
n-m	Present Theory	Leissa [9]	n-m	Present Theory	Leissa [9]	n-m	Present Theory	Leissa [9]
1-1	22.53	22.57	1-1	23.94	24.02	1-1	37.41	37.65
1-2	24.12	24.62	1-2	39.49	40.03	2-1	75.84	76.40
1-3	28.01	29.24	2-1	63.40	63.49	3-1	134.42	135.15
1-4	35.05	37.05	1-3	75.42	76.76	1-2	150.52	152.47
1-5	45.77	48.28	2-2	79.10	80.71	2-2	186.81	193.01
2-1	60.41	61.92	2-3	112.38	116.8	4-1	213.61	213.74

Table 2.10: Dimensionless frequencies variation of a clamped-free rectangular plate (CFFF, See Figure 2.3.J) as a function of side-length ratio

CFFF	λ							
	A/B=0.4		A/B=1			A/B=2.5		
n-m	Present Theory	Leissa [9]	n-m	Present Theory	Leissa [9]	n-m	Present Theory	Leissa [9]
1-1	3.49	3.51	1-1	3.47	3.49	1-1	3.42	3.45
1-2	4.75	4.78	1-2	8.51	8.524	1-2	17.97	17.98
1-3	8.03	8.11	2-1	21.35	21.42	2-1	21.43	21.56
1-4	13.75	13.88	1-3	27.14	27.33	2-2	49.41	57.45
2-1	21.67	21.63	2-2	30.96	31.11	3-1	57.27	60.58
2-2	22.92	23.73	2-3	53.82	54.44	3-2	106.03	106.54

Table 2.11: Dimensionless frequencies variation of a simply supported-free rectangular plate (SSSF, See Figure 2.3.K) as a function of side-length ratio

SSSF	λ							
	A/B=0.4		A/B=1			A/B=2.5		
n-m	Present Theory	Leissa [9]	n-m	Present Theory	Leissa [9]	n-m	Present Theory	Leissa [9]
1-1	10.15	10.12	1-1	11.68	11.68	1-1	18.79	18.8
1-2	12.90	3.057	1-2	27.54	27.75	2-1	50.54	50.54
1-3	18.42	18.83	2-1	41.29	41.19	3-1	100.35	100.23
1-4	26.86	27.55	2-2	58.24	59.06	1-2	109.08	110.22
1-5	38.39	39.33	1-3	61.14	61.86	2-2	143.96	147.63
2-1	39.75	39.61	3-1	90.72	90.29	4-1	169.83	169.10

Table 2.12: Dimensionless frequencies variation of a simply supported-free rectangular plate (SFSF, See Figure 2.3.L) as a function of side-length ratio

SFSF	λ							
	A/B=0.4		A/B=1			A/B=2.5		
n-m	Present Theory	Leissa [9]	n-m	Present Theory	Leissa [9]	n-m	Present Theory	Leissa [9]
1-1	9.81	9.76	1-1	9.65	9.63	1-1	9.49	9.48
1-2	11.05	11.03	1-2	16.13	16.13	1-2	33.62	33.62
1-3	14.89	15.06	1-3	36.44	36.72	2-1	38.46	38.36
1-4	21.28	21.70	2-1	39.14	38.94	2-2	75.17	75.20
1-5	30.49	31.17	2-2	46.78	46.73	3-1	87.44	86.96
2-1	39.48	39.23	2-3	69.73	70.74	3-2	127.52	130.35

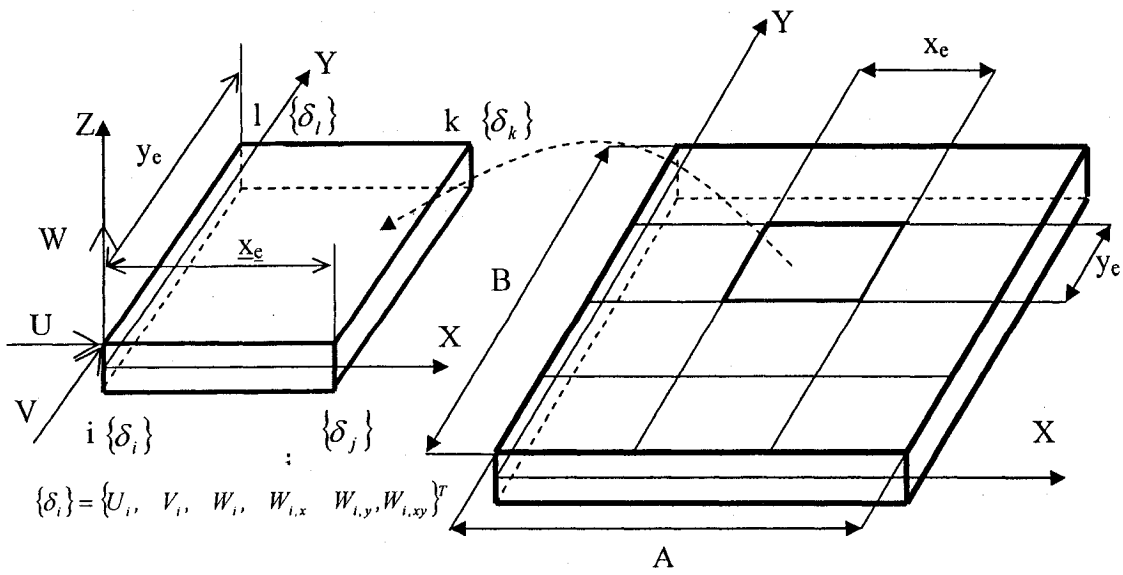

(A) (B)

Figure 2.1: A: Finite element discretization of a rectangular plate

B: Geometry and displacement field of a typical element

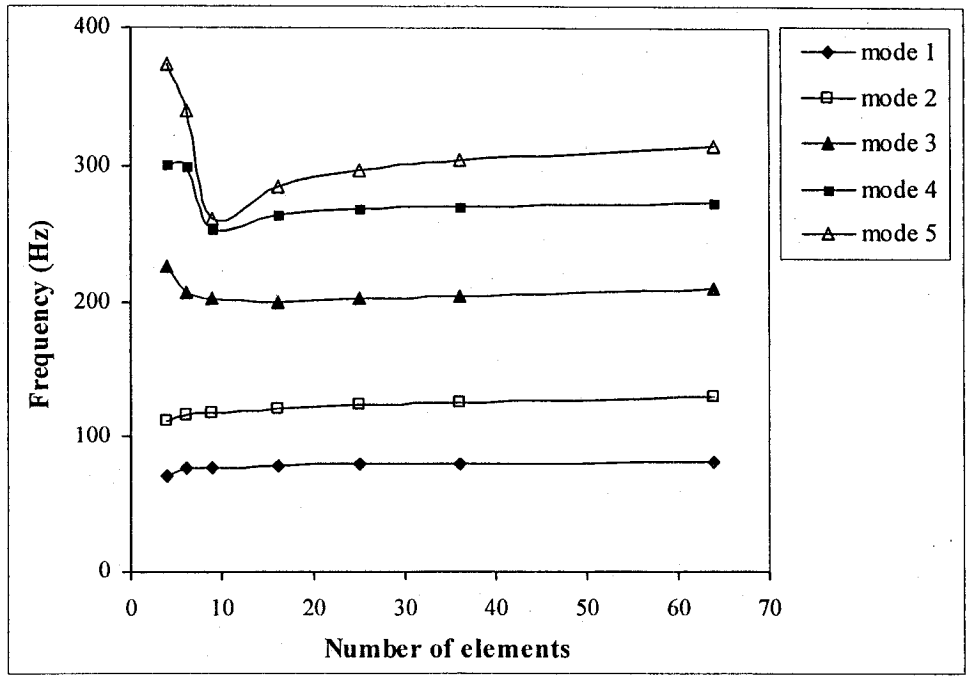

Figure 2.2: The first five natural frequencies of a four-side simply supported plate as a function of number of elements

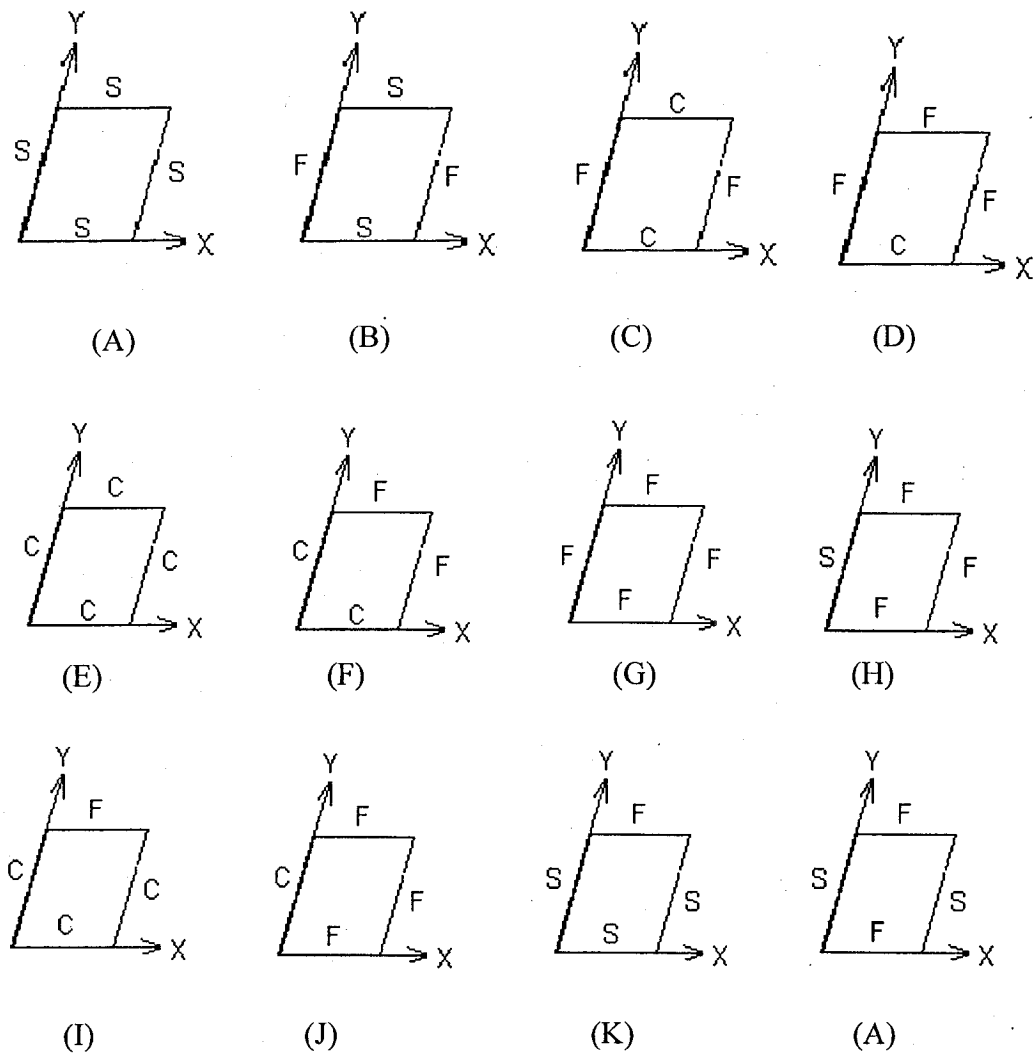

Figure 2.3: Boundary conditions of the plate

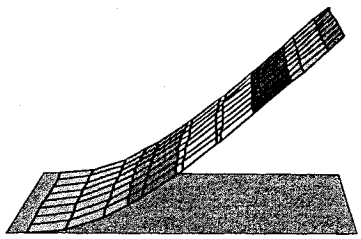

66.16 Hz

(n,m)=(1,1)

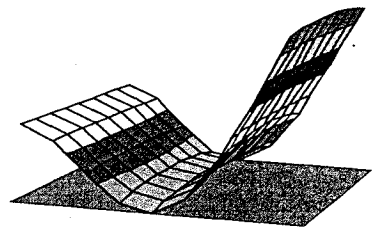

413.05 Hz

(n,m)=(1,2)

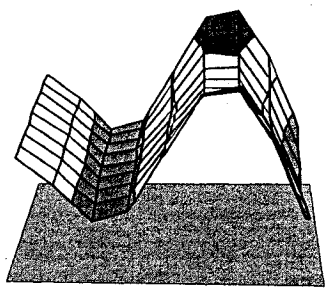

1159.04 Hz

(n,m) = (1,3)

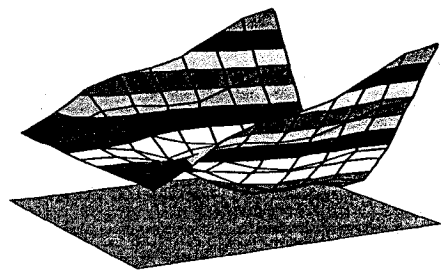

1557 Hz

(n,m) = (3,1)

Figure 2.4: The first four mode shapes of a cantilever rectangular plate

CHAPITRE III

VIBRATION ANALYSIS OF RECTANGULAR PLATES COUPLED WITH FLUID

Y. Kerboua[1], A.A. Lakis[1], M. Thomas[2], L. Marcouiller[3]

1. *Mechanical Engineering Dept., École Polytechnique of Montréal, Canada*
2. *Mechanical Engineering Dept., École de Technologie Supérieure, Canada*
3. *Institut de Recherche d'Hydro Québec, Montréal (Québec) Canada*

(Soumis pour publication dans **International Journal for Numerical Methods in Fluids)**

3.1 Abstract

The analytical approach developed in this paper applies to vibration analysis of rectangular plates coupled with fluid. This case is representative of certain key components of complex structures used in industries such as aerospace, nuclear and naval. The plates can be partially or totally submerged in fluid or floating on its free surface. The mathematical model for the structure is developed using a combination of the finite element method and Sanders' shell theory. The in-plane and out-of-plane displacement components are modelled using bilinear polynomials and exponential functions, respectively. The general equations of the displacement functions are derived from the equilibrium equations of a rectangular plate. The mass and stiffness matrices are then determined by exact analytical integration. The velocity potential and

Bernoulli's equation are adopted to express the fluid pressure acting on the structure. The product of the pressure expression and the developed structural shape function is integrated over the structure-fluid interface to assess the virtual added mass due to the fluid. Variations of physical and geometrical parameters such as structure and fluid boundary conditions and fluid level are considered in the calculation of the natural frequencies and mode shapes of the coupled fluid-structure system. The results are in close agreement with both experimental results and theoretical results using other analytical approaches.

3.2 INTRODUCTION

Plates have wide applications in areas such as; modern construction engineering, aerospace and aeronautical industries, aircraft construction, shipbuilding, rocket construction, and the components of nuclear power plants. It is therefore very important that the static and dynamic behaviour of plates when subjected to different loading conditions be clearly understood so that they may be safely used in these industrial applications.

It is well known that the natural frequencies of structures in contact with fluid are different from those in vacuo. As an elastic structure vibrates in a fluid, the fluid immediately surrounding the structure is set into motion and the structure will radiate sound waves into the far field. Therefore, the prediction of natural frequency changes due to the presence of the fluid is important for designing structures which are in contact with or immersed in fluid. This problem is referred to as the fluid-structure interaction

problem. Understanding this interaction is basic to a sound design of floating structure, i.e. ships and offshore structures. The presence of the fluid modifies the natural frequencies, damping ratios and mode shapes of the structure compared to those calculated in vacuo. In general, the effect of the fluid force on the structure is represented as added mass, which lowers the natural frequency of the structure from that which would be measured in a vacuum. This decrease in the natural frequency of the fluid-structure system is caused by increasing the kinetic energy of the coupled system without a corresponding increase in strain energy. The ratio between the kinetic energy of the water to that of the structure is referred to as the added virtual mass incremental (AVMI) factor.

An extraordinary amount of effort has been carried out in recent years on problems involving dynamic interaction between an elastic structure and a surrounding fluid medium. Consider the elastic vibration of a plate in a fluid medium. The high frequency oscillations are of primary concern in problems of noise or sound as the added pressure loading on the plate is mainly proportional to velocity while the effects of added mass are negligible. On the other hand, there are many interests in which knowledge of the structural vibration or low frequency characteristics of such elastic plates is of importance, and in this case the effects of the added mass dominate. Some examples include; flutter and other hydro-elastic problems of hydrofoils and control surfaces, impact forces on anti-pitching and shock loads on bottom plating and protuberances and even the singing of propeller blades.

Vibration analysis of rectangular plates has received considerable attention and has been the subject of numerous studies, many of which are well documented by Leissa [1]. Kirchhoff [2] is considered the founder of modern theory for plates in which both membrane and bending effects are taken into consideration. Love applied Kirchhoff's theory to the thick plates. Evolution in design of modern aircraft and space vehicles encouraged researchers to take some steps forward. Numerous computational approaches have been implemented for dynamic analysis of complex structures following the introduction of the finite element method and high-speed computers.

Lamb [3] calculated the first bending mode shape of a circular plate fixed at its circumference, in contact with fluid. The developed method was based on a calculation of the kinetic energy of the fluid. The resonant frequency was determined using Rayleigh's method. Powell and Robert [4] experimentally verified Lamb's results. They underlined that their frequencies were slightly higher than those of Lamb.

Lindholm et al. [5] carried out an extensive experimental study of the response of cantilever plates in air and in contact with fluid. The plates with different aspect ratios, and thickness were horizontally and vertically placed or inclined. The results were compared with theoretical predictions based on simple beam theory and thin plate theory and the chordwise hydrodynamic strip theory. An empirical correction factor was introduced to achieve good theoretical and experimental correlation. The free surface and partial submergence effects were also investigated. It was concluded that; *i)* natural frequencies of the plate decreased and node lines of mode shapes shifted when it was submerged in fluid and *ii)* the added mass factor changed with the submerged depth of

the plate, but significant change occurred only when the submerged depth was less than about one half span length of the plate.

Volcy et al. [6] reported the measured results of the fundamental natural frequencies of vertical cantilever plates partially and totally submerged in fluid. The experimental results were compared with results obtained using fluid finite element method. Values for the fundamental natural frequency obtained using the finite element method were about 15% larger than those measured in the experiments. This discrepancy was due to a difference in boundary conditions applied between the experiment and the theoretical approach. In some cases however, good agreement was reported between the measured and calculated values for the fundamental natural frequencies.

Fu and Price [7] studied the vibration responses of cantilevered vertical and horizontal plates partially or totally immersed in fluid. It was assumed that the plates vibrated in a semi-infinite fluid medium. The vibrational mode shapes of plates in vacuo and in contact with fluid were considered the same. They used a combination of finite element method and a singularity distribution panel approach to analyze the dynamic responses of plates in vacuo and also to determine the hydrodynamic coefficients for each element that is in contact with fluid. They also examined the effect of the free surface.

Kwak and Kim [8] studied the free vibrations of a floating circular plate in contact with the free surface of fluid. They only considered the axisymmetric vibrations. Their work was initiated due to the obvious contradictions between previous analytical and experimental results. They calculated the non-dimensional added virtual mass incremental (NAVMI) factors for clamped, simply supported and free plates. They

compared their results with other results from the literature. They indicated that their results could be extended to the case of submerged plates by multiplying the calculated values of the non-dimensional added virtual mass incremental (NAVMI) factors by a factor of 2.

The discrepancy in results of Lamb [3] and Powell et al. [4] is explained later by Kwak [23] on the basis of differences in the boundary conditions between the two methods. An analytical solution for a simply supported plate, carrying a free surface liquid with reservoir conditions at the edges is presented by Soedel [9].

The natural frequencies of annular plates in contact with a fluid on one side are theoretically obtained using the added mass approach [10]. The fluid is assumed to be incompressible and inviscid and the velocity potential describes its irrotational motion. The Hankel transfer is applied to solve the coupled fluid-structure system.

Haddara and Cao [11] investigated (analytically and experimentally) dynamic responses of plates submerged in water under various boundary conditions. They provided an analytical added mass factor depending on the height of the free surface and the depth of water under the plate. An approximate expression for the evaluation of the modal added mass has been derived.

Amabili et al. [12] studied the vibrations of circular plates resting on a sloshing liquid free surface. The fully coupled problem between sloshing modes of the free surface and bulging modes of the plate is solved using the Rayleigh-Ritz method.

The effect of free surface waves on free vibrations of circular plates resting on a free surface was studied by Amabili et al. [13]. The solution was achieved using a

combination of the perturbation technique and the Hankel transformation method, which produces two dual integral equations of Titchmarsh type. The fluid was considered inviscid and incompressible and the velocity potential describes its irrotational motion. The Kirchhoff theory of plates is used to model the elastic thin plate.

The hydroelastic vibrations of free edge circular plates are studied by Kwak and Han [14]. They adopted the Hankel transformation method, which resulted in dual integral equations. The solution of dual integral equations is calculated numerically using Fourier-Bessel series. The fluid is assumed to be inviscid and incompressible. The Kirchhoff theory of plates is used to model the elastic thin plate. The effects of fluid level on the dynamic behaviour of circular plates are also studied in this work.

Improving performance, reducing operation cost, lowering noise and other undesirable phenomenon and enhancing the structural reliability of complex and advanced structures are emerging challenges of the new century. The integrity of the mathematical model is a major factor in obtaining a satisfactory modal definition for the structure. If the model is of poor quality, mathematical rigor in the solution of the equations of motion will not improve results. The stiffness and mass distribution as well as the boundary conditions are basic parameters that should be given careful consideration in the synthesis of the mathematical model for structural dynamic analysis. Neglecting any of these parameters may result in a model that is not dynamically similar to the actual structure. It is therefore concluded that the accuracy of solutions reached by the finite element displacement formulation depends on the assumed functions used to model the deformation modes of structure. On the basis of aforementioned discussions, the need

for accurate and efficient methods for static/and dynamic analysis of rectangular plates becomes apparent. To meet requirements related to accuracy of the solution, a new model is developed; a combination of classical finite element method and Sanders' shell theory [15]. The displacement functions of the plate are derived using the equations of motion. Then, mass and stiffness matrices required by the finite element method are determined by precise analytical integration. The velocity potential and Bernoulli's equation are adopted to express the fluid pressure acting on the structure. The product of the pressure expression and the developed structural shape function is integrated over the structure-fluid interface to assess the virtual added mass due to the fluid.

3.3 STRUCTURAL MODEL

The geometry of plate reference surface and the co-ordinate systems used for this analysis are shown in Figure (3.1.B). A typical four-node element and nodal degrees of freedom are also shown in Figure (3.1.A). Each node has six degrees of freedom that represent the in-plane and out-of-plane displacement components and their spatial derivatives (see Figure 3.1.A). To develop the equilibrium equations of the rectangular plates, the Sanders' equations for cylindrical shells are used assuming the radius to be infinite, $\theta = y$ and $rd\theta = dy$. Both membrane and bending effects are taken into account in this theory.

3.3.1 Equilibrium Equations and Displacement Functions

The equilibrium equations of a rectangular plate as a function of displacement components of the reference surface resulting from the Sanders' theory can be written as follows:

$$P_{22}\frac{\partial^2 V}{\partial y^2}+P_{21}\frac{\partial^2 U}{\partial x\partial y}+P_{33}\left(\frac{\partial^2 U}{\partial x\partial y}+\frac{\partial^2 V}{\partial x^2}\right)=0 \tag{3.1}$$

$$P_{11}\frac{\partial^2 U}{\partial x^2}+P_{12}\frac{\partial^2 V}{\partial x\partial y}+P_{33}\left(\frac{\partial^2 V}{\partial x\partial y}+\frac{\partial^2 U}{\partial y^2}\right)=0 \tag{3.2}$$

$$P_{44}\frac{\partial^4 W}{\partial x^4}+\frac{\partial^4 W}{\partial x^2\partial y^2}(P_{45}+P_{54}+2P_{66})+P_{55}\frac{\partial^4 W}{\partial y^4}=0 \tag{3.3}$$

where U and V represent the in-plane displacement components of the middle surface in X and Y directions, respectively. W is the transversal displacement of the middle surface. P_{ij} (i=1,6 j=1,6) are the coefficients of elasticity matrix.

It is noted that both the circumferential and longitudinal hybrid elements used in dynamic analysis of the vertical and horizontal open cylindrical shells, respectively [16, 17] were developed based on exact solution of the equilibrium equations of cylindrical shells. This approach resulted in a very precise element that leads to a fast convergence and less numerical difficulties from the computational point of view. It encouraged us to develop a new finite element using the same approach for dynamic analysis of rectangular plates. Generally, exact solution of the equilibrium equations is difficult for the case of rectangular plates. To avoid this issue, we present the membrane

displacement components in terms of bilinear polynomials and the bending displacement component by an exponential function. Hence, the displacement field may be defined as follows:

$$U(x,y,t)=C_1+C_2\frac{x}{A}+C_3\frac{y}{B}+C_4\frac{xy}{AB} \tag{3.4}$$

$$V(x,y,t)=C_5+C_6\frac{x}{A}+C_7\frac{y}{B}+C_8\frac{xy}{AB} \tag{3.5}$$

$$W(x,y,t)=\sum_{i=9}^{24}C_j e^{i\pi\left(\frac{x}{A}+\frac{y}{B}\right)}e^{i\omega t} \tag{3.6}$$

where A and B are the plate dimensions in X and Y directions, respectively. "ω" is the natural frequency of the plate (rad/sec). "*i*" is a complex number and C_j are unknown constants. Solution of bending equation (3.3) is presented as follows:

$$W(x,y,t)=\sum_{q=0}^{3}\frac{A_q}{q!}\left(\frac{x}{A}\right)^q\sum_{p=0}^{3}\frac{B_p}{p!}\left(\frac{y}{B}\right)^p \tag{3.7}$$

Equation (3.7) can be developed in Taylor's series as [18]:

$$\begin{aligned}W(x,y,t)=&C_9+C_{10}\frac{x}{A}+C_{11}\frac{y}{B}+C_{12}\frac{x^2}{2A^2}+C_{13}\frac{xy}{AB}+C_{14}\frac{y^2}{2B^2}+C_{15}\frac{x^3}{6A^3}+C_{16}\frac{x^2y}{2A^2B}+C_{17}\frac{xy^2}{2AB^2}+\\&C_{18}\frac{y^3}{6B^3}+C_{19}\frac{x^3y}{6A^3B}+C_{20}\frac{x^2y^2}{4A^2B^2}+C_{21}\frac{xy^3}{6AB^3}+C_{22}\frac{x^3y^2}{12A^3B^2}+C_{23}\frac{x^2y^3}{12A^2B^3}+C_{24}\frac{x^3y^3}{36A^3B^3}\end{aligned} \tag{3.8}$$

The displacement field may be rewritten in the form of matrix relations as follows:

$$\begin{Bmatrix} U \\ V \\ W \end{Bmatrix} = [R]\{C\} \tag{3.9}$$

with:

$$\{C\} = \{C_1, C_1, \ldots, C_{24}\}^T \tag{3.10}$$

Where [R] is a matrix of order (3× 24) given in Appendix I and {C} is the vector for the unknown constant. The components of this last vector can be determined using twenty-four degrees of freedom presented for a plate element as shown in Figure (1A). The nodal displacement vector is given as:

$$\{\delta\} = \{\{\delta_i\}^T, \{\delta_j\}^T, \{\delta_k\}^T, \{\delta_l\}^T\}^T \tag{3.11}$$

Each node, i.e. "node i", possesses a nodal displacement vector composed of the following terms:

$$\{\delta_i\} = \{U_i, V_i, W_i, \partial W_i/\partial x, \partial W_i/\partial y, \partial^2 W/\partial x \partial y\}^T \tag{3.12}$$

where U_i and V_i are in-plane displacement components and W_i represent the displacement components normal to the middle surface. By introducing equations (3.4, 3.5 and 3.8) into relation (3.11), the elementary displacement vector can be defined as:

$$\{\delta\} = [A]\{C\} \tag{3.13}$$

The vector $\{C\}$ will be then replaced by the generalized displacement vector of a quadrilateral finite element. Multiplying equation (3.13) by $[A]^{-1}$ results in the following relation:

$$\{C\} = [A]^{-1}\{\delta\} \tag{3.14}$$

The terms of matrix $[A]^{-1}$ are given in [19]. Introducing equation (3.14) into equation (3.9), the displacement field may be described by the following relation:

$$\begin{Bmatrix} U \\ V \\ W \end{Bmatrix} = [R][A]^{-1}\{\delta\} = [N]\{\delta\} \tag{3.15}$$

where matrix [N] of order (3 ×24) is the displacement shape function of the finite element.

3.3.2 Kinematic Relations

Strain-displacement relations for the rectangular plates are given as [15]:

$$\begin{Bmatrix} \varepsilon_x \\ \varepsilon_y \\ 2\varepsilon_{xy} \\ \kappa_x \\ \kappa_x \\ \kappa_{xy} \end{Bmatrix} = \begin{Bmatrix} \partial U/\partial x \\ \partial V/\partial y \\ \partial V/\partial x + \partial U/\partial y \\ -\partial^2 W/\partial x^2 \\ -\partial^2 W/\partial y^2 \\ -2\partial^2 W/\partial x \partial y \end{Bmatrix} \tag{3.16}$$

Substituting the displacement components defined in equation (3.15) into the strain-displacement relationship (3.16), one obtains an expression for the strain vector as a function of nodal displacements.

$$\{\varepsilon\} = [Q][A]^{-1}\{\delta\} = [B]\{\delta\} \tag{3.17}$$

where matrix [Q], of order (6 ×24), is given in Appendix I.

3.3.3 Constitutive Equations

The stress-strain relationship of an anisotropic rectangular plate is defined as follows:

$$\{\sigma\} = [P]\{\varepsilon\} \tag{3.18}$$

where [P] is the elasticity matrix. The elements of the elasticity matrix for an isotropic plate, where no bending-membrane coupling is present, are defined as:

$$P_{11} = P_{22} = D \quad P_{44} = P_{55} = K \quad P_{12} = P_{21} = \nu D \quad P_{45} = P_{54} = \nu K$$
$$P_{33} = (1-\nu)D/2 \quad P_{66} = (1-\nu)K/2 \tag{3.19}$$

where;

$$K = \frac{Eh^3}{12(1-\nu^2)} \tag{3.20}$$

$$D = \frac{Eh}{1-\nu^2}$$

E is the modulus of elasticity, ν is the Poisson's coefficient and h is the plate thickness. Substituting equation (3.17) into equation (3.18) results in the following expression for the stress vector as a function of nodal displacements.

$$\{\sigma\} = [P][B]\{\delta\} \tag{3.21}$$

The mass and stiffness matrices for one finite element can be expressed as:

$$[k_s]^e = \iint_A [B]^T [P][B] dA \tag{3.22a}$$

$$[m_s]^e = \rho_s h \iint_A [N]^T [N] dA \tag{3.22b}$$

where dA is the element surface area and ρ is the material density and [P], [N] and [B] are defined in equations (3.15, 3.17 and 3.19); substituting them into equation (3.22) and carrying out the analytical integration with respect to x and y, we obtain:

$$[k_s]^e = [[A]^{-1}]^T \left(\int_0^{y_e} \int_0^{x_e} [Q]^T [P][Q] dxdy \right) [A]^{-1} \tag{3.23.a}$$

$$[m_s]^e = \rho h [[A]^{-1}]^T \left(\int_0^{y_e} \int_0^{x_e} [R]^T [R] dxdy \right) [A]^{-1} \tag{3.23.b}$$

where x_e and y_e are dimensions of an element according to the X and Y coordinates, respectively. These integrals are calculated using Maple mathematical software.

3.4 DYNAMIC BEHAVIOUR OF FLUID-STRUCTURE INTERACTION

The dynamic responses of a plate are affected by the presence of a fluid media. Generally, the fluid pressure acting upon the structure is expressed as a function of displacement and its derivatives i.e. velocity and acceleration. These three terms represent, respectively, the stiffness, Coriolis and inertia effects of the fluid forces. The fluid force matrices are superimposed onto the structural matrices to form the dynamic equations of a coupled fluid-structure system. The global equations for motion of a rectangular plate interacting with a fluid can be represented as follows [17]:

$$([M_s] - [M_f]) \{\ddot{\delta}_T\} - [C_f] \{\dot{\delta}_T\} + ([K_s] - [K_f]) \{\delta_T\} = \{F\} \tag{3.24}$$

where subscripts '*s*' and '*f*' refer to the shell in *vacuo* and fluid filled respectively. $[M_s]$ and $[K_s]$ are the global mass and stiffness matrices of the plate in *vacuo*. They have been previously defined by equation (3.23) for an element. $[M_f]$, $[C_f]$ and $[K_f]$, represents respectively the inertial, Coriolis and centrifugal force of the fluid; $\{\delta_T\}$ is the displacement vector, and $\{F\}$ represents the external forces. After applying the boundary conditions, these matrices are reduced to square matrices of order $6*(N)$-NC, where N and NC are the number of node and the restrictions imposed.

3.4.1 Fluid Modelling

The mathematical model which is developed is based on the following hypotheses: (i) the fluid flow is potential; (ii) vibration is linear; (iii) since the flow is inviscid, there is no shear and the fluid pressure is purely normal to the plate wall; and (v) the fluid is incompressible. Based on the aforementioned hypothesis the potential function, which satisfies the Laplace equation, is expressed in the Cartesian coordinate system as:

$$\nabla^2\phi = \frac{\partial^2\phi}{\partial x^2} + \frac{\partial^2\phi}{\partial y^2} + \frac{\partial^2\phi}{\partial z^2} = 0 \tag{3.25}$$

The Bernouilli equation for the case of stationary fluid when the fluid velocity is null, is expressed as:

$$\left.\frac{\partial \phi}{\partial t}+\frac{P}{\rho_f}\right|_{z=0}=0 \tag{3.26}$$

Equation (3.26) results in the following expression for pressure:

$$P|_{z=0}=-\rho_f \left.\frac{\partial \phi}{\partial t}\right|_{z=0} \tag{3.27}$$

The following separate variable relation is assumed for the velocity function:

$$\phi(x,y,z,t)=F(z)S(x,y,t) \tag{3.28}$$

where F(z) and S(x.y,z) are two separate functions to be determined.

The impermeability condition of the structure surface requires that the out-of-plane velocity component of the fluid on the plate surface should match the instantaneous rate of change of the plate displacement in the transversal direction. This condition implies a permanent contact between the plate surface and the peripheral fluid layer, which should be:

$$\left.\frac{\partial \phi}{\partial z}\right|_{z=0}=\frac{\partial W}{\partial t} \tag{3.29}$$

The following expression may be defined by introducing equation (3.28) into equation (3.29)

$$S(x,y,t)=\frac{1}{dF(0)/dz}\frac{\partial W}{\partial t} \tag{3.30}$$

Then, substituting equation (3.30) into relation (3.28) results in the following expression for the potential function:

$$\phi(x,y,z,t)=\frac{F(z)}{dF(0)/dz}\frac{\partial W}{\partial t} \tag{3.31}$$

Fluid boundary conditions are introduced separately for each element, which allows us to study partially or totally submerged plates, i.e. vertical plates or inclined plates as well as floating plates. Substituting equation (3.31) into relation (3.25) leads to the following differential equation of second order:

$$\frac{d^2F(z)}{dz^2}-\mu^2F(z)=0 \tag{3.32}$$

where;

$$\mu=\pi\sqrt{\frac{1}{A^2}+\frac{1}{B^2}} \tag{3.33}$$

The general solution of equation (3.32) is given as:

$$F(z) = A_1 e^{\mu z} + A_2 e^{-\mu z} \tag{3.34}$$

Substituting equation (3.34) into (3.31), one gets the following expression for the potential function:

$$\phi(x,y,z,t) = \frac{\left(A_1 e^{\mu z} + A_2 e^{-\mu z}\right)}{dF(0)/dZ} \frac{\partial W}{\partial t} \tag{3.35}$$

The potential function 'ϕ' must be verified for given boundary conditions at the fluid-structure interface and the fluid extremity surfaces as well.

3.4.2 Plate-fluid model with free surface

Assuming that perturbations due to free surface motion of the fluid are insignificant, the following condition may be applied at the fluid free surface to the velocity potential, See Figure (3.2).

$$\left.\frac{\partial \phi(x,y,z,t)}{\partial z}\right|_{z=h_1} = -\frac{1}{g}\frac{\partial^2 \phi}{\partial t^2} \tag{3.36}$$

where 'g' is acceleration due to gravity.

The introduction of equation (3.35) simultaneously into relation (3.36) and (3.29), results in the following expression for the potential function:

$$\phi(x,y,z,t)=\frac{1}{\mu}\left[\frac{e^{\mu z}+Ce^{-\mu(z-2h_1)}}{1-Ce^{2\mu h_1}}\right]\frac{\partial W}{\partial t} \tag{3.37}$$

where;

$$C=(g\mu-\omega^2)/(g\mu+\omega^2) \tag{3.38}$$

The graphical presentation in Figure A1 of appendix I demonstrates that the value of C tends asymptotically towards -1. This approximation is made to avoid problems that may arise due to non linear eigenvalue problem.

The corresponding dynamic pressure at the fluid-structure interface becomes:

$$P=-\frac{\rho_f}{\mu}\left[\frac{1+Ce^{2\mu h_1}}{1-Ce^{2\mu h_1}}\right]\frac{\partial^2 W}{\partial t^2}=Z_{f1}\frac{\partial^2 W}{\partial t^2} \tag{3.39}$$

Factor Z_{fl} is given in Appendix *I*.

3.4.3 Plate-fluid model bounded by a rigid wall

The boundary condition at the upper surface of the fluid represented in Figure (3.3) was studied by Lamb [3] and referred to as the null-frequency condition. This rigid wall boundary condition is expressed as:

$$\left.\frac{\partial \phi}{\partial z}\right|_{z=h_1} = 0 \tag{3.40}$$

Similarly, by introducing equation (3.35) into relations (3.40) and (3.29), we obtain the following expression for the velocity potential as follows:

$$\phi(x,y,z,t) = \frac{1}{\mu}\left[\frac{e^{\mu(z-2h_1)} + e^{-\mu z}}{e^{-2\mu h_1} - 1}\right]\frac{\partial W}{\partial t} \tag{3.41}$$

The dynamic pressure for this case is determined as:

$$P = -\frac{\rho_f}{\mu}\left[\frac{e^{-2\mu h_1} + 1}{e^{-2\mu h_1} - 1}\right]\frac{\partial^2 W}{\partial t^2} = Z_{f2}\frac{\partial^2 W}{\partial t^2} \tag{3.42}$$

Factor Z_{f2} is given in Appendix I.

3.4.4 Plate-fluid model with a null velocity potential at the fluid free surface

This last condition applied at the extreme surface of the fluid is presented in Figure (3.4). This case is known as the infinite frequency condition and expressed as:

$$\phi = 0 \tag{3.43}$$

Here again the potential function may be written as follows:

$$\phi(x,y,z,t)=\frac{1}{\mu}\left[\frac{e^{\mu z}-e^{-\mu(z-2h_1)}}{1+e^{2\mu h_1}}\right]\frac{\partial W}{\partial t} \tag{3.44}$$

The dynamic pressure corresponding to the fluid-structure interface is calculated as:

$$P=-\frac{\rho_f}{\mu}\left[\frac{1-e^{2\mu h_1}}{1+e^{2\mu h_1}}\right]\frac{\partial^2 W}{\partial t^2}=Z_{f3}\frac{\partial^2 W}{\partial t^2} \tag{3.45}$$

Factor Z_{f3} is given in Appendix I.

In the case of totally submerged plate, the total dynamic pressure will be a combination of the pressures corresponding to the fluid boundary conditions at both top and bottom surfaces of the plate.

3.4.5 Application cases

The fluid-structure contact may, for practical purposes, be presented in different ways. Depending on this presentation the expression of fluid dynamic pressure acting upon the structure would be different. We therefore present some practical cases more often encountered in industrial applications.

3.4.5.1 Totally submerged plate in fluid

As shown in Figure (3.5), the plate is subjected to fluid loading from both sides. The total dynamic pressure is therefore the sum of lower and upper pressures and can be

calculated using equations (3.39) and (3.42), respectively. The resulting pressure is obtained as:

$$P = -\frac{\rho_f}{\mu}\left[\frac{1+C_1 e^{2\mu h_1}}{1-C_1 e^{2\mu h_1}} + \frac{e^{-2\mu h_2}+1}{e^{-2\mu h_2}-1}\right]\frac{\partial^2 W}{\partial t^2} = Z_{f4}\frac{\partial^2 W}{\partial t^2} \tag{3.46}$$

Factor Z_{f4} is given in Appendix I.

3.4.5.2 Plate submerged in fluid bounded by two rigid walls

As we see in Figure (3.6), the plate is subjected to fluid loading from both superior and inferior surfaces and the fluid media is bounded by two rigid extremities. The resulting dynamic pressure is the sum of two expressions defined in equation (3.42) calculated at two different levels; 'h_1' and 'h_2'

$$P = -\frac{\rho_f}{\mu}\left[\frac{e^{-2\mu h_1}+1}{e^{-2\mu h_1}-1} + \frac{e^{-2\mu h_2}+1}{e^{-2\mu h_2}-1}\right]\frac{\partial^2 W}{\partial t^2} = Z_{f5}\frac{\partial^2 W}{\partial t^2} \tag{3.47}$$

Factor Z_{f5} is given in Appendix I.

If 'h_1' is equal to 'h_2', the corresponding dynamic pressure would be twice the pressure calculated in equation (3.42).

$$P = -\frac{2\rho_f}{\mu}\left[\frac{e^{-2\mu h_1}+1}{e^{-2\mu h_1}-1}\right]\frac{\partial^2 W}{\partial t^2} = Z'_{f5}\frac{\partial^2 W}{\partial t^2} \tag{3.48}$$

3.4.5.3 Floating plate on the fluid free surface

In this case the plate is subjected to fluid pressure acting on its bottom (inferior) surface as shown in Figure (3.7).

The resulting pressure is calculated using equation (3.39) at h_2 level.

$$P = -\frac{\rho_f}{\mu}\left[\frac{e^{-2\mu h_2}+1}{e^{-2\mu h_2}-1}\right]\frac{\partial^2 W}{\partial t^2} = Z_{f6}\frac{\partial^2 W}{\partial t^2} \tag{3.49}$$

3.4.6 Calculation of Fluid-Induced Force

Fluid forces are replaced by the added mass, representing inertia force, when the flow velocity is null. The fluid-induced force vector can be expressed by the following relation:

$$\{F\}^e = \iint_A [N]^T \{P\} dA \tag{3.50}$$

where [N] is the shape function matrix of the finite element defined in equation (3.15) and {P} is a vector expressing the pressure applied by the fluid on the plate (equations 3.39, 3.42 and 3.45 to 3.49). Substituting the transversal displacement (given in equation (3.15)) into the appropriate pressure expressions (3.39, 3.42 and 3.45 to 3.49), which depend on the fluid-structure contact model as well as the boundary conditions, one

obtains the fluid pressure that is applied on the plate. The dynamic pressure is then defined as:

$$\{P\} = Z_{fi}[R_f][A]^{-1}\{\ddot{\delta}\} \tag{3.51}$$

The coefficients Z_{fi} (i= 1to 6), which depend on the fluid-structure contact model (Figure 3.11), are given in Appendix I. The matrix $[R_f]$ is defined in Appendix I and $([A]^{-1})$ terms are given in Reference [19]. Placing equation (3.51), and displacement functions (3.15) into relation (3.50) leads to the vector of fluid forces as:

$$\{F\}^e = Z_{fi}\int_A [[A]^{-1}]^T [R]^T [R_f][A]^{-1} dA\{\ddot{\delta}\} \tag{3.52}$$

where dA is the fluid-structure interface area.

3.5 CALCULATION OF GLOBAL MASS AND STIFFNESS MATRICES

In the case of zero flow velocity, the Coriolis and centrifugal forces vanish and equation (3.24) may be rewritten as follows:

$$([M_s]-[M_f])\{\ddot{\delta}_T\} + [K_s]\{\delta_T\} = \{0\} \tag{3.53}$$

A rectangular plate is subdivided into a series of quadrilateral finite elements such that each of them is a smaller rectangular plate, see Figure (3.1.A). The positions of the nodal points of elements are chosen in such a way that the local and global coordinates are parallel. The global matrices are obtained by superimposing the mass and stiffness matrices for each individual element. After applying the boundary conditions, these matrices are reduced to square matrices of order NDF*N-NC where NDF, N and NC are; the number of degrees of freedom at each node, the number of nodes and the restriction imposed.

Assuming;

$$\{\delta_T\} = \{\delta_{0T}\}e^{i\omega t} \tag{3.54}$$

where $\{\delta_T\}$ is the global displacement vector, $\{\delta_{0T}\}$ is vector of mode shape amplitudes and ω is the natural frequency (rad/sec).

An in-house computer code has been developed to establish the structural matrices of each element based on the equations developed using this theoretical approach. The global matrices are obtained by superimposing the mass and stiffness matrices for each element. Once the global mass and stiffness matrices are constructed, equation (3.22) can be solved to obtain 6*(N)-NC eigenvalues and eigenvectors. By introducing equation (3.54) into relation (3.53), one obtains the typical eigenvalues and eigenvectors:

$$Det\left[\left[K_s\right]-\omega^2\left[M_s-M_f\right]\right]=0 \tag{3.55}$$

Equation (3.55) is then solved to obtain the natural frequencies and mode shapes of the coupled fluid-structure system.

3.6. RESULTS AND DISCUSSIONS

3.6.1 Convergence Test

The precision of the finite element method depends on the number of elements used to discretize the physical problem. The first set of calculations is therefore used to determine the requisite number of elements for a precise determination of the natural frequencies. The plate dimensions and mechanical properties are:

A = 0.20165m; B = 0.655m; h=2.54mm; E=196GPa; v=0.3 and ρ_s=7860kg/m^3.

The variation of the first five frequencies versus of number of finite elements is plotted in Figure (3.8) and shows the minimum number of elements required to assure a fast convergence in determining both low and high frequencies. Eight elements are sufficient to calculate the two first modes, whereas for other modes convergence requires at least twenty-five elements. This number of elements required by the proposed method is excellent compared to that of other existing approaches. In all of the following examples sixty-four elements are used, which assures that the results will be independent of mesh size.

3.6.2 Free vibration of rectangular plates in vacuo

The non-dimensional natural frequency parameter, λ, for a rectangular plate in vacuo is obtained using this theory for various boundary conditions and plate dimension ratios (A/B) and compared with corresponding results presented by Leissa [1]. The results are presented on Tables 3.1 to 3.6. The boundary conditions are shown in Figures (3.9) and (3.10).

$$\lambda = \omega A^2 / \sqrt{\rho h / K} \tag{3.56}$$

where:

$K = Eh^3 / 12(1-\nu^2)$

3.6.3 Natural frequencies of rectangular plates in contact with fluid

3.6.3.1 Submerged plates

The modal results obtained using the proposed theory are compared with those of experiments and other research work to show the applicability, reliability and effectiveness of the presented formulation.

This example involves the determination of non-dimensional natural frequencies of a rectangular plate totally submerged in fluid (water). The effect of boundary conditions shown in Figures (3.9) and (3.10), the plate dimension ratio and mode shape number on the dynamic responses of the submerged plates is investigated in this example. The non-dimensional natural frequency of a plate in contact with fluid is defined as the following:

$$\lambda_f = \omega_f A^2 \sqrt{\frac{\rho_s h}{K}} \tag{3.57}$$

The summarized results in Tables 3.1 to 3.6 show that the natural frequencies of the coupled fluid-structure system are lower than the corresponding values of plates in vacuo.

The next example calculates the natural frequencies of a steel rectangular plate simply supported at its two short sides as shown in Figure (3.9.A). The plate is totally submerged in fluid. This case was experimentally studied by Haddara and Cao [11]. The plate dimensions are:

A = 0.20165m, B = 0.655m and h=0.963mm.

The experimental apparatus was set up by placing the plate in a rectangular reservoir with dimensions 1.3m×0.55m×0.8m. The results obtained using the present theory are listed in Table 3.7 along with those of using the experimental and analytical approaches described in Reference [11]. As can be seen, there is good agreement between the theoretical results and corresponding experimental values.

The next case is the calculation of the natural frequencies of a submerged plate fixed at its two short sides (Figure 3.9.B). The same material and geometrical parameters as the previous example are used in this case, and the results are presented in Table 3.8.

The modal analysis of a cantilever square plate that is totally submerged in fluid is carried out in the next example. The steel plate dimensions are:

A = B = 10m and h =0.238m

This plate was studied analytically by Lindholm et al [5] and experimentally by Fu and Price [7]. According to the results listed in Table 3.9, we can conclude that the dynamic responses of the square plates are computed with a relatively good precision when compared with experimental and other analytical approaches.

The last example in this series deals with the dynamic analysis of a rectangular plate clamped at all sides and floated on the free surface of the fluid as shown in Figure (3.10.B). The eigenvalues calculated using the present theory are compared with those generated by experiments [20] and other theories [21]. Kwak [21] also studied the same plate in a fluid container bounded by an infinite rigid wall. Using the theoretical and experimental factors of NAVMI, the variation of normalized frequency (Frequency in vacuo / Frequency in presence of fluid) of a rectangular plate without a rigid wall is presented for different ratios of plate dimensions in Figure (3.12). The results coincide very well with the analytic and experimental values. It is noted that the results calculated using this theory are much closer to those of a floating plate on the fluid free surface than a plate put in a reservoir bounded by a rigid wall. This confirms that the proposed boundary conditions are similar to those of a plate in contact with fluid without a rigid wall.

3.6.3.2 Effects of fluid boundary conditions and fluid level on the plate's dynamic response

The dynamic behaviour of structures may be influenced by changing the fluid level and/or fluid boundary conditions, i.e. free surface or rigid wall. The variation of the

natural frequencies as a function of fluid height and fluid boundary conditions are verified in the following examples.

The first example involves vibration analysis of a submerged plate (fixed at its two short sides as discussed in section 5.3.1) with a variable fluid level, h_1. It is assumed that fluid level 'h_2' is sufficiently high that it has no significant influence on the natural frequencies of the structure. In case of free (top) surface fluid, the frequencies decrease as the fluid height increases (Figure 3.13.A), levelling off at a certain fluid level. They remain almost unchanged when the fluid level reaches 25% of the plate length. This fluid height/plate length ratio agrees very well with the percentage given in [11]. It means that the fluid level 'h_1' has no influence on the frequencies of the coupled fluid-structure system.

The next example concerns a floating plate fixed at its two short sides (section 5.3.1) with 'h_1=0' while 'h_2' varies. In case of the floating plate (h_1=0 and bounded by a rigid wall at h_2) shown in Figure (3.13.B), structural frequencies decrease abruptly when the fluid height (h_2) is less than 20% of the plate length. Beyond this percentage the frequencies are independent of the fluid level. This behaviour has been recognized in other theories and experiments [7 and 21].

It is well known that any change in the structural and fluid boundary conditions also changes the structural and fluid stiffness and consequently leads to different dynamic behaviours of structures. The effect of fluid height variation on the dynamic characteristics of a plate is investigated in the previous examples. In the next examples, plate frequencies are calculated while the boundary conditions and fluid level vary. This

allows determination of the modal frequencies of a cantilever square plate in contact at different fluid levels. This case has also been studied in [5 and 7]. It is assumed that the water height under the plate is sufficiently high so that it has no influence on the dynamic behaviour of the coupled system. According to Figure (3.14), we note that the frequencies decrease with increasing fluid level and they become independent of the fluid level when this reaches 50% of the plate length, which is the same percentage stated in References [5 and 7]. It is worthy to note that Kwak [14] concluded that the level of fluid at which the frequencies of a circular plate stop changing is equal to the plate radius.

However, the fluid level at which frequencies remain constant varies from one structure to another. In order to clarify this fact, a plate having a constant surface area of 4 square meters is considered whereas the boundary conditions and plate dimension ratio (A/B) varies. The physical parameters of this plate are given as:

$$h=0.05m;\ E=70GPa;\quad \nu=0.3;\ \rho_s=2700\ kg/m^3$$

The frequency variation of a clamped free plate (Figure 3.9.C) as a function of h_l/A (fluid level /plate length) ratio is plotted in Figures (3.15.A to 3.15.E) for the first five mode shapes. This figure shows that the h_l/A ratio, at which the frequencies cease changing, reaches its maximum for the case of a square plate (A/B=1). In case of a rectangular plate with dimension ratios (A/B= 4 /or A/B=0.25), the frequencies remain unchanged once the h_l/length ratio is equal to 0.125, although the plate boundary conditions are not symmetric in X and Y directions. Figures (3.15.B and 3.15.E) show

that frequencies of a rectangular plate with dimension ratios A/B=0.64 and 1.56, respectively, remain almost unchanged at a fluid level/plate length ratio equal to 0.3.

In the case of the plate fixed at two opposite sides shown in Figures (3.9.B) and that of the four sides simply supported plate shown in Figures (10.A), the variation of natural frequencies as a function of h_l/A (fluid level /plate length) ratio is plotted in Figure (16) and (17), respectively. The other input data are given within the Figures. These results show that whatever the boundary conditions are, the frequencies of coupled fluid-structure system become constant at fluid level/length ratios 0.5 and 0.35 for plate dimension ratios A/B=1 and A/B≠1, respectively.

3.6.3.3 Mode Shapes

Most of available theories assume that the mode shapes do not change under the influence of fluid, but this assumption is discarded in this theory. The following examples illustrate that this assumption may not be valid for all cases or for all vibrational modes. To visualize the existing gap between the plate's dry and wet displacement mode shapes, three eigenvectors of a rectangular plate are plotted in Figure (3.18). The plate is fixed at its two opposite short sides (as seen in section 3.6.3.1) and the transversal displacement, W, is drawn along the plate length. It is noted that the mode shapes corresponding to the lower frequencies are identical and differences may be seen from the thirteenth mode. In Figure (3.19), the out-of-plane displacement, W, of a cantilever square plate is drawn. The physical and geometrical parameters of this last example are given as:

A =2m; B=2m; h=0.05m; E=70GPa; ν=0.3; ρ_s=2700 kg/m^3

We begin to have a wet and dry mode shape differences from the tenth mode. Comparison of these two last examples shows a different dynamic behaviour from one case to another.

3.7 CONCLUSIONS

The purpose of the investigation described in this paper is to determine natural frequencies of rectangular plates in vacuo and in water, which constitute important structural components in various sectors of industry. The plates may be partially or completely submerged in fluid or floating on the free surface of fluid. The natural frequency is one of the critical factors in determining the responses of structures to various excitations including steady and turbulent flow forces, pump pulsation, and seismic motions etc. Natural frequency is affected by the added mass associated with the inertia of the fluid that is forced to oscillate when the structure vibrates. Thus it is necessary to evaluate the virtual added mass due to fluid when predicting and analyzing the vibratory responses and stresses of structures that are in contact with fluid. The structural mathematical model is developed based on a combination of the finite element method and Sanders' shell theory. The in-plane and out-of-plane displacement components are modelled using bilinear polynomials and exponential functions, respectively. The general equations of the displacement functions are derived from the equilibrium equations of a rectangular plate. The mass and stiffness matrices are then determined by exact analytical integration. The velocity potential and Bernoulli's

equation are adopted to express the fluid pressure acting on the structure. The product of the pressure expression and the developed structural shape function is integrated over the structure-fluid interface to assess the virtual added mass due to the fluid. The effects of several parameters; i.e. structure and fluid boundary conditions, the fluid depth and various plate aspect ratios on the dynamic behaviour of the rectangular plates are explored in this work. The results are in satisfactory agreement with both experimental results and those from other theoretical approaches.

3.8 REFERENCES

1. Leissa, A.W., "Vibration of plates", NASA, SP-160, 1969.
2. Kirchhoff, G., "UG berdas Gleichgewicht und die Bewegung einer elastischen Scheibe", Mathematical Journal (Crelle1s Journal) 40, pp. 51-58, 1850.
3. Lamb, H., "On the vibrations of an elastic plate in contact with water", Proceeding of Royal Society, A98, pp. 205-216, 1921.
4. Powell J. H", and Roberts, J. H. T., "On the frequency of vibration of circular diaphragms", Proceedings of the Physical Society London, 35, pp. 170-182, 1923.
5. Lindholm, U.S., Kana, D. D., Chu, W. H. and Abramson, H.N., "Elastic vibration characteristics of cantilever plates in water", Journal of Ship Research, pp11-22, 1965.
6. Volcy, G. C., Morel, P., Bureau, M., and Tanida, K., "Some studies and researches related to the hydro-elasticity of steel work", In Proc. 122nd Euromech Colloquium on numerical analysis of the dynamics of ship structures, Ecole Polytechnique, Paris, 403-406, 1979.
7. Fu, Y., and PRICE, W. G., "Interactions between a partially or totally immersed vibrating cantilever plate and the surrounding fluid", Journal of Sound and Vibration, 118 (3), pp495-513, 1987.
8. Kawk, M. K., and Kim, M. K., "Axisymmetric vibration of circular plates in contact with fluid", Journal of Sound and Vibration, 146, pp. 381-389,1991

9. Soedel, S. M., and Soedel, W., "On the free and forced vibration of a plate supporting a freely sloshing surface liquid", Journal of Sound and Vibration, 171(2), pp. 159-171, 1994.

10. Amabili, M., Frosali, G., Kawk, M. K., "Free vibrations of annular plates coupled with fluids", Journal of Sound and Vibration, 191 (5), pp. 825-846, 1996.

11. Haddara Mé. R., Cao, S., "A study of the dynamic response of submerged rectangular flat plates", Marine Structures, 9, pp. 913-933, 1996.

12. M. Amabili, "Vibrations of circular plates resting on a sloshing liquid, solution of the fully coupled problem", Journal of Sound and Vibration, 2001, 245(2), 261-283.

13. M. Amabili, M. K. Kwak, "Vibration of circular plates on a free fluid surface: effect of surface waves", Journal of Sound and Vibration 1999, 226(3) 404-424.

14. M. K. Kwak and S. B. Han, "Effect of fluid depth on the hydroelastic vibration of free-edge circular plate", Journal of sound and Vibration, 2000, 230(1), 171-185.

15. Sanders, J. L., "An improved first approximation theory for thin shell", NASA TR-24, 1959.

16. Lakis, A. A. and Paidoussis, M. P., "Free vibration of cylindrical shells partially filled with liquid", Journal of Sound and Vibration, 19 (1), pp1-15, 1971.

17. Selmane, A. and Lakis, A. A. "Vibration analysis of anisotropic open cylindrical shells subjected to a flowing fluid", Journal of Fluids and Structures, 11, pp111–134, 1997.

18. Charbonneau, E. and Lakis, A. A., "Semi-analytical shape functions in the finite element analysis of rectangular plates", Journal of Sound and vibration, 242 (3), 3, pp427-443, 2001.

19. Kerboua, Y., Lakis, A. A., Thomas, M., and Marcouiller, L., "Comportement dynamiques des plaques rectangulaires submerges", Technical Report, EPM-RT-2005-05, Ecole Polytechnique of Montreal, Canada, 2005.

20. Kim K. C., Kim, J. S., and Lee, H. Y., "An experimental study on the elastic vibration of plates in contact with water", Journal of the Society of Naval Architects of Korea, 16 (2), pp. 1-7, 1979.

21. Kwak, M. K., "Hydroelastic vibration of rectangular plates", Transactions of ASME, Journal of Applied Mechanics, 63 (1), pp. 110-115, 1996.

22. Leissa, A. W., "The free vibration of rectangular plates", Journal of Sound and Vibration, 13 (3), pp. 257-293, 1973.

23. Kwak, M. K., "Hydroelastic vibration of circular plates" Journal of Sound and Vibration, 201(3), pp293-303, 1997

3.9 APPENDIX I

This appendix contains some equations, which are referred to in this work.

$$[R]=\begin{bmatrix} 1 & \frac{x}{A} & \frac{y}{B} & \frac{xy}{AB} & 0 & 0 & 0 & 0 & 0 & 0 & 0 & 0 & 0 & 0 & 0 & 0 & 0 & 0 & 0 & 0 & 0 & 0 & 0 & 0 \\ 0 & 0 & 0 & 0 & 1 & \frac{x}{A} & \frac{y}{B} & \frac{xy}{AB} & 0 & 0 & 0 & 0 & 0 & 0 & 0 & 0 & 0 & 0 & 0 & 0 & 0 & 0 & 0 & 0 \\ 0 & 0 & 0 & 0 & 0 & 0 & 0 & 0 & 1 & \frac{x}{A} & \frac{y}{B} & \frac{x^2}{2A^2} & \frac{xy}{AB} & \frac{y^2}{2B^2} & \frac{x^3}{6A^3} & \frac{x^2y}{2AB} & \frac{xy^2}{2AB^2} & \frac{y^3}{6B^3} & \frac{x^3y}{6A^3B} & \frac{x^2y^2}{4A^2B^2} & \frac{xy^3}{6AB^3} & \frac{x^3y^2}{12A^3B^2} & \frac{x^2y^3}{12A^2B^3} & \frac{x^3y^3}{36A^3B^3} \end{bmatrix}$$

$$[Q]=\begin{bmatrix} 0 & \frac{1}{A} & 0 & \frac{y}{AB} & 0 & 0 & 0 & 0 & 0 & 0 & 0 & 0 & 0 & 0 & 0 & 0 & 0 & 0 & 0 & 0 & 0 & 0 & 0 & 0 \\ 0 & 0 & 0 & 0 & 0 & 0 & \frac{1}{B} & \frac{x}{AB} & 0 & 0 & 0 & 0 & 0 & 0 & 0 & 0 & 0 & 0 & 0 & 0 & 0 & 0 & 0 & 0 \\ 0 & 0 & \frac{1}{B} & \frac{x}{AB} & 0 & \frac{1}{A} & 0 & \frac{y}{AB} & 0 & 0 & 0 & 0 & 0 & 0 & 0 & 0 & 0 & 0 & 0 & 0 & 0 & 0 & 0 & 0 \\ 0 & 0 & 0 & 0 & 0 & 0 & 0 & 0 & 0 & 0 & 0 & -\frac{1}{A^2} & 0 & 0 & \frac{x}{A^3} & -\frac{y}{A^2B} & 0 & 0 & -\frac{xy}{A^3B} & -\frac{y^2}{2A^2B^2} & 0 & -\frac{xy^2}{2A^3B^2} & -\frac{y^3}{6A^2B^3} & -\frac{xy^3}{6A^3B^3} \\ 0 & 0 & 0 & 0 & 0 & 0 & 0 & 0 & 0 & 0 & 0 & 0 & 0 & -\frac{1}{B^2} & 0 & 0 & -\frac{x}{AB^2} & -\frac{y}{B^3} & 0 & -\frac{x^2}{2A^2B^2} & -\frac{xy}{AB^3} & -\frac{x^3}{2A^3B^2} & -\frac{x^2y}{6A^2B^3} & -\frac{x^3y}{6A^{2B^3}B^2} \\ 0 & 0 & 0 & 0 & 0 & 0 & 0 & 0 & 0 & 0 & 0 & 0 & -\frac{2}{AB} & 0 & 0 & -\frac{2x}{A^2B} & -\frac{2y}{A^2B} & 0 & -\frac{x^2}{A^3B} & -\frac{2xy}{A^2B^2} & -\frac{y^2}{AB^3} & -\frac{x^2y}{A^3B^2} & -\frac{xy^2}{A^2B^3} & -\frac{x^2y^2}{2A^3B^3} \end{bmatrix}$$

$$[R_f]=\begin{bmatrix} 0 & 0 & 0 & 0 & 0 & 0 & 0 & 0 & 0 & 0 & 0 & 0 & 0 & 0 & 0 & 0 & 0 & 0 & 0 & 0 & 0 & 0 & 0 & 0 \\ 0 & 0 & 0 & 0 & 0 & 0 & 0 & 0 & 0 & 0 & 0 & 0 & 0 & 0 & 0 & 0 & 0 & 0 & 0 & 0 & 0 & 0 & 0 & 0 \\ 0 & 0 & 0 & 0 & 0 & 0 & 0 & 0 & 1 & \frac{x}{A} & \frac{y}{B} & \frac{x^2}{2A^2} & \frac{xy}{AB} & \frac{y^2}{2B^2} & \frac{x^3}{6A^3} & \frac{x^2y}{2AB} & \frac{xy^2}{2AB^2} & \frac{y^3}{6B^3} & \frac{x^3y}{6A^3B} & \frac{x^2y^2}{4A^2B^2} & \frac{xy^3}{6AB^3} & \frac{x^3y^2}{12A^3B^2} & \frac{x^2y^3}{12A^2B^3} & \frac{x^3y^3}{36A^3B^3} \end{bmatrix}$$

Coefficients Z_{fi}

$$Z_{f1}=\frac{\rho_f}{\mu}\left[\frac{1-C_1e^{2\mu h_1}}{1+C_1e^{2\mu h_1}}\right] \qquad Z_{f2}=\frac{\rho_f}{\mu}\left[\frac{e^{-2\mu h_1}+1}{e^{-2\mu h_1}-1}\right]$$

$$Z_{f3}=\frac{\rho_f}{\mu}\left[\frac{1+e^{2\mu h_1}}{1-e^{2\mu h_1}}\right] \qquad Z_{f4}=\frac{\rho_f}{\mu}\left[\frac{1+C_1e^{2\mu h_1}}{1-C_{14}e^{2\mu h_1}}+\frac{e^{-2\mu h_2}+1}{e^{-2\mu h_2}-1}\right]$$

$$Z_{f5}=\frac{\rho_f}{\mu}\left[\frac{e^{-2\mu h_1}+1}{e^{-2\mu h_1}-1}+\frac{e^{-2\mu h_2}+1}{e^{-2\mu h_2}-1}\right] \qquad Z_{f6}=\frac{\rho_f}{\mu}\left[\frac{e^{-2\mu h_2}+1}{e^{-2\mu h_2}-1}\right]$$

Figure A.1 Variation of C with respect to frequency for different values of A and B

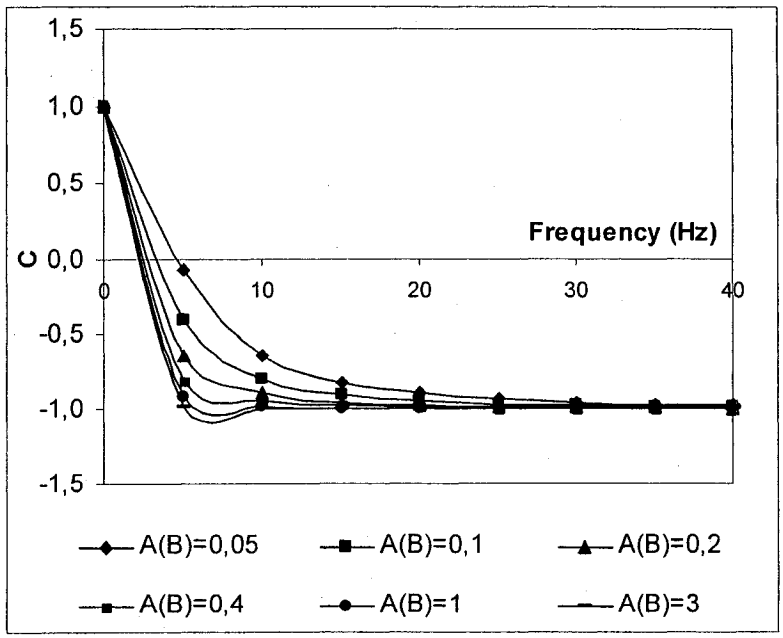

3.10. NOMENCALATURE

A, B	Plate side length along the X and Y axes, respectively
C_i	Constants defined by equation (3.10)
D	Membrane rigidity $Eh/(1-\nu^2)$
E	Modulus of elasticity
K	Bending rigidity $Eh^3/12(1-\nu^2)$
P	Fluid pressure
P_{ij}	Material elasticity matrix components defined by equation (3.19)
U, V	Displacement components of the plate reference surface in the X and Y directions, respectively
W	Normal displacement of the plate middle surface
U_i, V_i	Nodal displacement components at node *i* in the X and Y direction, respectively
W_i	Normal displacement of the plate at node *i*
$W_{i,x}$; $iW_{i,y}$	The first derivative of the plate's normal displacement with respect to X and Y, respectively, at node *i*
$W_{i,xy}$	Crossed derivative of the plate's normal displacement with respect to X and Y
X, Y, Z	Orthogonal coordinate system
Z_{fi}	Coefficient of fluid pressure acting on the plate
g	Gravity acceleration
h	Plate thickness

h_1	Fluid level on top of the plate
h_2	Fluid level below the plate surface
i	Complex number $i^2 = -1$
n, m	Mode shape number in the X and Y directions, respectively
x_e, y_e	Length of the element along the X and Y axes, respectively
λ	Non-dimensional frequency parameter of the plate
λ_f	Non-dimensional frequency of the coupled fluid-plate system
ω	Natural frequency of the plate in rad/sec
ω_f	Natural frequency of the plate in contact with fluid
ρ_s	Material density
ρ_f	Fluid density
ν	Poisson's coefficient
$\phi(x, y, z)$	Velocity potential function
$\{C\}$	Vector of unknown constants defined by equation (3.10)
$\{F\}^e$	Nodal force vector
$\{\delta\}$	Nodal displacement vector defined by equation (3.11)
$\{\delta_T\}$	Global displacement vector
$\{\delta_{0T}\}$	Vector of mode shape amplitudes
$\{\varepsilon\}$	Deformation vector
$\{\sigma\}$	Stress vector

[A]	Matrix (24 × 24) defined by equation (3.13)
[B]	Shape function derivative defined by equation (3.17)
$[k]^e$	Stiffness matrix of an element (24 × 24)
$[K_s]$	Structural global stiffness matrix
$[m]^e$	Mass matrix of an element (24 × 24)
$[M_s]$	Structural global mass matrix
$[M_f]$	Fluid global mass matrix
$[N]$	Shape function matrix (3 × 24) defined by equation (3.15)
$[P]$	Elasticity matrix (6 × 6)
$[Q]$	Matrix (6 × 24) defined by equation (3.17)
[R]	Matrix (3 × 24), defined by equation (3.9)
$[R_f]$	Defined by equation (3.51)

Table 3.1: Non-dimensional natural frequency variation of a rectangular plate (CCCC) totally submerged in fluid (water) as a function of side-length ratio (Figure 3.10.B)

CCCC	λ					
	A/B=0.4			A/B=1		
n-m[1]	No Fluid		With Fluid	n-m[1]	No Fluid		With Fluid
	Present Theory	Leissa [22]	Present Theory		Present Theory	Leissa [22]	Present Theory
1-1	23.31	23.64	7.46	1-1	35.45	35.99	12.80
1-2	26.69	27.81	8.54	2-1	72.03	73.41	26.01
1-3	33.48	35.44	10.72	1-2	72.03	73.41	26.01
1-4	44.21	46.70	14.15	2-2	103.70	108.27	37.44
1-5	59.01	61.55	18.89	3-1	129.41	131.64	46.73
2-1	62.24	63.1	19.92	1-3	130.28	132.24	47.04

(1) n and m represent the mode shape number in X and Y direction, respectively.

Table 3.2: Non-dimensional natural frequency variation of a rectangular plate (CCFF) totally submerged in fluid (water) as a function of side-length ratio

CCFF	λ					
	A/B=0.4			A/B=1		
n-m[1]	No Fluid		With Fluid	n-m[1]	No Fluid		With Fluid
	Present Theory	Leissa [22]	Present Theory		Present Theory	Leissa [22]	Present Theory
1-1	3.96	3.98	1.26	1-1	6.92	6.94	2.49
1-2	7.10	7.15	2.27	2-1	23.96	24.03	8.65
1-3	12.99	13.10	4.16	1-2	26.50	26.68	9.57
1-4	21.81	21.84	6.98	2-2	47.23	47.78	17.05
2-1	22.70	22.89	7.26	1-3	62.77	63.03	22.66
2-2	25.96	26.50	8.31	3-1	65.65	65.83	23.70

(1) n and m represent the mode shape number in X and Y direction, respectively.

Table 3.3: Non-dimensional natural frequency variation of a rectangular plate (FFFF) totally submerged in fluid (water) as a function of side-length ratio

FFFF	λ					
	A/B=0.4			A/B=1		
$n\text{-}m^{(1)}$	No Fluid		With Fluid	$n\text{-}m^{(1)}$	No Fluid		With Fluid
	Present Theory	Leissa [22]	Present Theory		Present Theory	Leissa [22]	Present Theory
1-3	3.431	3.46	1.62	2-2	13.48	13.48	4.86
2-2	5.28	5.28	8.46	1-3	19.61	19.78	7.08
1-4	9.56	9.62	10.10	3-1	24.31	24.43	8.78
2-3	11.34	11.43	26.99	3-2	34.79	35.02	12.56
1-5	18.72	18.79	28.43	2-3	34.79	35.02	12.56
2-4	18.94	19.1	49.41	4-1	61.32	61.52	22.14

(1) n and m represent the mode shape number in X and Y direction, respectively.

Table 3.4: Non-dimensional natural frequency variation of a rectangular plate (SFFF) totally submerged in fluid (water) as a function of side-length ratio

SFFF	λ					
	A/B=0.4			A/B=2.5		
$n\text{-}m^{(1)}$	No Fluid		With Fluid	$n\text{-}m^{(1)}$	No Fluid		With Fluid
	Present Theory	Leissa [22]	Present Theory		Present Theory	Leissa [22]	Present Theory
1-2	2.69	2.69	0.86	2-1	14.82	14.93	6.98
1-3	6.47	6.50	2.07	1-2	16.23	16.24	7.65
1-4	12.58	12.63	4.02	3-1	48.57	48.84	22.89
2-1	15.29	15.33	4.89	2-2	51.97	52.08	24.49
2-2	17.33	17.51	5.55	3-2	77.52	97.22	45.58
1-5	21.57	21.69	6.90	4-1	96.73	102.34	48.10

(1) n and m represent the mode shape number in X and Y direction, respectively.

Table 3.5: Non-dimensional natural frequency variation of a rectangular plate (CCCF) totally submerged in fluid (water) as a function of side-length ratio

CCCF	λ					
	A/B=0.4			A/B=2.5		
$n\text{-}m^{(1)}$	No Fluid		With Fluid	$n\text{-}m^{(1)}$	No Fluid		With Fluid
	Present Theory	Leissa [22]	Present Theory		Present Theory	Leissa [22]	Present Theory
1-1	22.53	22.57	7.21	1-1	37.41	37.65	17.63
1-2	24.12	24.62	7.72	2-1	75.84	76.40	35.74
1-3	28.01	29.24	8.96	3-1	134.42	135.15	63.35
1-4	35.05	37.05	11.22	1-2	150.52	152.47	70.93
1-5	45.77	48.28	14.65	2-2	186.81	193.01	88.03
2-1	60.41	61.92	19.34	4-1	213.61	213.74	100.67

(1) n and m represent the mode shape number in X and Y direction, respectively.

Table 3.6: Non-dimensional natural frequency variation of a rectangular plate (CFFF) totally submerged in fluid (water) as a function of side-length ratio (Figure 9.C)

CFFF	λ					
	A/B=0.4			A/B=2.5		
n-m[1]	No Fluid		With Fluid	n-m[1]	No Fluid		With Fluid
	Present Theory	Leissa [22]	Present Theory		Present Theory	Leissa [22]	Present Theory
1-1	3.49	3.51	1.12	1-1	3.42	3.45	1.61
1-2	4.75	4.78	1.52	1-2	17.97	17.98	8.46
1-3	8.03	8.11	2.57	2-1	21.43	21.56	10.10
1-4	13.75	13.88	4.40	2-2	49.41	57.45	26.99
2-1	21.67	21.63	6.94	3-1	57.27	60.58	28.43
2-2	22.92	23.73	7.34	3-2	106.03	106.54	29.41

(1) n and m represent the mode shape number in X and Y direction, respectively.

Table 3.7: Natural frequencies (Hz) of a plate, simply supported at two opposite sides, submerged in water

Mode Number	Experiment [11]	Theory [11]	Present Theory
1	28.72	28.71	31.28
2	117.125	122.59	126.40
3	154.51	N.A. (1)	141.78
4	281.79	296	285.98
5	335.04	N.A. (1)	304.57

(1) N. A. Not available

Table 3.8: Natural frequencies (Hz) of a plate, clamped at two opposite sides, submerged in water

Mode Number	Experiment [11]	Theory [11]	Present Theory
1	65.78	67.55	72.7
2	167	N.A. (1)	168.16
3	179.15	197.73	200.84
4	344.99	N.A. (1)	359.64
5	385.73	409.60	395.95

(1) N. A. Not available

Table 3.9: Natural frequencies (rad/sec) of a cantilever square plate submerged in water

Mode Number	No Fluid		Totally Submerged		
	Present	Fu and Price [7]	Present	Fu and Price [7]	Experiment
1	12.93	12.94	7.0	7.35	6.56
2	31.69	31.93	17.16	20.19	19.66
3	79.37	79.8	42.98	50.11	45.32

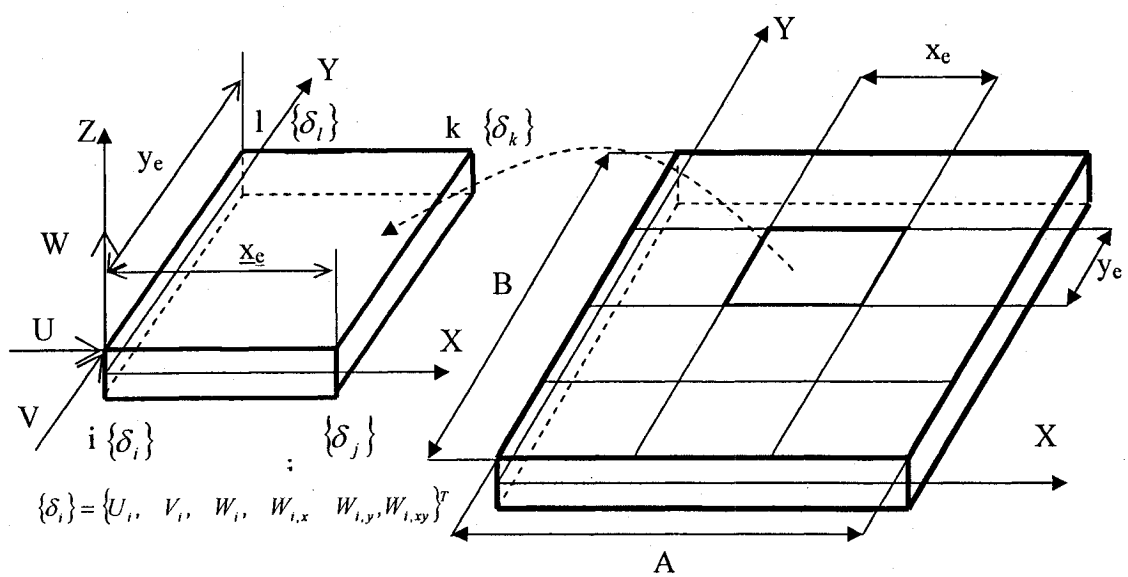

(A) (B)

Figure 3.1: A: Geometry and displacement field of a typical element
B: Finite element discretization of rectangular plate

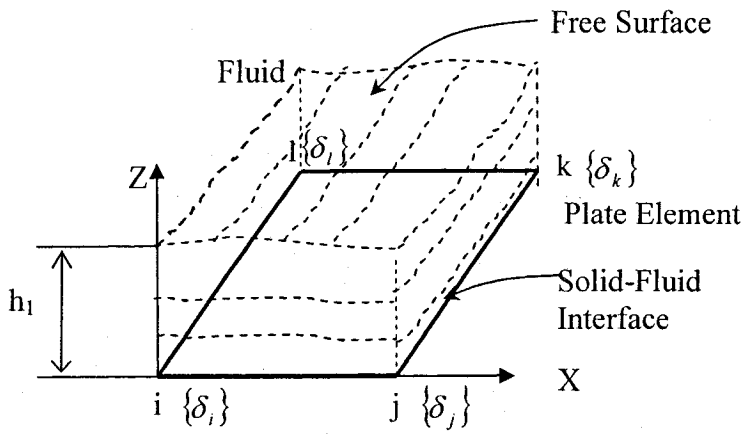

Figure 3.2: Coupled fluid-structure element possessing a free surface of fluid at $Z=h_1$

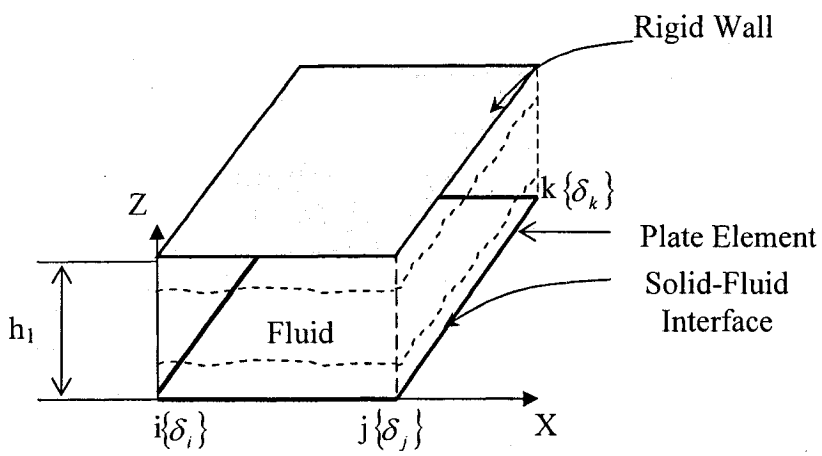

Figure 3.3: Plate element in contact with fluid bounded by a rigid wall

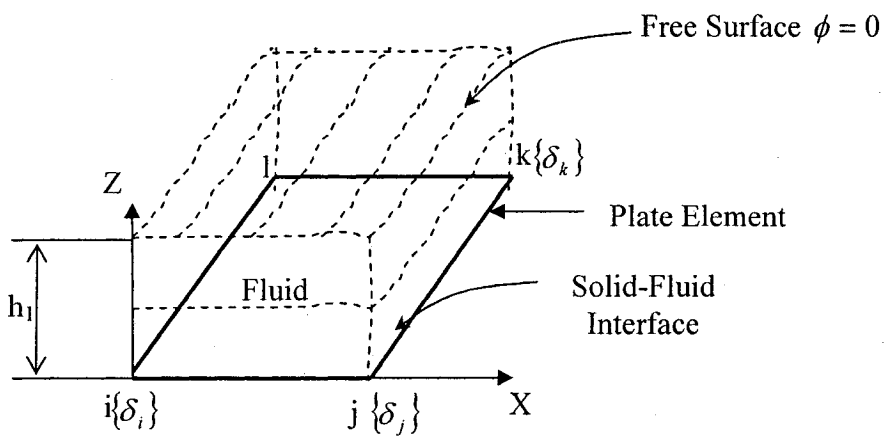

Figure 3.4: Plate element in contact with fluid having a free surface with null pressure

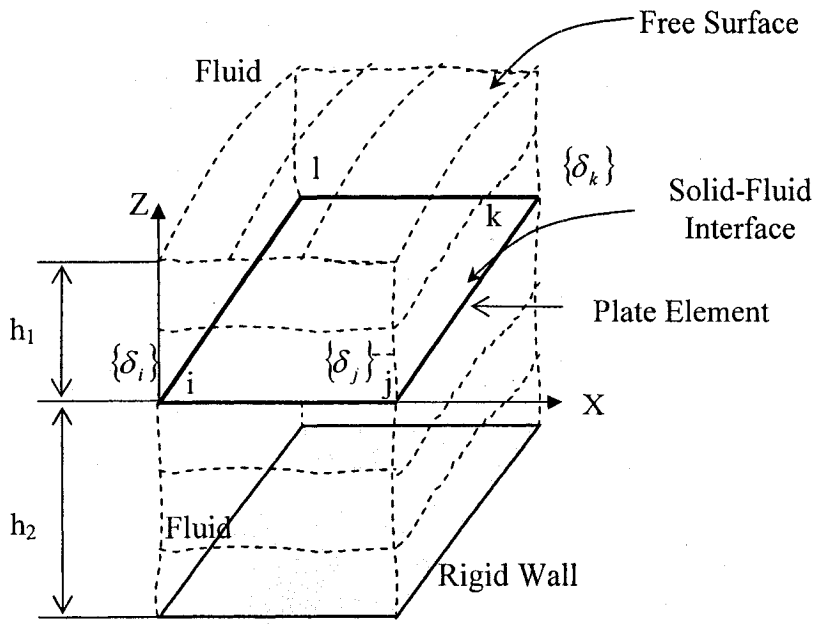

Figure 3.5: Plate element in contact with fluid bounded by a free surface on top and a rigid wall at its inferior surface.

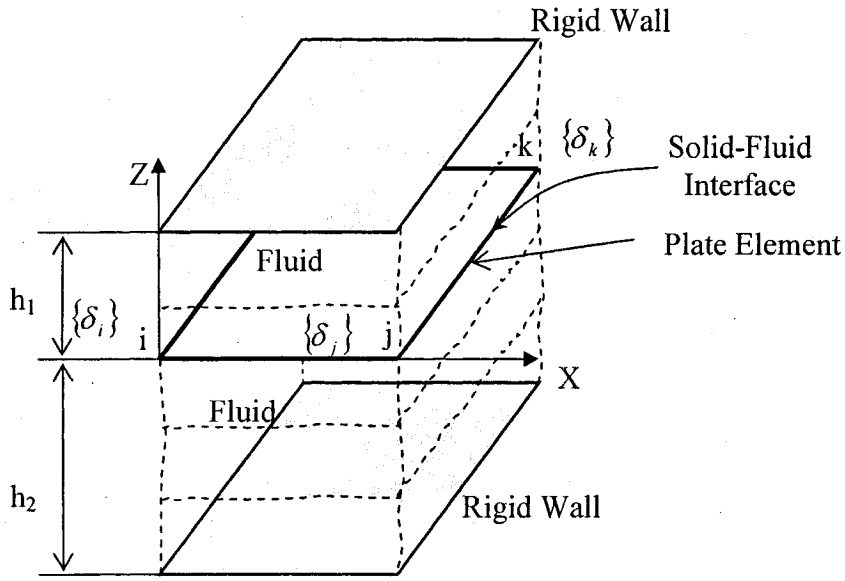

Figure 3.6: Plate element in contact with fluid bounded by two rigid walls at both upper and lower surfaces.

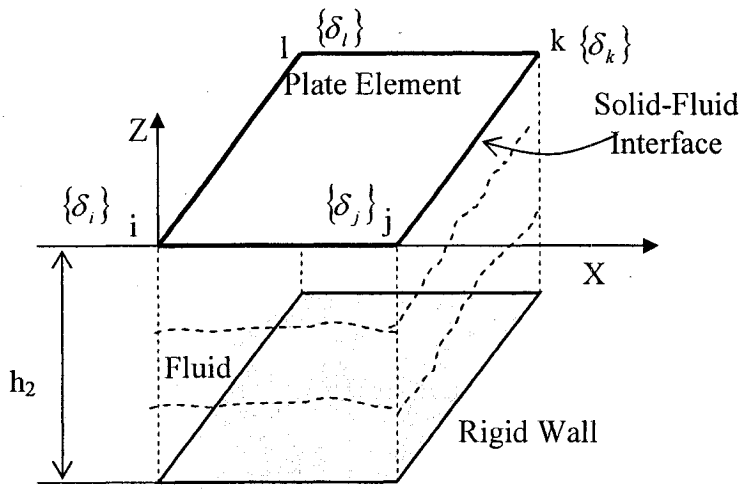

Figure 3.7: Plate element in contact with fluid bounded by a rigid wall at its lower surface.

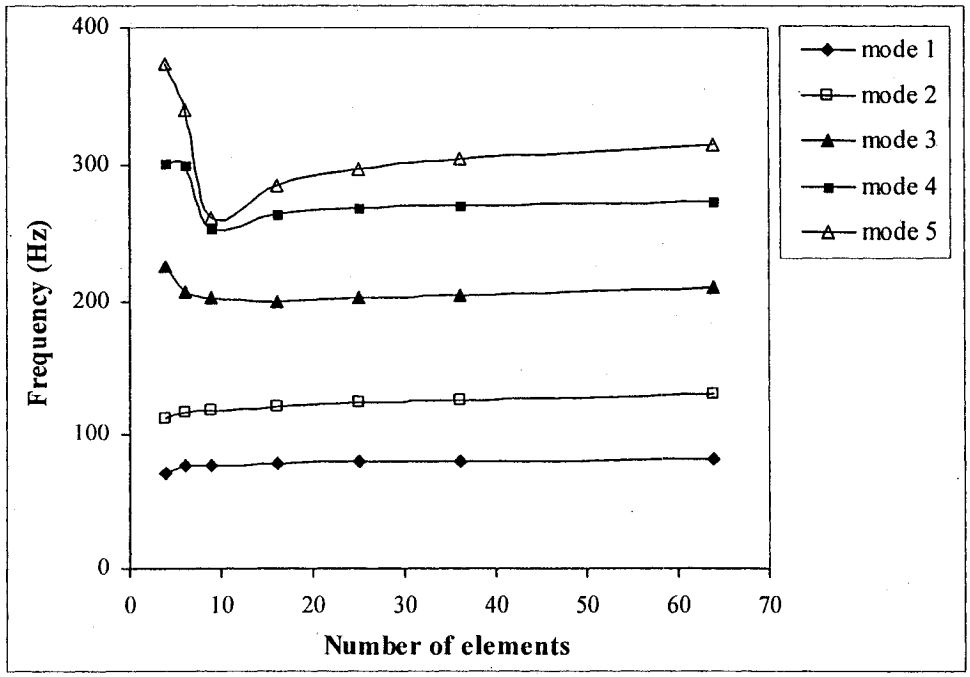

Figure 3.8: The five first natural frequencies of a four-side simply supported plate as a function of number of elements

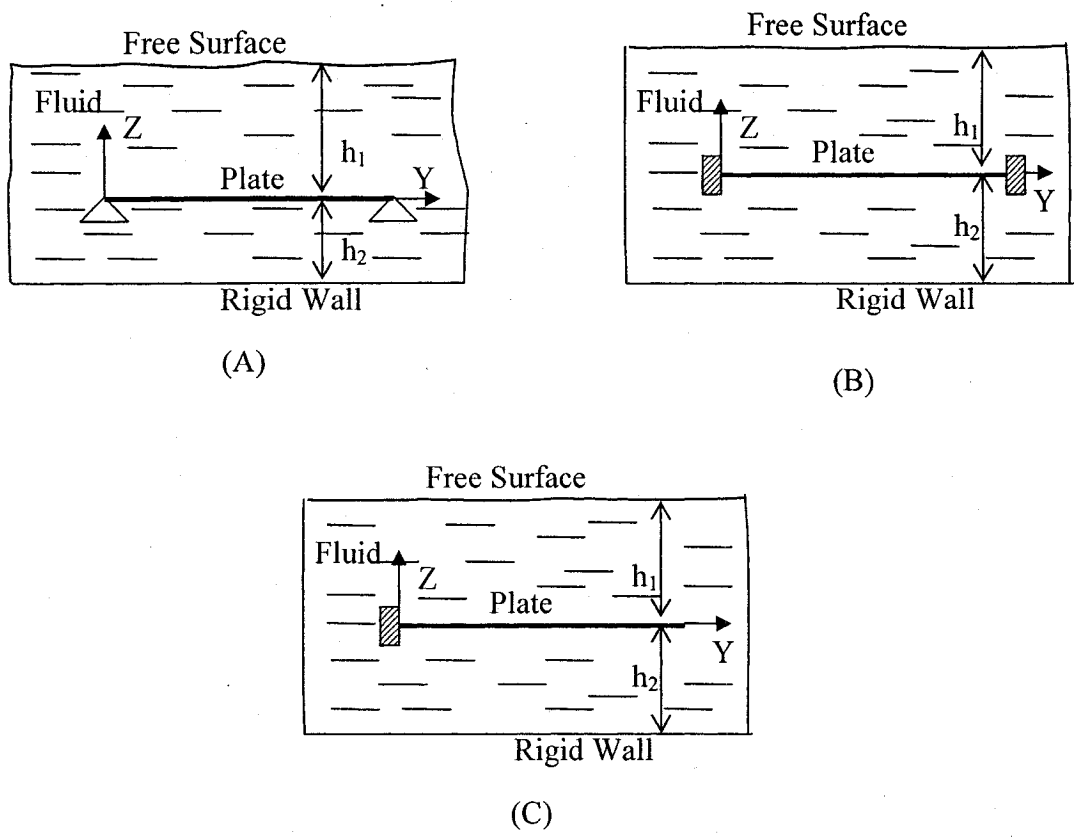

Figure 3.9: Plate boundary conditions, (A) Plate simply-supported at its two short sides (SFSF), (B) plate clamped at its two short sides (CFCF), (C) Cantilever plate (CFFF)

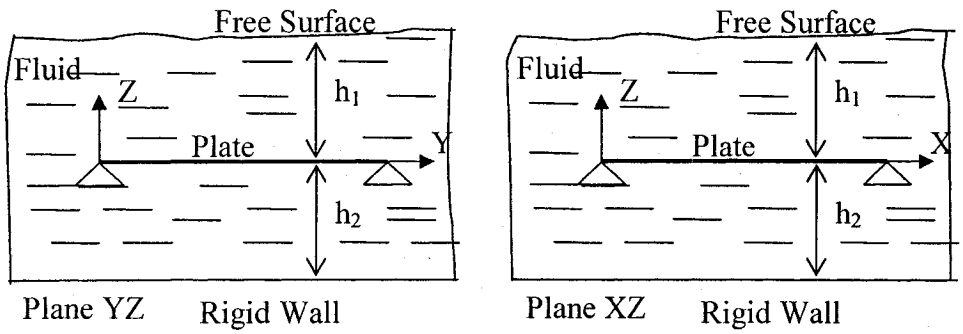

(A)

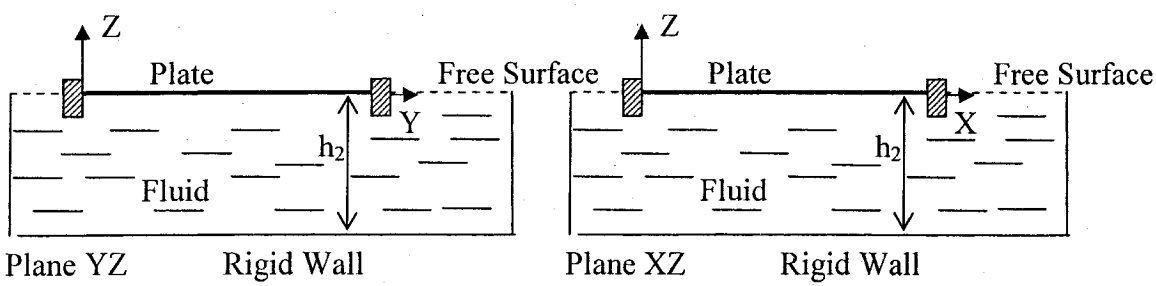

(B)

Figure 3.10: Plate boundary conditions, (A) Simply-supported submerged plate (SSSS), (B) Clamped floating plate (CCCC)

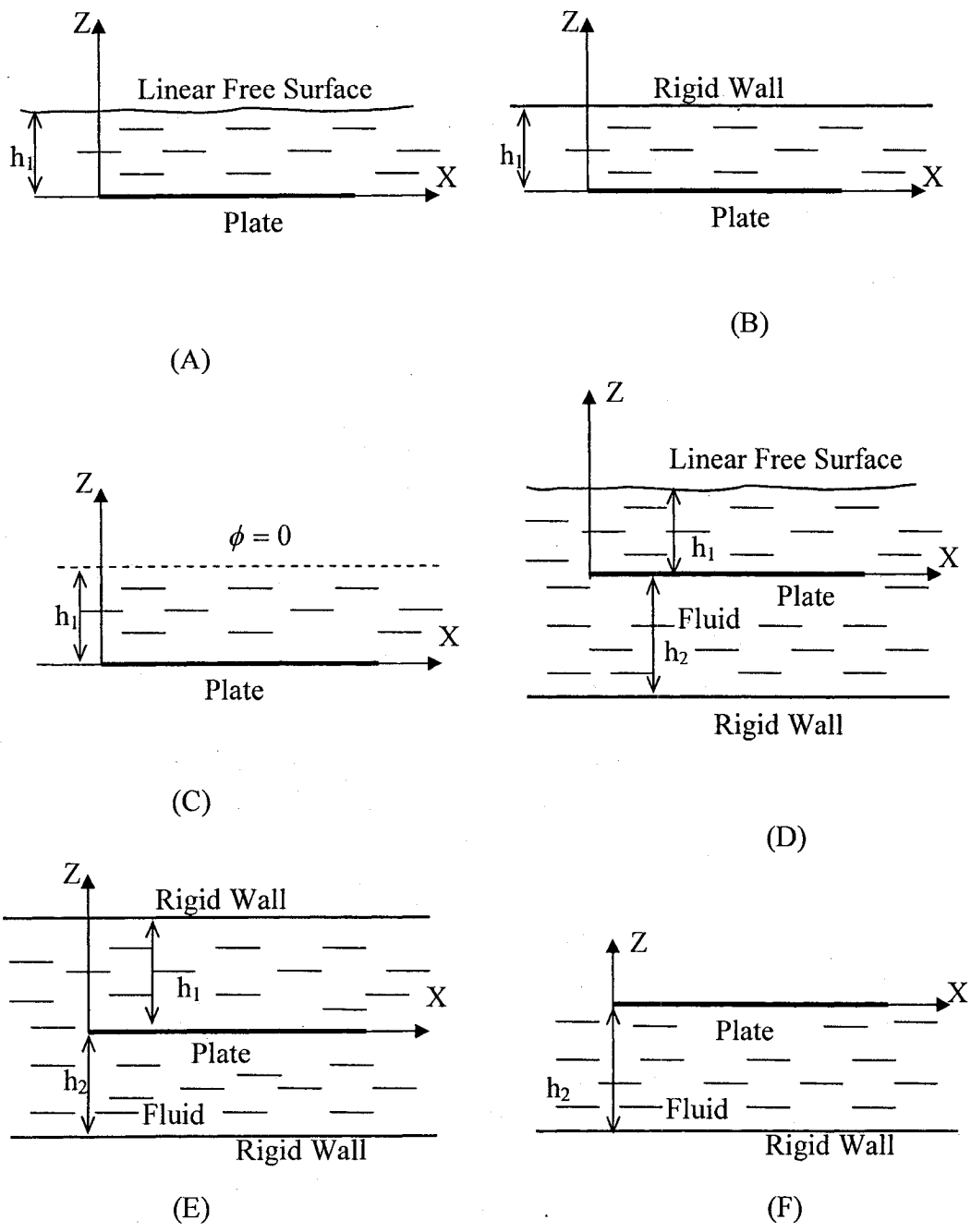

Figure 3.11: Plate boundary conditions used to determine the Z_{fi} coefficients

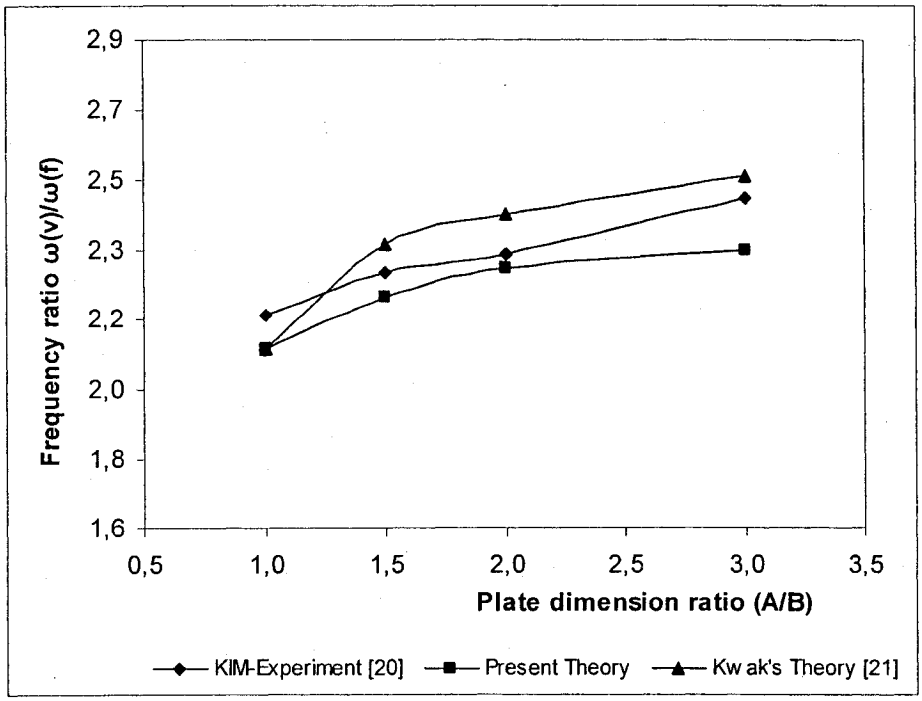

Figure 3.12: Air/fluid fundamental frequency ratio of a plate fixed at its four sides, floating on a fluid free surface, as a function of plate dimension ratio (A/B)

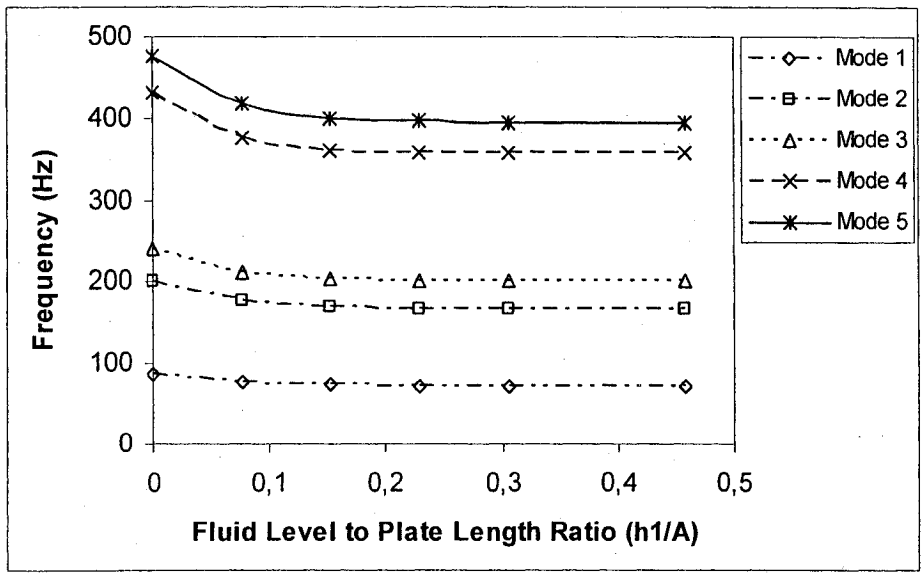

(a)

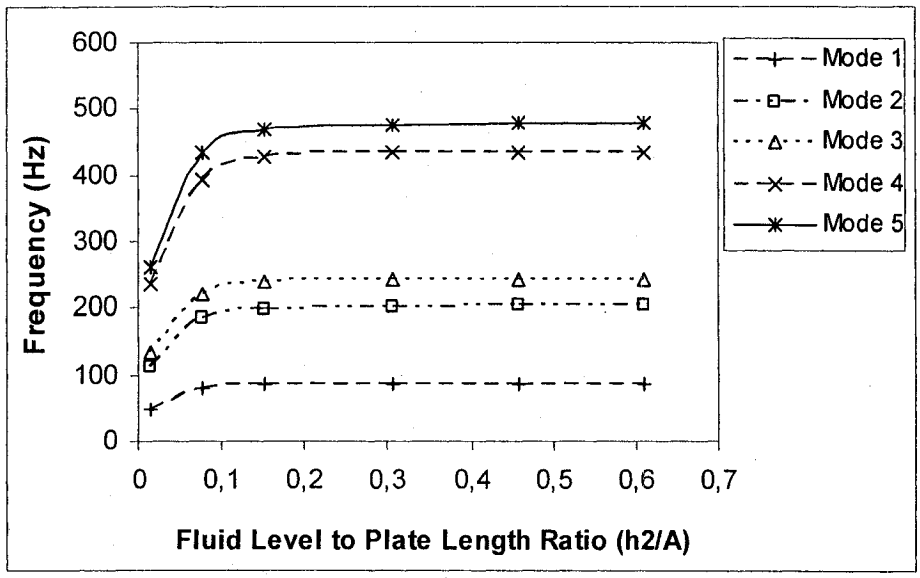

(b)

Figure 3.13: Natural frequency variation as a function of fluid height
(a) Submerged plate (h_1 variable, h_2>>0)
(b) Floating plate (h_1=0, h_2 variable), h_1 and h_2 are the distance between the plate's mean surface and the top and bottom surface of fluid, respectively. The inferior surface is bounded by a rigid wall

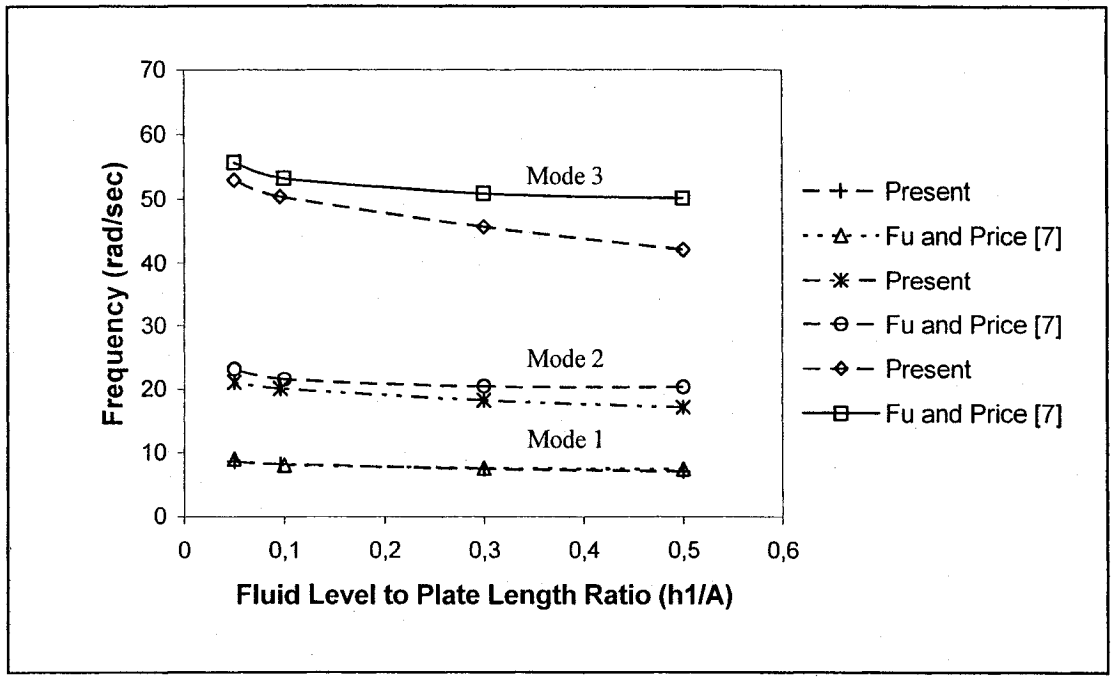

Figure 3.14: Natural frequency variation of a cantilever square plate [5 and 7] as a function of fluid level

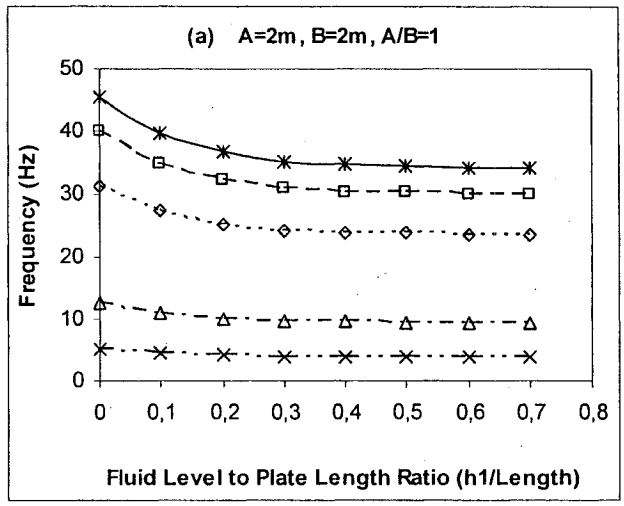

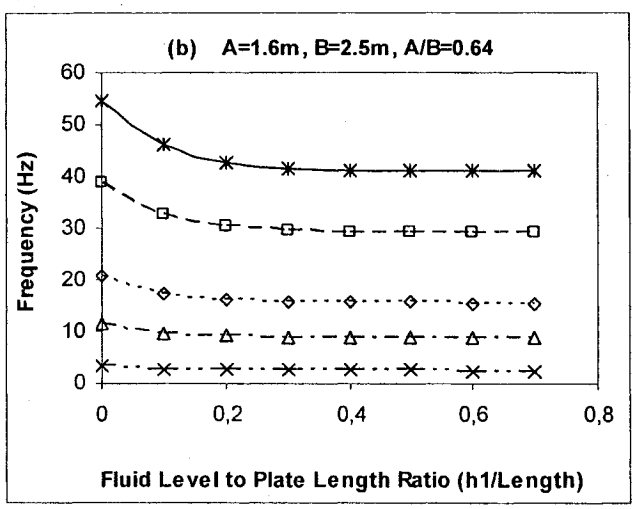

Figure 3.15: Natural frequency variation of a cantilever plate fixed at its long side parallel to the Y axis and submerged in fluid as a function of h_l/length ratio. The fluid is bounded by a far-off rigid wall and a free surface, at h_l level, at the inferior and superior surfaces, respectively (a) A/B=1, (b) A/B=0.64, (c) A/B=4, (d) A/B=0.25, (e) A/B=1.5625. (×) Mode1, (Δ) Mode 2, (◊) Mode 3, (□) Mode 4, (*) Mode 5

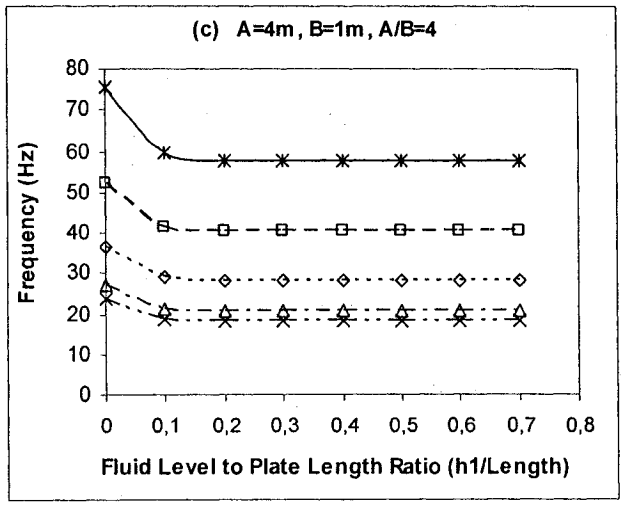

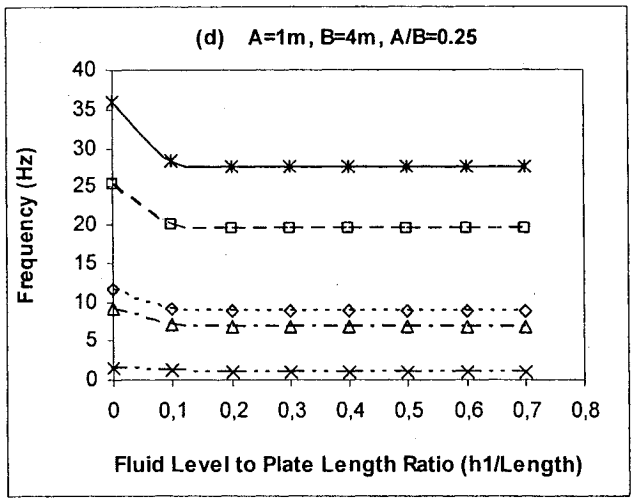

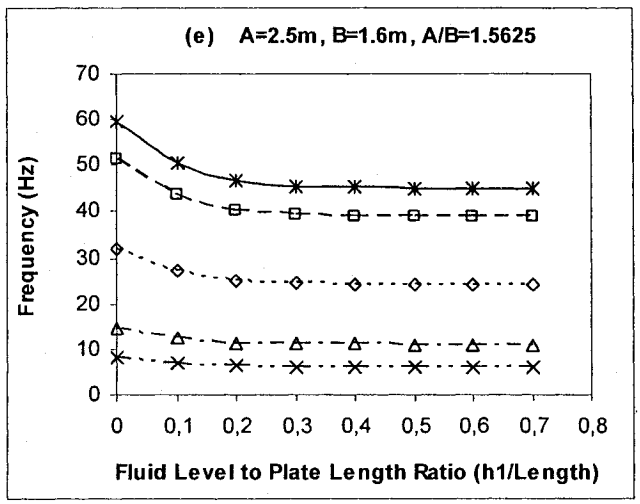

Figure 3.15 : (Suite)

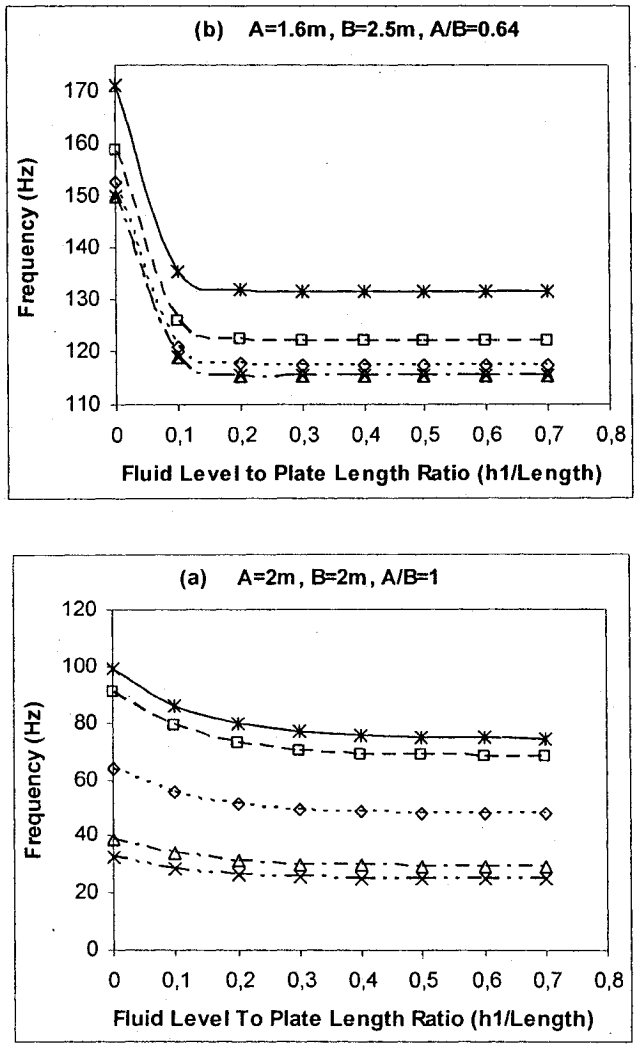

Figure 3.16: Natural frequency variation of a plate fixed at two opposite sides parallel to the Y axis and free at the other two, submerged in fluid as a function of h_1/ length ratio. The fluid is bounded by a far-off rigid wall and a free surface, at h_1 level, at the inferior and superior surfaces, respectively (a) A/B=1, (b) A/B=0.64, (c) A/B=4, (d) A/B=0.25, (e) A/B=1.5625 (×) Mode1, (Δ) Mode 2, (◊) Mode 3, (□) Mode 4, (*) Mode 5

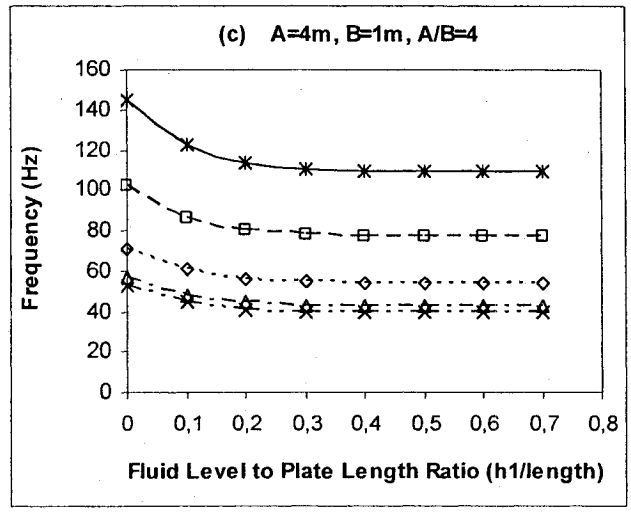

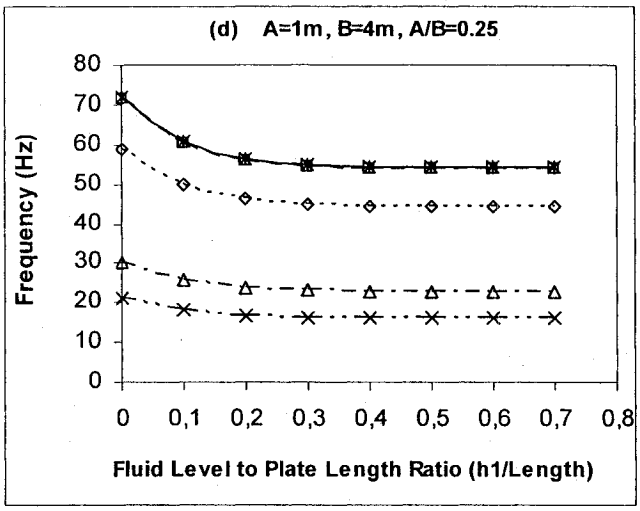

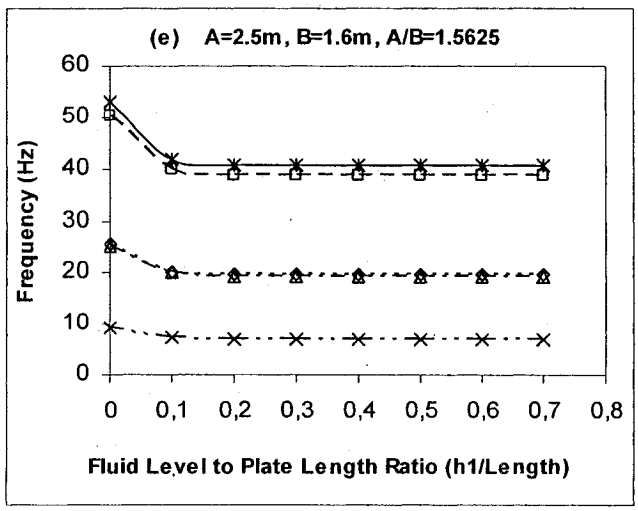

Figure 3.16: (Suite)

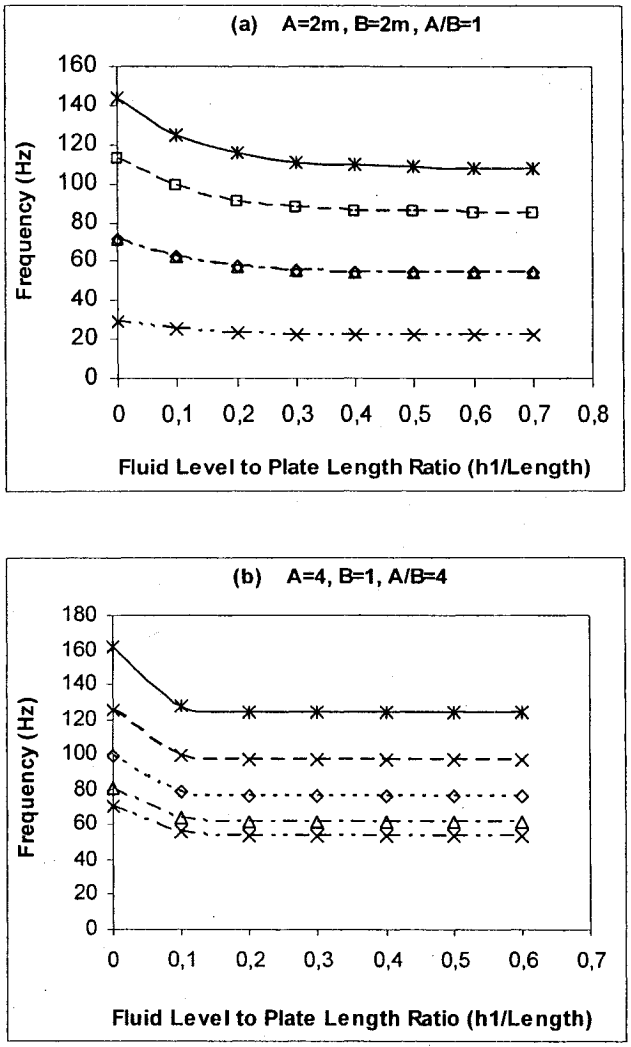

Figure 3.17: Natural frequency variation of a four-side simply supported plate submerged in fluid as a function of h_l/ length ratio. The fluid is bounded by a far-off rigid wall and a free surface, at h_l level, at the inferior and superior surfaces, respectively, A/B=1, (b) A/B=4, (c) A/B=1.5625, (×) Mode1, (Δ) Mode 2, (◊) Mode 3, (□) Mode 4, (*) Mode 5

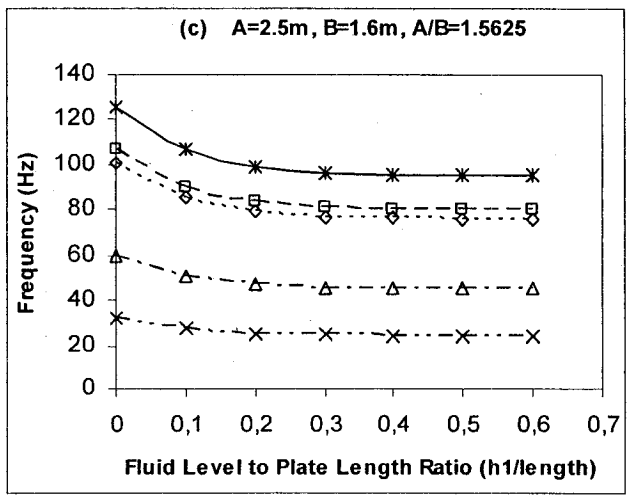

Figure 3.17 (Suite)

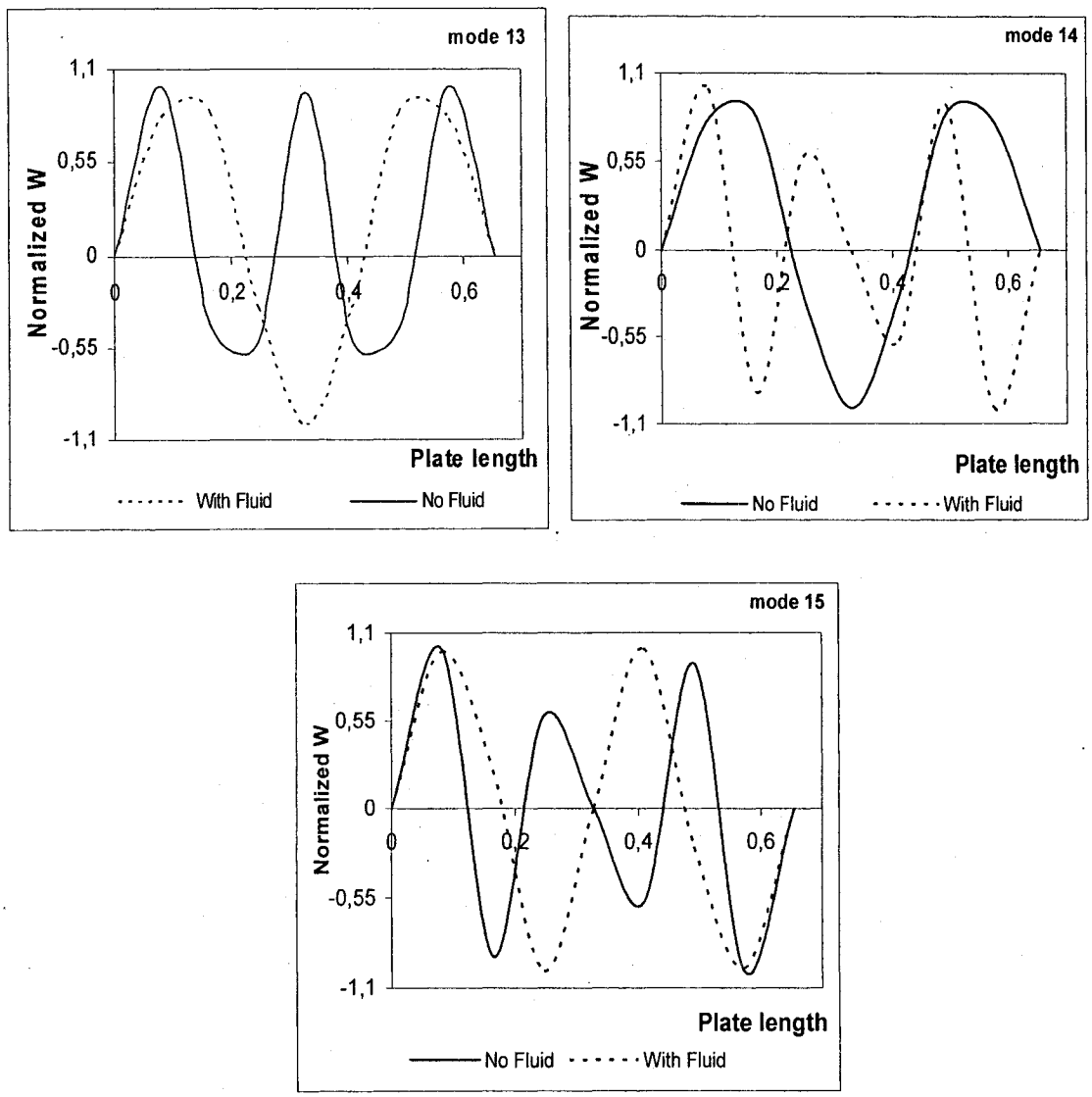

Figure 3.18: Normalized displacement of a plate, clamped at two-opposite-short sides, submerged in fluid

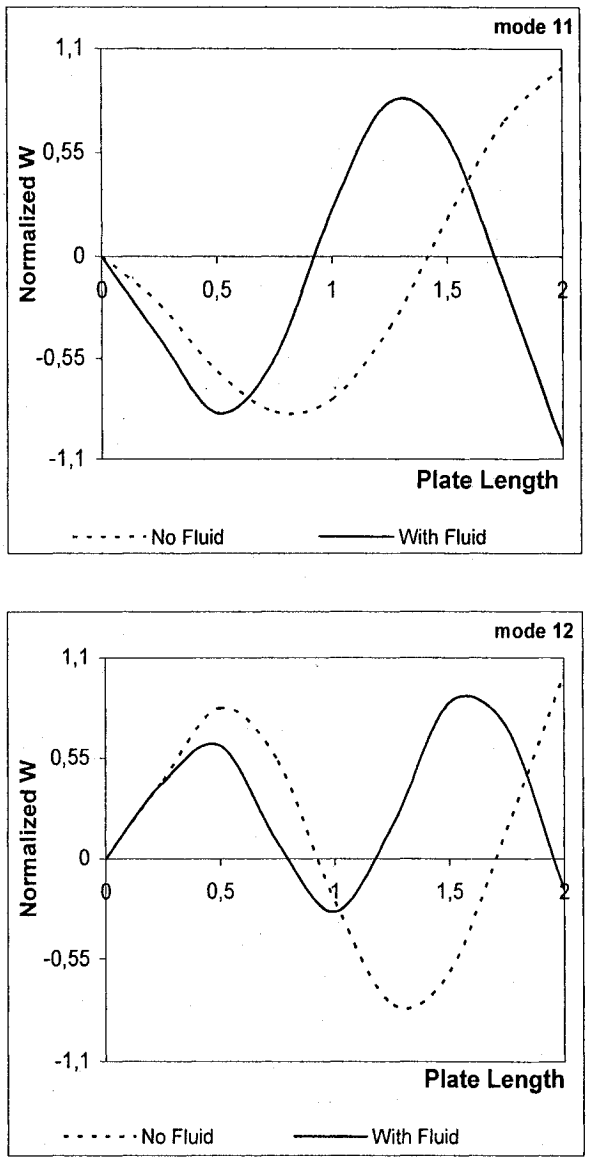

Figure 3.19: Normalized displacement of a cantilever plate submerged in fluid

CHAPITRE IV

COMPUTATIONAL MODELING OF COUPLED FLUID-STRUCTURE SYSTEMS WITH APPLICATIONS

Y. Kerboua[1], A.A. Lakis[1], M. Thomas[2], L. Marcouiller[3]

1. *Mechanical Engineering Dept., École Polytechnique de Montréal, Canada*
2. *Mechanical Engineering Dept., École de Technologie Supérieure, Canada*
3. *Institut de Recherche d'Hydro Québec, Montréal (Québec) Canada*

(Soumis pour publication dans **Computers and structures**)

4.1 Abstract

This paper outlines the development of a computational model in order to analyse the dynamic behaviour of a coupled fluid-structure systems such as a) liquid containers, b) a set of parallel /or radial plates used as hydraulic turbine /or turbo-reactor blades subjected to fluid forces. In this work, a fluid-solid element with using simultaneously the membrane and bending effects of plate element is developed. The structural mass and stiffness matrices are determined using exact integration of governing equations based on a classical theory of plates and finite element approach. The Bernoulli equation and velocity potential function are used to describe the liquid pressure applied on the solid-fluid element. Impermeability condition assures a permanent contact at the fluid-

structure interface. The applications of this model are presented for both parallel and radial plates as well as the fluid filled cylindrical and rectangular reservoirs. The effect of physical and geometrical parameters on the dynamic behavior of coupled fluid-structure system is investigated. The results indicate that the dynamic characteristics, i.e. natural frequency, obtained by this investigation are in a good agreement with corresponding results of other theories and experiments.

4.2 INTRODUCTION

Plates and shells constitute important components of the complex structures and are of great significance to modern constructions engineering, aerospace and aircraft structures, nuclear power plant components, naval structures to name a few. Therefore, knowledge of dynamic characteristics of structural components is of great interest in the study of structural responses to the various excitations.

Knowledge of the vibration characteristics of coupled fluid-structure systems is also of considerable practical interest since they have been used extensively in a various sectors of industry. One of the major concerns of axial-flow turbo-machine design is the minimization of the structural vibration of rotor/stator blades in presence of fluid media. The common design approach against blade structural vibration is to choose the optimal combination of operational and geometric design parameters of the rotor/stator pair so that blade vibration is minimal.

The structural systems composed of parallel plates, the cylindrical or rectangular reservoirs as well as turbine hub (dawn) are all of shell structural type. Often these

structures work in interaction with a stationary /or flowing fluid that considerably influences the structural dynamic responses.

The first works in the fluid-structure interaction domain were developed in nineteenth century by Rayleigh [1] and Lamb [2]. These works constitute the fundamental theory of fluid-filled cylindrical /or spherical shells. Later, Berry and Reissners [3] studied the behaviour of a fluid-filled cylindrical shell under pressure. Vibration analysis of partially fluid-filled cylindrical shells was investigated by Lindholm et al. [4]. Coale and Nagano [5] studied the axisymmetric vibrations of a cylindrical shell joined to a spherical shell; both were filled with liquid. Lakis and Paidoussis [6] developed a circumferential hybrid element based on the classical shell theory to dynamic analysis of a partially fluid-filled cylindrical shell. Néagu and Lakis [7] studied the same problem as Lakis and Paidoussis [6] while taking into account the effect of free surface motion of fluid. The vibration responses of an orthotropic cylindrical shell filled with an incompressible fluid were calculated by Jain [8]. In this work, the effect of transverse shear deformation and rotary inertia is taken into account. Amabili and Dalpiaz [9] developed an analytical approach to model a horizontal cylindrical shell partially /or fully filled with fluid and they also carried out some experimental tests. The effects of free surface parallel to the shell axis were also studied by Amabili [10]. Selmane and Lakis [11] developed a longitudinal hybrid element to dynamic analysis of open /and closed horizontal cylindrical shell partially /or fully filled with a liquid. The same element was used by Bursuc and Lakis [12] to study the effect of the free surface motion in case of partially fluid-filled horizontal cylindrical shell. Mistry and Menezes [13] used the finite element method to

model a fluid-filled cylindrical shell. The structural element is axi-symmetric to two nodes and liquid element is axi-symmetric to eight nodes. Yamaki et al. [14] studied the partially fluid-filled cylindrical shell fixed at two sides.

The circular and rectangular plates in interaction with fluid made the object of a large number of research works since the beginning of the twentieth century [1]. The effects of boundary conditions, free surface of fluid, and fluid level as well as the membrane effect have been studied on basis of experiments and computational approaches [15-23]. A detailed bibliographic survey on the plate dynamic behaviour in interaction with the stationary fluid is outlined in reference [24].

Jeong et al. [25] analytically studied the dynamic behaviour of two identical and parallel circular plates coupled with the movement of an ideal incompressible fluid using the Rayleigh method. The two elastic plates form the both ends of a rigid fluid-filled cylindrical shell. Some precise results were obtained in case of in-phase modes whereas out-of-phase modes results were dissatisfactory except for mode m=0. In order to improve the out-of-phase lateral vibration frequencies, Jeong [26] applied the Fourier-Bessel's finite set and Rayleigh-Ritz's approach to reanalyse his former model where the obtained results were very satisfactory. The influence of the fluid height between the two plates on the dynamic behaviour is also studied. It is concluded that when the height of fluid between the two plates increases, in-phase frequencies decrease and out-of-phase frequencies increase.

Jeong et al. [27] studied the case of two identical and parallel rectangular plates coupled with the movement of fluid. The two plates are fixed to the rigid walls of a reservoir

containing an ideal, incompressible fluid. The lateral vibrations in both in-phase and out-of-phase modes are considered. Each in-phase mode is a combination of beam-mode in air and each out-of-phase mode is approached by polynomials satisfying plate boundary conditions and the conservation of the fluid mass. The natural frequencies of coupled system are calculated using Rayleigh's method.

Kim and Lee [28] analysed the hydro-elastic behaviour of an open rectangular reservoir completely filled with water based on the MSC/NASTRAN DMAP's formulation. Only the first two frequencies for the in-phase and out-of-phase modes are analytically calculated.

Bauer [29] studied the hydro-elastic behaviour of a completely /or partially fluid-filled rectangular reservoir. This container is composed of rigid lateral walls and an elastic plate that forms its base. He also treated the case where the base of the tank is rigid and the free face of fluid is covered by an elastic plate or a flexible membrane.

Cheng and Zhou [30] calculated the natural frequencies of a plate forming the base of an open rectangular reservoir completely filled of liquid. The fluid free surface effect is not considered in that calculation. They applied the Ritz's method to dynamic analysis of this fluid-structure model. The rigid plate used at the base of a rectangular reservoir is modelled as a plate in contact with an infinite fluid domain.

The dynamic behaviour of a fluid-filled cylindrical shell, with a circular elastic plate at its base, considering the fluid free surface effect is studied by Cheng and Zhou [31]. The velocity potential function is used to model the fluid media and the Galerkin approach is adopted to calculate the natural frequencies of the coupled system.

The case of the circular plate composing the base of a rigid cylindrical tank filled with fluid was studied by Cheung and Zhou [34] by considering the fluid free surface effect. The velocity potential function is used to model the fluid media and the Galerkin approach is adopted to calculate the natural frequencies of the coupled system.

Mitra and Sinhamahapatra [32] studied the coupled slosh dynamics of fluid-filled containers. They calculated natural frequencies of sloshing and also studied the forced vibration responses of the fluid-structure system. They used one- and bi-dimensional finite element to model the structure and fluid media, respectively, and applied the weighted residual approach of Galerkin in solving the governing equations.

The objective of this work is to develop a computational model based on a fluid-plate element in order to study the dynamic responses of a fluid-structure systems, i.e. a set of parallel/ or radial plates which could represent turbine blades, that are in contact with an incompressible and non-viscous fluid. This new element permits us also to calculate the high and the low frequencies of the system with precision and it can take into account any combination of boundary conditions without changing the displacement field. This element is applied in order to simulate a number of industrial structures, i.e. cylindrical and rectangular reservoirs, a set of parallel /or radial plate in air or submerged in fluids.

4.3 STRUCTURAL MODELING

4.3.1 Mass and stiffness matrices of plate in local co-ordinates

A typical finite element in its local coordinates is shown in Figure (4.1). Each element is presented by four nodes and five degrees of freedom at each node consisting of three displacements and two rotations. The displacement functions in-plane (membrane) are presented by bilinear polynomials and those out-of-plane (bending) are derived from the plate's equation of equilibrium, see References [24, 33] for more details. The in-plane displacement field is defined as:

$$\begin{aligned} U(x,y,t) &= C_1 + C_2\frac{x}{A} + C_3\frac{y}{B} + C_4\frac{xy}{AB} \\ V(x,y,t) &= C_5 + C_6\frac{x}{A} + C_7\frac{y}{B} + C_8\frac{xy}{AB} \end{aligned} \tag{4.1}$$

where U and V are the displacement components of the reference surface in X and Y directions, respectively. A and B are the plate dimensions in X and Y directions. The transversal displacement component of the reference surface is defined as:

$$W(x,y,t) = \sum_{j=9}^{20} C_j e^{i\pi\left(\frac{x}{A}+\frac{y}{B}\right)} e^{i\omega t} \tag{4.2}$$

where W is the out-of-plane (bending) displacement component, ω is the natural frequency in rad/sec, i is the complex number i^2=-1, and C_i are the unknown constants. The transversal displacement W defined in equation (4.2) can be expressed in the Taylor's expansion set.

$$W(x,y,t)=C_9+C_{10}\frac{x}{A}+C_{11}\frac{y}{B}+C_{12}\frac{x^2}{2A^2}+C_{13}\frac{xy}{AB}+C_{14}\frac{y^2}{2B^2}+C_{15}\frac{x^3}{6A^3}+C_{16}\frac{x^2y}{2A^2B}+C_{17}\frac{xy^2}{2AB^2}+C_{18}\frac{y^3}{6B^3}+C_{19}\frac{x^3y}{6A^3B}+C_{20}\frac{xy^3}{6AB^3} \tag{4.3}$$

Finally, components of the displacement field are defined in the following form:

$$\begin{Bmatrix} U \\ V \\ W \end{Bmatrix} = [R]\{C\} \tag{4.4}$$

where $[R]$ is a matrix of order (3 × 20) given in [38] and $\{C\}$ is the constant vector. These constants can be defined as a function of twenty degrees of freedom of chosen element. Then, substituting the components of constant vector into equation (4.4) leads to the following relationship:

$$\begin{Bmatrix} U \\ V \\ W \end{Bmatrix} = [R][A]^{-1}\{\delta\} \tag{4.5}$$

where $[A]^{-1}$ is a matrix of order (20 × 20) defined in [38], $\{\delta\}$ is the displacement vector of finite element given in [38].

Introducing the displacement components defined by equation (4.5) into the deformation vector, one obtains the following equation that describes the deformation vector as a function of nodal displacements.

$$\{\varepsilon\} = [Q][A]^{-1}\{\delta\} \tag{4.6}$$

where $[Q]$ is a matrix of order (6 × 20) given in [38]. The stress vector is defined as the following relation:

$$\{\sigma\} = [P]\{\varepsilon\} \tag{4.7}$$

where $[P]$ is the elasticity matrix (6 × 6) whose components are given in [24].

Using equations (4.5 to 4.7), the stiffness and mass matrices in the local co-ordinates of developed element are expressed by the following equations:

$$\begin{aligned} [k]^e &= [[A]^{-1}]^T \left(\int_0^{y_e} \int_0^{x_e} [Q]^T [P][Q] dxdy \right) [A]^{-1} \\ [m]^e &= \rho_s h [[A]^{-1}]^T \left(\int_0^{y_e} \int_0^{x_e} [R]^T [R] dxdy \right) [A]^{-1} \end{aligned} \tag{4.8}$$

where ρ_s is the structural density, x_e and y_e are the element dimensions in X, and Y directions, respectively (see Figure 4.1).

4.3.2 Transformation matrix

As shown in Figure (4.2), the finite element is defined in its local co-ordinates, (X ; Y ; Z), that are not coincide with the global axes of the coupled fluid-structure system ($\bar{X}, \bar{Y}, \bar{Z}$). Therefore, the local mass and stiffness terms must be transformed to the global system before assembling into the global matrices that will describe the dynamic equations of motion. The displacement vector at each node in local co-ordinates may be defined as:

$$\{\delta_i'\} = \{U_i, V_i, W_i, \partial W_i/\partial x, \partial W_i/\partial y, 0\}^T \tag{4.9}$$

The nodal displacement relationships between the local and global co-ordinates are expressed by the following equation:

$$\{\delta_i'\} = \begin{bmatrix} cos(X,\bar{X}) & cos(X,\bar{Y}) & cos(X,\bar{Z}) & 0 & 0 & 0 \\ cos(Y,\bar{X}) & cos(Y,\bar{Y}) & cos(Y,\bar{Z}) & 0 & 0 & 0 \\ cos(X,\bar{X}) & cos(Z,\bar{Y}) & cos(Z,\bar{Z}) & 0 & 0 & 0 \\ 0 & 0 & 0 & -cos(Y,\bar{Y}) & -cos(Y,\bar{X}) & -cos(Y,\bar{Z}) \\ 0 & 0 & 0 & cos(X,\bar{Y}) & cos(X,\bar{X}) & cos(X,\bar{Z}) \\ 0 & 0 & 0 & cos(Z,\bar{Y}) & cos(Z,\bar{X}) & cos(Z,\bar{Z}) \end{bmatrix} \{\bar{\delta}_i\} = [T_i]\{\bar{\delta}_i\} \tag{4.10}$$

where $[T_i]$ is a transformation matrix and $\{\bar{\delta}_i\}$ is the nodal displacement vector in global co-ordinates whose components are given as :

$$\{\bar{\delta}_i\} = \{\bar{U}_i, \bar{V}_i, \bar{W}_i, \beta_{i,\bar{X}}, \beta_{i,\bar{Y}}, \theta_{i,\bar{Z}}\}^T \tag{4.11}$$

With application of equation (4.10) for all four nodes (i, j, k, l), one can obtain the following relation that describes the displacement components of each element in the global system.

$$\{\delta'\} = \begin{bmatrix} [T_i] & 0 & 0 & 0 \\ 0 & [T_j] & 0 & 0 \\ 0 & 0 & [T_k] & 0 \\ 0 & 0 & 0 & [T_l] \end{bmatrix} \{\bar{\delta}\} = [T^e]\{\bar{\delta}\} \tag{4.12}$$

where $\{\delta'\}$, $\{\bar{\delta}\}$ are the displacement vector of each element in the local and global co-ordinates. Consequently, the stiffness and mass matrices of each element in the global co-ordinates are determined by the following equations:

$$\begin{aligned} [\bar{k}]^e &= [T^e]^T [k']^e [T^e] \\ [\bar{m}]^e &= [T^e]^T [m']^e [T^e] \end{aligned} \tag{4.13}$$

where $[k']^e$ and $[m']^e$ are the stiffness and mass matrices of element, calculated by equation (4.8), and $[\bar{k}]^e$ et $[\bar{m}]^e$ are the corresponding matrices in the global co-ordinates.

4.4 FLUID MODELING

The fluid pressure applied on the structure can be expressed as a function of acceleration of system [24]. The effects of non-flowing fluid can be introduced by an added mass that increases the inertia of coupled system (Figure 4.3).

The set of equations of motion expressing the dynamic behaviour of coupled fluid-structure system is defined by the flowing relation:

$$[[M_s]-[M_f]]\{\ddot{\bar{\delta}}_T\}+[K_s]\{\bar{\delta}_T\}=\{0\} \tag{4.14}$$

where $[M_s]$ and $[K_s]$ are, respectively, the mass and stiffness matrices of structure and $[M_f]$ is the added mass matrix representing the inertia force effect due to the fluid presence, and finally, $\{\bar{\delta}_T\}$ is the global displacement vector.

The fluid-structure element in the local coordinates is shown in Figure (4.3). The boundary condition assures the permanent contact at the fluid-structure interface. To develop the governed dynamic equations in case of fluid-structure interaction, one assumes that the fluid is incompressible, inviscid and irrotational. Therefore, the velocity potential function is used to determine the fluid force relations. The velocity potential function in the Cartesian co-ordinates is expressed as:

$$\frac{\partial^2\phi}{\partial x^2}+\frac{\partial^2\phi}{\partial y^2}+\frac{\partial^2\phi}{\partial z^2}=0 \tag{4.15}$$

where ϕ is the velocity potential function.

Based on forgoing conditions, the Bernoulli equation at the fluid-structure interface is defined as:

$$\left.\frac{\partial \phi}{\partial t}+\frac{P}{\rho_f}\right|_{z=0}=0 \tag{4.16}$$

The fluid pressure at interface is expressed as:

$$P|_{z=0}=-\rho_f \left.\frac{\partial \phi}{\partial t}\right|_{z=0} \tag{4.17}$$

Using the mathematical technique of separation of variables, the velocity potential function is defined by the following relationship:

$$\phi(x,y,z,t)=F(z)S(x,y,t) \tag{4.18}$$

At the fluid-structure interface, the impermeability conditions, which assures the permanent contact between the fluid and structure, is defined by:

$$\left.\frac{\partial \phi}{\partial z}\right|_{z=0} = \frac{\partial W}{\partial t} \tag{4.19}$$

where W *is* the transversal displacement of plate in local co-ordinates and ϕ is the potential flow. Using equations (4.18) and (4.19), one can express the potential function as follow:

$$\phi(x,y,z,t) = \frac{F(z)}{dF(0)/dz}\frac{\partial W}{\partial t} \tag{4.20}$$

To determine the potential function, one has to calculate the function F(z). Substituting equation (4.20) into equation (4.15), one obtains the following differential equation:

$$\frac{d^2F(z)}{dz^2} - \mu^2 F(z) = 0 \tag{4.21}$$

With

$$\mu = \pi\sqrt{\frac{1}{A^2} + \frac{1}{B^2}}$$

where A and b A, B are the plate length along the X and Y directions, respectively.

The function F(z) is obtained by solving the differential equation (4.21). The general solution of F(z) is defined as:

$$F(z) = A_1 e^{\mu z} + A_2 e^{-\mu z} \tag{4.22}$$

Substituting equation (4.22) into equation (4.20), one obtains the following expression for the velocity potential function.

$$\phi(x,y,z,t) = \frac{\left(A_1 e^{\mu z} + A_2 e^{-\mu z}\right)}{dF(0)/dZ} \frac{\partial W}{\partial t} \tag{4.23}$$

The fluid boundary conditions are, separately, introduced for each element that allows us to investigate the dynamic behaviour of totally or partially fluid-filled structures as well as the submerged structures. The potential function ϕ has to verify the boundary conditions at the various locations, i.e. (z=0, or z=h_1) of each element (Figure 4.3). The coupled fluid-structure system can take various forms. The solution of equation (4.23) is already developed for some cases [38] in which the upper surface of fluid is bounded by free surface /or a rigid wall (see Appendix A). In the following sections, the solution of equation (4.23) will be applied to two parallel or radial walls that are in contact with fluid.

4.4.1 Fluid-solid element for the parallel /and radial plates

In case of a rectangular reservoir, (Figures 4.5 and 4.12) as well as in case of parallel plates (Figures 4.6 and 4.7) and radial plates (Figure 4.9), the fluid interacts at inner part of elastic walls. These components can vibrate according to in-phase or out-of-phase modes with each other. The impermeability condition for each element of fluid-structure

system remains unchanged, while the boundary conditions vary in terms of vibrational modes. Both cases are discussed, hereafter.

4.4.1.1 In-phase vibrational mode of parallel plates

In case of in-phase vibration of two walls (see Figure 4.4), the boundary condition at the fluid level ($z=h_1$) is defined by the following relation.

$$\left.\frac{\partial \phi}{\partial z}\right|_{z=h_1} = \frac{\partial W}{\partial t} \tag{4.24}$$

Substituting equation (4.23), simultaneously, into equations (4.19 and 4.24), one obtains the constants A_1 and A_2. Introducing these constants into equation (4.23), one can express the following velocity potential function:

$$\phi(x,y,z,t) = \frac{1}{\mu}\left[\frac{(1-e^{-\mu h_1})e^{\mu z} + (1-e^{\mu h_1})e^{-\mu z}}{e^{\mu h_1} - e^{\mu h_1}}\right]\frac{\partial W}{\partial t} \tag{4.25}$$

Substituting relation (4.25) into equation (4.17), the dynamic pressure is expressed as:

$$P = -\frac{\rho_f}{\mu}\left[\frac{2-e^{-\mu h_1} - e^{\mu h_1}}{e^{\mu h_1} + e^{-\mu h_1}}\right]\frac{\partial^2 W}{\partial t^2} = Z_{f4}\frac{\partial^2 W}{\partial t^2} \tag{4.26}$$

When the two walls are radials (Figure 4.8), the given term in the right-side of equations (4.24 to 4.26) must be multiplied by a factor of *cos(α)*, where α is the angle between two walls.

4.4.1.2 Out-of-phase vibrational modes of parallel plates

In case of out-of-plane vibrational modes, the boundary condition at the fluid level ($z=h_1$) is given by:

$$\left.\frac{\partial \phi}{\partial z}\right|_{z=h_1} = -\frac{\partial W}{\partial t} \tag{4.27}$$

Substituting, simultaneously, equation (4.23) into equations (4.19) and (4.27), the constants A_1 and A_2 can be calculated. Introducing these constants into equation (4.23) results in the following expression for the velocity potential function:

$$\phi(x,y,z,t) = \frac{1}{\mu}\left[\frac{(1+e^{\mu h_1})e^{\mu z} + (e^{\mu h_1} + e^{2\mu h_1})e^{-\mu z}}{1-e^{2\mu h_1}}\right]\frac{\partial W}{\partial t} \tag{4.28}$$

The fluid pressure at fluid-structure interface is determined by substitution of the potential function (4.28) into equation (4.17):

$$P = -\frac{\rho_f}{\mu}\left[\frac{1+2e^{\mu h_1}+e^{2\mu h_1}}{1-e^{2\mu h_1}}\right]\frac{\partial^2 W}{\partial t^2} = Z_{f5}\frac{\partial^2 W}{\partial t^2} \tag{4.29}$$

When both walls are elastic and radial (Figure 4.8), the right-hand terms in equations (4.27 to 4.29), must be multiplied by a factor of *cos(α)*, where α is the angle between two walls.

4.5 CALCULATION OF FLUID-INDUCED FORCE

The fluid-induced force vector in the local coordinate can be expressed as:

$$\{F\}^e = \int_A \left[[A]^{-1}\right]^T [R]^T \{P\} dA \tag{4.30}$$

where $\{P\}$ is the vector of fluid pressure acting on the fluid-structure element.

Replacing the transversal displacement component of equation (4.3) into fluid pressure expression, which depends on the case in question, the fluid pressure acting on the structure is obtained as:

$$\{P\} = Z_{fi}[R_f][A]^{-1}\{\ddot{\delta}\} \tag{4.31}$$

where Z_{fi} ($i=1,5$) that depends on the contact mode between the plate and fluid and the boundary conditions at fluid-structure interface as well. The expression Z_{fi} is defined in

Appendix A for i=1 to 3 and also equations (4.26) and (4.29) for cases i=4 and 5. Matrix $[R_f]$ is given in Appendix A.

Replacing pressure expression (4.31) into equation (4.30), the force vector for each element is given by:

$$\{F\}^e = Z_{fi} \int_A \left[[A]^{-1}\right]^T [R]^T [R_f][A]^{-1} dA \{\ddot{\delta}\} = [m_f]^e \{\ddot{\delta}\} \tag{4.32}$$

where dA is elementary surface.

4.6 CALCULATION OF [K_S], [M_S] and [M_F]

The structure is subdivided into a set of quadrilateral elements. The stiffness and mass (solid and fluid) matrices are determined for each element in its local co-ordinates. Then, they are transferred to the global system of co-ordinates in order to assemble in the global matrices that are defined in equation (4.14).

Assuming:

$$\{\bar{\delta}_T\} = \{\bar{\delta}_{0T}\} e^{i\omega t} \tag{4.33}$$

where $\{\bar{\delta}_T\}$ is the global displacement vector, ω is the natural frequency of system (rad/sec) ; and $\{\bar{\delta}_{0T}\}$ is global displacement amplitude vector for each mode.

Substituting equation (4.33) into equation (4.14) leads to the following eigenvalue problem:

$$Det\left[\left[K_s\right]-\omega^2\left[M_s-M_f\right]\right]=0 \tag{4.34}$$

Solution of this system results in the natural frequencies and mode shapes of the structure.

4.7 RESULTS AND DISCUSSIONS

The most studied fluid-structure systems concern plates, cylindrical, spherical or conical shells. Rare works deal with hydro-elastic analysis of complicated structures composed of plate and shell components.

The developed fluid-solid element in this work is used to study the hydro-elastic behaviour of:

a. Two identical parallel plates in interaction with a bounded fluid
b. A set of plates used in a heat exchanger
c. A set of plates fixed at a rigid wall
d. A set of radial plates
e. A set of plates fixed at an elastic wall
f. A vertical rectangular plate gradually submerged in a fluid reservoir
g. An open rectangular reservoir
h. A simplified model of turbine hub (dawn)

i. A clamped cylindrical shell

a. The first structure is a fluid-filled rectangular reservoir that was studied by Jeong et al. [27]. The vessel dimensions given in Figure (4.5) and the plate thickness is h = 2mm. The mechanical properties used in this example are:

$$E = 69 \text{ GPa}, \rho_s = 2700 \text{ kg/m}^3, \nu = 0.3, \rho_f = 1000 \text{ kg/m}^3$$

The lateral walls of the reservoir are rigid. The top and base plates are elastic and fixed to the lateral walls (Figure 4.5). The elastic plates vibrate in the presence of fluid in both in-phase and out-of-phase modes. Some vibration modes are not permitted in order to not violate the mass conservation of incompressible fluid. The results, presented in Table (4.1), show an excellent agreement between the present theory and that of Jeong et al. [27]. Table (4.1) lists natural frequencies for in-phase modes of the two plates coupled with the movement of an incompressible fluid.

The natural frequencies of the two parallel plates coupled with an incompressible fluid and vibrating in out-of-phase mode (0,1) are listed in Table (4.2). Only the frequency corresponding to the mode (0,1) is presented since it reserves the mass conservation that was also met by Jeong et al. [25] in the analysis of two circular plates coupled with fluid. We note that the obtained results are in good agreement with those of Jeong et al. [27].

In connection with dynamic analysis of two identical rectangular plates in interaction with fluid studied by Jeong et al. [27], the displacement field for the in-phase and out-of-phase modes is not the same. Another displacement field is adopted so that the mode shape compensates the change of fluid volume in the Z direction. Therefore, to calculate the other mode one must impose some conditions in the displacement field in such a way

that the assumption for incompressible fluid is respected. This problem arises in the closed structures completely filled with an incompressible fluid.

b. There are some complex structures composed of a set of identical parallel /or radial plates that are in interaction with the fluid i.e. MTR-type flat-plate fuel element in nuclear industry. If the height of fluid between plates is relatively low, the fluid transports the kinetic energy from one plate to another. Therefore, one studies the case of three parallel plates fixed to a rigid wall as shown in Figure (4.6). The material properties are given as:

$$E = 69 \text{ GPa}, \nu = 0.3, \rho_s = 2700 \text{ kg/m}^3, h = 2 \text{ mm}$$

When the system is submerged into a big reservoir, every plate undergoes a different pressure at its two sides caused by the fluid being, respectively, on top and bottom of the plate. In addition, the plates vibrate between them according to in-phase /or out-of-phase modes. For each mode, there is a distinct fluid pressure that is presented in Table (4.3). Among several possible combinations, one distinguishes three modes of vibration of the system. The remainder cases are only repetitions of one of the three modes. Table (4.4) presents the vibrational frequencies according to the three distinct modes of plate. According to these results, we note that the dynamic behaviour of this system can be studied while considering only one plate that vibrates in out-of-phase mode in relation to the two others since this mode provides the lowest frequency [34].

c. The assembled parallel plates are often used in different sector of industry i.e. tubes support plates in steam generator. Figure (4.7) shows a part of a structural system

composed of a set of thin plates having each two parallel sides fixed to the lateral rigid walls. All plates have the same properties and they are distributed uniformly.

Guo and Paidoussis [34] studied an identical system submitted to a flowing fluid in a channel formed by rectangular plates. Here, it is assumed that the fluid velocity is null and only the inertia force due to the fluid is taken into account. They only considered the out-of-phase vibration modes since they are most problematic. One arranges a dimensionless frequency parameter defined by the following expression:

$$\omega = \frac{l}{b^2}\sqrt{\frac{K}{\rho_s h_p}}\,\bar{\omega}$$

where ω is vibration frequency in rad/sec.

Parameters 'h_p', 'b', and 'l' are represented in Figure (4.7). The dimensionless parameters η, ζ, and ψ are defined by the following relations:

$$\eta = \rho_f b/\rho_s h = 1; \qquad \zeta = l/b = 0.5; \qquad \psi = h_p/b = 0.05$$

The structure is discretized into a number of quadrilateral elements. All nodal degrees of freedom belonging to the rigid walls are eliminated. Table (4.5) lists the natural frequencies of fluid-structure model, in case of non-flowing fluid, along with corresponding results of Reference [34]. In out-of-phase mode, the applied pressure on the middle plate is the sum of the calculated pressure acting on the top and bottom plates. Because of the geometrical symmetry, the applied pressure on the top and bottom plates is the same. It is for this reason that the analysis of a set of plates comes back to study only one plate subject to the calculated pressure at out-of-phase vibration mode of side walls.

d. The dynamic behavior of a system composed of several radial plates having one side of each plate welded to a rigid axis as shown in Figure (4.8). The angle between every two plates is 45 degrees. All plates have the same geometrical dimensions and mechanical properties which are given as follows:

$B = 0.655$ m, $A = 0.2016$ m, $h = 9.36$ mm, $E=207$ GPa, $\rho_s = 7850$ kg/m^3

and $\nu = 0.3$

In this structural model, the fluid level on top and bottom of plates vary from one element to another. Considering the axial symmetry of the system and the uniform distribution of plates in the circumferential direction indicates that the dynamic analysis of such system comes back to study only one plate that vibrates according to three different modes in relations with neighbouring plates [34]. The fluid pressures applied, on plate 2, corresponding to each mode of vibration are listed in Table (4.6).

Natural frequencies of this structure without /and with fluid (when totally submerged in a water reservoir) effects according to the three distinct modes are enumerated in Table (4.7).

It is important to note that the dynamic analysis of a set of parallel /or radial plates can be reduced to the dynamic analysis of only one plate when all plates have the same dimensions and the same mechanical properties. In addition, the fluid height has to be even between every two plates and the axis (Figure 4.8) or the wall (Figures 4.6 and 4.7) that attaches all plates together be rigid.

e. The dynamic behaviour of a system represented in Figure (4.6) is studied while assuming that the vertical wall plate is elastic and also no displacement condition is

imposed (free-free). In Table (4.8), we have the natural frequencies in vacuum of the system calculated by our program and by ANSYS software as well as the frequencies corresponding to in-phase mode vibration of the three plates when the system is completely submerged in a reservoir of infinite size. We note that the frequencies are not repeated contrary to the case of the plates clamped to the rigid wall (see Figure 4.6), this repetition is due to the effects of the boundary conditions. In this case, it is necessary to study all the possible combinations of in-phase and out-of-phase mode of the plates.

In the structural systems composed of parallel plates (Figures 4.6 and 4.7), the fluid height between the plates is a very important parameter in fluid-structure interaction problems. Resonance frequency variation as a function of h/L ratio (fluid height /plate length ratio) for the structural system is plotted in Figure (4.9) when the three plates vibrate according to in-phase and out-of-phase. We note that when we increase the fluid-height between the plates the in-phase frequency increases whereas the out-of-phase frequency decreases. This behaviour was underlined by Jeong and al in the case of two circular plates [26] and that of two parallel rectangular plates [27] in interaction with the fluid. As shown in Figure (4.9), the fluid height at which there is no difference between the in-phase and out-of-phase frequencies is equal to the plate length.

f. When a vertical plate is partially immersed in a container of fluid, its behaviour is completely different from that of the horizontal submerged plate studied in reference [24], since the immersed finite elements are subjected to the fluid pressure, on the other hand the dry elements vibrate in vacuum.

The dynamic behaviour of a vertical plate partially or totally immersed in fluid reservoir is investigated (Figure 4.10). Natural frequencies are calculated for a plate vibrating in both air and water. The following boundary conditions are considered:

i.1 A cantilever plate (CFFF)

i.2 A plate fixed at two opposite sides and simply supported at two others (CFCF)

i.3 A plate simply supported at one side and free at other sides (SFFF)

i.4 A plate simply supported at two opposite sides and free at two others (SFSF)

In each case, the vibration analysis is carried out for four levels of immersion (25%, 50%, 75%, 100%). The fluid pressure applied on the submerged part of plate is equal to twice of the pressure expressed by (A.5). In order to validate our model we considered a plate belonging to the series of the cantilevered plates studied experimentally by Lindholm [4]. Its dimensions and mechanical properties are:

$E = 206$ GPa, $\nu = 0.3$, $\rho_s = 7830$ kg/m^3, $\rho_f = 1000$ kg/m^3,

$A = 0.2032$ m, $B = 1.016$ m and $h = 4$ mm

The obtained frequencies are listed in Table (4.9). It is noted that results are in good agreement with those of Lindholm [4]. One underlines that the natural frequency of a cantilever plate significantly decreases when the immersed part is less than of plate's half-length.

To investigate the boundary condition effects on the dynamic behaviour of the vertical submerged plates, the same plate as forgoing example is considered by changing the boundary conditions and calculated results are presented in Figure (4.11). We note that the plates supported on two sides (SFSF and CFCF) undergo to a significant change in

natural frequencies of the first three modes when the level of immersion is situated between 25% and 75%. Below 25% the influence of fluid is insignificant. On the other hand for plates supported on only one side (CFFF and SFFF), the fluid presence has a very important influence on frequencies even at a level of immersion below 25%. From the fourth mode, frequency decreasing is almost linear for all four plates. The natural frequencies change slightly, whatever the boundary conditions are, for immersion level above 75% of plate length.

g. Kim and Lee [28] studied the hydro-elastic behaviour of an open rectangular reservoir completely filled with water. Vessel geometry and its dimensions are given in Figure (4.12). The plates perpendicular to the Y-axis and the base plate are supposed rigid, but those perpendiculars to X-axis are elastic and simply supported at four sides. The material properties are:

$$E = 200 \text{ GPa}, \nu = 0.3, \rho_s = 7970 \text{ kg/m}^3, h = 5 \text{ mm}, \rho_f = 1000 \text{ kg/m}^3$$

The natural frequencies of fluid-filled reservoir calculated by Kim and Lee [28] are only given for in-phase modes and the first out-of-phase mode. Referring to Kim and Lee's results (Table 4.10), it is noted that the frequency for in-phase modes is more precise than the frequency of out-of-phase mode. One says that our solution is more exact since when the ratio between the height of the fluid and reservoir dimensions passes at certain value, there is no difference between in-phase and out-of-phase modes, which was confirmed in this work (see Figure 4.9).

h. The dynamic characteristics of a simplified two-wing structure shown in Figure (4.13) are calculated in this example. The structure (bird) is composed of two plates in

aluminium welded to a solid box made of same material whose mechanical properties are:

$$E = 72 \text{ GPa}, \nu = 0.3, \rho_s = 2720 \text{ kg/m}^3, h = 3.2\text{mm}$$

This structure made the object of an experimental work [36] in which the tests firstly were performed in air and with the free-free conditions; a suspension system was conceived to assure these limit conditions. This structure is also studied to the laboratory of the IREQ (Institute of research of hydro Quebec).

The developed element is used to calculate the natural frequencies of this structure in vacuo while adapting the program to consider a variable thickness from one element to another. The obtained results are listed in Table (4.11). It is noted that the determined results on basis of present theory are very precise and agree with those of ANSYS software.

An experiment is also carried out for this structure submerged in an open rectangular reservoir with free surface on top and a rigid wall at the base of vessel. The fluid height was 37.5 cm. The numerical and experimental results are listed in Table (4.11). It is important to note that at out of this fluid height the structural frequencies do not change when one increases the level of fluid on the plate [24].

We calculated the vibration frequencies of the same structure completely submerged in water while satisfying the same boundary conditions imposed during the experimental tests. The applied water pressure on the walls is the sum of the pressure applied by the fluid on the upper and lower surfaces of structure expressed by the equations (A.3) and

(A.5), respectively. The results listed in Table (4.11) reveal that the frequencies calculated by our model are in good agreement with those obtained experimentally [36].

i. The dynamic behaviour of a cylindrical shell fixed at its two ends (Figure 4.14) is investigated in this example. The effect of geometrical parameter on the natural frequency of this structure is also verified. The results are listed in Table (4.12) along with those of [35] that show a good agreement between two models. The mechanical properties of cylindrical shells are

$$E = 206 \text{ GPa}, \nu = 0.3, \rho_s = 7680 \text{ kg/m}^3, \rho_f = 1000 \text{ kg/m}^3$$

4.8 CONCLUSIONS

A new element is developed to dynamic analysis of a coupled fluid-structure system i.e. 'n' parallel or radial plates open and closed rectangular reservoirs, and cylindrical shells. The structure may be empty, partially or completely filled with fluid or submerged in a liquid. The structural mass and stiffness matrices are determined by exact analytical integration. The fluid pressure applied on structure is expressed according to the acceleration of the transverse displacement of the structure and the density of the fluid.

It is noted that the increase of the fluid height results in a reduction of frequencies for in-phase modes and an increase of frequencies for out-of-phase modes. This behaviour is underlined by Jeong et al. for the case of two circular plates and also two parallel rectangular plates in interaction with the fluid. It is noted that when the height of the fluid is equal to the length of the plate, there is no difference between the in-phase and out-of-phase modes. It means that the fluid transports the kinetic energy from one plate

to another along a limited distance. According to Figure (9.b), the same behaviour is also valid for the system of three plates attached to an elastic wall.

While calculating frequencies and vibration modes of several structures having the different geometry, it is proved that the utilisation of developed computational approach is a powerful and reliable tool to dynamic analysis of a variety of plate and shell structures. While comparing our results with those of the other researchers, either analytical or experimental works, we can conclude that the developed fluid-structure element results in satisfactorily results. This element can be applied to vibration analysis of non-uniform structures supported by any combinations of various boundary conditions.

The major importance in this work is to verify the applicability of this element to represent the hydro-elastic behaviour of different structures. The next step is to apply this element to study the effect of other aspects i.e. material and structural discontinuity, structural curvature on the dynamic responses of coupled fluid-structure systems.

4.9 REFERENCES

1. J.W.S. Lord Rayleigh, '*Theory of Sound*', New-York: Dover, second edition (First edition, 1877), 1945.
2. H. Lamb, '*Hydrodynamics*', New York Dover Publications sixth edition, 1945.
3. J. G. Berry, E. Reissner, '*The effect of an internal compressible fluid column on the breathing vibrations of a thin pressurized cylindrical shell*', Journal of Aerospace Science N 25,P288-294, 1958.
4. U. S. Lindholm, D. D. Kana, H. N. Abramson. '*Breathing vibrations of a circular cylindrical shell with an internal liquid*', Journal of the Aerospace Sciences N 29. P1052-1059, 1962.
5. C. W. Coale, M. Nagano, '*Axisymmetric modes of an elastic cylindrical-hemispherical tank partially filled with liquid*', AIAA Symposium on Structural Dynamics and Aeroelasticity, 1965.
6. A.A. Lakis, M.P. Paidoussis, '*Free vibration of cylindrical shells partially filled with liquid*', Journal of Sound and Vibration, V19, N1, P1-15, 1971.
7. A.A. Lakis, S. Neagu, '*Free surface effects on the dynamics of cylindrical shells partially filled with liquid*', Journal of Sound and Vibration, V207, N2, P175-205, 1997.
8. R. K . Jain, '*Vibration of fluid filled orthotropic cylindrical shells*', Journal of Sound and Vibration N39, P379-388, 1974.

9. M. Amabili, G. Dalpiaz, '*Breathing vibrations of a horizontal circular cylindrical tank shells partially filled with liquid*', Transactions of the American Society of Mechanical Engineers. Journal of Vibration and Acoustics. N117, P187-191, 1995.

10. M. Amabili, '*Free vibration of partially filled horizontal cylindrical shells*', Journal of Sound and Vibration N191, P5 757-5780, 1996.

11. A.A. Lakis and A. Selmane, '*Vibration analysis of anisotropic open cylindrical shells subjected to a flowing fluid*', Journal of Fluids and Structures, N11, P111–134, 1997.

12. G. Bursuc, A.A. Lakis, and M. H. Toorani, 'Sloshing effect on the dynamic behaviour of horizontal cylindrical shells', Submitted to International Journal for Numerical Methods in Engineering, June 2006.

13. J. Mistry, J.C. Menezes, '*Vibration of cylinders partially-filled with liquids*', Journal of Sound and Vibration, V117, P 87-93, 1995.

14. N. Yamaki, J. Tani and T. Yamaji, '*Free vibration of a clamped-camped circular cylindrical shell partially filled with liquid*', Journal of Sound and Vibration N94, P531-550, 1984.

15. H. Lamb, '*On the vibrations of an elastic plate in contact with water*', Proceeding of Royal Society, A98, P205-216. London, 1921.

16. U.S. Lindholm, D.D. Kana, W.H. Chu and H.N. Abramson, '*Elastic vibration characteristics of cantilever plates in water*', Journal of Ship Research, P11-22, 1965.

17. Y. Fu and W. G. Price, '*Interactions between a partially or totally immersed vibrating cantilever plate and the surrounding fluid*', Journal of Sound and Vibration, V118, N3, P495-513, 1987.

18. M.K. Kwak, '*Hydroelastic vibration of circular plates*', Journal of Sound and Vibration, V201, N3, P293-303, 1997.

19. M.K. Kwak, '*Vibration of circular membranes in contact with water'*, Journal of Sound and Vibration, V178, N5, P688-690, 1994.

20. M. Amabili, G. Frosali and M.K. Kwak, '*Free vibrations of annular plates coupled with fluids*', Journal of Sound and Vibration V191, N5, P825-846, 1996.

21. M. Amabili and M.K. Kwak, '*Vibration of circular plates on a free fluid surface: effect of surface waves*', Journal of Sound and Vibration, V226, N3, P407-424, 1999.

22. M.K. Kwak and S.B. Han, '*Effect of fluid depth on the hydroelastic vibration of free-edge circular plate*', Journal of Sound and Vibration, V230, N1, P171-85, 2000.

23. M. Amabili, '*Effect of finite fluid depth on the hydroelastic vibrations of circular and annular plates*', Journal of Sound and Vibration, V193, N4, P909-925, 1996.

24. Y. Kerboua, A.A.Lakis, M. Thomas and L. Marcouiller, '*Comportement dynamique des plaques rectangulaires submergées*', Ecole Polytechnique of Montreal, EPM-RT-2005-05.

25. Kyeong_Hoon Jeong Tae-Wan Kim and Keun_Bae Park, '*Free vibration analysis of two circular disks coupled with fluid*', PVP-Vol 366, Technologies in Reactor safety, Fluid-Structure interaction, sloshing and Natural Hazard engineering ASME 1998. P157- 164.

26. Kyeong_Hoon Jeong, '*Free vibration of two identical circular plates coupled with bounded fluid*', Journal of Sound and Vibration, V260, N4. P653-670, 2003.

27. Kyeong_Hoon Jeong; Gye-Hyoung Yoo and Seong-Cheol Lee, '*Hydroelastic vibration of two identical rectangular plates*', Journal of Sound and Vibration, V272, N3-5, P539-555, 2004.

28. M.C. Kim and S.S. Lee, '*Hydroelastic analysis of rectangular tank*', The aerospace corporation El Segundo, California 90245, 1997.

29. H.F. Bauer, '*Hydroelsatic vibrations in rectangular container'*, International Journal of Solids and Structures. V17 P639-652, 1980.

30. Y.K. Cheung and D. Zhou, '*Coupled vibratory characteristics of a rectangular container bottom plate*', Journal of fluids and structures V14, P339-357, 2000.

31. Y.K. Cheung and D. Zhou, '*Hydroelastic vibration of circular container bottom plate using the Galerkin method*', Journal of fluids and structures V16(4), P561-580, 2002.

32. Santana Mitra and K.P. Sinhamahapatra, '*Coupled slosh dynamics of liquid filled containers using pressure based finite element method'*, Exploring innovation in education and research Tainan, 1-5, 2005.

33. R. Szilard, '*Theory and Analysis of Plate'*, Englewood Cliffs, NJ: Prentice-Hall, 1974.

34. C. Q. Guo, M. P. Paidoussis, '*Analysis of hydroelastic instabilities of rectangular parallel-plate assemblies*', Transactions of the ASME, Journal of Pressure Vessel Technology. N4. V122, P502-508, 2000.

35. A.A. Lakis and M. P. Paidoussis, Feb 1972. Dynamic analysis of axially non-uniform thin cylindrical shells. Journal of Mechanical Engineering Science, V14, N1, P49-71.

36. K. Abassi and M. Thomas, '*Analyse modale expérimentale d'une structure vibrant dans l'eau*', Ecole de technologie supérieure, Montreal, Canada, 2005.

37. N.W. Mclachlan, '*The accession to inertia of flexible discs vibrating in a fluid*', Proceedings of the Physical Society, London: 44, P546-555, 1932.

38. Y. Kerboua, A.A.Lakis, M. Thomas and L. Marcouiller, 'Analyse dynamique des systèmes de plaques en interaction avec un fluide et application', Ecole Polytechnique of Montréal, EPM-RT-2006-01.

4.10 APPENDIX A

Matrix R_f (3 × 20)

$$[R_f]=\begin{bmatrix} 0 & 0 & 0 & 0 & 0 & 0 & 0 & 0 & 0 & 0 & 0 & 0 & 0 & 0 & 0 & 0 & 0 & 0 & 0 & 0 \\ 0 & 0 & 0 & 0 & 0 & 0 & 0 & 0 & 0 & 0 & 0 & 0 & 0 & 0 & 0 & 0 & 0 & 0 & 0 & 0 \\ 0 & 0 & 0 & 0 & 0 & 0 & 0 & 0 & 1 & \frac{x}{A} & \frac{y}{B} & \frac{x^2}{2A^2} & \frac{xy}{AB} & \frac{y^2}{2B^2} & \frac{x^3}{6A^3} & \frac{x^2y}{2A^2B} & \frac{xy^2}{2AB^2} & \frac{y^3}{6B^3} & \frac{x^3y}{6A^3B} & \frac{xy^3}{6AB^3} \end{bmatrix} \quad \text{(A.1)}$$

Fluid-structure element including a fluid free surface

Assuming the perturbations of fluid motion at free surface are small and negligible (Figure 3), then, the following condition can be applied on velocity potential function

$$\left.\frac{\partial\phi(x,y,z,t)}{\partial z}\right|_{z=h_l} = -\frac{1}{g}\frac{\partial^2\phi}{\partial t^2} \quad \text{(A.2)}$$

where 'g' is the gravity acceleration

Using this relation and the impermeability condition, the fluid pressure at the fluid-structure interface becomes:

$$P = -\frac{\rho_f}{\mu}\left[\frac{1+Ce^{2\mu h_l}}{1-Ce^{2\mu h_l}}\right]\frac{\partial^2 W}{\partial t^2} = Z_{fl}\frac{\partial^2 W}{\partial t^2} \quad \text{(A.3)}$$

It is proved [24] that coefficient C tends asymptotically toward –1.

Fluid-structure element including a rigid wall

The applied boundary condition on the fluid as illustrated by Figure (4.15) is adopted by Lamb and McLachlan [15, 37]. This case is known as a null-frequency case and the rigid-wall condition is expressed as:

$$\left.\frac{\partial \phi}{\partial z}\right|_{z=h_1} = 0 \tag{A.4}$$

Again, considering this definition and the impermeability condition, the fluid-pressure applied at the fluid-structure interface is defined as:

$$P = -\frac{\rho_f}{\mu}\left[\frac{e^{-2\mu h_1}+1}{e^{-2\mu h_1}-1}\right]\frac{\partial^2 W}{\partial t^2} = Z_{f2}\frac{\partial^2 W}{\partial t^2} \tag{A.5}$$

Fluid-structure element including a free surface with null-potential

The boundary condition presented in Figure (4.16) is known as infinite-frequency condition and is expressed as:

$$\phi = 0 \tag{A.6}$$

Using this relation and the impermeability condition, the fluid pressure acting on the fluid-structure interface is given by:

$$P = -\frac{\rho_f}{\mu}\left[\frac{1-e^{2\mu h_1}}{1+e^{2\mu h_1}}\right]\frac{\partial^2 W}{\partial t^2} = Z_{f3}\frac{\partial^2 W}{\partial t^2} \tag{A.7}$$

Mass and stiffness matrices in local co-ordinates

We rearrange the matrices (mass and stiffness) in order to facilitate the passage to the global coordinates.

$$[k]^e = \begin{bmatrix} [k_{ii}] & [k_{ij}] & [k_{ik}] & [k_{il}] \\ & [k_{jj}] & [k_{jk}] & [k_{jl}] \\ & & [k_{kk}] & [k_{kl}] \\ Sym & & & [k_{ll}] \end{bmatrix} \tag{A.8}$$

$$[k']^e = \begin{bmatrix} [k_{ii}] & \{0\} & [k_{ij}] & \{0\} & [k_{ik}] & \{0\} & [k_{il}] & \{0\} \\ & 0 & \{0\}^T & 0 & \{0\}^T & 0 & \{0\}^T & 0 \\ & & [k_{jj}] & \{0\} & [k_{jk}] & \{0\} & [k_{jl}] & \{0\} \\ & & & 0 & \{0\}^T & 0 & \{0\}^T & 0 \\ & & & & [k_{kk}] & \{0\} & [k_{kl}] & \{0\} \\ & & & & & 0 & \{0\}^T & 0 \\ & & & & & & [k_{ll}] & \{0\} \\ Sym & & & & & & & 0 \end{bmatrix} \tag{A.9}$$

4.11 NOMENCLATURE

A, B	Plate length along the X and Y directions, respectively
X, Y, Z	Orthogonal local coordinate system
$\overline{X}, \overline{Y}, \overline{Z}$	Orthogonal global coordinate system
D	Membrane rigidity $Eh/(1-\nu^2)$
E	Modulus of elasticity
g	Gravity acceleration
h	Plate thickness
h_1	Fluid level above the finite element
h_2	Fluid level below the finite element
i	Complex number i^2=-1
K	Bending rigidity $Eh^3/12(1-\nu^2)$
n, m	Mode shape number in X and Y directions, respectively
P	Fluid pressure
P_{ij}	Material elasticity matrix's components defined by equation (4.7)
U, V	Displacement components of the plate reference surface in the X and Y directions, respectively
$\overline{U}, \overline{V}$	Displacement components of the plate reference surface in the $\overline{X}$ and $\overline{Y}$ directions, respectively
U_i, V_i	Nodal displacement components at node *i* in X and Y direction, respectively

$\overline{U}_i, \overline{V}_i$	Nodal displacement components at node *i* in $\overline{X}$ and $\overline{Y}$ direction, respectively:
W	Normal displacement of the plate middle surface in Z direction
$\overline{W}$	Normal displacement of the plate middle surface in $\overline{Z}$ direction
W_i	Normal displacement of the plate at node *I* in Z direction
$\overline{W}_i$	Normal displacement of the plate at node *I* in $\overline{Z}$ direction
$W_{i,x}$; $W_{i,y}$	The first derivative of the plate's normal displacement with respect to X and Y, respectively, at node *i*
x_e, y_e	Length of the element along the X- and Y-axis, respectively
Z_{fi}	Coefficient of induced fluid pressure
$\beta_{i,\overline{X}}$	Rotation about $\overline{Y}$ axis at node i
$\beta_{i,\overline{Y}}$	Rotation about $\overline{X}$ axis at node i
$\theta_{i,\overline{Z}}$	Rotation about $\overline{Z}$ axis at node i
ω	Natural frequency of the plate in rad/sec
ρ_s	Structural density
ρ_f	Fluid density
ϕ (x, y, z,t)	Velocity potential function
ν	Poisson's coefficient
λ	Non-dimensional frequency parameter of the plate
$[A]^{-1}$	Matrix (20 × 20) defined by equation (4.5)

$\{C\}$	Vector of unknown constants defined by equation (4.4)
$\{F\}^e$	vector
$\{F\}^e$	Nodal force vector in local co-ordinates
$[k]^e$	Stiffness matrix of an element in local co-ordinate system (20 × 20)
$[\bar{k}]^e$	Stiffness matrix of an element in global co-ordinate system (20 × 20)
$[K_s]$	Global stiffness matrix
$[m]^e$	Mass matrix of an element in local co-ordinate system (20 × 20)
$[m_f]^e$	Added mass matrix of an element in local co-ordinate system (20 × 20)
$[\bar{m}]^e$	Mass matrix of an element in global co-ordinate (20 × 20)
$[M_s]$	Global mass matrix
$[M_f]$	Global added mass matrix due to fluid-induced inertia force
$[P]$	Elasticity matrix (6 × 6)
$\{P\}$	Fluid pressure vector
$[Q]$	Matrix (6 × 20) defined by equation (4.6)
[R]	Matrix (3 × 20), defined by equation (4.5)
[Rf]	Matrix (3 × 20), defined by equation (4.31)
$[T]$	Transformation matrix of nodal displacements
$[T]^e$	Transformation matrix of elementary displacements
$\{\varepsilon\}$	Deformation vector

$\{\sigma\}$	Stress vector
$\{\delta\}$	Displacement vector in local co-ordinate system X, Y, Z
$\{\bar{\delta}\}$	Displacement vector in global co-ordinate system $\bar{X}, \bar{Y}, \bar{Z}$
$\{\bar{\delta}_T\}$	Global displacement vector
$\{\bar{\delta}_{0T}\}$	Vector of mode shape amplitudes

TABLE 4.1: In-phase vibrational frequencies (Hz) of a fluid-filled reservoir

Mode number (n, m)	Jeong et al. [27]	Present Theory
(0,0)	113.3	112.9
(0,1)	192.5	188.7
(1,0)	272.4	265.6
(0,2)	326.5	314.0
(1,1)	348.4	332.9
(1,2)	479.6	447.7
(0,3)	516.1	485.6
(2,0)	525.9	498.2

TABLE 4.2: Out-of-phase vibrational frequencies (Hz) of a fluid-filled reservoir

Mode number (n, m)	Jeong et al. [27]	Present Theory
(0,1)	61.2	66.5

TABLE 4.3: Number of equations for expressing the pressure corresponding to each vibrational mode of submerged plates

Vibrational Mode	Plate 1		Plate 2		Plate 3	
	Superior Pressure	Inferior Pressure	Superior Pressure	Inferior Pressure	Superior Pressure	Inferior Pressure
Three plates vibrating in-phase	(4.26)	(A.5)	(4.26)	(4.26)	(A.3)	(4.26)
Plate (2) is out-of-phase with plates (1) and (3)	(4.29)	(A.5)	(4.29)	(4.29)	(A.3)	(4.29)
Plate (2) is out-of-phase with plate (3) and is in-phase with plate (1)	(4.26)	(A.5)	(4.29)	(4.26)	(A.3)	(4.29)

TABLE 4.4: Vibrational frequencies (Hz) of a set of three plates fixed to rigid wall

Mode Number	Three submerged plates vibrating in-phase	Plate (2) is out-of-phase with plates (1) and (3)	Plate (2) is out-of-phase with plate (3) and is in-phase with plate (1)
1	12.3	9.7	10.5
2	12.3	10.5	11.1
3	13.4	15.7	12.3
4	30.1	23.8	25.7
5	30.1	25.7	27.3
6	32.8	38.5	30.1
7	75.9	60.0	64.6
8	75.9	64.6	68.7
9	82.7	75.7	75.9
10	95.7	81.5	81.5

TABLE 4.5: Non-dimensional out-of-phase vibration frequencies

Mode number	Present Theory	Guo and Paidoussis [34]
1	16.3	16.6
2	26.5	32.5
3	45.0	48.5

TABLE 4.6: Number of equations for expressing the pressure corresponding to each vibrational mode of radial submerged plates

Vibrational Mode	Plate 2	
	Upper Pressure	Lower Pressure
Three plates vibrating in-phase	$(4.26)\cos\alpha$	$(4.26)\cos\alpha$
Plate (2) is out-of-phase with plates (1) and (3)	$(4.29)\cos\alpha$	$(4.29)\cos\alpha$
Plate (2) is out-of-phase with plate (3) and is in-phase with plate (1)	$(4.29)\cos\alpha$	$(4.26)\cos\alpha$

TABLE 4.7: Vibrational frequencies (Hz) of three N radial plates

Mode Number	In vacuo	In fluid		
		Three plates vibrating in-phase	Plate (2) is out-of-phase with plates (1) and (3)	Plate (2) is out-of-phase with plate (3) and is in-phase with plate (1)
1	199.1	140.0	116.4	126.5
2	242.6	170.6	141.6	154.0
3	361.9	255.1	210.7	229.5
4	558.1	394.3	323.6	353.4
5	851.5	602.6	491.9	538.4
6	1243.6	885.1	683.0	773.0
7	1251.1	917.6	699.1	780.6
8	1311.6	957.9	732.2	815.0
9	1440.9	1056.7	785.3	889.3
10	1679.4	1233.8	911.2	1034.2

TABLE 4.8: Vibrational frequencies (Hz) of a set of three plates fixed to elastic wall

Mode Number	Present Theory (in vacuum)	ANSYS (in vacuum)	Three submerged plates vibrating in-phase
1	28,71	28,71	7,58
2	37,73	37,739	10.49
3	ND	52,6	ND
4	83,35	84,98	29.59
5	97,74	93,29	54.06
6	105,3	105,26	57.58
7	ND	134	ND
8	147	150	59.6
9	174,7	174,4	68.09
10	186	ND	74.25
11	246,4	245,31	92.17
12	290,7	289,21	92.93
13	317,8	316,09	93.38
14	357,4	358,94	100
15	358,8	360,57	104.7

TABLE 4.9: Natural frequencies (Hz) of a vertical cantilever plate gradually submerged in a fluid reservoir

Mode Number °	In vacuo	Submerged height Ratio							
		25%		50%		75%		100%	
		Present Theory	Lindhom [4]	Present Theory	Lindhom [4]	Present Theory	Lindhom [4]	Present Theory	Lindhom [4]
1	3.9	2.3	2.2	2.0	1.8	1.9	1.8	1.9	1.8
2	24.7	20.7	21.0	14.7	15.5	12.1	12.0	11.8	11.5
3	39.3	25.4	29.8	20.4	25.5	19.1	24.2	18.9	24.2
4	69.2	55.8	57.4	49.1	51.6	35.6	38.3	33.2	33.5

TABLE 4.10: Vibrational frequencies (Hz) of a fluid-filled reservoir

Theory	In-Phase	Out-of-Phase
Kim and Lee [28]	49.8	42.2
Present Theory	50.7	49.9

TABLE 4.11: Vibrational frequencies (Hz) a simplified wing model (bird structure)

Mode Number	In vacuo			Submerged in Water	
	ANSYS [36]	Experiment [36]	Present Theory	Experiment [36]	Present Theory
1	38.0	38.0	38.0	16.9	18.3
2	115.9	106.0	118.9	42.0	48.2
3	133.3	137.0	141.3	N. A.	52.9
4	159.2	N. A.	157.3	79.0	82.1
5	216.4	218.0	224.3	95.0	98.1
6	357.2	317.0	349.8	151.0	159.5
7	437.5	N. A.	463.9	N. A.	164.3
8	N. A.[1]	393.0	471.9	206.0	207.8
9	N. A.	N. A.	618.1	265.0	248.0

1. N. A. Not Avaialable

TABLE 4.12: Vibration frequencies of a fluid-filled clamped-clamped cylindrical shell

Mode Number	L=0.664m, R=0.175m, h=1mm		L=0.9m, R=0.25m, h=2mm		L=0.9m, R=0.25m, h=1mm	
	Present Theory	Ref. [35]	Present Theory	Ref. [35]	Present Theory	Ref. [35]
1	137.9	138.6	135.0	135.9	74.1	79.7
2	146.2	152.8	149.9	138.8	80.4	80.2
3	165.9	158.3	154.6	166.9	81.6	94.0
4	178.0	201.9	195.6	177.7	98.2	96.4
5	224.4	205.3	212.9	223.3	105.6	119.9
6	234.3	256.9	228.3	245.7	120.7	129.8

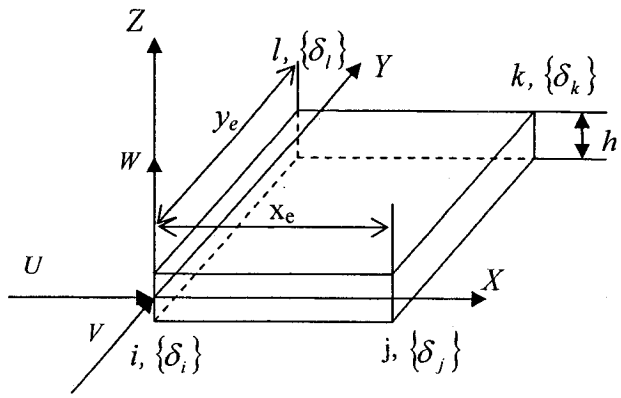

$$\{\delta_i\} = \{U_i, U_j, W_i, W_{i,x}, W_{i,y}\}^T$$

FIGURE 4.1: Finite element geometry and nodal displacement vector in local co-ordinates *X, Y, Z.*

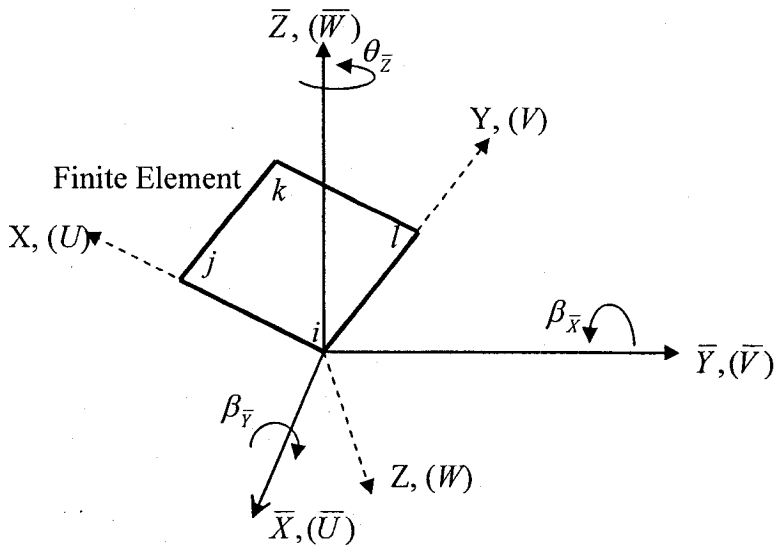

FIGURE 4.2: Local and global co-ordinate systems of the structure

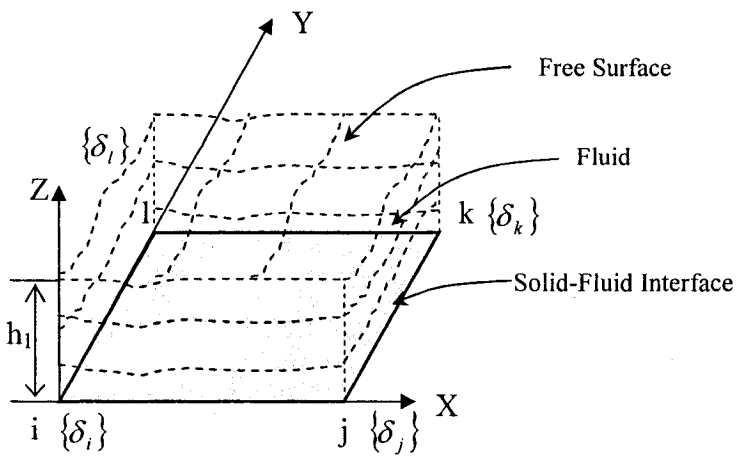

FIGURE 4.3: Solid-fluid finite element in local co-ordinates X, Y, Z

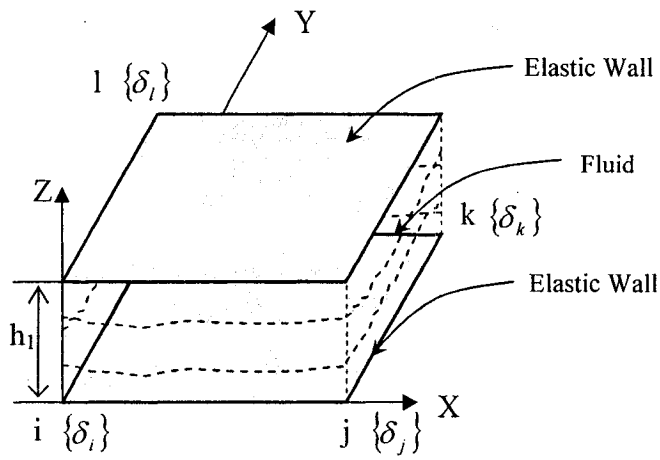

FIGURE 4.4: Solid-fluid finite element, in local co-ordinates X; Y; Z, bounded by an elastic wall at level $z=h_l$

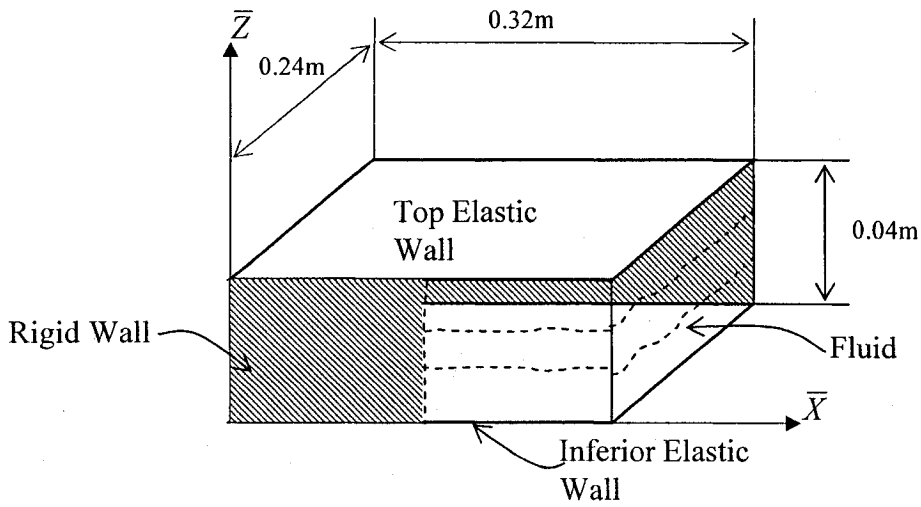

FIGURE 4.5: Fluid-filled rectangular reservoir with vertical rigid walls

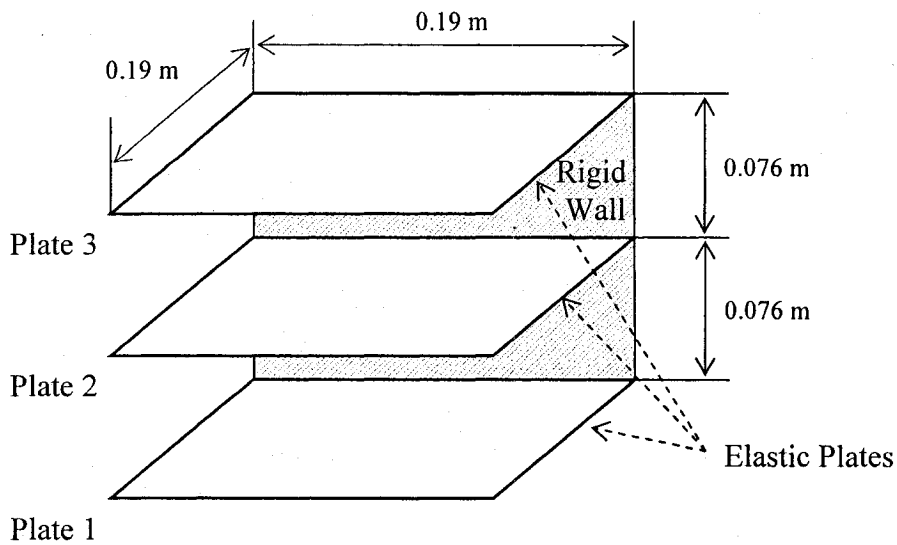

FIGURE 4.6: A set of parallel plates

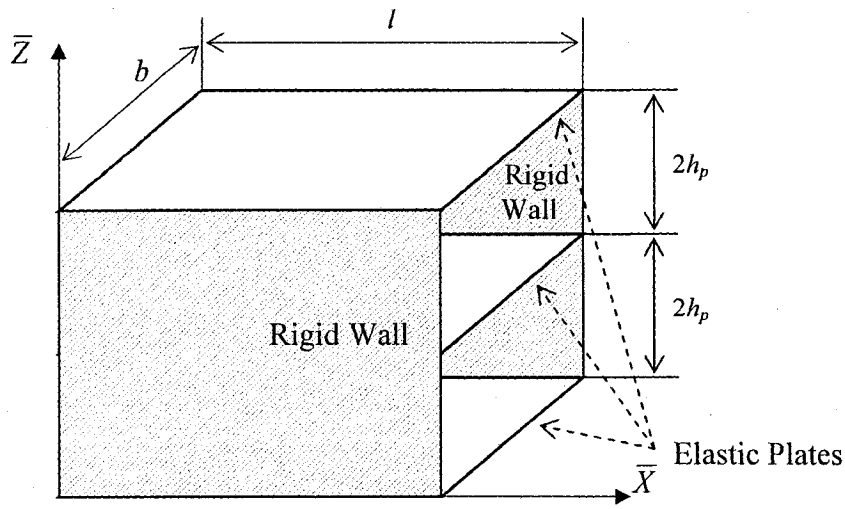

FIGURE 4.7: A set of parallel plates fixed at a rigid wall and totally submerged in fluid

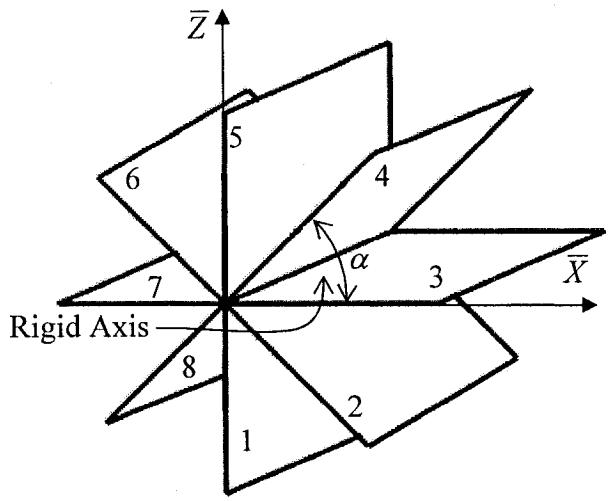

FIGURE 4.8: A structural system composed of n radial plates welded to a common axis

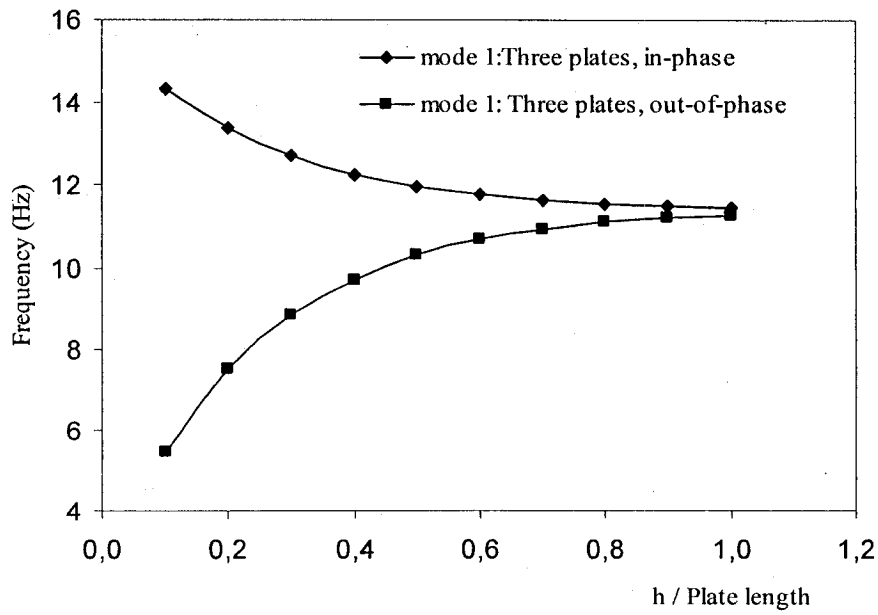

(A) Three plates fixed at a rigid wall

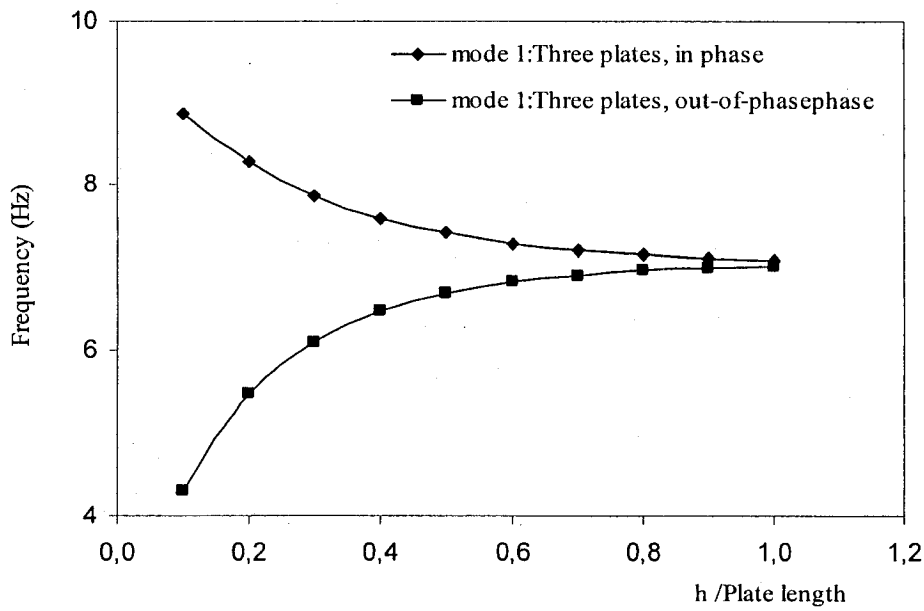

(B) Three plates fixed at an elastic wall

FIGURE 4.9: In-phase and out-of-phase vibration frequencies of a set of parallel plates as a function of fluid level

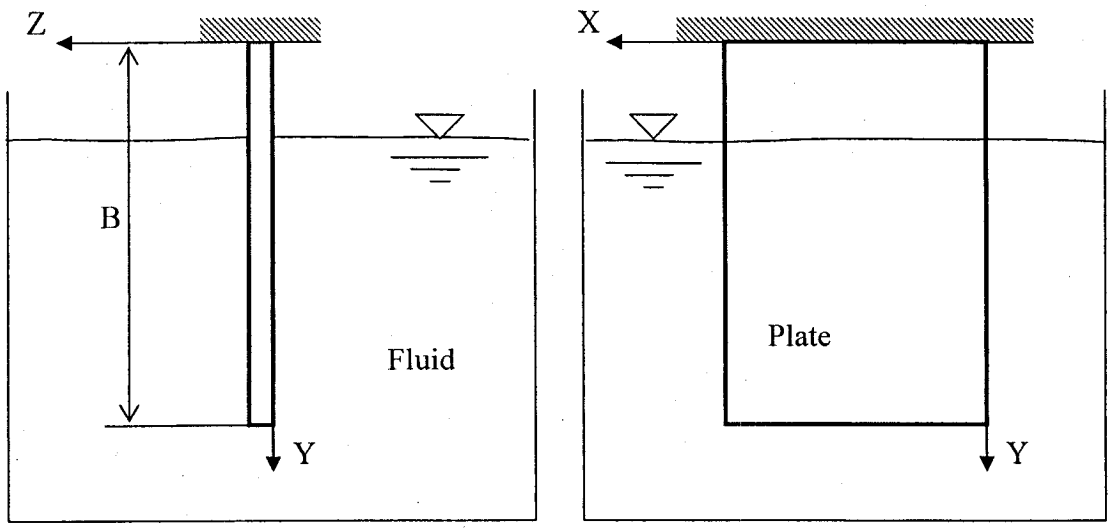

FIGURE 4.10: Vertical rectangular plate gradually submerged in a fluid reservoir

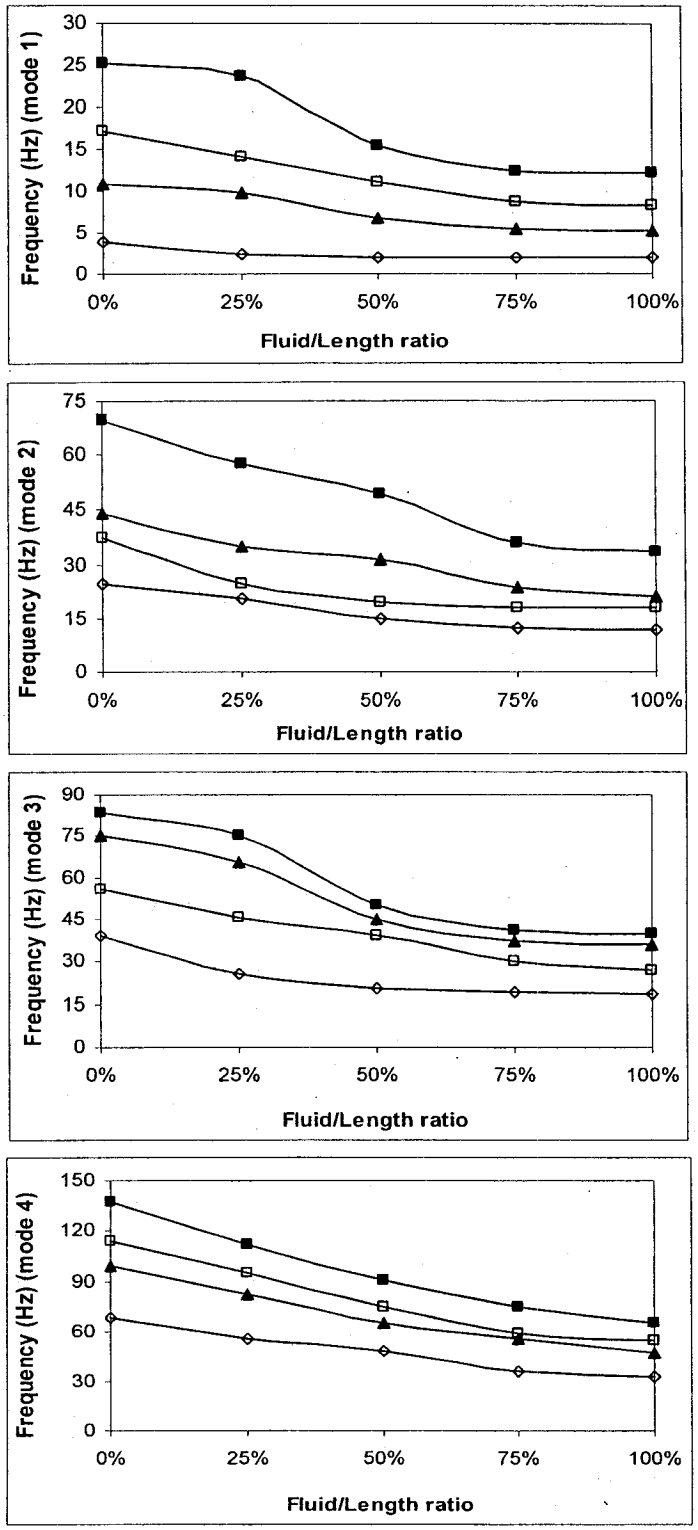

FIGURE 4.11: Frequency variation of a partially submerged plate as a function of fluid level (■ CFCF, ▲ SFSF, □ SFFF, ◊ CFFF)

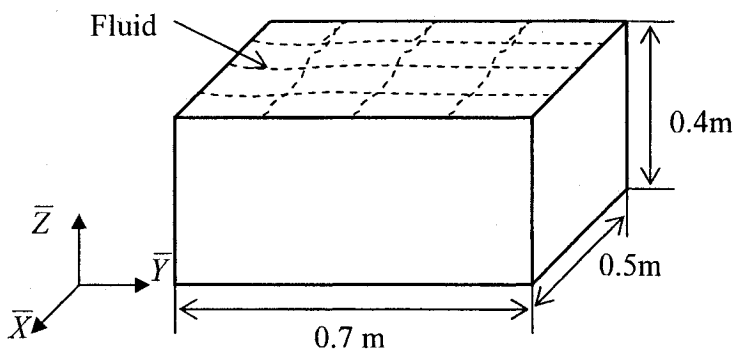

FIGURE 4.12: Fluid-filled open rectangular reservoir

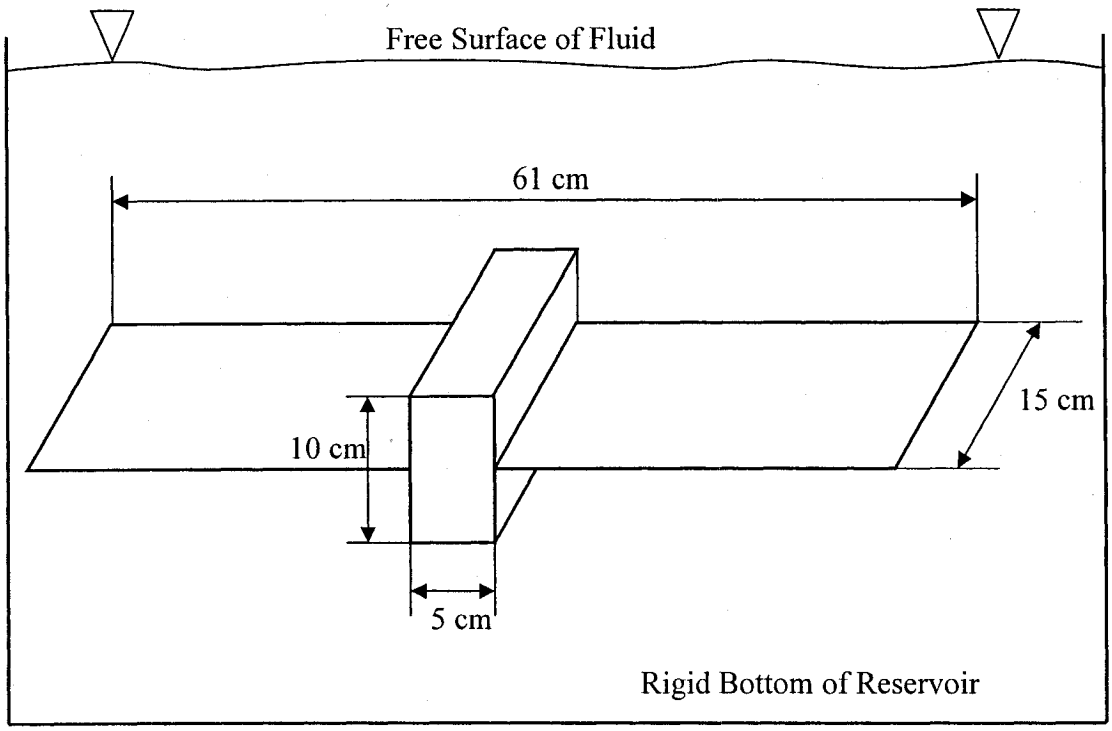

FIGURE 4.13: Simplified model of wing structure (bird structure)

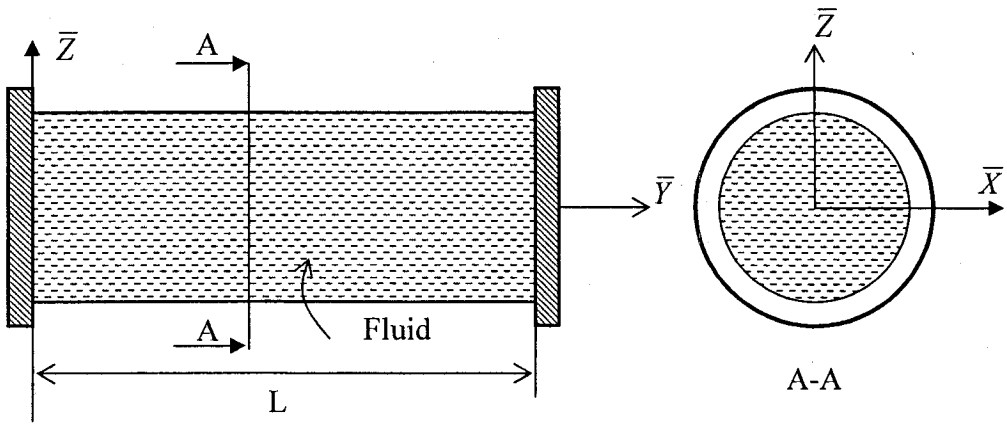

FIGURE 4.14: Cylindrical shell fixed at x=0 and x=L.

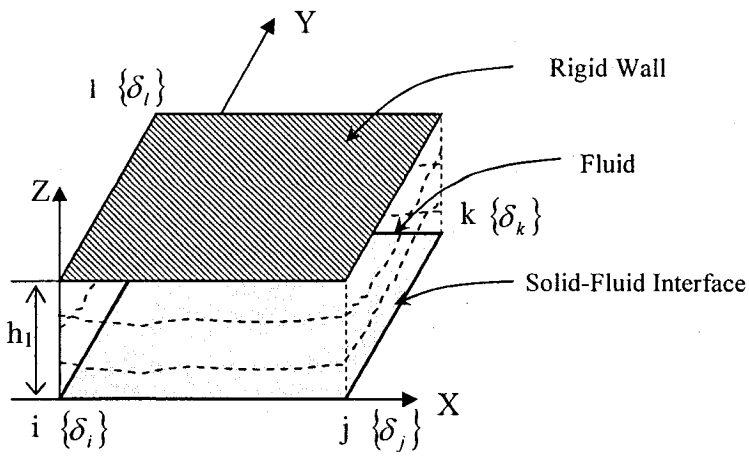

FIGURE 4.15: Solid-fluid finite element, in a local co-ordinate X, Y, Z, bounded by a rigid wall

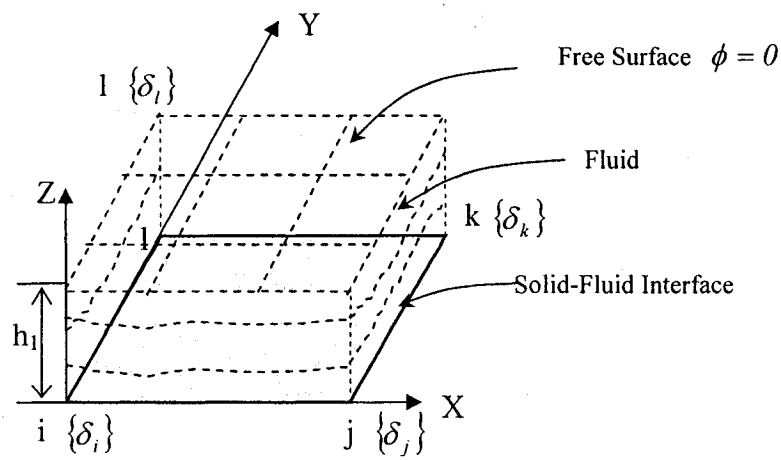

FIGURE 4.16: Solid-fluid finite element, in local co-ordinate X, Y, Z, bounded by a free surface where the fluid-pressure is null ($\phi = 0$)

CHAPITRE V

MODELING OF PLATES SUBJECTED TO FLOWING FLUID UNDER VARIOUS BOUNDARY CONDITIONS

Y. Kerboua[1], A.A. Lakis[1], M. Thomas[2], L. Marcouiller[3]

1. *Mechanical Engineering Dept., École Polytechnique of Montréal, Canada*
2. *Mechanical Engineering Dept., École de Technologie Supérieure, Canada*
3. *Institut de Recherche d'Hydro Québec, Montréal (Québec) Canada*

(Soumis pour publication dans **International Journal for Numerical Methods in Fluids)**

5.1 Abstract

Elastic structures subjected to fluid flow undergo a considerable change in their dynamic behaviour and can lose their stability. In this article we describe the development of a fluid-solid finite element to model plates subjected to flowing fluid under various boundary conditions. A new method is applied which combines this finite element with the classical theory of plates. The membrane displacement field is approximated by bilinear polynomials and the transversal displacement by an exponential function which is the solution of equilibrium equations. Fluid pressure is expressed by inertial, Coriolis and centrifugal fluid forces, written respectively as function of acceleration, velocity and

transversal displacement. Bernoulli's equation for the fluid-solid interface and partial differential equation of potential flow are applied to calculate the fluid pressure. An impermeability condition ensures contact between the system of plates and the fluid. Mass and rigidity matrices for each element are calculated by exact integration. Calculated results are in reasonable agreement with other analytical theories.

5.2 INTRODUCTION

Systems of plates subjected to fluid flow are often found in contemporary industries such as nuclear reactors and aerospace. Generally these industries require high rates of fluid flow and low plate thicknesses. Under these conditions, if the length of the plates is excessive the structure becomes very susceptible to failure.

Earlier works in this field were carried out on the ETR (engineering test reactor) systems consisting of many thin plates stacked in parallel with narrow channels between the plates to let coolant flow through.

Miller [1] was the first to present a theoretical analysis predicting the flow velocity at which the system collapses. It corresponds to the coolant velocity at which the change in dynamic pressure resulting from plate deflexion equals the elastic restoring force in the plate. Both flat and curved plate assemblies with various boundary conditions are considered. He has derived relations expressing the collapse velocities of ETR systems.

Rosenberg and Youngdahl [2] have formulated a dynamic model describing the motion of a fuel plate in a parallel plate assembly. They obtained the critical flow velocity of Miller.

Groninger and Kane [3] investigated three parallel-plate assemblies to determine the flow-induced deflection of individual plates. They detected a violent flutter of the plates at a velocity corresponding to 1.9 times the Miller velocity. The model showed that adjacent plates always move in opposite directions at high flow rates, causing alternate opening and a closing of the channel. This dynamic instability was observed to be a wave vibration originating at the leading edges and travelling along the plates in the direction of the flow.

Ishii [4] observed two different types of instability; small amplitude oscillation at a high frequency and large amplitude oscillation at a low frequency. He explained these instabilities by the fact that the pressure gradient along the flow direction has a destabilizing effect that creates flutter.

The assumptions of Miller [1] and, Rosenberg and Youngdahl [2] were the same, they linearized the pressure drop expression using only a first-order approximation. Wambsganss [5] retained the second-order terms in an attempt to assess their influence on stability. He derived a new expression for critical velocity.

Dowell [6] studied the stability of a plate system using a non-linear plate model and linearized potential flow theory. His numerical results show that there is divergence at certain critical velocities but there is no flutter above divergence.

Smissaert [7, 8] studied the hydroelastic instabilities that occur in MTR-type flat plates both experimentally and theoretically. His experimental results [7] demonstrate that for low velocities the plates will deform as a result of static pressure in the channels between them. At high fluid velocities a high-amplitude flutter vibration is observed.

This flutter does not appear below a minimum average water velocity referred to as the flutter velocity, which is approximately equal to two times the Miller velocity of the assembly. The flutter vibration starts at the leading edge of the plates and travels along the plates in the form of a flexural wave in the direction of the flow. Smissaert's theoretical analysis [8] includes the development of an analytical model of a parallel plate system of infinite dimensions. This approach enables two-dimensional consideration of the problem. Results of this treatment of the system indicated that a plate assembly is characterized by two velocities; Miller's velocity and flutter velocity. He concluded that the system is subject to a number of instabilities. Miller's velocity corresponds to static divergence of Class "A". At this velocity, the plates deflect at infinite wave length. Class B type dynamic instabilities generate small-amplitude traveling waves in the plates. These class B instabilities are very mild. When the flutter velocity is reached, a coupling takes place between Class B and flutter instabilities at the leading edges of the plates. This phenomenon creates high amplitude waves which travel along the plate in the flow direction. Flutter velocity is approximately two times Miller's velocity.

Weaver and Unny [9] studied the dynamic behaviour of a single flat plate, one side of which is exposed to high velocity flow of a heavy fluid such as water. The model used is a two-dimensional plate of finite length in the direction of flow and simply supported at its ends. They examined the variation of natural frequencies according to the rate of flow. They concluded that for a given mass rapport, the neutral zone of stability is

followed by a zone of static instability. After this stage, the plate quickly returns to neutral stability, which continues until the occurrence of dynamic instability.

Gislason [10] completed an experimental study on a rectangular plate with a chord-to-span ratio of 2 subjected to a flowing fluid. He reported that no dynamic instability was observed when the dynamic pressure was increased up to about two times the Miller's velocity.

Kornecki et al. [11] considered a flat panel of infinite width and finite length embedded in an infinite rigid plane with uniform incompressible potential flow over its upper surface. The studied plates were constrained (clamped or simply supported) along their leading and trailing edges. The case of a panel clamped at its leading edge and free at its trailing edge was investigated both theoretically and experimentally. The obtained results demonstrate that a panel fixed at its leading and trailing edges loses its stability by divergence, while the cantilevered panel loses its stability by flutter.

Holmes [12] investigated the behaviour of a panel subjected to fluid flow by taking into account structural nonlinearity and damping. He recast the differential equations of motion using Galerkin method and modal truncation. He obtained results in good agreement with those of Dowell [6].

Davis and Kim [13] developed an analytical model of a system of thin rectangular flat plates. Their model was used to investigate static and dynamic instabilities of the system. The plates are assumed laterally fixed and elastically restrained in rotation along two opposite edges which are attached to the assembly walls.

Guo and Paidoussis [14] conducted an analytical study of the stability of rectangular plates with free side-edges in inviscid channel flow. They considered a finite length rectangular plate, treating the plate as one-dimensional and the channel flow as two-dimensional. Galerkin method was employed to solve the plate equation and the perturbation of pressure was obtained from the potential equations using the Fourier transform technique. They investigated every possible combination of classical supports at the leading and trailing edges of the plates. They concluded that divergence and coupled mode flutter may occur for plates with any type of end supports, while single mode flutter only arises for nonsymmetrically supported plates.

Guo and Paidoussis [15] have also conducted a theoretical study of the hydro-elastic instabilities of rectangular parallel-plate assemblies. In the analysis the plates are treated as two-dimensional, and the flow field is taken as inviscid, three-dimensional. They mention two types of instability; single-mode flutter divergence, mostly in the first mode, and coupled-mode flutter involving adjacent modes. They also concluded that the frequency at a given flow velocity decreases as the aspect ratio increases and the channel height to plate-width ratio decreases. They confirmed that structural damping has little effect on the frequency and critical velocity, but does have a major influence on the post divergence behaviour and coupled-mode flutter.

This subject has been studied by several researchers, but has not received the attention focused on analysis of the behaviour of a plate subjected to supersonic flow. It is clear that, in spite of the conclusions reached during these various studies, the subject is far from being understood considering the number of contradictory results.

In this work we develop a finite element model to investigate the dynamic behaviour of a rectangular plate or system of flat plates subjected to potential fluid flow.

5.3 SOLID FINITE ELEMENT

The solid plate finite element used in this work was already employed to study the dynamic behaviour of a plate without fluid [16]. The computed natural frequencies were compared to those obtained by other theories and from experiments and the results were in very good agreement.

The finite element is shown in Figure (5.1). It is a portion of a flat plate with a thickness h and four nodes (i, j, k, l). Each node has six degrees of freedom that represent the in-plane and out-of-plane displacement components and their spatial derivatives.

The approximation of transversal displacement by exponential function and the membrane displacements by bilinear polynomials was justified when we developed the fluid-solid finite element [16].

The displacement field is expressed as:

$$U(x,y,t)=C_1+C_2\frac{x}{A}+C_3\frac{y}{B}+C_4\frac{xy}{AB} \tag{5.1.a}$$

$$V(x,y,t)=C_5+C_6\frac{x}{A}+C_7\frac{y}{B}+C_8\frac{xy}{AB} \tag{5.1.b}$$

$$W(x,y,t)=\sum_{j=9}^{24}C_j\, e^{i\pi\left(\frac{x}{A}+\frac{y}{B}\right)}e^{i\omega t} \tag{5.1.c}$$

where U and V represent the in-plane displacement components of the middle surface in X and Y directions, respectively, W is the transversal displacement of the middle surface, A and B are the plate dimensions in X and Y directions, "ω" is the natural frequency of the plate (rad/sec), "i" is a complex number and C_j are unknown constants; Equation (5.1.c) can be developed in Taylor's series as follows [16]:

$$W(x,y,t)=C_9+C_{10}\frac{x}{A}+C_{11}\frac{y}{B}+C_{12}\frac{x^2}{2A^2}+C_{13}\frac{xy}{AB}+C_{14}\frac{y^2}{2B^2}+C_{15}\frac{x^3}{6A^3}+C_{16}\frac{x^2y}{2A^2B}+C_{17}\frac{xy^2}{2AB^2}+C_{18}\frac{y^3}{6B^3}+$$

$$C_{19}\frac{x^3y}{6A^3B}+C_{20}\frac{x^2y^2}{4A^2B^2}+C_{21}\frac{xy^3}{6AB^3}+C_{22}\frac{x^3y^2}{12A^3B^2}+C_{23}\frac{x^2y^3}{12A^2B^3}+C_{24}\frac{x^3y^3}{36A^3B^3} \qquad (5.2)$$

The displacement field may be rewritten in the form of matrix relations as follows:

$$\begin{Bmatrix} U \\ V \\ W \end{Bmatrix}=[R]\{C\} \qquad (5.3)$$

where [R] is a matrix of order (3× 24) given in Appendix A and $\{C\}$ is the vector for the unknown constants.

To determine these constants, we need to define twenty-four boundary conditions for the finite element. These twenty four boundary conditions will be the degrees-of-freedom per element, which means six degrees-of-freedom per node (see Appendix B). By replacing them in Equation (5.3), the field of displacements becomes:

$$\begin{Bmatrix} U \\ V \\ W \end{Bmatrix} = [R][A]^{-1}\{\delta\} = [N]\{\delta\} \tag{5.4}$$

where $[A]^{-1}$ is a matrix of order (24 ×24) defined in Appendix A, $\{\delta\}$ is a vector of nodal displacement given in Appendix A and [N] is a matrix of order (3 ×24) and is the displacement shape function of the finite element.

Substituting the displacement components defined Equation (5.4) into the strain-displacement relationship given in Appendix A; one obtains an expression for the strain:

$$\{\varepsilon\} = [Q][A]^{-1}\{\delta\} \tag{5.5}$$

where [Q] is a (6 ×24) matrix listed in Appendix A.

The corresponding stresses may be related to the strains by the elasticity matrix [P] as follows:

$$\{\sigma\} = [P]\{\varepsilon\} \tag{5.6}$$

where [P] is a (6x6) symmetric elasticity matrix. In the case of an isotropic material there is no coupling between membrane and bending effects, and the only non-vanishing terms are given in Appendix B.

By using Equations (5.4), (5.5) and (5.6), the mass and stiffness matrices for one finite element may be expressed as:

$$[k]^e = [[A]^{-1}]^T \left(\int_0^{y_e} \int_0^{x_e} [Q]^T [P][Q] dx dy \right) [A]^{-1} \tag{5.7}$$

$$[m]^e = \rho_s h [[A]^{-1}]^T \left(\int_0^{y_e} \int_0^{x_e} [R]^T [R] dx dy \right) [A]^{-1} \tag{5.8}$$

where ρ_s is the material density, and x_e and y_e are dimensions of an element according to the X and Y coordinates. These integrals are calculated using Maple mathematical software.

5.4 FLUID-SOLID INTERACTION

The aim of our work is to develop a fluid-solid finite element which takes into account the effects of potential fluid flow on the plate under all possible boundary conditions.

The fluid pressure acting upon the structure is generally expressed as a function of displacement and its derivatives i.e. velocity and acceleration. These three terms are respectively known as the stiffness, Coriolis and inertia effects of the fluid forces[17]. The fluid matrices will be combined with solid matrices as follows:

$$[[M_s]-[M_f]]\{\ddot{\delta}_T\}+[[C_s]-[C_f]]\{\dot{\delta}_T\}+[[K_s]-[K_f]]\{\delta_T\}=\{F\} \tag{5.9}$$

where $[M_s]$, $[C_s]$ and $[K_s]$ are the global matrices of mass, damping and rigidity of the solid plate, $[M_f]$, $[C_f]$ and $[K_f]$ represent the inertial, Coriolis and centrifugal forces of potential flow, $\{\delta_T\}$ is the displacement vector and $\{F\}$ represents the external forces. We start by calculating the virtual added matrices at the element level and then apply the usual techniques of assembly to build the total matrices of equation (5.9).

5.4.1 Fluid-solid finite element

The fluid-solid model is developed based on the following hypotheses: (i) the fluid flow is potential; (ii) vibration is linear (small deformations); (iii) the fluid mean velocity distribution is constant and (iv) the fluid is incompressible.

Taking account these assumptions, the velocity potential must satisfy the Laplace equation. This relation is expressed in the Cartesian system by:

$$\frac{\partial^2\phi}{\partial x^2}+\frac{\partial^2\phi}{\partial y^2}+\frac{\partial^2\phi}{\partial z^2}=\frac{1}{c^2}\left(\frac{\partial^2\phi}{\partial t^2}+2U_x\frac{\partial^2\phi}{\partial x\partial t}+U_x^2\frac{\partial^2\phi}{\partial x^2}\right) \tag{5.10}$$

where ϕ is the potential function that represents the velocity potential, c is the velocity of sound in a fluid medium and U_x is the mean velocity of fluid in the x-direction. Therefore we have:

$$V_x = U_x + \frac{\partial \phi}{\partial x} \qquad V_y = \frac{\partial \phi}{\partial y} \qquad V_z = \frac{\partial \phi}{\partial z} \tag{5.11}$$

where V_x, V_y, V_z are the components of fluid velocity along X, Y, Z directions, respectively.

The Bernoulli equation is given by:

$$\frac{\partial \phi}{\partial t} + \frac{1}{2} V^2 + \frac{P}{\rho_f}\bigg|_{z=0} = 0 \tag{5.12}$$

where P is the fluid dynamic pressure.

Figure (5.2) depicts a fluid-solid finite element subjected to flowing fluid on its upper surface. Introducing Equation (5.11) into (5.12) and neglecting the nonlinear terms we can write the dynamic pressure at the solid-fluid interface as follows (see Figure. 5.2):

$$P\big|_{z=0} = -\rho_f \left(\frac{\partial \phi}{\partial t} + U_x \frac{\partial \phi}{\partial x} \right)\bigg|_{z=0} \tag{5.13}$$

The impermeability condition ensures contact between the shell and the fluid. This is represented by the following expression:

$$\left.\frac{\partial\phi}{\partial z}\right|_{z=0} = \left(\frac{\partial W}{\partial t} + U_x \frac{\partial W}{\partial x}\right) \tag{5.14}$$

If we assume that:

$$\phi(x, y, z, t) = F(z)S(x, y, t) \tag{5.15}$$

where *F(z)* and *S(x. y, z)* are two separate functions to be defined, one can use Equations (5.14) and (5.15) to develop the potential function as:

$$\phi(x, y, z, t) = \frac{F(z)}{dF(0)/dz}\left(\frac{\partial W}{\partial t} + U_x \frac{\partial W}{\partial x}\right) \tag{5.16}$$

The only unknown function in equation (5.16) is *F(z)*. By introducing equation (5.15) into (5.10), we obtain the following differential equation of second order:

$$\left[\frac{1}{c^2}\left(\omega^2 + 2U_x \frac{\pi}{A}\omega + U_x^2 \frac{\pi^2}{A^2}\right) - \mu^2\right]F(z) + \frac{d^2F(z)}{dz^2} = 0 \tag{5.17}$$

where:

$$\mu = \pi\sqrt{\frac{1}{A^2}+\frac{1}{B^2}}$$

In order to avoid the nonlinear eigenvalue problem and as our fluid is incompressible we can assume that:

$$\left(\omega^2 + 2U_x\frac{\pi}{A}\omega + U_x^2\frac{\pi^2}{A^2}\right) << c^2 \tag{5.18}$$

In this case equation (5.17) may be reduced to:

$$\frac{d^2F(z)}{dz^2} - \mu^2 F(z) = 0 \tag{5.19}$$

The general form of this last equation is:

$$F(z) = A_1 e^{\mu z} + A_2 e^{-\mu z} \tag{5.20}$$

By substituting equation (5.20) into (5.16) the potential function becomes:

$$\phi(x,y,z,t) = \frac{\left(A_1 e^{\mu z} + A_2 e^{-\mu z}\right)}{dF(0)/dZ}\left(\frac{\partial W}{\partial t} + U_x\frac{\partial W}{\partial x}\right) \tag{5.21}$$

A_1 and A_2 are two constants to be determined using boundary conditions. We note that at solid-fluid interface (z=0) we have the impermeability condition (5.14) which is common for all cases and at the second limit of fluid ($z=h_1$ and/or $z=h_2$), we have a boundary condition corresponding to either a rigid wall, an elastic plate, or an infinite fluid level. For each case we have a distinct solution.

Below we will calculate the pressure of fluid acting on only one side of the plate. If the fluid pressure acts on two sides, the total dynamic pressure will be a combination of the pressures corresponding to the fluid boundary conditions at both top and bottom surfaces of the plate.

5.4.1.1 Fluid-solid finite element subject to flowing fluid with infinite level of fluid

When the level of fluid on and/or under the plate (h_1 and/or h_2) is very large (see Figure. 5.3), we assume that very far from the plate the potential is null, this boundary condition is written as follows:

$$\begin{aligned} &\phi = 0 \\ &z \to \pm\infty \end{aligned} \tag{5.22}$$

In order to avoid an infinite potential, the constant A_1 must be null. Equation (5.14) permits us to calculate the second constant A_2. The potential expression becomes:

$$\phi(x.y,z,t) = -\frac{F'(0)e^{-\mu z}}{\mu}\left(\frac{\partial W}{\partial t} + U_x \frac{\partial W}{\partial x}\right) \tag{5.23}$$

The introduction of Equation (5.23) into relation (5.13), results in the following expression for the pressure function

$$P = \frac{\rho_f}{\mu}\left[\frac{\partial^2 W}{\partial t^2} + 2U_x \frac{\partial^2 W}{\partial x \partial t} + U_x^2 \frac{\partial^2 W}{\partial x^2}\right] \tag{5.24}$$

or:

$$P = Z_{fl}\left[\frac{\partial^2 W}{\partial t^2} + 2U_x \frac{\partial^2 W}{\partial x \partial t} + U_x^2 \frac{\partial^2 W}{\partial x^2}\right] \tag{5.25}$$

Z_{fl} is given in Appendix B.

5.4.1.2 Fluid-solid finite element subject to flowing fluid bounded by rigid wall

As shown in Figure (5.4), fluid flows between the rigid wall and elastic plate. This provides another boundary condition at $z=h_1$ and/or $z=h_2$ when the impermeability condition is taken into account. This boundary condition is adopted by Lamb and McLachlan [18, 19] and is expressed by:

$$\left.\frac{\partial \phi}{\partial z}\right|_{z=h_1 (z=h_2)} = 0 \tag{5.26}$$

Using Equations (5.14) and (5.26) we can calculate the constants A_1 and A_2 corresponding to this last boundary condition. Substituting these constants in (5.21) we obtain:

$$\phi(x.y,z,t) = \frac{F'(0)}{\mu}\frac{(e^{-2\mu h_1}e^{\mu z} + e^{-\mu z})}{(e^{-2\mu h_1} - 1)}\left(\frac{\partial W}{\partial t} + U_x\frac{\partial W}{\partial x}\right) \tag{5.27}$$

Replacing Equation (5.27) in (5.13), the corresponding dynamic pressure becomes:

$$P = -\frac{\rho_f(e^{-2\mu h_1} + 1)}{\mu(e^{-2\mu h_1} - 1)}\left[\frac{\partial^2 W}{\partial t^2} + 2U_x\frac{\partial^2 W}{\partial x \partial t} + U_x^2\frac{\partial^2 W}{\partial x^2}\right] \tag{5.28}$$

or:

$$P = Z_{f2}\left[\frac{\partial^2 W}{\partial t^2} + 2U_x\frac{\partial^2 W}{\partial x \partial t} + U_x^2\frac{\partial^2 W}{\partial x^2}\right] \tag{5.29}$$

Z_{f2} is given in Appendix B

5.4.1.3 Fluid-solid finite element subject to flowing fluid bounded by elastic plate

When the fluid flows through two parallel elastic plates (see Figure 5.5) we can observe in-phase and out-of-phase transverse vibration modes. The impermeability condition for each element remains the same, while the boundary condition at $z=h_1$ and/or $z=h_2$ changes according to the mode of vibration (in-phase or out-of-phase).

5.4.1.3.1 In-phase mode

In the case of in-phase mode the boundary condition at fluid limits $z=h_1$ and/or $z=h_2$ is expressed as follows [20]:

$$\left.\frac{\partial\phi}{\partial z}\right|_{z=h_1} = \left(\frac{\partial W}{\partial t} + U_x \frac{\partial W}{\partial x}\right) \tag{5.30}$$

Similarly, A_1 and A_2 can be calculated by introducing Equation (5.21) into relations (5.14) and (5.30). The substitution of these constants in (5.21) enables us to develop the following expression for the potential.

$$\phi(x,y,z,t) = \frac{1}{\mu}\left[\frac{(1-e^{-\mu h_1})e^{\mu z} + (1-e^{\mu h_1})e^{-\mu z}}{e^{\mu h_1} - e^{\mu h_1}}\right]\left(\frac{\partial W}{\partial t} + U_x \frac{\partial W}{\partial x}\right) \tag{5.31}$$

By replacing (5.31) into (5.13), we obtain the following expression for pressure:

$$P = -\frac{\rho_f}{\mu}\left(\frac{2-e^{-\mu h_1} - e^{\mu h_1}}{e^{\mu h_1} + e^{-\mu h_1}}\right)\left[\frac{\partial^2 W}{\partial t^2} + 2U_x \frac{\partial^2 W}{\partial x \partial t} + U_x^2 \frac{\partial^2 W}{\partial x^2}\right] \tag{5.32}$$

or:

$$P = Z_{f3}\left[\frac{\partial^2 W}{\partial t^2} + 2U_x \frac{\partial^2 W}{\partial x \partial t} + U_x^2 \frac{\partial^2 W}{\partial x^2}\right] \tag{5.33}$$

Z_{f3} is given in Appendix B

5.4.1.3.2 Out-of-phase mode

The boundary condition for the out-of-phase mode is expressed as follows [20]:

$$\left.\frac{\partial\phi}{\partial z}\right|_{z=\frac{h_1}{2}} = 0 \tag{5.34}$$

Here again the potential function may be written as follows:

$$\phi(x.y,z,t) = \frac{F'(0)}{\mu}\frac{(e^{-\mu h_1}e^{\mu z} + e^{-\mu z})}{(e^{-\mu h_1} - 1)}\left(\frac{\partial W}{\partial t} + U_x\frac{\partial W}{\partial x}\right) \tag{5.35}$$

Using Equations (5.35) and (5.13) we obtain the following dynamic pressure:

$$P = -\frac{\rho_f(e^{-\mu h_1} + 1)}{\mu(e^{-\mu h_1} - 1)}\left[\frac{\partial^2 W}{\partial t^2} + 2U_x\frac{\partial^2 W}{\partial x\partial t} + U_x^2\frac{\partial^2 W}{\partial x^2}\right] \tag{5.36}$$

or:

$$P = Z_{f4}\left[\frac{\partial^2 W}{\partial t^2} + 2U_x\frac{\partial^2 W}{\partial x\partial t} + U_x^2\frac{\partial^2 W}{\partial x^2}\right] \tag{5.37}$$

Z_{f4} is given in Appendix B

5.4.2 Matrices of mass, damping and stiffness induced by flowing fluid

The elementary vector of distributed load is expressed by:

$$\{F\}^e = \int_A [N]^T \{P\} dA \tag{5.38}$$

where $[N]$ is the shape function matrix of the finite element defined in equation (5.4), $\{P\}$ is a vector expressing the pressure applied by the fluid on the plate and dA is the fluid-structure interface area.

By placing the matrix $[N]$ of Equation (5.4) into Equation (5.38), the element load vector becomes:

$$\{F\}^e = \int_A \left[[A]^{-1}\right]^T [R]^T \{P\} dA \tag{5.39}$$

The dynamic pressures of Equations (5.25, 5.29, 5.33 and 5.37) may be rewritten as:

$$P = Z_{fi}\left[\frac{\partial^2 W}{\partial t^2} + 2U_x \frac{\partial^2 W}{\partial x \partial t} + U_x^2 \frac{\partial^2 W}{\partial x^2}\right] \tag{5.40}$$

where Z_{fi} ($i=1, 4$), depends on the boundary conditions (see Appendix B) and P is the only non-zero component in the pressure tensor. Substituting Equation (5.1.c) into Equation (5.40) the pressure expression becomes:

$$P = Z_{fi}\left[\frac{\partial^2 W}{\partial t^2} + 2U_x \frac{i\pi}{A}\frac{\partial W}{\partial t} + U_x^2 \frac{i^2\pi^2}{A^2} W\right] \tag{5.41}$$

The transversal displacement can be separated from Equation (5.4) as follows:

$$\begin{Bmatrix} 0 \\ 0 \\ W \end{Bmatrix} = [R_f][A]^{-1}\{\delta\} \tag{5.42}$$

where [*Rf*] is a (3x24) matrix given in Appendix A. Substituting (5.42) into (5.41), we obtain the following expression for pressure:

$$\{P\} = Z_{fi}[R_f][A]^{-1}\left(\{\ddot{\delta}\} + 2U_x \frac{i\pi}{A}\{\dot{\delta}\} + U_x^2 \frac{i^2\pi^2}{A^2}\{\delta\}\right) \tag{5.43}$$

By combining Equations (5.43), (5.39) and (5.4) the element load vector is given by the following relation:

$$\{F\}^e = Z_{fi}\begin{pmatrix} \int_A \left[[A]^{-1}\right]^T [R]^T [R_f][A]^{-1}\{\ddot{\delta}\}dA + 2U_x \frac{i\pi}{A}\int_A \left[[A]^{-1}\right]^T [R]^T [R_f][A]^{-1}\{\dot{\delta}\}dA \\ + U_x^2 \frac{i^2\pi^2}{A^2}\int_A \left[[A]^{-1}\right]^T [R]^T [R_f][A]^{-1}\{\delta\}dA \end{pmatrix} \tag{5.44}$$

Note that the force induced by flowing fluid is a function of acceleration, velocity and displacement of the solid finite element. From Equation (5.44) we can separate the added matrices induced by flowing fluid, respectively describing inertial, Coriolis and centrifugal effects as follows:

$$\left[m_f\right]^e = Z_{fi} \int_A \left[\left[A\right]^{-1}\right]^T \left[R\right]^T \left[R_f\right] \left[A\right]^{-1} \left\{\ddot{\delta}\right\} dA \tag{5.45}$$

$$\left[c_f\right]^e = 2U_x Z_{fi} \frac{\pi}{A} \int_A \left[\left[A\right]^{-1}\right]^T \left[R\right]^T \left[R_f\right] \left[A\right]^{-1} \left\{\dot{\delta}\right\} dA \tag{5.46}$$

$$\left[k_f\right]^e = U_x^2 Z_{fi} \left(\frac{i\pi}{A}\right)^2 \int_A \left[\left[A\right]^{-1}\right]^T \left[R\right]^T \left[R_f\right] \left[A\right]^{-1} \left\{\delta\right\} dA \tag{5.47}$$

Dynamic equilibrium requires a combination of the last three elementary matrices with corresponding matrices given in Equations (5.7) and (5.8) as follows:

$$\left[\left[m\right]^e - \left[m_f\right]^e\right]\left\{\ddot{\delta}\right\} - i\left[c_f\right]^e \left\{\dot{\delta}\right\} + \left[\left[k\right]^e - \left[k_f\right]^e\right]\left\{\delta\right\} = \left\{0\right\} \tag{5.48}$$

5.5 EIGENVALUE PROBLEM

Assembly of the element matrices for mass, damping and rigidity enables us to develop a system of Equations (5.9) representing the dynamic behaviour of plate subjected to flowing fluid.

The eigenvalue problem is solved by means of the equation reduction technique. Equation (5.9) may be rewritten as follows:

$$\begin{bmatrix} [0] & [M] \\ [M] & [C] \end{bmatrix} \begin{Bmatrix} \{\ddot{\delta}_T\} \\ \{\dot{\delta}_T\} \end{Bmatrix} + \begin{bmatrix} -[M] & [0] \\ [0] & [K] \end{bmatrix} \begin{Bmatrix} \{\dot{\delta}_T\} \\ \{\delta_T\} \end{Bmatrix} = \{0\} \tag{5.49}$$

where:

$$[M] = [M_s] - [M_f], \quad [C] = [C_f], \quad [K] = [K_s] - [K_f]$$

$\{\delta_T\}$ is the global displacement vector,

$[K]$, $[M]$ *et* $[C]$ are square matrices of order *NDF(NNODE)-NC,* where *NDF* is the number of degrees of freedom by node, *NNODE* is the number of nodes in structure and *NC* is the number of constraints applied.

The eigenvalue problem is given by:

$$[[DD] - \Lambda[I]] = 0 \tag{5.50}$$

where:

$$[DD] = \begin{bmatrix} 0 & [I] \\ [K]^{-1}[M] & [K]^{-1}[C] \end{bmatrix};$$

and $\Lambda = 1/i\omega^2$;

$[I]$ is the identity matrix.

If the velocity of the fluid is (U_x=0), the eigenvalue problem in this particular case may be reduced to:

$$\left|[K]^{-1}[M]\right| - \Lambda[I] = 0 \tag{5.51}$$

5.6 RESULTS and DISCUSSIONS

The solid finite element used here has already been used for testing the model in the case of a plate without fluid and the obtained results were compared to those obtained by other theories and from experiments [16]. The results were in good agreement. Here we present some calculations to test the fluid-solid model in the case of a plate subjected to flowing fluid.

5.6.1 Plate subjected to flowing fluid with infinite level of fluid (h_1 and h_2 >>A and B)

a. The first example is a thin plate clamped on two opposite edges (see Figure 5.6) subjected to flowing fluid on its upper and lower surfaces. The fluid level is assumed to be very high (h_1 and h_2 >>A and B). The corresponding dynamic pressure would be twice the pressure calculated in Equation (5.25). The following characteristics are defined below; mass ratio (ψ), dimensionless frequency ($\overline{\omega}$) and dimensionless velocity ($\overline{U}$):

$$\psi = \frac{\rho_f B}{\rho_p h} \tag{5.52}$$

$$\overline{\omega} = B^2 \sqrt{\frac{\rho_s h}{K}}\omega \tag{5.53}$$

$$\overline{U} = B\sqrt{\frac{\rho_s h}{K}}U_x \tag{5.54}$$

Geometric ratios and dimensionless parameters for the structure are:

$$\psi = 0.93,\ h_1/A \to \infty,\ h_2/A \to \infty,\ A/B = 1, h_1/A >> 1,\ h_2/A >> 1$$

Numerical results were used to plot the curves shown in Figure (5.7). We note that the plate becomes increasingly vulnerable to static instability as the rate of flow increases. Beyond the critical velocity we expect a large deflection of the plate to occur [13].

b. In order to compare the influence of boundary conditions on critical velocity, we change our analysis to consider the preceding plate with simply supported edges (see Figure 5.8) instead of clamped edges. Figure (5.9) shows the variation of dimensionless frequencies for the first three modes versus dimensionless velocity of the fluid. It can be seen that the critical velocities for the first three modes are lower than those of the clamped plate. It can be concluded that clamped plates are more stable than simply supported plates which is in good agreement with the observations of Kim and Davis [13].

c. The case of a cantilevered plate subjected to flowing flow is often encountered in practice. We will compare the critical velocity of this plate with those already calculated above. As shown in Figure (5.10) the fluid level is infinite on two edges.

Table (5.1) compares the critical velocities of the three boundary conditions studied. We conclude that the cantilevered plate is more vulnerable to static instability.

5.6.2 System of parallel plates

Parallel-plate assemblies are used as core elements in nuclear reactors. Many thin plates are stacked in parallel with channels between them for fluid flow (see Figure 5.11). When channel height is relatively low, kinetic energy travels through the fluid from one plate to another. Vibration of the plates modifies the distribution of pressure and velocity along the channel. Therefore the fluid in the channels interacts simultaneously with both higher and lower plates. As mentioned previously, the plates vibrate according to two modes; in-phase and out-of-phase. The dynamic pressure for each case is distinct.

It has been proven that the dynamic behaviour of parallel-plate assemblies clamped at two lateral walls (see Figure 5.11) can be sufficiently predicted using only one plate which vibrates out-of-phase with respect to its adjacent upper and lower plates. This condition corresponds to a lower critical velocity [21]. The model of Groninger and Kana [3] showed that the adjacent plates always move in opposite directions at high flow rates, causing alternate opening and closing of the channel.

Miller [1] derived relations expressing the collapse velocity of an ETR (engineering test reactor) system. For the case of a flat plate clamped on two opposite edges (see Figure 5.11), the developed formula is:

$$U_{Miller} = \sqrt{\frac{15Eh_1h^3}{\rho_f(1-\nu^2)B^4}} \tag{5.55}$$

where E is Young modulus, ρ_f is the fluid density, h_1 is the fluid level on the plate, ν Poisson's coefficient and B is the width of plate.

We studied the case of an internal plate vibrating out-of-phase with respect to its adjacent upper and lower plates; the same assumptions applied in Miller's work. The corresponding dynamic pressure would be twice the pressure calculated in Equation (5.37). Figure (5.12) shows the critical velocities for the first mode computed by the present method compared with those calculated using Miller's formula. By examining Figure (5.12), it is clear that at low fluid levels the results are in good agreement with the available analytical data. But for high fluid levels a large discrepancy is observed. It is important to note here that beyond a certain fluid height, increasing h_1 or h_2 does not have any influence on the dynamic behaviour of a plate subjected to flowing fluid. This will be confirmed in the following examples. Miller's formula was developed specifically for ETR systems with very low h_1/A ratio.

Miller [1] also derived a relation expressing the collapse velocity of an ETR system when the plates are simply supported on two opposite edges, the developed formula is:

$$U_{Miller} = \sqrt{\frac{5Eh^3 h_1}{2\rho_f B^4 (1-\nu^2)}} \tag{5.56}$$

where E is Young modulus, ρ_f is the fluid density, h_1 is the fluid level on the plate, ν Poisson's coefficient and B is the width of plate.

We used the solid-fluid finite element developed in this work to calculate the critical velocity corresponding to the first mode when the adjacent plates move in opposite directions (out-of-phase mode). The obtained results are shown in Figure (5.13). There is a good agreement between our results and those calculated by Miller's formula.

5.6.3 Limit value of fluid level

The next step in our analysis was to determine the limit values of fluid level (h_{1lim}) beyond which the increase of fluid level does not have any influence on the dynamic behaviour of structure.

We initially considered the case of a plate clamped on two lateral sides placed in a channel of rigid walls (see Figure 5.14). The corresponding pressure is twice the pressure calculated in Equation (5.29). We gradually increased fluid height and calculated (for each value of h_1 and h_2) the corresponding critical velocity for the first two modes. As plotted in Figure (5.15), an initial phase occurs during which the critical velocities increase as the ratio (h_1/A) increases. However, there is limit value for the ratio (h_1/A) beyond which an increase in the fluid level doesn't change the critical velocity. For the case of a plate subjected to flowing fluid bounded by two rigid walls the limit value of this ratio is 0.5.

We then considered the case of an internal plate in an ETR system (see Figure. 5.11). As shown in Figure (5.16), for a given plate the critical velocity first increases as channel height increases. When the h_1/A ratio reaches a value of 1, the critical velocity remains constant even if we increase the channel height.

5.7 CONCLUSIONS

In this work we have developed a solid-fluid finite element and demonstrated how it can be used to predict the dynamic behaviour of a plate subjected to the dynamic pressure induced by potential flow.

The membrane displacement field is approximated by bilinear polynomials and the transversal displacement by an exponential function which is the solution of equilibrium equations. The mass, damping and stiffness matrices corresponding to a solid and fluid are determined by exact analytical integration for each element.

The fluid pressure is derived from a potential, it is function of acceleration, velocity and the transverse displacement of the plate, respectively known as inertial, Coriolis and centrifugal effects.

Several plates with various boundary conditions were studied. The frequencies of vibration were calculated for each mean velocity of flow and for each fluid height, until the critical velocity was reached. Establishment of the critical velocity is very important for the design of plate systems subjected to fluid flow. We note that the boundary conditions and the fluid level on the plate strongly influence the dynamic behaviour of the plate.

The developed element can be used for analysis of rectangular anisotropic plates with any boundary conditions contrary to previous analytical methods which were developed for particular cases.

The critical velocities calculated using our element agree well with those obtained using the analytical formulas derived by Miller, especially for the low fluid heights.

The limit value of fluid height was calculated for a plate subjected to flowing fluid bounded by two rigid walls and for an internal plate in an ETR system.

The fluid-solid finite element developed in this work can be adapted to study a rectangular plate or structure made of more complex forms subjected to turbulent flow.

5.8 REFERENCES

1. Miller, D.R., *Critical flow velocities for collapse of reactor parallel-plate fuel assemblies.* American Society of Mechanical Engineers -- Transactions -- Journal of Engineering for Power Series A, 1960. **82**(2): p. 83-95.
2. Rosenberg, G.S. and C.K. Youngdahl, *A simplified dynamic model for the vibration frequencies and critical coolant flow velocities for reactor parallel plate fuel assemblies.* Nuclear Science and Engineering, 1962. **13**(2): p. 91-102.
3. Groninger, R.D. and J.J. Kane, *Flow induced deflections of parallel flat plates.* Nuclear science and engineering, 1963. **16**: p. 218–226
4. Ishii, T., *Aeroelastic instabilities of simply supported panels in subsonic flow.* AIAA 1965. **65**: p. 772.
5. Wambsganss, M.W., *Second-order effects as related to critical coolant flow velocities and reactor parallel plate fuel assemblies.* Nuclear Engineering and design, 1967. **5**: p. 268-276.
6. Dowell, E.H., *Nonlinear oscillations of a fluttering plate. II.* AIAA Journal, 1967. **5**(10): p. 1856-62.
7. Smissaert, G.E., *Static and dynamic hydroelastic instabilities in MTR-type fuel elements.* Nuclear Engineering and Design, 1968. **7**(6): p. 535-546.
8. Smissaert, G.E., *Static and dynamic hydroelastic instabilities in MTR-type fuel elements -- 2.* Nuclear Engineering and Design, 1969. **9**(1): p. 105-122.

9. Weaver, D.S. and T.E. Unny, *The hydroelastic stability of a flat plate.* Transactions of the ASME. Series E, Journal of Applied Mechanics, 1970. **37**(3): p. 823-27.

10. Gislason, J.T., *Experimental investigation of panel divergence at subsonic speeds.* AIAA journal 1971. **9**(11): p. 2252-2258.

11. Kornecki, A., E.H. Dowell, and J. O'Brien, *On the aeroelastic instability of two-dimensional panels in uniform incompressible flow.* Journal of Sound and Vibration, 1976. **47**(2): p. 163-78.

12. Holmes, P.J., *BIFURCATIONS TO DIVERGENCE AND FLUTTER IN FLOW-INDUCED OSCILLATIONS: A FINITE DIMENSIONAL ANALYSIS.* Journal of Sound and Vibration, 1977. **53**(4): p. 471-503.

13. Kim, G. and D.C. Davis, *Hydrodynamic instabilities in flat-plate-type fuel assemblies.* Nuclear Engineering and Design, 1995. **158**(1): p. 1-17.

14. Guo, C.Q. and M.P. Paidoussis, *Stability of rectangular plates with free side-edges in two-dimensional inviscid channel flow.* Journal of Applied Mechanics, Transactions ASME, 2000. **67**(1): p. 171-176.

15. Guo, C.Q. and M.P. Paidoussis, *Analysis of hydroelastic instabilities of rectangular parallel-plate assemblies.* Transactions of the ASME. Journal of Pressure Vessel Technology, 2000. **122**(4): p. 502-8.

16. Kerboua, Y., et al., *Comportement dynamique des plaques rectangulaires submergées*. 2005, Ecole polytechnique de Montréal: Montreal.

17. Selmane, A. and A.A. Lakis, *Vibration analysis of anisotropic open cylindrical shells subjected to a flowing fluid.* Journal of Fluids and Structures, 1997. **11**(1): p. 111-134.

18. Lamb, H., *On the Vibrations of an Elastic Plate in Contact with Water.* Proceedings of the Royal Society of London., 1920. **98**(690): p. 205-216.

19. McLachlan, N.W., *Accession to inertia of flexible discs vibrating in a fluid.* Proceedings of the Physical Society, 1932. **44**: p. 546-555.

20. Kyeong-Hoon, J., Y. Gye-Hyoung, and L. Seong-Cheol, *Hydroelastic vibration of two identical rectangular plates.* Journal of Sound and Vibration, 2004. **272**(3-5): p. 539-55.

21. Kerboua, Y., et al., *Analyse dynamique des systémes de plaques en interaction avec un fluide et application* EPM-RT-2006-01, Editor. 2006, Ecole polytechnique de Montréal: Montréal.

5.9 APPENDIX A

A.1. Matrix [R]

$$[R]=\begin{bmatrix} 1 & \frac{x}{A} & \frac{y}{B} & \frac{xy}{AB} & 0 & 0 & 0 & 0 & 0 & 0 & 0 & 0 & 0 & 0 & 0 & 0 & 0 & 0 & 0 & 0 & 0 & 0 & 0 & 0 \\ 0 & 0 & 0 & 0 & 1 & \frac{x}{A} & \frac{y}{B} & \frac{xy}{AB} & 0 & 0 & 0 & 0 & 0 & 0 & 0 & 0 & 0 & 0 & 0 & 0 & 0 & 0 & 0 & 0 \\ 0 & 0 & 0 & 0 & 0 & 0 & 0 & 0 & 1 & \frac{x}{A} & \frac{y}{B} & \frac{x^2}{2A^2} & \frac{xy}{AB} & \frac{y^2}{2B^2} & \frac{x^3}{6A^3} & \frac{x^2y}{2AB} & \frac{xy^2}{2AB^2} & \frac{y^3}{6B^3} & \frac{x^3y}{6A^3B} & \frac{x^2y^2}{4A^2B^2} & \frac{xy^3}{6AB^3} & \frac{x^3y^2}{12A^3B^2} & \frac{x^2y^3}{12A^2B^3} & \frac{x^3y^3}{36A^3B^3} \end{bmatrix}$$

A.2. Matrix [R_f]

$$[R_f]=\begin{bmatrix} 0 & 0 & 0 & 0 & 0 & 0 & 0 & 0 & 0 & 0 & 0 & 0 & 0 & 0 & 0 & 0 & 0 & 0 & 0 & 0 & 0 & 0 & 0 & 0 \\ 0 & 0 & 0 & 0 & 0 & 0 & 0 & 0 & 0 & 0 & 0 & 0 & 0 & 0 & 0 & 0 & 0 & 0 & 0 & 0 & 0 & 0 & 0 & 0 \\ 0 & 0 & 0 & 0 & 0 & 0 & 0 & 0 & 1 & \frac{x}{A} & \frac{y}{B} & \frac{x^2}{2A^2} & \frac{xy}{AB} & \frac{y^2}{2B^2} & \frac{x^3}{6A^3} & \frac{x^2y}{2AB} & \frac{xy^2}{2AB^2} & \frac{y^3}{6B^3} & \frac{x^3y}{6A^3B} & \frac{x^2y^2}{4A^2B^2} & \frac{xy^3}{6AB^3} & \frac{x^3y^2}{12A^3B^2} & \frac{x^2y^3}{12A^2B^3} & \frac{x^3y^3}{36A^3B^3} \end{bmatrix}$$

A.3. Matrix [Q]

$$[Q]=\begin{bmatrix} 0 & \frac{1}{A} & 0 & \frac{y}{AB} & 0 & 0 & 0 & 0 & 0 & 0 & 0 & 0 & 0 & 0 & 0 & 0 & 0 & 0 & 0 & 0 & 0 & 0 & 0 & 0 \\ 0 & 0 & 0 & 0 & 0 & 0 & \frac{1}{B} & \frac{x}{AB} & 0 & 0 & 0 & 0 & 0 & 0 & 0 & 0 & 0 & 0 & 0 & 0 & 0 & 0 & 0 & 0 \\ 0 & 0 & \frac{1}{B} & \frac{x}{AB} & 0 & \frac{1}{A} & 0 & \frac{y}{AB} & 0 & 0 & 0 & 0 & 0 & 0 & 0 & 0 & 0 & 0 & 0 & 0 & 0 & 0 & 0 & 0 \\ 0 & 0 & 0 & 0 & 0 & 0 & 0 & 0 & 0 & 0 & 0 & \frac{1}{A^2} & 0 & 0 & \frac{x}{A^3} & \frac{y}{A^2B} & 0 & 0 & \frac{xy}{A^3B} & \frac{y^2}{2A^2B^2} & 0 & \frac{xy^2}{2A^3B^2} & \frac{y^3}{6A^2B^3} & \frac{xy^3}{6A^3B^3} \\ 0 & 0 & 0 & 0 & 0 & 0 & 0 & 0 & 0 & 0 & 0 & 0 & \frac{1}{B^2} & 0 & 0 & \frac{x}{AB^2} & \frac{y}{B^3} & 0 & \frac{x^2}{2A^2B^2} & \frac{xy}{AB^3} & \frac{x^2}{2A^2B^3} & \frac{x^2y}{6A^2B^3} & \frac{x^2y}{6A^{2B^3}B^2} \\ 0 & 0 & 0 & 0 & 0 & 0 & 0 & 0 & 0 & 0 & 0 & \frac{2}{AB} & 0 & 0 & \frac{2x}{A^2B} & \frac{2y}{A^2B} & 0 & \frac{x^2}{A^2B} & \frac{2xy}{A^2B^2} & \frac{y^2}{AB^3} & \frac{x^2y}{A^2B^3} & \frac{xy^2}{A^2B^3} & \frac{x^2y^2}{2A^2B^3} \end{bmatrix}$$

A.4. Elementary displacement vector $\{\delta\}$

$$\{\delta\}=\{U_i,V_i,W_i,W_{i,x},W_{i,y},W_{i,xy},U_j,V_j,W_j,W_{j,x},W_{j,y},W_{j,xy},U_k,V_k,W_k,W_{k,x},W_{k,y},W_{k,xy},U_l,V_l,W_l,W_{l,x},W_{l,y},W_{l,xy}\}^T$$

A.5. Matrix $[A]^{-1}$

The nonzero elements of Matrix A^{-1} are:

$$A^{-1}(1,1) = 1, A^{-1}(2,1) = A^{-1}(2,7) = -\frac{A}{x_e}, A(3,1) = -A(3,19) = -\frac{B}{y_e}, \; A^{-1}(4,1) = -A^{-1}(4,7)) = A^{-1}(4,13) = -A^{-1}(4,19) = -\frac{AB}{x_e y_e}$$

$$A^{-1}(5,2) = 1, \; A^{-1}(6,2) = -A^{-1}(6,8) = -\frac{A}{x_e}, \; A^{-1}(7,2) = -\frac{B}{y_e}, \; A^{-1}(7,20) = -\frac{AB}{x_e y_e},$$

$$A^{-1}(8,2) = -A^{-1}(8,8) = A^{-1}(8,14) = A^{-1}(8,14) = -A^{-1}(8,20) = \frac{AB}{x_e}, \; A^{-1}(9,3) = 1, \; A^{-1}(10,4) = A, \; A^{-1}(11,5) = B,$$

$$A^{-1}(12,3) = -A^{-1}(12,9) = -\frac{6A^2}{x_e^2}, \; A^{-1}(12,4) = 2A^{-1}(12,10) = -4\frac{A^2}{x_e}, \; A^{-1}(13,6) = A.B, \; A^{-1}(14,3) = -A^{-1}(14,21) = -12\frac{A^3}{x_e^2},$$

$$A^{-1}(14,5) = A^{-1}(14,3) = 2A^{-1}(14,23) = 2\frac{B^2}{y_e}, \; A^{-1}(15,3) = -A^{-1}(15,9) = 12\frac{A^3}{x_e^3}, \; A^{-1}(15,4) = A^{-1}(15,10) = \frac{6A^3}{x_e^2},$$

$$A^{-1}(16,5) = -A^{-1}(16,11) = -6\frac{A^2B}{x_e^2}, \; A^{-1}(16,6) = A^{-1}(16,12) = -2\frac{A^2B}{x_e}, \; A^{-1}(17,4) = -A^{-1}(17,22) = -6\frac{AB^2}{y_e^2},$$

$$A^{-1}(17,6) = A^{-1}(17,24) = -\frac{4AB^2}{y_e}, \; A^{-1}(18,3) = -A^{-1}(18,21) = 12\frac{B^3}{y_e^3}, \; A^{-1}(18,5) = A^{-1}(18,23) = 6\frac{B^3}{y_e^2},$$

$$A^{-1}(19,5) = A^{-1}(19,11) = 12\frac{A^3B}{x_e^3}, \; A^{-1}(19,6) = A^{-1}(19,12) = 6\frac{BA^3}{x_e^2},$$

$$A^{-1}(20,4) = 2A^{-1}(20,10) = -A^{-1}(20,16) = -A^{-1}(20,22) = 24\frac{B^2A^2}{xy_e^2},$$

$$A^{-1}(20,5) = -\frac{2A^{-1}(20,9)}{3} = -A^{-1}(20,11) = -2A^{-1}(20,17) = 2A^{-1}(20,23) = 24\frac{A^2B^2}{x_e^2 y_e},$$

$$A^{-1}(20,6) = 2A^{-1}(20,12) = 4A^{-1}(20,18) = \frac{2}{3}A(20,24) = 16\frac{A^2B^2}{x_e y_e}, \; A^{-1}(21,4) = -A^{-1}(21,22) = 12\frac{AB^3}{y_e^3},$$

$$A^{-1}(21,6) = A^{-1}(21,24) = 6\frac{AB^3}{y_e^2},$$

$$A^{-1}(22,3) = -A^{-1}(22,9) = A^{-1}(22,15) = -A^{-1}(22,21) = 72\frac{AB^2}{x_e^3 y_e^2}, \; A^{-1}(22,4) = A^{-1}(22,10) = -A^{-1}(22,16) = -A^{-1}(22,22) = -36\frac{A^3B^3}{x_e^2 y_e^2},$$

$$A^{-1}(22,5) = -A^{-1}(22,11) = -2A^{-1}(22,17) = 2A^{-1}(22,23) = -48\frac{A^3B^2}{x_e^3 y_e},$$

$$A^{-1}(22,6) = A^{-1}(22,12) = 2A^{-1}(22,18) = 2A^{-1}(22,24) = -24\frac{A^3B^2}{x_e^2 y_e}$$

$$A^{-1}(23,3) = -A^{-1}(23,9) = A^{-1}(23,15) = A^{-1}(23,21) = 72\frac{A^2B^3}{x_e^2 y_e^2},$$

$$A^{-1}(23,4) = 2A^{-1}(23,10) = -2A^{-1}(23,16) = -A^{-1}(23,22) = -48\frac{A^2B^3}{x_e y_e^3},$$

$$A^{-1}(23,5) = -A^{-1}(23,11) = -A^{-1}(23,17) = A^{-1}(23,23) = -36\frac{A^2B^3}{x_e^2 y_e^2},$$

$$A^{-1}(23,6) = 2A^{-1}(23,12) = 2A^{-1}(23,18) = A^{-1}(23,24) = -24\frac{A^2B^3}{x_e y_e^2}$$

$$A^{-1}(24,3) = -A^{-1}(24,9) = A^{-1}(24,15) = -A^{-1}(24,21) = 144\frac{A^3B^3}{x_e^3 y_e^3},$$

$$A^{-1}(24,4) = A^{-1}(24,10) = -A^{-1}(24,16) = -A^{-1}(24,22) = 72\frac{A^3B^3}{x_e^2 y_e^3},$$

$$A^{-1}(24,5) = -A^{-1}(24,11) = -A^{-1}(24,17) = A^{-1}(24,23) = -72\frac{A^3B^3}{x_e^2 y_e^2}, \quad A^{-1}(24,6) = A^{-1}(24,12) = A^{-1}(24,18) = A^{-1}(24,24) = 36\frac{A^3B^3}{x_e^2 y_e^2}$$

5.10 APPENDIX B

B.1. Determination of vector $\{C\}$:

Each node (i) has a displacement vector given by:

$$\{\delta_i\} = \{U_i, V_i, W_i, \partial W_i/\partial x, \partial W_i/\partial y, \partial^2 W_i/\partial y \partial x\}^T$$

U_i, V_i, represent the in-plane nodal displacements of the middle surface in X and Y directions, respectively and W_i is the transversal nodal displacement of the middle surface.

The elementary vector of displacement is:

$$\{\delta\} = \left\{\{\delta_i\}^T, \{\delta_j\}^T, \{\delta_k\}^T, \{\delta_l\}^T\right\}^T$$

From Equation (5.3), the displacement vector {δ} can be written as follows:

$$\{\delta\} = [A]\{C\}$$

From the last equation we express the constant vector by:

$$\{C\} = [A]^{-1}\{\delta\}$$

The terms of matrix $[A]^{-1}$ are given in Appendix A.

Substitution of vector $\{C\}$ into Equation (5.3) gives:

$$\begin{Bmatrix} U \\ V \\ W \end{Bmatrix} = [R][A]^{-1}\{\delta\}$$

B.2. Kinematics equations

The relation between the strain and the displacement for a rectangular plate is given as [44]:

$$\begin{Bmatrix} \varepsilon_x \\ \varepsilon_y \\ 2\varepsilon_{xy} \\ \kappa_x \\ \kappa_y \\ \kappa_{xy} \end{Bmatrix} = \begin{Bmatrix} \partial U/\partial x \\ \partial V/\partial y \\ \partial V/\partial x + \partial U/\partial y \\ -\partial^2 W/\partial x^2 \\ -\partial^2 W/\partial y^2 \\ -2\partial^2 W/\partial x \partial y \end{Bmatrix}$$

B.3. Elasticity matrix P

Stresses may be related to the strains by the elasticity matrix [P].

where $[P]$ is matrix of order (6x6). In the case of isotropic material the non vanishing terms of the elasticity matrix are:

$$P_{11} = P_{22} = D,\ P_{44} = P_{55} = K,\ P_{12} = P_{21} = \nu D,\ P_{45} = P_{54} = \nu K P_{33} = (1-\nu)D/2,$$
$$P_{66} = (1-\nu)K/2$$

where : $K = \dfrac{Eh^3}{12(1-\nu^2)}$, $D = \dfrac{Eh}{1-\nu^2}$,

B.4. dynamic pressure coefficients Z_{fi}

$$Z_{f1} = \frac{\rho_f}{\mu}$$

$$Z_{f2} = -\frac{\rho_f (e^{-2\mu h_1} + 1)}{\mu (e^{-2\mu h_1} - 1)}$$

$$Z_{f3} = -\frac{\rho_f}{\mu}\left(\frac{2 - e^{-\mu h_1} - e^{\mu h_1}}{e^{\mu h_1} + e^{-\mu h_1}}\right)$$

$$Z_{f4} = -\frac{\rho_f (e^{-\mu h_1} + 1)}{\mu (e^{-\mu h_1} - 1)}$$

5.11 NOMENCLATURE

U, V	Displacement components of the plate reference surface in the X and Y directions, respectively
W	Normal displacement of the plate middle surface
A, B	Plate side length along the X and Y axes, respectively
h	Plate thickness
h_1	Fluid level on top of the plate
h_2	Fluid level below the plate surface
U_i, V_i	Nodal displacement components at node i in the X and Y direction, respectively
W_i	Normal displacement of the plate at node i
$W_{i,x}$; $W_{i,x,y}$	The first derivative of the plate's normal displacement with respect to X and Y, respectively, at node i
$W_{i,xy}$	Crossed derivative of the plate's normal displacement with respect to X and Y
ω	Natural frequency (rad/sec)
$\overline{\omega}$	Dimensionless natural frequency
U_x	Mean velocity of fluid
ψ	Mass ratio defined in Equation (5.52)
X, Y, Z	Orthogonal coordinate system
ρ_s	Material density
ρ_f	Fluid density

Z_{fi}	Coefficient of fluid pressure acting on the plate
K	Bending stiffness, $Eh^3/12(1-\nu^2)$
D	Membrane stiffness, $Eh/(1-\nu^2)$
i	Complex number i^2=-1
C_i	Constants defined by Equations (5.1) and (5.2)
ν	Poisson's coefficient
E	Elasticity Modulus
P_{ij}	Material elasticity matrix components
x_e, y_e	Length of the element along the X and Y axes, respectively
P	Fluid dynamic pressure
c	Velocity of sound in the fluid
V	Fluid velocity $V=\sqrt{V_x^2+V_y^2+V_z^2}$
V_x, V_y, V_z	Fluid velocity components in X, Y, Z directions, respectively
ϕ(x, y, z)	Velocity potential function
[R]	Matrix (3 × 24), defined by Equation (5.3)
$[R_f]$	Defined by Equation (5.42)
$\{C\}$	Vector of unknown constants defined by Equation (5.3)
$\{\delta\}$	Elementary vector of displacement define in (5.4)
$[A]^{-1}$	Matrix (24x24), define in Appendix A
$[N]$	Shape function matrix (3 × 24) defined by Equation (5.4)

$\{\varepsilon\}$	Deformation vector
$\{\sigma\}$	Stress vector
$[Q]$	Matrix (6 × 24) defined by Equation (5.5)
$[P]$	Elasticity matrix (6x6), given in Appendix B
$[k]^e$	Stiffness matrix of a solid element (24 × 24)
$[m]^e$	Mass matrix of a solid element (24 × 24)
$[k_f]^e$	Stiffness matrix of a fluid element (24 × 24)
$[m_f]^e$	Mass matrix of a fluid element (24x24)
$[c_f]^e$	Damping matrix of a fluid element (24x24)
$\{F\}^e$	Nodal force vector
$\{F\}$	Global force vector
$[M_s]$	Global solid mass matrix
$[K_s]$	Global solid stiffness matrix
$[C_s]$	Global solid damping matrix
$[M_f]$	Global fluid mass matrix
$[C_f]$	Global fluid damping matrix
$[K_f]$	Global fluid stiffness
$\{\delta_T\}$	Global displacement vector

Table 5.1: Dimensionless critical velocity $(\overline{U})$ of plates with various boundary conditions ($\psi = 0.93$, $h_1/A \to \infty$, $h_2/A \to \infty$, $A/B = 1$).

Boundary conditions	$\overline{U} = B\sqrt{\frac{\rho_s h}{K}}U_x$		
	Mode 1	Mode 2	Mode 3
Clamped plate on two opposite edges (Figure 5.6) (CFCF)	9.58	11.36	18.83
Simply supported plate on two opposite edges (Figure 5.8) (SFSF)	4.22	6.98	15.83
Cantilevered plate (Figure 5.10) (FFFC)	1.494	3.73	9.25

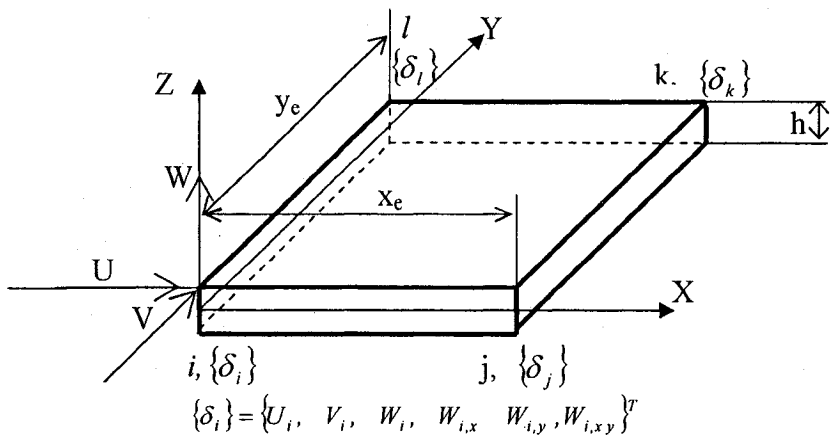

Figure 5.1: Geometry of the finite element and nodal vector of displacements

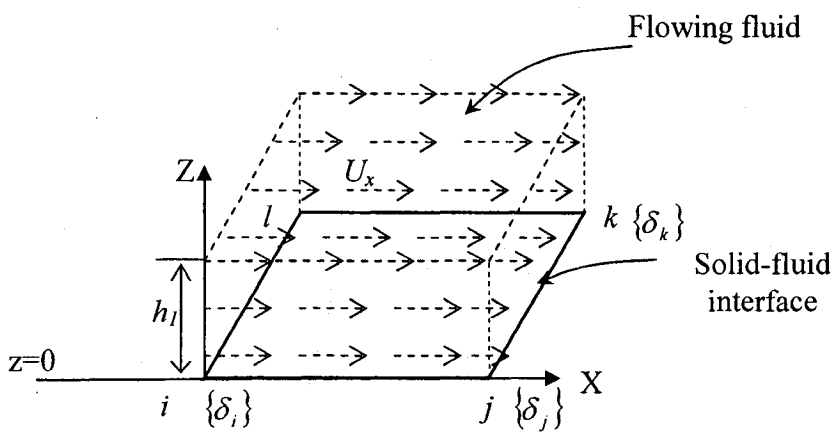

Figure 5.2: Fluid-solid finite element.

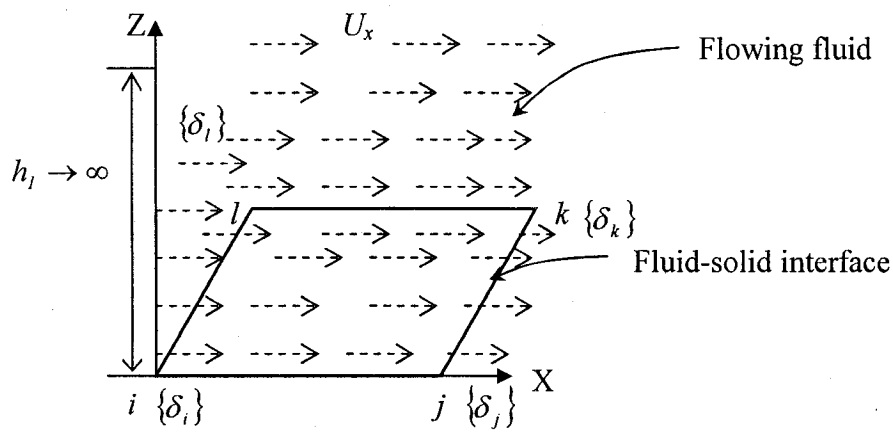

Figure 5.3: Fluid-solid finite element subjected to flowing fluid with infinite height

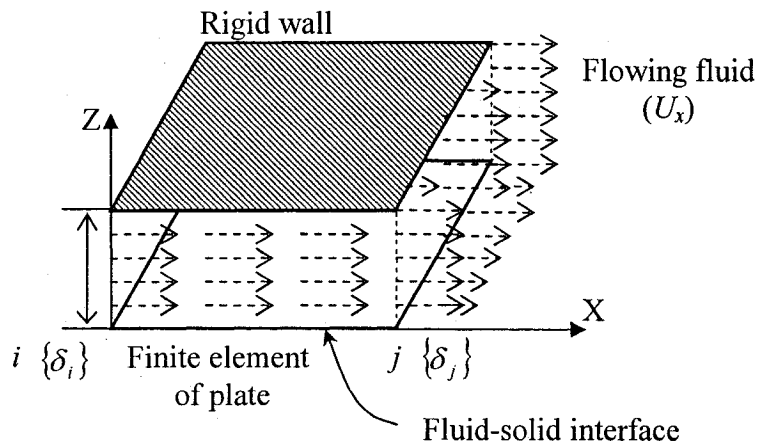

Figure 5.4: fluid solid finite element in contact with flowing fluid bounded by a rigid wall.

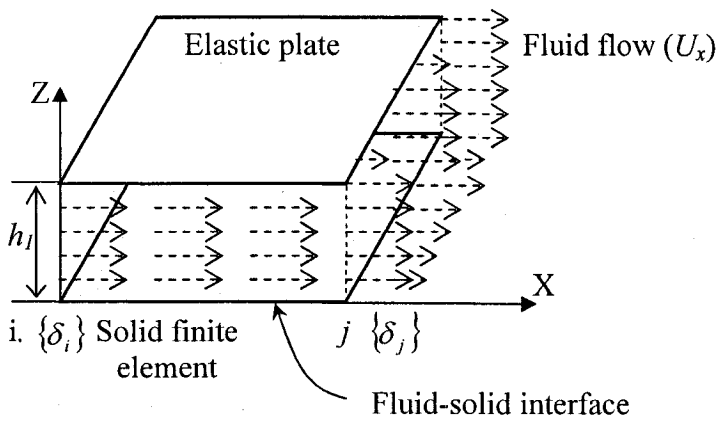

Figure 5:5 fluid-solid finite element in contact with flowing fluid bounded by an elastic plate

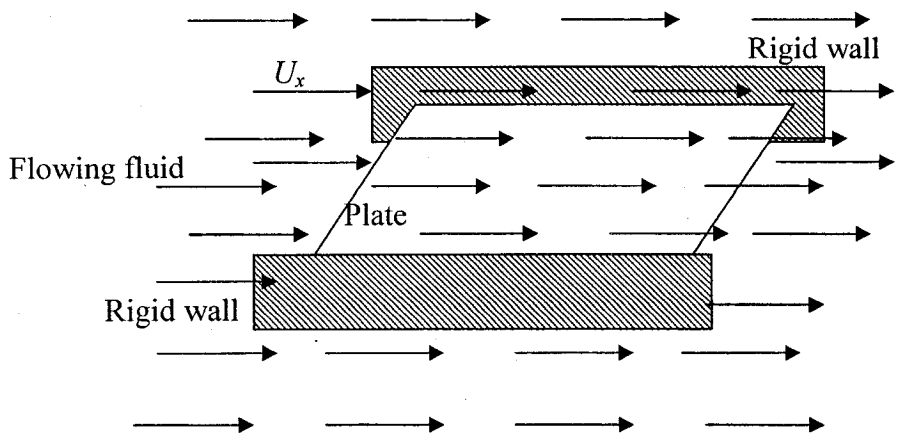

Figure 5.6: Plate clamped on two opposite edges subjected to flowing fluid (h_1 and h_2 >>A and B).

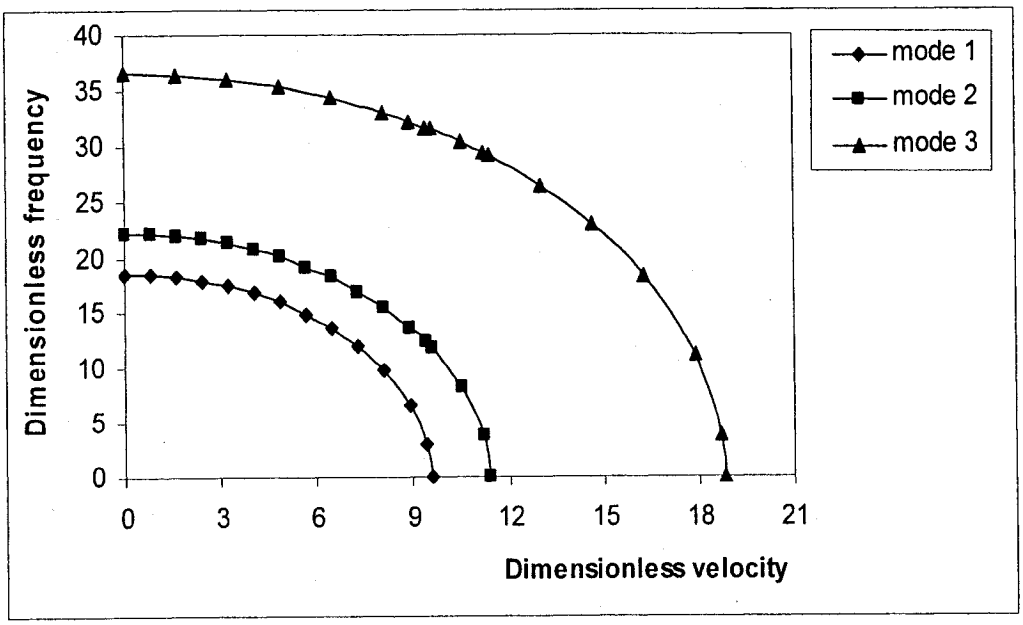

Figure 5.7: Variation of frequency ϖ versus fluid velocity $\overline{U}$ for plate clamped on two opposite edges subjected to flowing fluid.

$\psi = 0.93,\ h_1/A \to \infty,\ h_2/A \to \infty,\ A/B = 1, h_1/A >> 1,\ h_2/A >> 1$

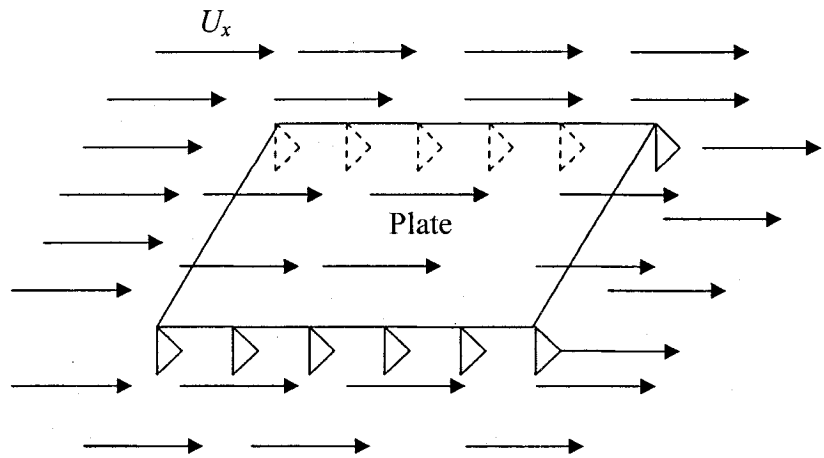

Figure 5.8: Plate simply supported on two opposite edges subjected to flowing fluid (h_1 and h_2 >>A and B)

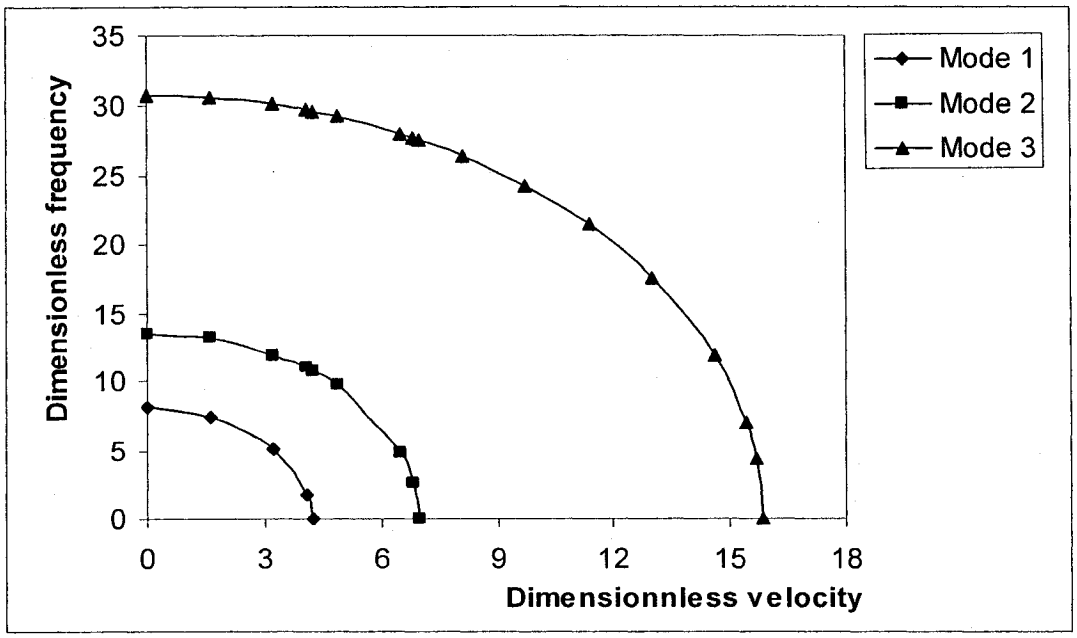

Figure 5.9: Variation of frequency ϖ versus fluid velocity $\overline{U}$ for plate simply supported on two opposite edges subjected to flowing fluid.

$\psi = 0.93,\ h_1/A \to \infty,\ h_2/A \to \infty,\ A/B = 1.$

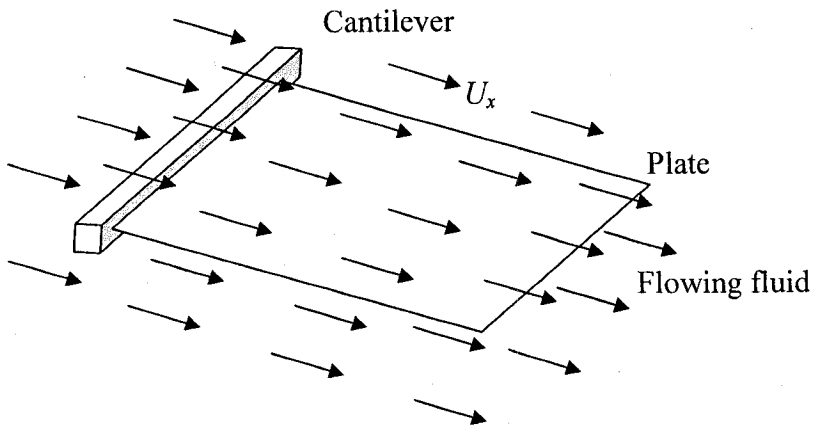

Figure 5.10: cantilevered plate subjected to flowing fluid (h_1 and h_2 >>A and B).

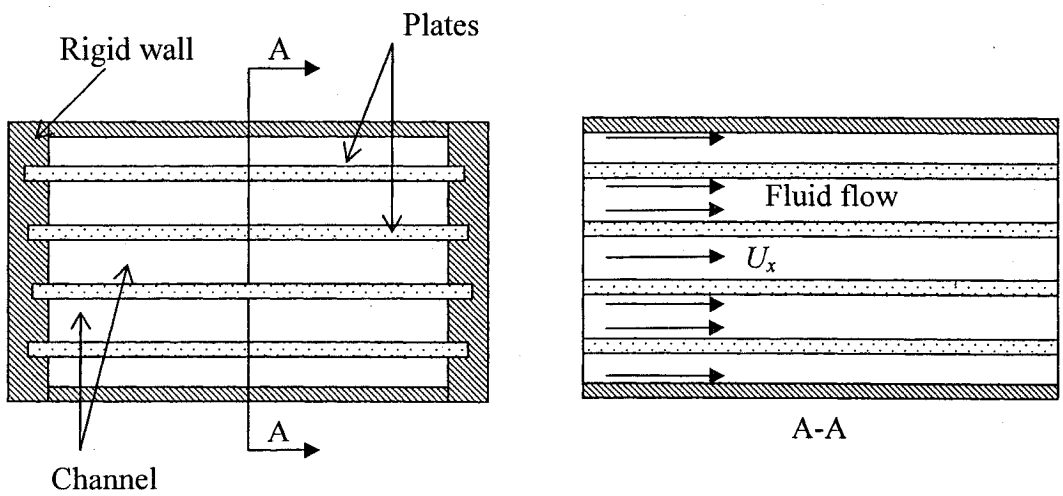

Figure 5.11: ETR (engineering test reactor) system subjected to flowing fluid

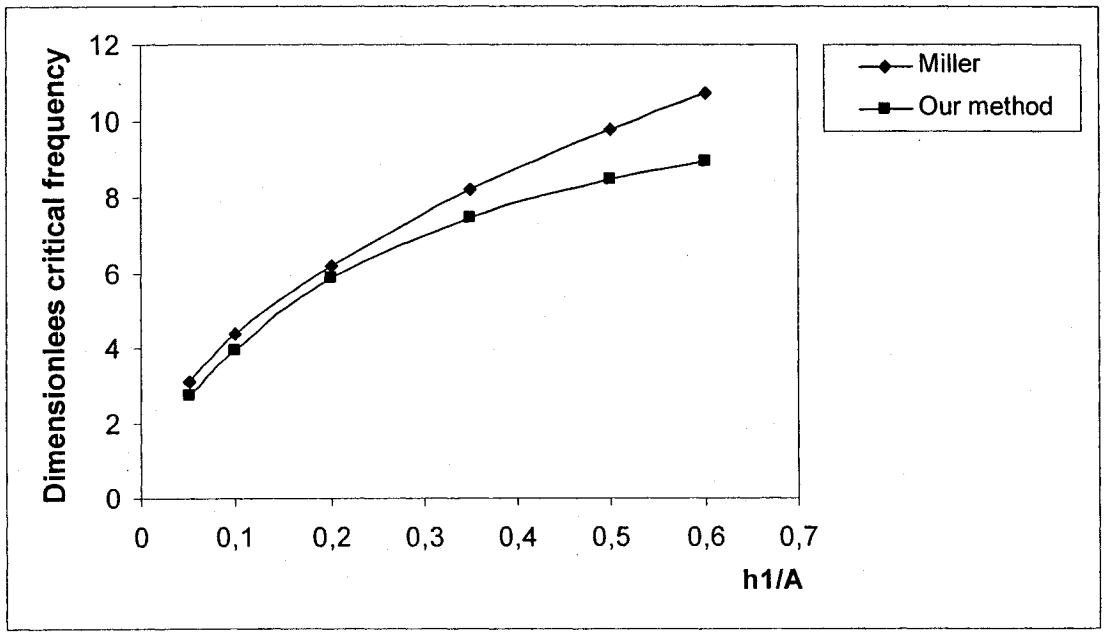

Figure 5.12: Dimensionless critical velocity $\left(\overline{U}\right)$ versus ratio (h_1/A) for a plate clamped on two opposite edges, $\psi = 0.93$, $h_1/A \to \infty$, $h_2/A \to \infty$, $A/B = 1$.

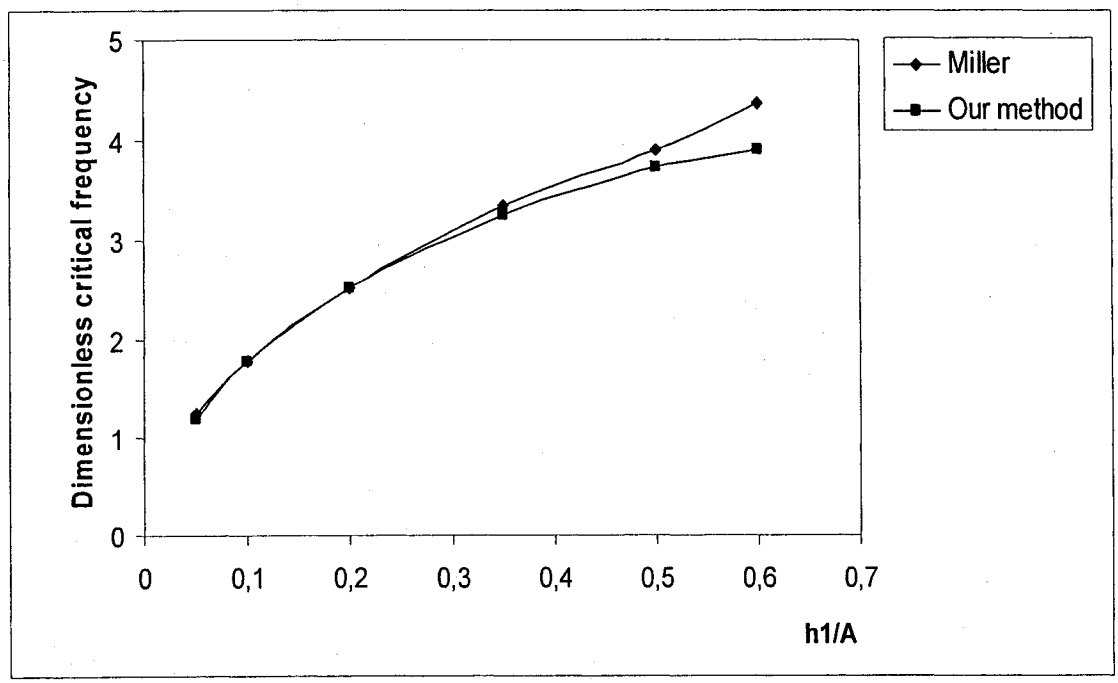

Figure 5.13: Dimensionless critical velocity $(\overline{U})$ versus ratio (h_1/A) for a plate simply supported on two opposite edges, $\psi = 0.93$, $h_1/A \to \infty$, $h_2/A \to \infty$, $A/B = 1$

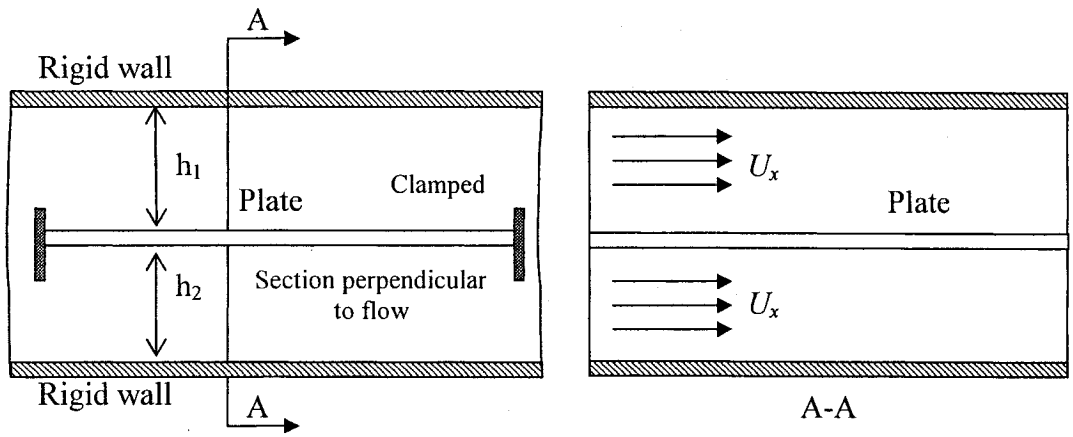

Figure 5.14: Plate subjected to flowing fluid bounded by two rigid walls

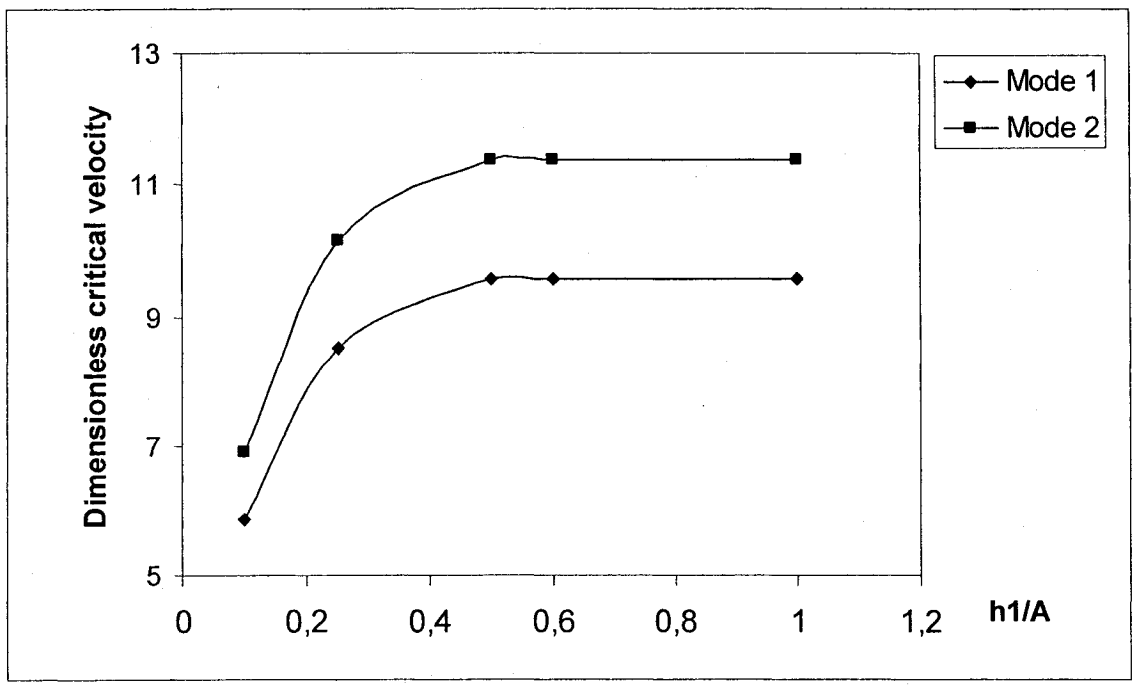

Figure 5.15: Critical velocity of plate clamped on two opposite edges subjected to flowing fluid bounded by two rigid walls versus ratio (h_1/A)

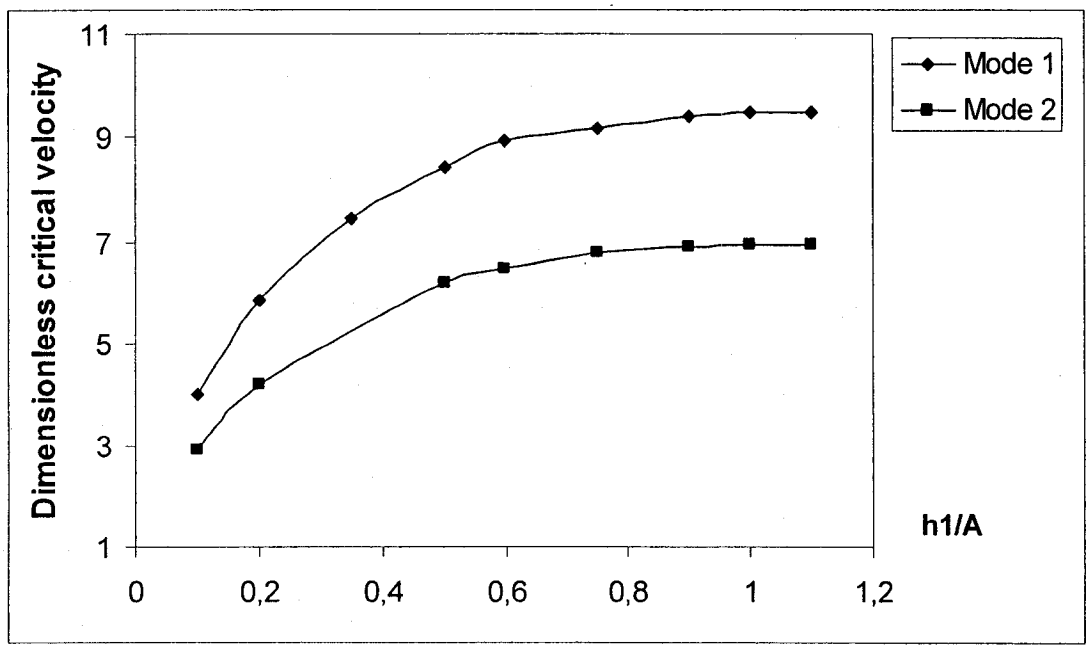

Figure 5.16: Critical velocity of an internal plate in an ETR system clamped on two opposite edges subjected to flowing fluid bounded by two elastic plates which vibrate in out-of-phase mode versus ratio (h_1/A)

CHAPITRE VI

DISCUSSION GÉNÉRALE

Le modèle d'éléments finis développé dans ce travail a été utilisé pour l'analyse d'une variété de structures en vibration à vide ou en interaction avec le fluide. Certaines structures nous ont servi de modèle de validation et d'autres ont été étudiées afin de comprendre leur comportement lorsque leur mouvement est couplé avec celui du fluide. Les résultats obtenus éprouvent généralement une bonne précision et une représentation correcte du comportement dynamique des structures étudiées lorsque nous varions certains paramètres d'interaction.

Nous avons commencé évidemment par l'analyse des plaques rectangulaires sans fluide, nous avons comparé les modes et les fréquences calculées pour des plaques ayant des conditions aux rives variées avec des méthodes analytiques, numériques et expérimentales. Nous avons constaté que nos résultats sont très précis et convergent rapidement.

Lorsque la plaque rectangulaire horizontale est en interaction avec le fluide, les fréquences de vibration diminuent d'une façon remarquable. Les résultats obtenus montrent que les fréquences de vibration sont sensibles au niveau du fluide sous et/ou sur la plaque lorsque la hauteur du fluide est inférieure à la moitié de la longueur de la plaque. En même temps, l'effet de niveau du fluide sur les fréquences est intimement lié aux conditions limites du fluide. Nous avons constaté que les fréquences diminuent en augmentant la hauteur de fluide lorsque la limite de fluide est une surface libre. En revanche, les fréquences augmentent lorsqu'on augmente la

hauteur du fluide lorsque la limite de fluide est un mur rigide. Il est aussi important de souligner que les conditions aux rives et l'aspect géométrique sont des paramètres à considérer lors du calcul des plaques submergées dans le fluide.

Les premiers modes de vibration de la plaque submergée sont les mêmes que ceux de la plaque à vide. Ceci signifie que l'hypothèse des modes invariables adoptés par la majorité des travaux est une approximation valable.

Les réservoirs rectangulaires, les systèmes de plaques et les coques cylindriques ouvertes et fermées ont été étudiés en utilisant l'élément fini de plaque développé dans ce travail après la transformation des matrices élémentaires calculées au niveau local à un repère global représentant toute la structure. Les fréquences naturelles calculées pour ces structures à vide coïncident parfaitement avec les fréquences calculées en utilisant le logiciel ANSYS. Les structures courbes nécessitent plus d'éléments afin de minimiser l'erreur commise provenant du fait d'approcher une surface courbe par une surface plane.

La singularité numérique causée par l'apparition d'un nouveau degré de liberté lorsque nous passons du repère local au repère global est résolue en introduisant des raideurs et des masses fictives aux termes diagonaux correspondant à ce degré de liberté dans chaque nœud de l'élément.

Lorsque le fluide est situé entre deux parois élastiques se trouvant l'une en face de l'autre, un transfert de mouvement se fait entre ces deux parois. Il est donc nécessaire de calculer la pression lorsque les deux parois vibrent selon le mode en phase et lorsqu'elles vibrent selon le mode antiphase. Dans le cas d'un réservoir renfermant un fluide incompressible, les modes en phase vérifient toujours la conservation de

masse du fluide alors que les modes en antiphase nécessitent le choix d'un champ de déplacement qui impose d'emblée des conditions de conservation de masse.

Lors de l'analyse de l'interaction solide-fluide des systèmes de plaques parallèles identiques encastrées à des murs latéraux, il s'est avéré que l'étude d'une seule plaque interne en vibration en mode antiphase par rapport aux plaques adjacentes est suffisant pour avoir les fréquences critiques de tout le système.

D'après les résultats obtenus pour un système de plaques ou pour un réservoir rectangulaire, nous soulignons que la hauteur de fluide entre chaque deux parois élastiques au-delà de laquelle les fréquences de vibration cessent de changer est égale à la longueur des plaques parallèles. Nous notons aussi que l'augmentation progressive de la hauteur de fluide entre chaque deux parois élastiques cause une diminution de fréquences pour le mode en phase et une augmentation de fréquences des modes en antiphase, jusqu'à ce qu'elles coïncident à une valeur finale. À ce point, n'importe quelle augmentation de nouveau de fluide n'influence pas le comportement dynamique du système.

Dans le cas des plaques radiales, la pression du fluide appliquée sur les parois élastiques est différente d'un élément fini à l'autre puisque la hauteur de fluide change en fonction des dimensions des plaques et de l'angle d'inclinaison.

Un élément fini solide-fluide a été développé pour prédire le comportement dynamique d'une plaque rectangulaire soumise aux efforts induits par le passage d'un écoulement potentiel d'un fluide incompressible. La pression du fluide dans ce cas est exprimée en fonction de l'accélération, de la vitesse et du déplacement transversal de la plaque, appelées respectivement l'effet de l'inertie, l'effet de force de Coriolis et l'effet de la force centrifuge.

Les fréquences de vibration ont été calculées pour chaque vitesse moyenne d'écoulement et pour chaque hauteur de fluide séparant les plaques des systèmes ETR (engineering test reactor) jusqu'à ce qu'on atteigne la vitesse critique. Les résultats obtenus en utilisant cet élément s'accordent bien avec ceux calculés par les formules analytiques dérivées par Miller, spécialement pour les hauteurs de fluide faibles.

Ce travail rentre dans le cadre d'un projet de modélisation des aubes de turbines hydrauliques soumises aux efforts induits par un écoulement turbulent lorsque cette dernière est soudée à un arbre rigide ou élastique.

CHAPITRE VII

CONCLUSIONS ET RECOMMANDATIONS

L'objectif de cette thèse était de développer un modèle d'éléments finis capable de représenter adéquatement les vibrations libres des plaques rectangulaires et des systèmes de plaques tels que les réservoirs rectangulaires et les plaques parallèles et radiales et de tenir compte des efforts induits par un fluide en contact avec ces systèmes solides.

Les fonctions de déplacement assurant le couplage de mouvement des parois élastiques avec le fluide incompressible à l'interface solide-fluide ont été inspirées des éléments finis hybrides développés par Lakis et al. [43, 47] pour les coques cylindriques fermées et ouvertes.

Un modèle d'éléments finis solide quadrilatère à quatre nœuds a été développé en utilisant un champ bipolynomial pour les déplacements membranaires et une fonction exponentielle dérivée des équations d'équilibre des plaques en flexion pour le déplacement transversal.

L'équation de Bernoulli et l'équation différentielle du potentiel de vitesses ont été utilisées pour calculer la pression du fluide exercée sur la paroi solide de chaque élément fini. La pression est exprimée en fonction de la masse volumique du fluide, des conditions aux limites du fluide (mur rigide, surface libre, etc.), de la vitesse moyenne d'écoulement et du champ de déplacement de la paroi solide et ses dérivées par rapport au temps. Cette pression s'introduit dans les équations d'équilibre dynamiques du système comme étant une masse, un amortissement et une rigidité

connus respectivement par l'effet de l'inertie, l'effet de force de Coriolis et l'effet de la force centrifuge. Lorsque la vitesse moyenne du fluide est nulle, la force de Coriolis et la force centrifuge n'interviennent pas dans les équations puisqu'elles sont fonctions de la vitesse.

En effectuant les transformations géométriques nécessaires, l'élément fini de plaque a été utilisé pour l'analyse des réservoirs rectangulaires et des coques cylindriques ouvertes et fermées.

Dans le cas des systèmes plaques parallèles ou radiales et des réservoirs rectangulaires, la pression de fluide a été calculée pour les modes de vibrations en phase et en antiphase. Lorsque le fluide est renfermé dans des parois rigides, certains modes en antiphase ne sont pas permis puisqu'ils violent le principe de conservation de volume d'un fluide incompressible.

L'élément solide-fluide a été utilisé pour le calcul d'une série de structures telles les plaques parallèles et radiales submergé dans le fluide ou soumises aux efforts induits par un écoulement potentiel , les réservoirs rectangulaires ouverts ou fermés et les coques cylindriques. Les résultats obtenus sont très encourageants.

Jusqu'à maintenant, aucun logiciel ni modèles analytiques ne peuvent représenter correctement le comportement dynamique d'une plaque rectangulaire ou d'un système composé de plaques submergées dans un fluide ou soumis à un écoulement potentiel en tenant compte de tous les paramètres tels que l'effet de niveau de fluide, l'effet de surface libre, les discontinuités de matériaux, les conditions aux limites quelconques ainsi que la non-uniformité géométrique. À partir de cela, nous pouvons assumer que les éléments solide-fluide développés dans ce travail sont un pas en avant du domaine de l'interaction fluide-structure.

L'élément fini fluide-structure développé est en cours d'être utilisé pour :

a) modéliser une aube de turbine soumise à une pression aléatoire induite par un écoulement turbulent ;

b) modéliser un ensemble d'aubes encastrées à un axe rigide ou élastique ;

c) prédire expérimentalement et/ou numériquement les effets de l'amortissement et des mécanismes d'interaction à différentes positions des aubes;

d) finalement, cet élément sera utilisé pour trouver la réponse d'un système de turbine hydraulique soumise à des forces certaines (deterministic).

BIBLIOGRAPHIE

1. Love, A.E.H., *A treatise on the mathematical theory of elasticity*. 4th Édition ed. 1944, New York: Dover.
2. Reissner, E., *A new derivation of the equations for the deformation of elastic shells.* Amer, J. Math, 1941. **63**: p. 177-184
3. Knowles, J.K. and E. Reissner, *Derivation of equations of shell theory for general orthogonal coordinates.* Journal of Mathematics and Physics, 1957. **35**(4): p. 351-358.
4. Sanders, J.L., *An improved first approximation theory for thin shells.* . 1959, NASA.
5. Kirchhoff, G., *Über das Gleichgewicht und die Bewegung einer elastischen Scheibe. J Reine Mathe 40, 51-58.* J Reine Mathe, 1850. **40**: p. 51-58.
6. Reissner, E., *The effect of transverse shear deformation on the bending of elastic plates.* Journal of Applied Mechanics, 1945. **12**: p. A69-A77.
7. Mindlin, R.D., *Influence of rotatory inertia and shear on flexural motions of isotropic, elastic plates.* American Society of Mechanical Engineers -- Transactions -- Journal of Applied Mechanics, 1951. **18**(1): p. 31-38.
8. Rayleigh, L., *Theory of sound.* Second Edition ed. 1877, New York: Dover
9. Lamb, H., *Vibrations of an elastic plate touching water.* Proceedings of the Royal Society of London, 1920. **98**: p. 205-216.
10. Powell, J.H. and J.H.T. Roberts, *Frequency of circular diaphragms [with discussion].* Proceedings of the Physical Society, 1923. **35**: p. 170-181.
11. McLachlan, N.W., *Accession to inertia of flexible discs vibrating in a fluid.* Proceedings of the Physical Society, 1932. **44**: p. 546-555.

12. Peake, W.H. and E.G. Thurston, *The lowest resonant frequency of a water-loaded circular plate.* Journal of the Acoustical Society of America, 1954. **26**: p. 166-168.

13. Montero De Espinosa, F. and J.A. Gallego-Juarez, *On the resonance frequencies of water-loaded circular plates.* Journal of Sound and Vibration, 1984. **94**(2): p. 217-22.

14. Lindholm, U.S., et al., *Elastic vibration characteristics of cantilever plates in water.* Journal of Ship Research, 1965. **9**(1): p. 11-22.

15. Muthuveerappan, G., N. Ganesan, and M.A. Veluswami, *A note on vibration of a cantilever plate immersed in water.* Journal of Sound and Vibration, 1979. **63**(3): p. 385-91.

16. Zienkiewicz, O.C., *The finite element method in engineering sciences.* 1971, Maindenhead, Bearks McGraw-Hill Publishing Compagny Limited.

17. Muthuveerappan, G., N. Ganesan, and M.A. Veluswami, *Influence of fluid added mass on the vibration characteristics of plates under various boundary conditions.* Journal of Sound and Vibration, 1980. **69**(4): p. 612-15.

18. Joseph, P., G. Muthuveerappan, and N. Ganesan, *Vibrations of generally orthotropic plates in fluids.* Composite Structures, 1990. **15**(1): p. 25-42.

19. Aggarwal, K.R., R. Sinhasan, and G.K. Grover, *Free vibrations of a rectangular plate submerged in fluid.* Journal of the Institution of Engineers (India) Mechanical Engineering Division, 1980. **60**: p. 184-90.

20. Fu, Y. and W.G. Price, *Interactions between a partially or totally immersed vibrating cantilever plate and the surrounding fluid.* Journal of Sound and Vibration, 1987. **118**(3): p. 495-513.

21. Haddara, M.R. and S. Cao, *Study of the dynamic response of submerged rectangular flat plates.* Marine Structures, 1996. **9**(10): p. 913-933.

22. Kwak, M.K. and K.C. Kim, *Axisymmetric vibration of circular plates in contact with fluid.* Journal of Sound and Vibration, 1991. **146**(3): p. 381-9.

23. Kwak, M.K., *Vibration of circular plates in contact with water.* Journal of Applied Mechanics, Transactions ASME, 1991. **58**(2): p. 480-483.

24. Kwak, M.K., *Vibration of circular membranes in contact with water.* Journal of Sound and Vibration, 1994. **178**(5): p. 688-690.

25. Amabili, M. and M.K. Kwak, *Free Vibrations of Circular Plates Coupled with Liquids: Revising the Lamb Problem.* Journal of Fluids and Structures, 1996. **10**(7): p. 743.

26. Amabili, M., G. Frosali, and M.K. Kwak, *Free vibrations of annular plates coupled with fluids.* Journal of Sound and Vibration, 1996. **191**(5): p. 825-846.

27. Amabili, M., *Effect of finite fluid depth on the hydroelastic vibrations of circular and annular plates.* Journal of Sound and Vibration, 1996. **193**(4): p. 909-25.

28. Kwak, M.K. and S.B. Han, *Effect of fluid depth on the hydroelastic vibration of free-edge circular plate.* Journal of Sound and Vibration, 2000. **230**(1): p. 171-85.

29. Kwak, M.K., *Hydroelastic vibration of rectangular plates.* Transactions of the ASME. Journal of Applied Mechanics, 1996. **63**(1): p. 110-15.

30. Amabili, M. and M.K. Kwak, *Vibration of circular plates on a free fluid surface: Effect of surface waves.* Journal of Sound and Vibration, 1999. **226**(3): p. 407-424.

31. Cheung, Y.K. and D. Zhou, *COUPLED VIBRATORY CHARACTERISTICS OF A RECTANGULAR CONTAINER BOTTOM PLATE.* Journal of Fluids and Structures, 2000. **14**(3): p. 339-357.

32. Cheung, Y.K. and D. Zhou, *Hydroelastic vibration of a circular container bottom plate using the Galerkin method* Journal of fluids and structures 2002. **16**(4): p. 561-580.

33. Chiba, M., *Axisymmetric free hydroelastic vibration of a flexural bottom plate in a cylindrical tank supported on an elastic foundation.* Journal of Sound and Vibration, 1994. **169**(3): p. 387-94.

34. Soedel, S.M. and W. Soedel, *On the free and forced vibration of a plate supporting a freely sloshing surface liquid.* Journal of Sound and Vibration, 1994. **171**(2): p. 159-171.

35. Ergin, A. and B. Ugurlu, *Linear vibration analysis of cantilever plates partially submerged in fluid.* Journal of Fluids and Structures, 2003. **17**(7): p. 927-939.

36. Sinha, J.K., S. Singh, and A. Rama Rao, *Added mass and damping of submerged perforated plates.* Journal of Sound and Vibration, 2003. **260**(3): p. 549-64.

37. Kyeong-Hoon, J. and K. Kwi-Ja, *Hydroelastic vibration of a circular plate submerged in a bounded compressible fluid.* Journal of Sound and Vibration, 2005. **283**(1-2): p. 153-72.

38. Amabili, M., *Vibrations of circular plates resting on a sloshing liquid: solution of the fully coupled problem.* Journal of Sound and Vibration, 2001. **245**(2): p. 261-83.

39. Lamb, H., *Hydrodynamics* ed. D.P.S. edition. 1945 New York.

40. Berry, J.G. and E. Reissner, *The effect of an internal compressible fluid column on the breathing vibrations of a thin pressurized cylindrical shell.* Journal of Aerospace Science 1958. **25**(1958): p. 288-294.

41. Lindholm, U.S., D.D. Kana, and H.N. Abramson, *Breathing vibrations of circular cylindrical shell with internal liquid.* Journal of the Aero/Space Sciences, 1962. **29**(9): p. 1052-1059.

42. Coale, C.W. and M. Nagano, *Axisymmetric modes of an elastic cylindrical-hemispherical tank partially filled with liquid.* AIAA Symposium on Structural Dynamics and Aeroelasticity. , 1965.

43. Lakis, A.A. and Paidoussis, *Free vibration of cylindrical shells partially filled with liquid.* Journal of Sound and Vibration, 1971. **19**(1): p. 1-15.

44. Lakis, A.A. and S. Neagu, *Free surface effects on the dynamics of cylindrical shells partially filled with liquid.* Journal of Sound and Vibration, 1997. **207**(2): p. 175-205.

45. Jain, R.K., *Vibration of fluid-filled, orthotropic cylindrical shells.* Journal of Sound and Vibration, 1974. **37**(3): p. 379-88.

46. Amabili, M. and G. Dalpiaz, *Breathing vibrations of a horizontal circular cylindrical tank shell, partially filled with liquid.* Journal of Vibration and Acoustics, Transactions of the ASME, 1995. **117**(2): p. 187-191.

47. Selmane, A. and A.A. Lakis, *Vibration analysis of anisotropic open cylindrical shells subjected to a flowing fluid.* Journal of Fluids and Structures, 1997. **11**(1): p. 111-134.

48. Bursuc, G., *effect de la surface libre sur la dynamique des coques cylindriques horizontales partiellement remplies de liquide.*, in *Département de génie mécanique*. 2003, École polytechnique de Montréal: Montréal.

49. Mistry, J. and J.C. Menezes, *Vibration of cylinders partially-filled with liquids.* Journal of Vibration and Acoustics, Transactions of the ASME, 1995. **117**(1): p. 87-93.

50. Kyeong-Hoon Jeong, et al. *Free vibration analysis of two circular disks coupled with fluid.* 1998. San Diego, CA, USA: ASME, Fairfield, NJ, USA.

51. Kyeong-Hoon, J., *Free vibration of two identical circular plates coupled with bounded fluid.* Journal of Sound and Vibration, 2003. **260**(4): p. 653-70.

52. Kyeong-Hoon, J., Y. Gye-Hyoung, and L. Seong-Cheol, *Hydroelastic vibration of two identical rectangular plates.* Journal of Sound and Vibration, 2004. **272**(3-5): p. 539-55.

53. Kim, M.C. and S.S. Lee. *Hydroelastic analysis of rectangular tank.* in *The aerospace corporation El Segundo, .* 1997. California 90245.

54. Bauer, H.F., *Hydroelastic vibrations in a rectangular container.* International Journal of Solids and Structures, 1981. **17**(7): p. 639-52.

55. Koh, H.M., J.K. Kim, and J.-H. Park, *Fluid-structure interaction analysis of 3-D rectangular tanks by a variationally coupled BEM-FEM and comparison with test results.* Earthquake Engineering & Structural Dynamics, 1998. **27**(2): p. 109-124.

56. Miller, D.R., *Critical flow velocities for collapse of reactor parallel-plate fuel assemblies.* American Society of Mechanical Engineers -- Transactions -- Journal of Engineering for Power Series A, 1960. **82**(2): p. 83-95.

57. Rosenberg, G.S. and C.K. Youngdahl, *A simplified dynamic model for the vibration frequencies and critical coolant flow velocities for reactor parallel plate fuel assemblies.* Nuclear Science and Engineering, 1962. **13**(2): p. 91-102.

58. Groninger, R.D. and J.J. Kane, *Flow induced deflections of parallel flat plates.* Nuclear science and engineering, 1963. **16**: p. 218–226

59. Dowell, E.H., *Nonlinear oscillations of a fluttering plate. II.* AIAA Journal, 1967. **5**(10): p. 1856-62.

60. Smissaert, G.E., *Static and dynamic hydroelastic instabilities in MTR-type fuel elements.* Nuclear Engineering and Design, 1968. **7**(6): p. 535-546.

61. Smissaert, G.E., *Static and dynamic hydroelastic instabilities in MTR-type fuel elements -- 2.* Nuclear Engineering and Design, 1969. **9**(1): p. 105-122.

62. Weaver, D.S. and T.E. Unny, *The hydroelastic stability of a flat plate.* Transactions of the ASME. Series E, Journal of Applied Mechanics, 1970. **37**(3): p. 823-27.

63. Gislason, J.T., *Experimental investigation of panel divergence at subsonic speeds.* AIAA journal 1971. **9**(11): p. 2252-2258.

64. Kornecki, A., E.H. Dowell, and J. O'Brien, *On the aeroelastic instability of two-dimensional panels in uniform incompressible flow.* Journal of Sound and Vibration, 1976. **47**(2): p. 163-78.

65. Holmes, P.J., *Bifurcations to divergence and flutter in flow-induced oscillations : a finite dimensional analysis.* Journal of Sound and Vibration, 1977. **53**(4): p. 471-503.

66. Kim, G. and D.C. Davis, *Hydrodynamic instabilities in flat-plate-type fuel assemblies.* Nuclear Engineering and Design, 1995. **158**(1): p. 1-17.

67. Guo, C.Q. and M.P. Paidoussis, *Stability of rectangular plates with free side-edges in two-dimensional inviscid channel flow.* Transactions of the ASME. Journal of Applied Mechanics, 2000. **67**(1): p. 171-6.

68. Guo, C.Q. and M.P. Paidoussis, *Analysis of hydroelastic instabilities of rectangular parallel-plate assemblies.* Transactions of the ASME. Journal of Pressure Vessel Technology, 2000. **122**(4): p. 502-8.